Influence du climat sur les transferts de carbone organique dissous, nitrates et phosphates dans une tête de bassin versant agricole

Laurent Strohmenger

DOCTORAT ECOLOGIE
BRETAGNE GEOSCIENCES
LOIRE AGRONOMIE ALIMENTATION

l'institut Agro
agriculture • alimentation • environnement
AGRO CAMPUS OUEST

THESE DE DOCTORAT DE

L'institut national d'enseignement supérieur pour l'agriculture, l'alimentation et l'environnement
Ecole interne AGROCAMPUS OUEST

ECOLE DOCTORALE N° 600
Ecole doctorale Ecologie, Géosciences, Agronomie et Alimentation
Spécialité : Sciences de la terre et de l'environnement

Par

Laurent STROHMENGER

Influence du climat sur les transferts de carbone organique dissous, nitrate et phosphate dans une tête de bassin versant agricole

Thèse présentée et soutenue à Rennes, le 10 décembre 2020
Unité de recherche : UMR SAS, INRAE, Institut Agro
Thèse N° : D-91

Rapporteurs avant soutenance

Ilja VAN MEERVELD	Senior researcher, University of Zurich
Vazken ANDREASSIAN	Directeur de recherche, INRAE

Composition du Jury

Président :	Christophe CUDENNEC	Professeur, Institut Agro
Examinateurs :	Florence HABETS	Directrice de recherche, CNRS
	Cécile DAGES	Chargée de recherche, INRAE
Dir. de thèse :	Chantal GASCUEL-ODOUX	Directrice de recherche, INRAE
Co-dir. de thèse :	Ophélie FOVET	Chargée de recherche, INRAE

Invité

Markus HRACHOWITZ :	Associate professor, Delft University of Technology

DOCTORAT ECOLOGIE
BRETAGNE GEOSCIENCES
LOIRE AGRONOMIE ALIMENTATION

THESE DE DOCTORAT

L'institut national d'enseignement supérieur pour l'agriculture, l'alimentation et l'environnement

Ecole interne AGROCAMPUS OUEST

ECOLE DOCTORALE N° 600
Ecole doctorale Ecologie, Géosciences, Agronomie et Alimentation

Par

Laurent STROHMENGER

Influence du climat sur les transferts de carbone organique dissous, nitrate et phosphate dans une tête de bassin versant agricole

Unité de recherche : UMR SAS, INRAE, Institut Agro, 35 000 Rennes, France

Dir. de thèse : *Chantal Gascuel*
Co-encadrante de thèse : *Ophélie Fovet*

Résumé de la thèse

Au XXe siècle, l'agriculture a perturbé les écosystèmes naturels et notamment la qualité des masses d'eaux de surface. Ces dégradations se manifestent par des développement anormaux d'espèces végétales au détriment de la biodiversité aquatique causés par des concentrations excessives en nitrate (NO_3) et phosphate (SRP), deux élément dont l'origine agricole a été démontrée. Outre les pratiques agricoles, le climat influence également les processus biogéochimiques qui contrôle la réactivité et les transferts de ces éléments au sein d'un bassin versant. La compréhension de ces processus de transferts est cruciale pour en permettre la gestion à l'échelle du paysage dans un objectif de reconquête de la qualité des eaux. Les premières directives de mitigation des pollutions agricoles ont amorcé des tendances à la diminution des concentrations en NO_3 et SRP dans les rivières. Cependant, la distinction entre les effets du climat et ceux des pratiques agricoles sur l'évolutions des concentrations reste incertaine.

L'objectif de la thèse est d'identifier les relations entre le climat et les transferts de carbone organique dissous (DOC), NO_3 et SRP dans une tête de bassin versant agricole. Ces trois éléments sont complémentaires par leurs origines (naturelle pour DOC, agricole pour NO_3 et SRP), leurs distributions spatiales (en surface pour DOC et SRP, en profondeur pour le NO_3) et la sensibilité présumée du DOC par rapport au climat (notamment à la température). Cette étude s'appuie sur un jeu de données hydro-climatiques et chimiques acquis à haute fréquence sur le bassin versant agricole de Kervidy-Naizin (Morbihan, Bretagne, France) entre 2002 et 2017.

Le premier volet de recherche porte sur l'analyse de ce jeu de données pour identifier les conditions hydro-climatiques qui contrôlent les concentrations en solutés à l'exutoire du bassin versant pour plusieurs échelles temporelles (long terme, saisonnier et évènementielle). Le second volet de recherche porte sur la modélisation des dynamiques annuelles et évènementielles du débit et des concentrations en DOC et NO_3 à l'exutoire du bassin versant de Kervidy-Naizin dans le but de mieux contraindre nos connaissances sur les sources et chemins d'écoulement de l'eau et des solutés jusqu'à la rivière.

Les résultats montrent que les pratiques agricoles et le climat contrôlent les dynamiques des concentrations en solutés sur le long terme, alors que les conditions hydrologiques (humidité du bassin versant et précipitations) contrôlent davantage les dynamiques saisonnières et évènementielles. De plus, les concentrations en DOC et NO_3 montrent des dynamiques opposées pour les trois échelles temporelles. La modélisation a mis en évidence que ces oppositions entre DOC et NO_3 sont principalement contrôlées par la distribution spatiale de leurs concentrations dans deux compartiments dont les temps de résidence sont contrastés. Le réservoir souterrain, dont l'écoulement est lent et saisonnier, présente des concentrations fortes en NO_3 et faibles en DOC. A l'inverse, le réservoir superficiel de bas de versant (la zone riparienne), dont la réponse à un évènement de pluie est rapide et qui soutient les écoulements en crue, présente des concentrations faibles en NO_3 et fortes en DOC.

Le climat influence indirectement les dynamiques saisonnières et évènementielles des concentrations en DOC et NO_3 dans la rivière par son effet sur les chemins d'écoulement de l'eau dans le bassin versant. En effet, ces derniers dépendent de l'état hydrologiques du bassin versant (humidité des sols, niveaux de nappes) qui à leur tour, contrôlent les contributions relatives des compartiments souterrain et riparien au débit, et par conséquent les concentrations dans la rivière.

Summary of the thesis

Over the twentieth century, agriculture has disturbed the biogeochemical cycles in natural ecosystems and in particular in the surface waters. These disturbances have caused degradation of the ecosystem such as the unusual organic matter production at the expense of aquatic biodiversity. This phenomenon, called eutrophication, is caused by excessive concentrations of nitrate (NO_3) and phosphate (SRP), two elements whose agricultural origin has been shown. In addition to agricultural practices, climate also influences the biogeochemical processes and the transfer processes of chemical elements from land to surface water. However, the distinction between the effects of climate and those of agricultural practices on the river concentrations variability remains unclear. Understanding these processes is crucial to allow their management at the landscape scale in order to restore the water quality.

This thesis aims at identifying the relationships between climate and transfers of dissolved organic carbon (DOC), nitrogen focusing on nitrate and phosphorus focusing on soluble reactive phosphorus (SRP) in an agricultural headwater catchment. These three elements are complementary in terms of origin (natural for DOC, agricultural for NO_3 and SRP), spatial distributions (mostly in surface soil layers for DOC and SRP, rather in the vadose zone and groundwater for NO_3) and their presumed sensitivity to climate (high for DOC especially to temperature). This study used a set of hydro-climatic and chemical data acquired at high (daily) frequency on the agricultural catchment of Kervidy-Naizin (AgrHyS observatory, Brittany, France) between 2002 and 2017.

The first part of the thesis focuses on the analysis of the dataset in order to identify the hydro-climatic controls of solute concentrations at the outlet of the catchment for three time scales (long-term, seasonal and event-driven). The second part of the research focuses on the modeling of the annual and event-driven dynamics of DOC and NO_3 concentrations at the outlet of the Kervidy-Naizin catchment in order to better constrain our knowledge about the sources and flow paths of water and solutes from land to stream. The third part discusses the links between the analysis and the modelling results and the perspectives of model evolutions to investigate the effect of climatic scenarios on these elements.

The results showed that agricultural practices and climate control the long-term dynamics of solute concentrations, while wetness conditions (catchment wetness index and precipitation) control seasonal and event-driven dynamics. In addition, DOC and NO_3 concentrations show opposite dynamics for the three time scales. The model tended to support that these oppositions between DOC and NO_3 were mainly controlled by the mixing between two source compartments with contrasting residence times. The slow reservoir, with seasonal flow contribution, has high NO_3 and low DOC concentrations and is interpreted as the shallow groundwater. Conversely, the faster reservoir supports storm flows, has low NO_3 and high DOC concentrations, and is interpreted as a more superficial compartment in the riparian zone. Climate indirectly influences the seasonal and event-driven dynamics of DOC and NO_3 concentrations in the river through its effects on water flow paths that connect the sources of the solute to the river.

Remerciements

Pendant ces 3 années, j'ai eu la chance d'être encadré par Ophélie et Chantal, que je remercie profondément pour la confiance, l'écoute et la patience dont elles ont su faire preuve, et qui ont permis de faire de la réalisation de cette thèse un excellent souvenir.

Je remercie également Gérard Gruau, Jérôme Molénat et Markus Hrachowitz, Patrick Durand, Jordy Salmon Monviola, Laurent Ruiz, Zahra Thomas, et Rémi Dupas pour l'intérêt porté à mes travaux, leurs critiques et leurs précieux conseils, année après année.

J'en profite pour remercier Marie-Claire Pierret et Damien Lemarchand car vous m'avez donné l'envie et la conviction que faire une thèse pouvait être agréable! Mission réussie!

Markus, merci pour l'accueil à Delft, les discussions scientifiques et méthodologiques au bureau, les discussions plus conceptuelles hors du bureau, et tes conseils de lectures qui se sont avérées passionnantes!

Un grand merci évidemment à l'ensemble de l'UMR SAS pour les conditions de travail bienveillantes et conviviales, les pauses et les activités ludiques. Je pense particulièrement à Monique, Karine, Maryvonne, Tiphaine et Séverine, déjà pour leurs disponibilités et efficacités, mais surtout pour leur bonne humeur communicative! Je pense également à Yannick H., Mikael, Yannick B., Nicolas, Yannick F., Laurence et Béatrice avec qui j'ai toujours eu plaisir à échanger.

Une unité de recherche, c'est aussi une armée de jeunes têtes (ou encore jeune !) avec qui partager des moments conviviaux autours d'un apéro ou d'un repas pendant lesquels naissent des rencontres inoubliables. Coucou Elisa, Mamadou, Charlotte, Lucie, Stella, Kevin, Thomas, …, Sophie, Monique et Guénola!

Et puis il y a les doctorants avec qui partager nos expériences, nos doutes et nos joies: Hugo (et l'autre Hugo aussi !), Stéphane, Laurène, Yossra, Youssra, Inès, PA, Laurène, Bia, Antonin, Aymeric, Joshua. Claire, merci pour ces repas partagés ensemble, et pour nos discussions sur les avancés de thèse et de rédaction de manuscrit mais également sur des questions existentielles. Antoine, on a un peu ramé dans le même bateau, merci d'avoir été présent pour m'écouter me plaindre, partager tes astuces autours d'un café ou à l'occasion d'une pause. Ovidiu, tu as forcément ta place parmi ces remerciements pour tes précieux conseils sur l'organisation au travail et la gestion efficace d'un emploi du temps (et plein d'autre trucs encore).

Enfin, il y a l'entourage, ceux qui m'ont permis de garder l'équilibre, Titouan, Tiphaine, Josselin, Jeanne, Coralie et Damien merci pour votre présence et pour les soirées passées ensemble (les vraies, et les fausses aussi!). Mavi, j'ai été ravi de partagé un toit avec toi, merci pour les repas collectifs à la maison, et pour les soirées à partager un doute, un verre, ou les deux, qui sont le reflet de ta générosité tant appréciée.

Je ne pouvais évidemment pas oublier les collègues de bureau Allemand, Brésilien et Ecossais qui sont devenus bien plus que cela: Seb, Bia et Céline. Vous me manquerez, mais on se reverra très prochainement, n'est-ce pas ?

Et puisque personne n'est parfait, je tiens à remercier toutes les personnes que j'ai pu oublier ici.

Table des matières

Liste des figures du manuscrit

Liste des figures du premier article

Liste des figures du deuxième article

Liste des tables

1. Introduction

1.1. Contexte sociétal

L'influence de l'homme sur les écosystèmes, notamment sur les milieux aquatiques, ne fait plus aucun doute aujourd'hui, à tel point que la réduction de la pollution de l'eau résultante des activités terrestres compte parmi les objectifs de développement durables de l'organisation des nations unies. Pourtant, l'évolution de la vision de la nature comme un stock de ressources à exploiter vers une vision des écosystèmes pourvoyeurs de services écosystémiques à préserver est le fruit de nombreuses années de débats publiques, politiques et scientifiques.

Les évolutions de l'agriculture du XX^{e} siècle

Les années 1950 à 1970 ont été marquées par l'augmentation de la natalité et une pénurie alimentaire dans un contexte de reconstruction de l'Europe et de la France d'après-guerre. La politique agricole des années 1950 visait à produire, et pour cela à transformer le paysage rural français afin d'assurer la sécurité alimentaire du pays. Le déploiement des plans Monnet et Marshall ont permis, en France, de moderniser et d'intensifier l'agriculture par la mécanisation des techniques de production, le remembrement des terres cultivées, la sélection d'espèces animales et végétales en fonction de leurs potentiels de rendement, l'utilisation d'intrants sous formes d'amendement et d'engrais, etc. Les rendements de céréales et la production de lait et de viande ont explosé.

Conséquences de ces changements

Au cours des années 1970, dans plusieurs pays de l'hémisphère nord, la qualité de certaines masses d'eaux de surface s'est dégradée et a été marquée par le développement d'algues, accompagné d'un appauvrissement en oxygène des milieux aquatiques. En France, le lac du Bourget en est un des premiers exemples, suivies d'épisodes de marées vertes sur les côtes bretonnes, conséquence du développement excessif de macro-algues. Dans un cas comme dans l'autre, le phénomène est identifié et nommé : il s'agit de l'eutrophisation des masses d'eau continentales et marines.

L'eutrophisation peut être un processus naturel de l'évolution de la masse trophique (la matière organique) d'un plan d'eau continental ou littoral qui se manifeste par le développement de producteurs primaires au détriment d'autres formes de vie tels que le phytoplancton, la faune benthique et piscicole. Ce phénomène est considérablement accéléré par l'excès de nutriments lié à l'activité humaine et la modification des conditions physico-chimiques du milieu. Ainsi, l'eutrophisation est provoquée par une perturbation de l'équilibre entre les concentrations de nutriments dont les facteurs limitants sont les concentrations en azote et en phosphore.

Outre les menaces pour le développement de la biodiversité, l'eutrophisation impacte aussi la société par ses effets sur le tourisme suite à la fermeture de plages, sur l'industrie via l'activité conchylicole et piscicole ou la production hydro-électrique, et sur la santé publique pour la toxicité des sources d'eau destinée à la production d'eau potable. La mutation agricole a été questionnée du fait de ses conséquences sur l'environnement et est devenu un enjeu politique majeur à partir des années 1970.

Réaction politique

C'est dans ce contexte qu'ont été financés les premiers projets de recherche visant à la compréhension des processus responsables de la détérioration de la qualité de l'eau, notamment sur les transferts d'azote et de phosphore dans les milieux terrestres et aquatiques. Ces missions ont été confiées à des organismes de recherche en lien avec l'hydrologie et l'agronomie tels que le CEMAGREF[1] et l'INRA[2].

Dispositifs de suivis

Les travaux de recherches menés par ces organismes portaient sur les transferts de pollution d'origine agricole vers les cours d'eau. Ces études se sont appuyées sur des sites-laboratoires instrumentés pour mesurer et étudier l'évolution des bilans et de la qualité des eaux dans le temps : les bassins versant de recherche expérimentale (BVRE) ont été créés au début des années 1970. La vocation d'un BVRE était de collecter l'information la plus complète possible (topographie, géologie, pédologie, occupation du sol, climat, hydrologie) pour comprendre et conceptualiser le fonctionnement hydrologique, géochimique et biologique d'un écosystème.

En Bretagne, territoire particulière concerné par les systèmes d'élevage intensif et des systèmes de culture étroitement liés à l'alimentation du bétail, les premières observations destinées à la compréhension et la quantification des flux de pesticides, d'azote et de phosphore émis par les cultures et les élevages ont été réalisées dès 1971 sur le BVRE du Coët-Dan. L'expertise du CEMAGREF, puis de l'INRA ont permis de dresser les premiers bilans des transferts de nutriments et de mettre en évidence le lien entre l'utilisation d'azote et de phosphore en excès et l'augmentation de leurs concentrations dans le cours d'eau à l'exutoire du bassin versant. Le phénomène d'eutrophisation littoral, bien que localisé, prend en réalité sa source à plus large échelle, celle des bassins versant situés très en amont des zones impactées.

Plans de gestion

Forts de ce constat, les pouvoirs politiques ont élaboré un programme national de maitrise de la pollution d'origine agricole (PMPOA) visant la reconquête de la qualité de l'eau en zone vulnérable. Ces programmes accompagnaient financièrement et techniquement les acteurs des systèmes agricoles vers une optimisation de l'agriculture, plus respectueuse de l'environnement. Le premier volet de ce programme (PMPOA 1), appliqué de 1994 à 2000, était axé vers la réglementation de la qualité des effluents d'élevage et de l'épandage dans de grosses exploitations animales. Le second volet (PMPOA 2), appliqué de 2001 à 2007, a élargi le champ d'application du PMPOA 1, ajouté l'exigence de mise en conformité des bâtiments d'élevage, et incité les agriculteurs à une gestion plus raisonnée de la fertilisation. Les répercussions de ces actions sur qualité de l'eau étaient attendues dans les années suivantes, mais elles ont été plus lentes en raison de l'inertie des systèmes hydrologiques.

[1] **CE**ntre national du **M**achinisme **A**gricole, du **G**énie **R**ural, des **E**aux et **F**orêts, rebaptisé IRSTEA (**I**nstitut national de **R**echerche en **S**ciences et **T**echnologies pour l'**E**nvironnement et l'**A**griculture) en 2012 puis fusionné en 2020 dans INRAE

[2] **I**nstitut **N**ational de la **R**echerche **A**gronomique, fusionné en 2020 dans INRAE (Institut National de Recherche pour l'Agriculture, l'Alimentation et l'Environnement.

Les effets de la diminution de la pression de la fertilisation instaurée par ces programmes ont été visibles, en Bretagne, en 2004. En effet, le réseau de surveillance de la qualité de l'eau indiquait alors une amorce de diminution des concentrations en nitrates dans les cours d'eau dans les bassins à forte densités d'élevage, et une stabilisation des concentrations dans la plupart des autres bassins autour de la Loire. Cependant, le retour au bon état des masses d'eau, c'est-à-dire des concentrations suffisamment basses, a été plus ou moins retardé selon les caractéristiques hydrologiques (temps de résidence) et climatiques des bassins versants.

En effet, le climat influence directement les fonctionnements hydrologiques (pluviométrie, transferts d'eau), biologique (transformations biogéochimiques des nutriments, production primaire) et physico-chimiques (température, oxygénation, pH) du bassin versant. La distinction entre les effets du climat et ceux liés aux changements de pratiques agricoles sur les exports de nutriments représente un des enjeux de la recherche actuelle dans l'optique de protéger et de restaurer la qualité de l'eau.

1.2. Contexte scientifique

Le carbone, l'azote et le phosphore sont des éléments fondamentaux pour l'activité biologique telles que la production, la respiration et la décomposition de la matière organique par les micro-organismes (*Finzi et al.*, 2011). Les cycles de ces trois éléments sont couplés entre eux par un effet de facteur limitant, notamment par des ratios stœchiométriques de C:N:P nécessaires à l'équilibre de l'activité biologique (*Finzi et al.*, 2011). Les cycles du carbone, de l'azote et du phosphore ont été perturbés, du fait des intrants, par les pratiques agricoles du 20^{e} siècle, provoquant des concentrations en excès en nitrate (NO_3) et en phosphate (SRP) dans eaux continentales et côtières. Une des approches pour étudier ces processus de transfert de pollution d'origine agricole est l'analyse des évolutions spatiales ou temporelles des concentrations de ces éléments au sein d'un ou plusieurs bassins versants. L'objectif de telles études est d'identifier les processus de production, transformation et mobilisation de ces éléments au sein du paysage.

Facteurs de variabilité spatiale de la qualité de l'eau

L'influence de l'activité humaine sur les écosystèmes, et notamment celle de l'occupation du sol et de l'agriculture sur la qualité de l'eau, a été mise en évidence par plusieurs auteurs (*Bartley et al.*, 2012; *Howarth et al.*, 1996; *Jordan et al.*, 1997). Les principales sources d'azote dans les eaux de surface sont d'origine agricole à l'échelle mondiale (*Howarth*, 2008; *Potter et al.*, 2010), régionale (*Jordan et al.*, 1997; *Lapointe et al.*, 2004) et locale (*Cann*, 1998; *Schilling and Spooner*, 2006). Plusieurs travaux ont montré que le niveau d'apports azotés (Figure 1) et la proportion de terres cultivés sur un territoire ont pour effet d'augmenter les flux d'azote exportés par les cours d'eau (*Howarth et al.*, 1996; *Jordan et al.*, 1997) (*Dupas et al.*, 2015b; *Ebeling et al.*, 2020).

Cette relation est valable pour les grands bassins versants, mais il existe une forte hétérogénéité des réponses des transferts de C, N et P entre des bassins versants de petite taille (*Ecrepont*, 2019; *Guillemot et al.*, 2020; *Lintern et al.*, 2018). A l'échelle des bassins versant de superficie inférieure à 5 km² (*Temnerud et al.*, 2007), les dynamiques d'export de C, N et P sont davantage contrôlées par les caractéristiques hydromorphologiques du bassin versant tels que l'épaisseur des sols, les temps de résidence dans les sols et la nappe et l'aménagement du paysage (*Dick et al.*, 2015; *Thomas et al.*, 2016; *Thompson et al.*, 2011; *Viaud et al.*, 2004).

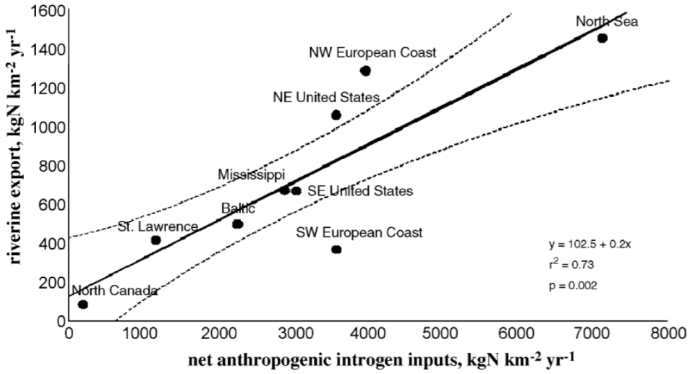

Figure 1 Exports annuels d'azote dans le cours d'eau en fonction du surplus d'azote sur les parcelles agricoles. Source : Howarth et al. (1996)

Les principales sources de carbone dissous sont localisées dans les zones de bas de versant (*Birkel et al.*, 2014; *Casson et al.*, 2019; *Dick et al.*, 2015), et plus spécifiquement dans les 30 premiers cm de sol des zones humides ripariennes sur le bassin de Kervidy-Naizin (*Humbert*, 2015; *Morel*, 2009). Cette source de carbone est répartie dans deux compartiments producteurs : le premier qui s'épuise pendant l'automne; le second, mobilisé en hiver et au printemps, et dont le stock parait très largement supérieur aux exports dans le cours d'eau (*Morel et al.*, 2009). Les travaux de modélisation de *Morel* (2009) ont également évoqué la production de carbone autochtone dans le cours d'eau lorsque le débit est faible en été.

La matière organique est donc produite et accumulée dans le bas de versant (Figure 2) (*Bende-Michl et al.*, 2013; *Wen et al.*, 2020). La reconnexion hydrologique de cette source avec le cours d'eau est assurée en automne par la montée des niveaux de nappe qui permet le transport latéral du carbone dissous vers le cours d'eau (*Humbert*, 2015). Les travaux de *Morel* (2009) et *Humbert et al.* (2019) n'ont pas permis d'identifier d'effet de l'activité agricole (en comparaison avec des bassins alpins et forestiers) sur les transferts de carbone vers le cours d'eau.

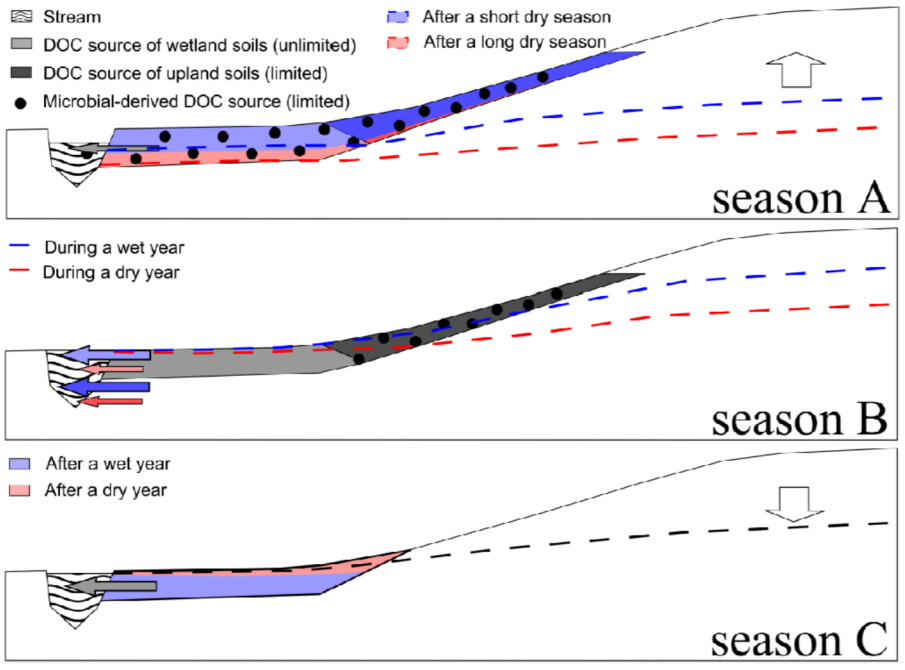

Figure 2 Schéma conceptuel des mécanismes de transfert du DOC depuis le bas de versant vers le cours d'eau. Les saisons A, B et C correspondent à la période de remontée de la nappe de base versant, montée de la nappe en haut de versant et diminution du niveau de nappe de haut de versant jusqu'à l'assec du cours d'eau, respectivement. Source : Humbert (2015)

L'origine agricole du NO_3 présent dans les eaux souterraines et de surface (*He et al.*, 2019) a été suspectée par *Cann* (1998), puis démontrée par *Molénat et al.* (2002) et *Ruiz et al.* (2002b). Lors des périodes de recharge de la nappe, le surplus de NO_3 du sol est infiltré vers les eaux souterraines (nappe superficielle). Les fortes concentrations en NO_3 dans le réservoir souterrain et, à l'inverse, les faibles concentrations en bas de versant (en raison de la dénitrification hétérotrophe qui s'y opère), ont été mises en évidence par comparaison des signatures moyennes des différents compartiments du bassin versant (*Aubert*, 2013; *Molénat et al.*, 2008). *Molénat et al.* (2002) conclut que le réservoir souterrain a un effet tampon sur les concentrations en NO_3, ce qui implique que les effets de changements de pratiques agricoles ne peuvent être suivies d'une diminution rapide des concentrations dans le cours d'eau (*Basu et al.*, 2012; *Basu et al.*, 2010; *Howden et al.*, 2011; *Hrachowitz et al.*, 2015; *Wang et al.*, 2013).

La concentration en NO_3 dans le cours d'eau est le résultat d'un mélange d'eaux en provenance de plusieurs compartiments plus ou moins riches en NO_3 spatialement distribués dans le bassin versant (*Bende-Michl et al.*, 2013; *Molénat et al.*, 2008; *Molénat et al.*, 2002; *Shrestha et al.*, 2013). La contribution des compartiments riches en NO_3 dépend des gradients de nappes qui contrôlent la connexion hydrologique entre le haut de versant et le cours d'eau (Figure 3).

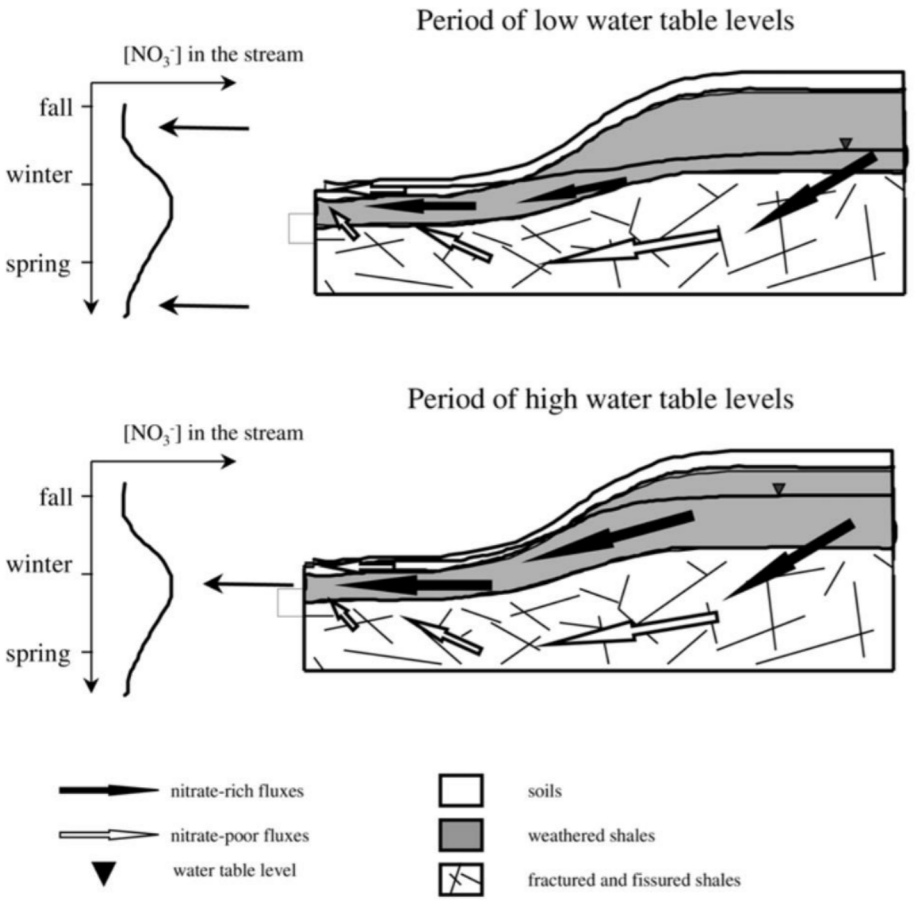

Figure 3 Schéma conceptuel du transport du NO_3 dans le bassin versant de Kervidy-Naizin. Source : Molénat et al. (2002)

Des bilans de flux de phosphore à l'échelle du bassin versant ont été réalisés par *Cann* (1998) et *Haygarth et al.* (2014). Il a été démontré depuis que le phosphore reste dans les horizons superficiels du sol, et qu'il est mobilisé par les écoulements latéraux depuis les parcelles du versant vers les zones ripariennes moins pentues (*Bende-Michl et al.*, 2013; *Bowes et al.*, 2005; *Dupas*, 2015; *Ford et al.*, 2018).

Les principales sources de phosphore dissous sont les zones ripariennes (*Gu et al.*, 2017), où le phosphore est accumulé pendant les périodes de sécheresse estivale (*Dupas*, 2015). Le phosphore solubilisé est exporté vers le cours d'eau lorsque la connexion hydrologique est assurée par la nappe en automne (Figure 4) (*Bende-Michl et al.*, 2013; *Dupas*, 2015; *Jordan et al.*, 1997).

La nappe, sous l'effet de la topographie et du climat, contrôle également les conditions physico-chimiques (redox, pH) des zones de bas de versant, donc les mécanismes biogéochimiques de dissolution du phosphore (*Casson et al.*, 2019; *Gu et al.*, 2017). La stagnation et la saturation prolongée des sols de bas de versant, en hiver, sont les moteurs de la réduction d'hydroxydes de fer accompagnée par la mobilisation de phosphore (*Gu et al.*, 2017).

Le phosphore dissous trouve également sa source dans les processus internes au cours d'eau, en raison de l'augmentation de la température et du temps de résidence pendant les périodes de basses eaux, en été (*Dupas*, 2015).

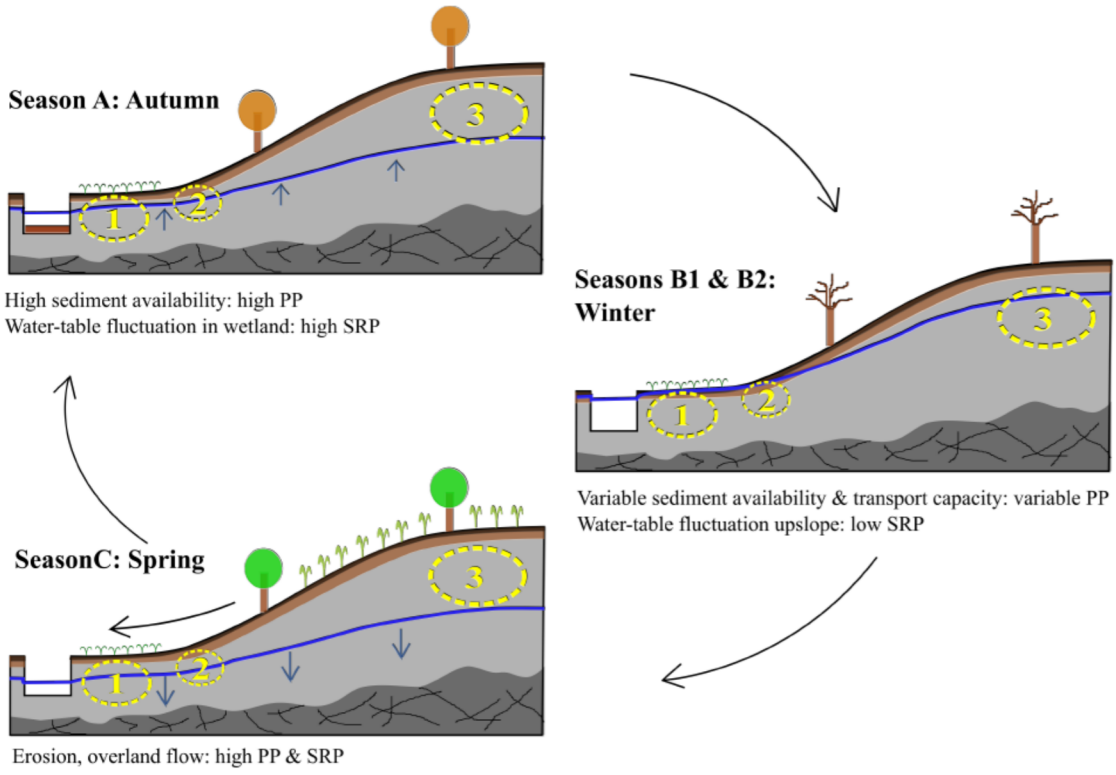

Figure 4 Schéma conceptuel du transport de phosphore dissous et particulaire dans un versant agricole. Source : Dupas (2015)

Emergence des approches multi-élémentaires

Aussi, les dynamiques des concentrations en DOC, NO_3 et SRP dans les cours d'eau sont le reflet d'une diversité de processus hydrologiques et biogéochimiques (*Burns et al.*, 2019). La diversité de caractéristiques biogéochimiques représente une opportunité pour mieux contraindre et améliorer le réalisme des modèles de transfert en terme de chemin d'écoulement et de distribution des sources d'éléments dans le paysage (*Hrachowitz et al.*, 2013).

Bien que le couplage de ces éléments semble critique dans la compréhension du fonctionnement des bassins versants (*Finzi et al.*, 2011), à notre connaissance, peu d'études intègrent les concentrations en DOC, NO_3 et SRP dans leurs analyses. Pourtant, une analyse comparative de ces trois éléments permettrait de synthétiser et comparer les connaissances acquises et de répondre à plusieurs questions telles que :

- Quelles évolutions à long terme présentent les concentrations en DOC, NO_3 et SRP dans le cours d'eau?
- Les sources et processus de transfert de solutés ont-ils des conséquences sur les dynamiques annuelles des concentrations ? sont-elles synchronisées?
- Comment et pourquoi ces dynamiques sont-elles liées ?

Effets du climat sur les dynamiques des solutés

Le cycle hydrologique est intrinsèquement lié avec celui du climat (*Michalak*, 2016). D'après *Salmon-Monviola et al.* (2013), le débit annuel, la recharge de la nappe et l'extension des zones humides diminuent dans un contexte d'augmentation de la température et d'une diminution des précipitations, et par extension les flux d'azotes diminuent également. D'autres facteurs, tels que les vitesses d'écoulement, les temps de résidence et la température de l'eau sont susceptibles d'influencer le transfert des solutés (*Howarth*, 2008; *Tavakoly et al.*, 2019).

Howarth (2008) a observé que le pourcentage de NO_3 d'origine anthropique exporté par le cours d'eau est plus élevé dans les régions humides que dans les régions sèches et dans une moindre mesure dans les régions froides que dans les régions chaudes. La modification des régimes de pluies et de températures influence également les niveaux de nappes, l'humidité des sols et les périodes d'assec susceptibles d'impacter les transferts de NO_3 (*Gascuel-Odoux et al.*, 2010), la production de matière organique en bas de versant (*Birkel et al.*, 2014; *Humbert*, 2015) et la solubilisation du SRP (*Forber et al.*, 2017).

Bien que complexes en raison des nombreux processus biogéochimiques en jeu, distinguer les effets du climat sur les transferts de solutés vers les eaux de surface représente un des enjeux actuels majeurs pour anticiper la réponse d'un écosystème dans un contexte de changement global (*Cross et al.*, 2015; *Fu et al.*, 2019; *Mellander et al.*, 2018; *Thompson et al.*, 2011). Les études des effets du climat sur plusieurs éléments, comme le DOC, NO_3 et SRP sont rares à ce jour, et la question de l'évolution de la qualité de l'eau en lien avec les variations climatiques reste ouverte.

Cette thèse s'appuie sur l'analyse de données et la modélisation pour étudier les dynamiques des concentrations en DOC, NO_3 et SRP dans les cours d'eau amont à plusieurs échelles temporelles. Les objectifs sont notamment d'identifier les (a)synchronies des concentrations en DOC, NO_3 et SRP, ainsi que leur sensibilité aux effets du climat et de l'hydrologie, et de caractériser la variabilité des zones sources et les processus moteurs des dynamiques des transferts de ces éléments. L'hypothèse avancée présuppose que les solutés répondent différemment aux forçages hydro-climatiques selon leur voie de transfert et leur réactivité biogéochimique.

Ces relations ont été étudiées à partir d'un jeu de données hydro-climatiques et chimiques acquis à haute fréquence (1 par jour) sur un bassin versant agricole de recherche. Le site d'étude et les données acquises sont présentés plus en détail dans le deuxième chapitre de ce manuscrit.

Le troisième chapitre a pour objectif d'identifier les co-évolutions temporelles des variables climatiques, hydrologiques et chimiques à plusieurs échelles temporelles. L'analyse des données s'appuie sur des outils statistiques et d'analyses fréquentielles adaptées aux différentes temporalités des chroniques : les tests de Mann Kendall et Theil Sen pour le long terme, la transformée de Fourier pour la saisonnalité et l'analyse fréquentielle pour les relations journalières. Ces travaux ont permis de relier les sources et mécanismes des transferts des solutés avec les principaux facteurs anthropiques, climatiques et hydrologiques.

Le quatrième chapitre présente le développement d'un modèle conceptuel, représentant les différents compartiments du bassin versant pour reproduire les dynamiques annuelles et évènementielles du débit et des concentrations en DOC et NO_3 à l'exutoire du bassin versant. L'objectif est de tester les hypothèses de transfert précédemment identifiées et de profiter de la richesse des chroniques chimiques pour proposer une conception plus réaliste du fonctionnement hydrologique du bassin versant en ajoutant des contraintes relatives aux observations de concentrations en éléments chimiques aux comportements opposés du DOC et du NO_3.

Le cinquième chapitre propose de croiser les travaux des deux chapitres précédents pour répondre à plusieurs questions : les simulations du modèle reproduisent-elles les signatures hydro-chimiques observées par l'analyse de données ? Ce modèle est-il apte à simuler des dynamiques de concentrations en tenant compte des variations climatiques ? Quelles sont les pistes d'améliorations envisageables pour représenter plus finement les processus de mobilisation des solutés ? Enfin, peut-on et comment utiliser ce modèle pour analyser les impacts prédits de projections climatiques ou contextuelles ?

2. Matériel et Méthodes

2.1. Observatoire de recherche en Environnement – Observatoire de la Zone Critique

L'étude in-situ des mécanismes hydrologiques et géochimiques contrôlant le transport des solutés vers l'exutoire d'un bassin versant requiert des données mesurées sur le terrain pendant une période assez longue pour capturer les évolutions à long terme (pluriannuelle, >10 ans) et la variabilité interannuelle des conditions hydro-climatiques, et avec une résolution temporelle suffisamment élevée pour capturer les variations à court terme, en particulier celles liées aux évènements hydrologiques Pluie-Débit. Produire ce type de jeu de données est la vocation d'un Observatoire de Recherche en Environnement (ORE) tel que l'ORE AgrHyS, dédié aux AgroHydroSystèmes, c'est-à-dire aux bassins versants agricoles, et situé en contexte de socle cristallin dans le massif armoricain.

L'ORE AgrHyS est l'un des nombreux observatoires français de la Zone Critique de l'Infrastructure de recherche nationale OZCAR (Figure 5, https://www.ozcar-ri.org). Chaque observatoire est spécialisé sur des questions de recherche en cohérence avec son contexte local. Progressivement, les infrastructures de recherche s'organisent au niveau européen, tel le réseau eLTER (European Long-Term Ecosystem Research infrastructure, https://www.lter-europe.net) qui regroupe pour la France OZCAR et RZA (le Réseau des Zones Ateliers, https://www.za-inee.org/) et des observatoires de près de 30 Pays Européens. Ces infrastructures de recherche ont pour but de fournir des services (plateformes d'observation in-situ et données) et de favoriser ainsi les échanges et collaborations scientifiques et techniques à l'échelle nationale et internationale.

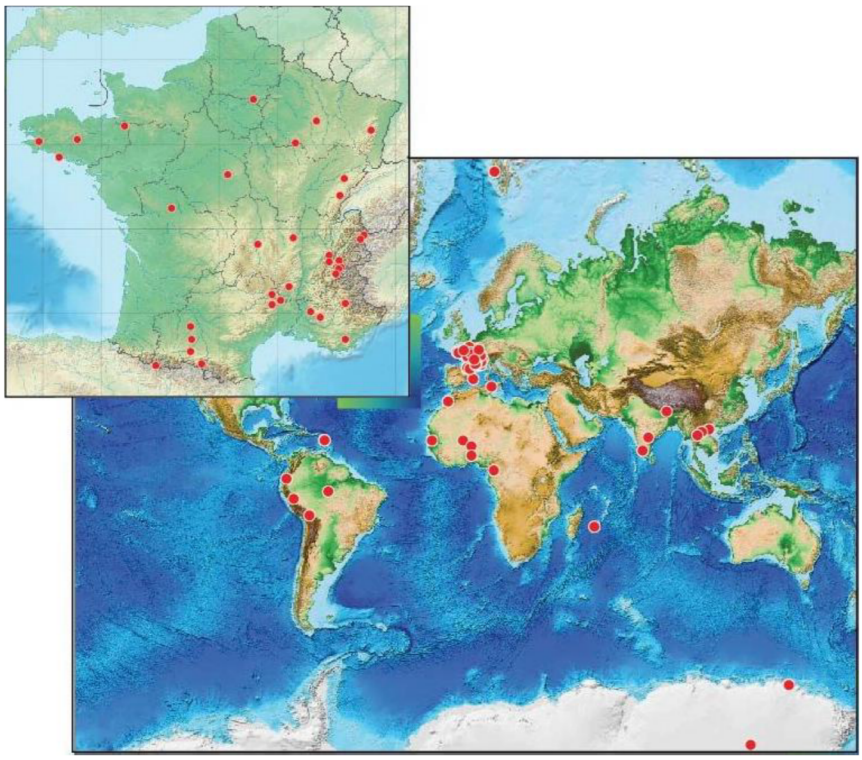

Figure 5 Répartition des observatoires du réseau OZCAR en France et dans le monde. Source : Gaillardet et al. (2018)

2.1.1. Observer les relations entre systèmes agricoles et qualité de l'eau

Les relations entre l'agriculture et la qualité de l'eau, en particulier concernant la concentration en nutriments dans l'eau, sont étudiées dans divers contextes pédoclimatiques à l'internationale, par plusieurs réseaux d'observatoires qui ont émergé pendant la décennie 2000-2010. Par exemple, le programme « Demonstration Test Catchment » au Royaume-Uni (http://www.demonstratingcatchmentmanagement.net/) vise à démontrer l'efficacité des changements de pratiques agricoles sur les pollutions diffuses agricoles. Un autre exemple, le réseau irlandais « Agricultural Catchment Programme » a été mis en place pour fournir une évaluation scientifique des « bonnes pratiques agricoles » implémentées suite à la Directive Nitrates, dans des bassins versants représentatifs de l'agriculture irlandaise. Les suivis mis en place dans ces observatoires portent principalement sur l'azote et le phosphore.

Parmi les observatoires français de l'infrastructure OZCAR qui étudient les interactions entre systèmes agricoles et qualité de l'eau, on peut aussi citer:

- L'observatoire OMERE (Observatoire Méditerranéen de l'Environnement Rural et de l'Eau, https://www.obs-omere.org/), qui étudie les hydro-systèmes méditerranéens (Languedoc et Tunisie) cultivés et naturels (viticulture et cultures céréalières) ;
- L'observatoire ORACLE (https://gisoracle.inrae.fr/) qui étudie des bassins sédimentaires en milieu rural (grandes cultures céréalières dans le bassin Parisien) ;
- Le bassin expérimental d'Auradé (https://www.ozcar-ri.org/fr/aurade/) représentatif des bassins versants des coteaux de Gascogne (blé, tournesol) ;
- L'Observatoire M-TROPICS (Multi-scale Tropical Catchments, https://mtropics-fr.obs-mip.fr/) inclut plusieurs bassins où sont étudiés les effets des pressions agricoles sur l'eau, les cycles biogéochimiques et l'érosion hydrique en Inde du Sud (polyculture irriguée) et en Asie du Sud-Est (conversion rapide en plantations et monocultures en zone vulnérable de Montagne)
- Le bassin versant du Tensift au Maroc (https://www.cesbio.cnrs.fr/la-recherche/activites/observatoires/maroc-observatoire-du-tensift/) est étudié pour suivre et comprendre le fonctionnement d'un hydro-système semi-aride soumis aux effets conjoints du changement climatique, du développement de l'agriculture irriguée et du développement urbain

Chacun de ces observatoires présentent des spécificités pédoclimatique, géologique et agricole, qui justifient l'intérêt de leur mise en réseau. On peut noter que parmi tous ces observatoires, les suivis combinant les trois éléments azote, phosphore et carbone sont, à notre connaissance, plutôt rares et généralement restreints à soit N et C, soit N et éventuellement P.

2.1.2. L'ORE AgrHyS

L'Observatoire AgrHyS a été créé formellement au début des années 2000 en réunissant plusieurs sites déjà suivis par des équipes d'INRAE depuis les années 1990. L'observatoire est alors défini comme un observatoire agro-hydrologique (*Richard et al.*, 2018) focalisé sur les interactions entre agriculture, hydrologie et la qualité des eaux.

Dans un contexte international et national, les spécificités de l'ORE AgrHyS sont (i) du point de vue hydrologique, des bassins versants dits « de socle » où les cours d'eau sont alimentés par une nappe superficielle, (ii) du point de vue agricole, une activité de production associant polyculture et élevage qui s'est intensifiée dans les années 1970, avec de forts intrants de nutriments sous formes

minérales et organiques, de l'élevage hors sol, et (iii) du point de vue climatique, un climat océanique tempéré.

Les missions de l'ORE AgrHyS sont :

1) d'accueillir des travaux de recherche pour leur phase d'acquisition de données. Ces travaux s'inscrivent généralement dans un enjeu scientifique de compréhension des processus en lien avec les cycles du carbone, de l'azote et du phosphore;
2) de produire et diffuser des séries de données (hydrologiques, climatiques, chimiques, atmosphériques et agricoles) dans le but d'alimenter les travaux de recherches, comme cela a été le cas dans le cadre de cette thèse;
3) de permettre de tester des outils méthodologiques et instrumentaux;
4) de contribuer à la formation d'étudiants en hydrologie ou en agronomie;
5) de servir de support de communication avec les acteurs (agriculteurs, acteurs agricoles, gestionnaires de l'eau et de l'environnement).

Les travaux de recherche menés par l'ORE AgrHyS sont pluridisciplinaires et l'existence de l'observatoire a favorisé les collaborations entre hydrologues, agronomes, pédologues et écologues. Ces travaux portent sur les liens entre agriculture et qualité de l'eau, les éléments structurant du paysage (haies, zones humides) et les relations entre la nappe et la rivière (nappe, ripisylves, zone hyporhéique) sur deux sites complémentaires localisés en Bretagne (Figure 6):

- Le site de Kerbernez
- Le site de Kervidy-Naizin, le site d'étude de cette thèse

Figure 6 Localisation des sites d'études de l'ORE AgrHyS en Bretagne, France. (Source: GéoSAS)

2.1.3. Le bassin versant de « Naizin »

Le bassin versant « Naizin », drainant le cours d'eau Coët-Dan, est localisé à proximité de la commune de Naizin-Evellys dans le Morbihan, en centre Bretagne (Figure 6). Ce site a été choisi en raison du « dynamisme supérieur à la moyenne qu'ont manifesté les agriculteurs locaux pour se développer » (*Cheverry*, 1998) qui se traduit, entre autres, par un remembrement du paysage entre 1971 et 1976 (triplement de la surface moyenne des parcelles, diminution de la longueur des haies et talus). *Gascuel-Odoux et al.* (2018) ont proposé un historique de l'observatoire de Kervidy-Naizin. L'évolution chronologique des thèmes de recherche y est mise en relation avec l'évolution des techniques et des protocoles d'observation mis en œuvre sur le site, ainsi que l'évolution des modes de gouvernance de ce type d'infrastructure de recherche. Les grandes lignes de la succession des questions scientifiques abordées sur l'observatoire sont reprises ici afin de positionner la thèse dans l'historique des recherches menées sur l'observatoire.

L'instrumentation du bassin versant a été initiée par le CEMAGREF[3] en 1971, avec l'ambition de d'étudier l'impact du remembrement et de l'intensification agricole sur le bilan hydrologique, la qualité de l'eau et l'érosion des sols. Ces instruments mesuraient la pluviométrie et le débit à l'exutoire d'un bassin versant de 12 km^2 appelé Stimoes (Figure 7), complétés à partir de 1975 par un suivi de la composition chimique de l'eau (prélèvements analysés pour MES, SRP, NO_3, NH_4 et pesticides) ainsi que des enquêtes auprès des exploitants agricoles pour estimer les bilans d'azote et de phosphore (*Gascuel-Odoux et al.*, 2018).

Suite à l'aménagement d'un plan d'eau récréatif au sein du bassin versant de Naizin-Stimoès en 1991, l'exutoire du bassin versant instrumenté a été déplacé en amont, au niveau du lieu-dit de Kervidy dont le sous bassin draine une superficie de 5 km^2 (Figure 7), appelé Kervidy-Naizin. L'INRA a repris le suivi en 1993 dans le but d'étudier la genèse du ruissellement, la dynamique des zones contributives et la spatialisation des propriétés des sols hydromorphes (*Chaplot and Walter*, 2003; *Chaplot et al.*, 2003; *Crave and Gascuel-Odoux*, 1997; *Jaffrézic and Mérot*, 1998; *Mérot et al.*, 1994). Un seuil de mesure de débit est installé à l'exutoire du bassin versant (*Carluer*, 1998) ainsi qu'une station météo environ 1 km à l'est de l'exutoire (Figure 8).

Au cours des années 1996-1998 le bassin versant a été équipé d'une dizaine de piézomètres situés sur deux versants (Figure 8) pour étudier plus précisément la contribution de la nappe dans les transferts d'eau et de nitrate vers la rivière (*Molénat and Gascuel-Odoux*, 2002; *Molénat et al.*, 2005; *Molénat et al.*, 2008). De même, l'étude du fonctionnement biogéochimique des zones humides vis-à-vis des cycles de l'Azote, du Carbone, du Fer, et des éléments traces a fait intervenir des travaux de biogéochimie et d'hydrologie, avec une complémentarité d'approches in-situ (*Morel et al.*, 2009; *Oehler*, 2006) et expérimentales (*Davranche et al.*, 2011; *Davranche et al.*, 2013; *Grybos et al.*, 2009; *Pourret et al.*, 2007).

[3] **CE**ntre national du **M**achinisme **A**gricole, du **G**énie **R**ural, des **E**aux et **F**orêts, rebaptisé IRSTEA (**I**nstitut national de **R**echerche en **S**ciences et **T**echnologies pour l'**E**nvironnement et l'**A**griculture) en 2012 puis fusionné en 2020 dans INRAE

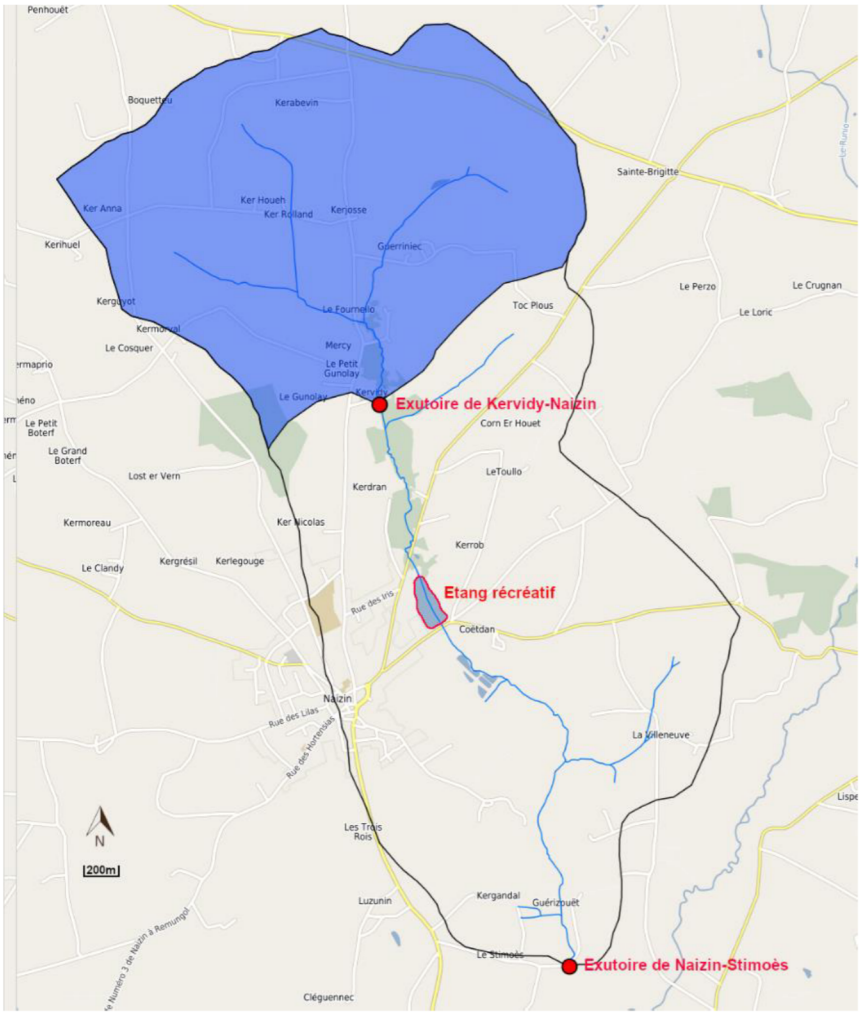

Figure 7 Carte des bassins versant de Naizin-Stimoès et Kervidy-Naizin, Morbihan, Bretagne, France. Source: GéoSAS

Dès le début des années 2000, les données de l'observatoire servent aussi de support au développement de la modélisation intégrée : de modèles agrohydrologique (*Beaujouan et al.*, 2002; *Durand*, 2004) et de modèles prenant en compte le paysage, en particulier le réseau bocager (*Benhamou et al.*, 2013; *Viaud et al.*, 2005), permettant de développer des travaux d'évaluation de scénarios de pratiques agricoles ou agro-paysagers (*Casal et al.*, 2018). Une approche multi-compartiments des transferts se généralise, d'abord sur le lien sol-eau en mesurant les transferts particulaires (*Lefrançois*, 2007; *Vongvixay et al.*, 2018), puis sur les échanges avec l'atmosphère pour aborder la cascade de l'azote (*Drouet et al.*, 2012; *Flechard et al.*, 2011).

La diversification des espèces chimiques mesurées à la fin des années 1990 a permis une première analyse multi-élémentaire sur les anions majeurs et le carbone dissous et de la variabilité temporelle de la qualité de l'eau sur le bassin versant (*Aubert*, 2013; *Aubert et al.*, 2013a; *Aubert et al.*, 2013c) à partir des 10 années de séries journalières dans le cours d'eau. Les mesures sur le cycle du carbone sont alors complétées en couplant des mesures de stocks, de flux (*Buysse et al.*, 2016; *Jeanneau et al.*, 2020) et des techniques de traçages variées (*Denis et al.*, 2017; *Humbert et al.*, 2019; *Lambert et al.*, 2014). Les mesures sur le phosphore dans les sols et les eaux viennent compléter le jeu de données de l'observatoire (*Dupas et al.*, 2015a; *Dupas et al.*, 2015c; *Dupas et al.*, 2015d; *Gu et al.*, 2018; *Gu et al.*, 2019; *Gu et al.*, 2017).

Le présent travail se situe dans le prolongement de ces travaux i) en proposant une première synthèse multi-élémentaires sur les transferts de C, N et P dissous, en mettant en relation les précédents résultats obtenus sur chaque éléments séparemment, ii) en explorant les effets du climat sur ces transferts grâce à une serie temporelle qui dépasse désormais la décennie, et iii) en allant jusqu'à proposer une conceptualisation des transferts de ces éléments dans un même modèle, ce qui avait été amorcé dans les précédents travaux avec des formalismes différents selon les éléments.

Les nouvelles questions de recherche abordées ces dernières années sur l'observatoire concernent d'une part les fonctions et services des sols en caractérisant les abondances et diversités biologiques des sols (*Le Guillou et al.*, 2019; *Viaud et al.*, 2018), et d'autre part l'extrapolation et la transposition des processus identifiés sur l'observatoire à d'autres bassins et d'autres échelles dans un contexte similaire (régional notamment). Des premiers travaux sur la transposition d'hydrogramme ont pu s'appuyer sur l'observatoire pour évaluer des méthodes de modélisation en bassins non jaugés (*de Lavenne et al.*, 2015). En parallèle de cette thèse, des travaux sur la variabilité spatiale des concentrations en C, N et P dissous dans les cours d'eau ont été menés sur d'autres sites ou en mobilisant des bases de données régionales, et ont été mis en relation avec les résultats du présent travail donnant lieu à un article collectif actuellement en discussion publique (*Guillemot et al.*, 2020).

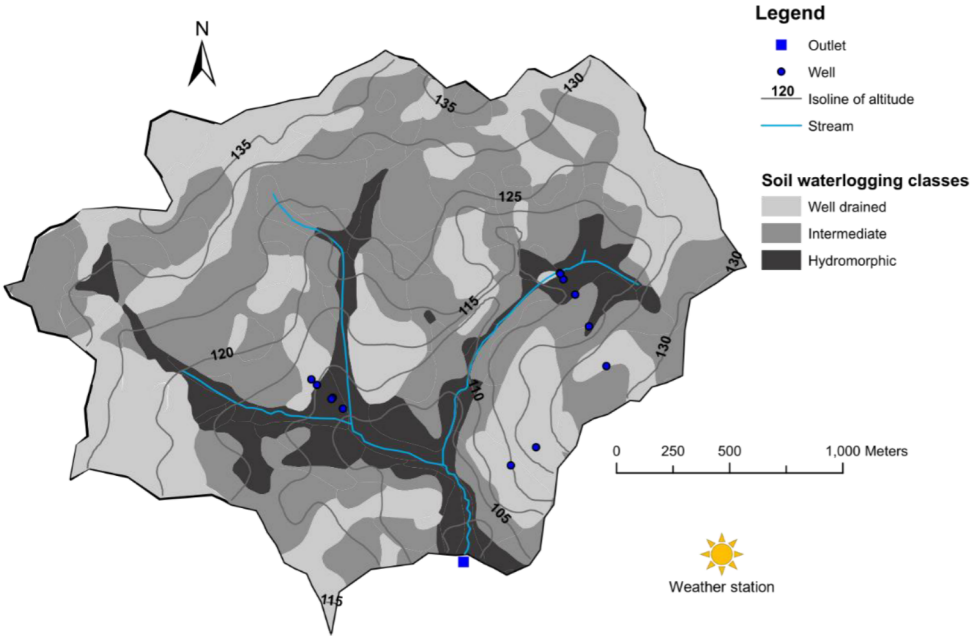

Figure 8 Carte du réseau hydrographique et de l'hydromorphie des sols sur le bassin versant de Kervidy-Naizin, Morbihan, France. Source : Salmon-Monviola (2017)

2.1.3.1. *Caractéristiques du bassin versant de Kervidy-Naizin*

Ce site d'étude est un bassin versant de tête d'une superficie de 5 km². Le paysage est dominé par l'agriculture, avec des productions végétales (céréales, maïs, prairies, légumes) représentent 91% de l'occupation du sol (Figure 9) et animales (bovins, porcs, volailles) avec une densité de bétail de 5 unités.ha^{-1}, principalement conduites en hors sol.

Ce bassin versant repose sur un socle semi-imperméable composé d'un schiste Briovérien surmonté par un schiste localement fracturé puis une couche de schiste altéré dont la profondeur varie entre 1 m en bas de versant et 30 m en haut de versant (*Molénat et al.*, 2005). La profondeur des sols varie entre 35 et 150 cm, ils sont composés de Luvisols bien drainés en haut de versant et de Cambisols hydromorphes (Figure 9 classification FAO, *WRB* (2006)) en bas de versant (Figure 8). La teneur en matière organique des sols est élevée (2,5 à 6,5%) dans les 40 premiers cm de sol (*Walter and Curmi*, 1998).

L'exutoire se situe à une altitude de 98 m et le point le plus haut est à 140 m au-dessus du niveau de la mer. La topographie du bassin versant est relativement modérée avec des pentes maximums de l'ordre de 5%. Le climat est océanique tempéré avec des températures journalières qui fluctuent entre -2 et 32,6 C pour une moyenne de 11,2 C, des précipitations s'élevant à 810 mm.an^{-1} en moyenne (± 180 mm) et une évapotranspiration potentielle estimée à 699 mm.an^{-1} (± 58 mm).

Le Coët Dan prend sa source, au plus loin, à 2 km en amont de l'exutoire. A Kervidy, il s'agit d'un ruisseau d'ordre de Strahler 2 dont l'écoulement est intermittent, souvent en assec strict durant plusieurs semaines pendant les périodes sèches de l'été. Il est alimenté par une nappe superficielle dont l'amplitude de battements dans l'altérite de schiste atteint 8 m en haut de versant et 1 à 2 m en bas de versant (*Molénat and Gascuel-Odoux*, 2002).

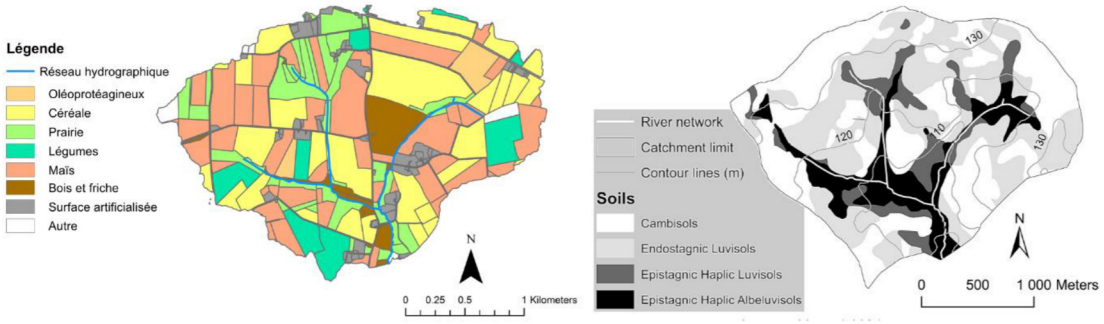

Figure 9 Carte de l'occupations des sols en 2013 (à gauche, Source: Dupas (2015)) et des sols (à droite, source : Fovet et al. (2018)) du bassin versant de Kervidy-Naizin.

2.1.3.2. *Instrumentation hydro-météorologique de Kervidy-Naizin*

Le bassin versant est équipé d'une station météo (Cimel), située 1 km à l'est de l'exutoire (Figure 8). Celle-ci mesure plusieurs variables météorologiques à une fréquence horaire : température de l'air et du sol, rayonnement net, vitesse et direction du vent, pluviométrie et hygrométrie. La station fait partie du réseau agroclimatique d'INRAE géré par l'Unité de service AgroClim, qui effectue un traitement et la diffusion de ces données via le portail CLIMATIK, dans lequel des variables calculées à partir de ces variables horaires sont aussi disponibles comme l'ETP Penmann (au pas de temps journalier).

La hauteur d'eau à l'exutoire est mesurée par un capteur à flotteur (Thalimède) toutes les minutes (Figure 10). Cette hauteur est par la suite convertie en débit à l'aide d'une courbe de tarage (*Carluer*, 1998). Les variations de niveaux de nappes sont mesurées toutes les 15 minutes par des transducteurs (Orpheus mini) placés dans des piézomètres dont les profondeurs varient entre 3 et 8 m selon leur position sur le versant.

Figure 10 Photographie de l'exutoire du bassin versant de Kervidy-Naizin.

2.1.3.3. Suivis de la qualité de l'eau de Kervidy-Naizin

Un prélèvement manuel est effectué par une personne de la commune chaque jour vers 17h pour évaluer la qualité de l'eau. L'eau est prélevée, filtrée à 0.22 ou 0.45 µm, puis stockée dans des flacons en propylène conservés dans un réfrigérateur avant d'être transportés aux laboratoires. Un préleveur automatique (ISCO) complète ces prélèvements journaliers. L'enclenchement de ce préleveur est asservi aux variations de la hauteur d'eau et permet de collecter des échantillons toutes les 10 à 30 minutes lors des crues. Les eaux de pluies et de nappe sont également prélevées mensuellement depuis 2013 et trimestriellement depuis 2000, respectivement tous les mois. La synthèse des variables mesurées, le pas de temps associé et la date de mise en place du suivi sont présentés dans le Tableau 1.

Les échantillons ainsi collectés sont analysés en laboratoire au maximum deux semaines après le prélèvement pour analyser la composition chimique de l'eau, notamment les concentrations en anions majeurs, en carbone organique et inorganique dissous, ainsi qu'en phosphore réactif et total. Les anions majeurs (Cl, NO_2, NO_3, SO_4) sont analysés par chromatographie ionique (DIONEX DX 100, *ISO 10304* (1995)) dans un échantillon d'eau filtré à 0,22 µm au laboratoire de Géosciences Rennes. Le carbone total dissous (DTC) et inorganique dissous (DIC) sont mesurés, après filtration à 0,22 µm, par un analyseur de carbone (Shimadzu TOC 5050A, *Petitjean et al.* (2004)) au laboratoire de Géosciences Rennes. La concentration en carbone organique dissous correspond à la différence entre DTC et DIC. Le phosphore total et dissous réactif sont mesurés par colorimétrie (réaction au molybdate d'ammonium), après filtration à 0.45 µm pour le SRP, et après digestion au peroxodisulfate de potassium pour le phosphore total (*ISO 15681*, 2005) au laboratoire de l'UMR SAS.

2.1.3.4. Disponibilité et accès aux données

Ces acquisitions hautes fréquences pendant bientôt 20 ans constituent un jeu de données riche d'information. Dans le cadre de la politique de partage et de diffusion, ce jeu de données est accessible via un outil de visualisation et de téléchargement sur le site internet de l'ORE : https://www6.inra.fr/ore_agrhys_eng/Data. La licence associée à l'utilisation de ces données est une licence de type Creative Common Attribution (CC BY 2.0 FR), le crédit devant être attribué à : *UMR SAS. 2010. Observatoire de Recherche en Environnement sur les Agro-Hydrosystèmes (ORE AgrHyS). INRA.* https://doi.org/10.15454/1.5499682911557678E12.

Tableau 1 Localisations, fréquences, et dates de début du suivi des variables atmosphériques, hydrologiques et physico-chimiques du bassin versant de Kervidy-Naizin. Adaptée d'après Fovet et al. (2018)

Stations	Atmospheric variables			Hydrological variables			Other physical variables			Chemical variables		
	Variable	Time step	First date	Variable	Time step	First date	Variable	Time step	First date	Variable	Time step	First date
Weather station	air and soil temperature global radiation and PAR wind speed and direction rain humidity	1 h	1993							bulk in rain water: NO_3, Cl, SO_4, NH_4, Ca, Mg, Na, total N	1 month	2013
Kervidy outlet				stream level	1 minute	1994	temperature	10 min	2010	NO_3	1 d + 15 min + 5 storms/yr	1993 (<daily), 1999 (daily), 2010 (15 min)
										DOC	1 d + 15 min + 5 storms/yr	1999 (daily), 2010 (15 min)
							EC		2013	SO_4, Cl	1 d + 5 storms/yr	1993 (<daily), 1999 (daily)
										DIC	1 d + 5 storms/yr	1999 (daily)
							turbidity		2004	SS	3 d + 5 storms/yr	2007
										total P, SRP	1 d + 30 min + 5 storms/yr	2007 (biweekly), 2013 (daily), 2016 (30 min)
Piezometers				water table level	15 min	1998	temperature	10 min	2007 or 2010	NO_3, SO_4, Cl, DOC, DIC	4/yr	2000

2.2. Cadre méthodologique d'acquisition de connaissances

L'acquisition de données environnementales pour la recherche s'inscrit dans une démarche d'apprentissage faisant intervenir des expérimentateurs sur le terrain, des modélisateurs, ainsi que les acteurs et usagers d'un site d'étude dans le but de faire progresser les connaissances sur le site instrumenté (*Dunn et al.*, 2008; *Hrachowitz et al.*, 2016). Cette démarche repose sur une série d'étapes successives depuis l'acquisition de données jusqu'à la production de scénario anticipatifs (Figure 11).

C'est via l'analyse de données d'observation que sont interprétées les interactions entre les différents compartiments du bassin versant (atmosphère, écosystème et ici agroécosystème, sol, sous-sol et rivière) (*Hrachowitz et al.*, 2016). Ces interprétations permettent à leurs tours de formuler les hypothèses sur les processus écologiques, hydrologiques et biogéochimiques nécessaires à la construction d'un modèle perceptuel, puis conceptuel du système étudié (Figure 11).

Une fois calibré et validé, un modèle peut être utilisé comme :

- un outil d'apprentissage pour identifier les principaux mécanismes d'intérêt pour répondre à une problématique (*Birkel et al.*, 2010);
- un outil de prédiction de la réponse attendue du système à des évolutions de nature anthropiques ou environnementales (*Dunn et al.*, 2008);
- un outil pour reconstituer les périodes de données manquantes d'un jeu de données;
- ou pour identifier des lacunes dans la compréhension du système et par conséquent adapter ou proposer de future campagnes de collecte de données (*Dunn et al.*, 2008).

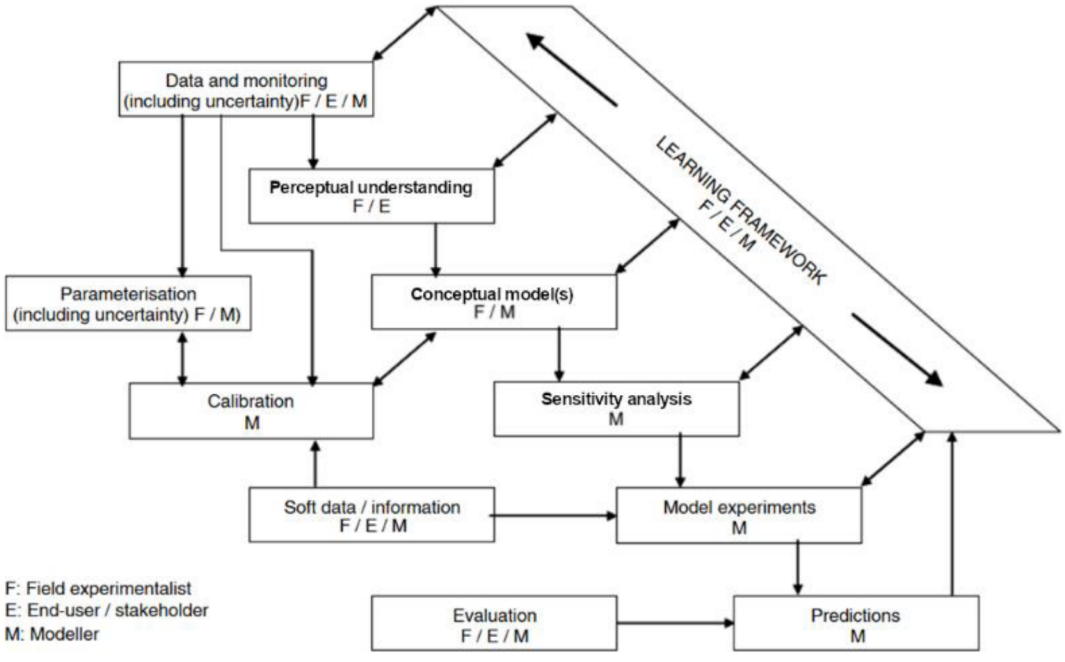

Figure 11 Learning framework proposé par Dunn et al. (2008)

2.3. Interprétation de séries temporelles hydrochimiques

Les jeux de données hydrochimiques, souvent acquis à l'exutoire des bassins versants, sont le fruit d'interactions complexes entres des processus spatio-temporels de différentes natures. Ces chroniques présentent généralement des variations à plusieurs échelles temporelles : long terme (ici > 10 ans), interannuelle, saisonnière et évènementielle (Figure 12) qui peuvent être analysées et interprétées à l'aide de méthodes spécifiques (Figure 13, *Lloyd et al.* (2014)) dans le but de produire un schéma perceptuel du fonctionnement du bassin versant.

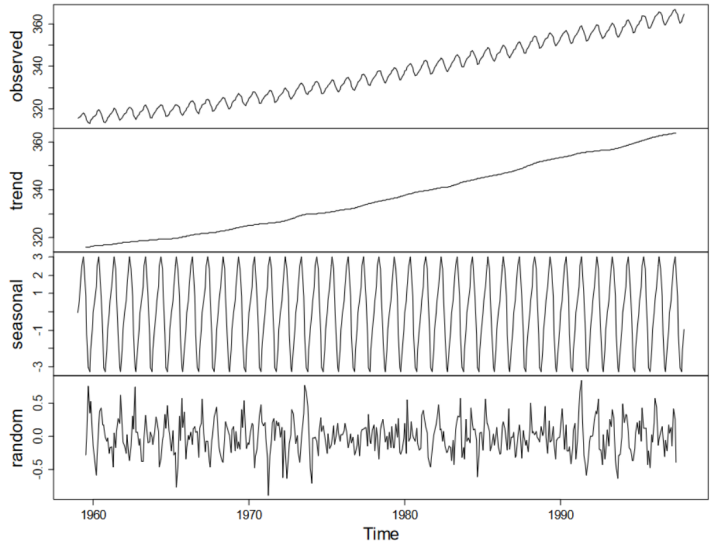

Figure 12 Décomposition d'un signal brut (observed) en composantes long terme (trend), saisonnière (seasonal) et en bruit (random). Source: Dettling (2013)

L'évolution des débits et concentrations sur le long terme permet d'identifier les effets de changements globaux liés à l'activité humaine, notamment agricole dans notre contexte d'étude, ou climatiques. Ces évolutions se manifestent par des tendances à long terme que l'on peut détecter à l'aide d'outils tels que les tests de Mann Kendall et de Theil Sen ou bien par régressions linéaires (*Lloyd et al.*, 2014). Les séries temporelles présentent parfois des changements de valeurs abrupts qui peuvent être détectés par des méthodes telles que le t-test ou l'ANOVA (*Lloyd et al.*, 2014).

Les variations interannuelles reflètent l'effet « mémoire » de la réponse hydro-chimique suite à une année particulièrement sèche ou humide, ou bien en réponse à la variabilité climatique dont les cycles peuvent atteindre quelques années en réponse à un forçage régional comme les oscillations Nord Atlantiques (*Gascuel et al.*, 2010; *Loecke et al.*, 2017; *Mellander et al.*, 2018; *Monteith et al.*, 2000). Ces variations sont subtiles à identifier, mais on peut cependant calculer des corrélations sur des indicateurs pour les détecter (*Ringard et al.*, 2019).

En contexte de climat tempéré, l'évolution saisonnière informe sur le fonctionnement hydrologique et biogéochimique des bassins versants. En effet, les signatures saisonnières reflètent la

structure, la distribution et la composition des compartiments qui contribuent à l'écoulement de la rivière (*Fovet et al.*, 2015; *Ruiz et al.*, 2002a; *Woodward et al.*, 2013). L'analyse des variations saisonnières est réalisée à l'aide de méthodes de traitement du signal telles que la décomposition en ondelettes, la transformée de Fourier ou encore des variogrammes (*Aubert et al.*, 2013c; *Lloyd et al.*, 2014).

Les dynamiques évènementielles nous renseignent sur les caractéristiques des compartiments rapidement mobilisés lors d'un évènement pluvieux, et sur les connexions hydrologiques entre les compartiments superficiels et la rivière (*Ebeling et al.*, 2020; *Zuecco et al.*, 2016). Ces analyses s'appuient sur des paramètres de relations concentrations-débit (*Ebeling et al.*, 2020; *Minaudo et al.*, 2019; *Zuecco et al.*, 2016), ou d'autres méthodes d'exploration de données tels que *Latent Dirichlet Allocation* (*Aubert et al.*, 2013b) ou *Dynamic Time Warping* (*Dupas et al.*, 2015d).

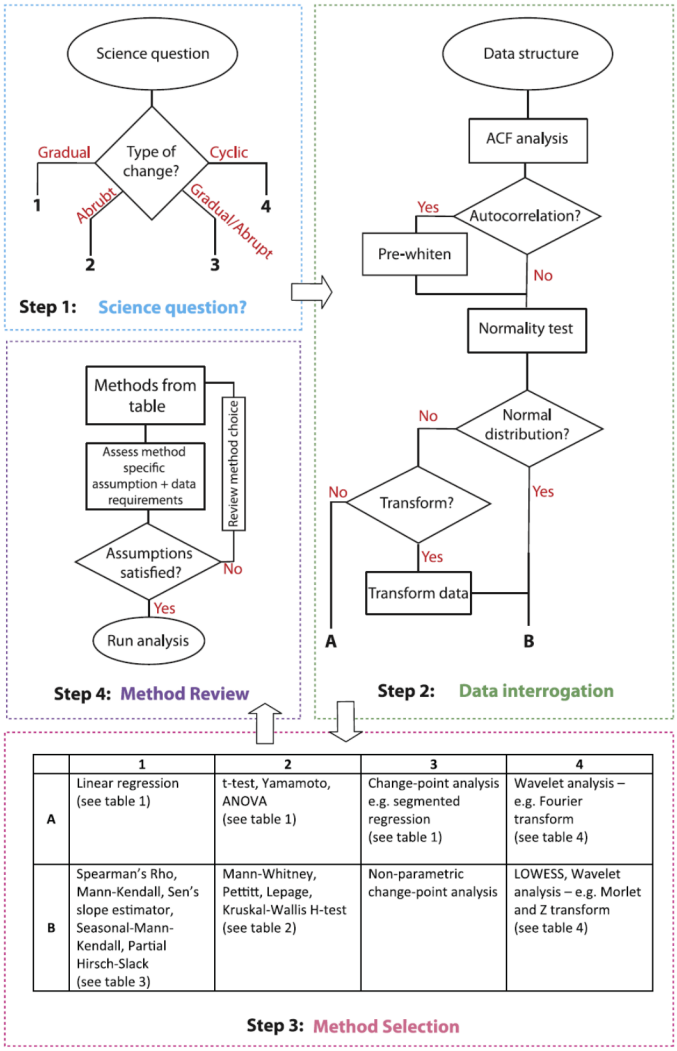

Figure 13 Diagramme d'aide au choix d'une méthode d'analyse selon la nature des données et la temporalité liée à la question scientifique. Source : (Lloyd et al., 2014)

2.4. Modélisation

La démarche de modélisation consiste à traduire le modèle perceptuel en modèle conceptuel à l'aide d'outils mathématiques et informatiques. Il existe plusieurs types de modèles (Figure 14), de la simple relation empirique entre deux variables jusqu'à la représentation dynamique et tridimensionnelle des processus physiques, chimiques et biologiques qui ont lieu au sein d'un bassin versant (*Dunn et al.*, 2008; *Hrachowitz and Clark*, 2017; *Pettersson et al.*, 2001). La modélisation fine des processus physiques dans l'espace requiert une représentation discrétisée du système, où les propriétés de chaque élément du maillage sont renseignées, on parle alors de modèle distribué (*Fu et al.*, 2019; *Hrachowitz et al.*, 2016). A l'inverse, un modèle global intègre l'hétérogénéité du système et permet d'exprimer les processus dominants à l'échelle du système étudié (*Fu et al.*, 2019; *Hrachowitz et al.*, 2016). Il existe un gradient intermédiaire, celui des modèles semi-distribués, pour lequel le système est subdivisé en sous-éléments regroupant les zones dont les propriétés sont communes (Figure 15). D'autres typologies ont été proposées, par exemple en fonction des utilisations visées par le modèle : cognition, prédiction, décision, etc. Le choix du type de modèle est orienté par les questions de recherche posées mais aussi par les informations disponibles sur le système étudié (*Hrachowitz and Clark*, 2017; *Hrachowitz et al.*, 2016).

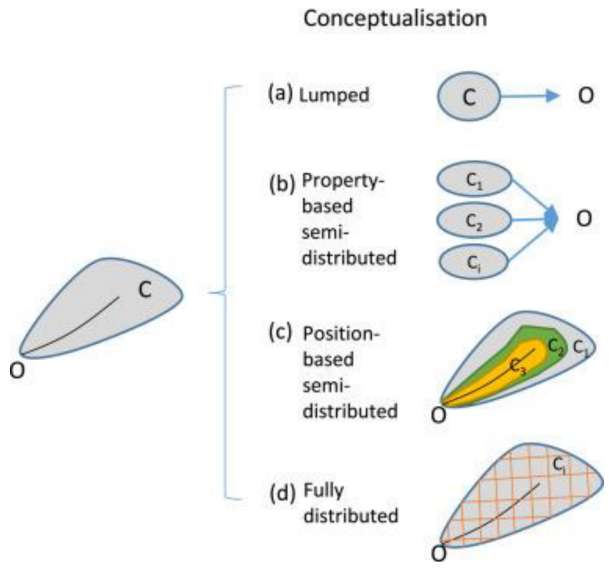

Figure 14 Discrétisation spatiale d'un bassin versant selon une approche globale (a), semi-distribuée (b et c) ou distribuée (d). Source : Fu et al. (2019)

Les modèles développés pour simuler les concentrations en NO_3, DOC ou SRP à Kervidy-Naizin ou en contexte similaire sont hétérogènes. Ainsi, la modélisation du NO_3 dans la nappe superficielle a été effectuée avec des modèles mécanistes et distribués tels que Modflow-MT3D (*Molénat and Gascuel-Odoux*, 2002), FEFMPW (*Kolbe et al.*, 2016) dans le but d'estimer les temps de résidence dans le bassin versant. Le modèle distribué et conceptuel TNT2 a également été développé pour représenter explicitement l'hétérogénéité spatiale des pratiques agricoles et des sols et leurs effets sur les exports de NO_3 (*Beaujouan et al.*, 2001). Des approches semi-intégrées (INCA, *Durand* (2004)) et plus globales (ETNA,

Fovet et al. (2015)) ont également été développées pour étudier l'influence de scenario agricoles et l'évolution à long terme des concentrations en NO_3, respectivement. Les concentrations en DOC ont été modélisées par une approche semi-distribuée avec une adaptation de TOPMODEL (*Fovet et al.*, 2013; *Morel*, 2009). Enfin, les concentrations en SRP ont été modélisées par une approche distribuée avec une adaptation de TNT2 (*Dupas et al.*, 2016).

L'objectif des travaux de modélisation présentés dans le cadre de cette thèse est de conceptualiser les sources de solutés et le fonctionnement hydrologique du bassin versant. Dans cette optique cognitive, une approche globale et multi-élémentaires développée à partir de de l'analyse de données parait pertinente pour identifier les trajets de l'eau et les zones sources des éléments à l'échelle des compartiments du bassin versant (haut de versant, souterrain et bas de versant). Aussi, ce type approche présente l'avantage de rester parcimonieux en terme de paramètres et de temps de calcul (*Birkel et al.*, 2014; *Perrin et al.*, 2001; *Perrin et al.*, 2003b; *Woodward et al.*, 2013) tant que le niveau de complexité du modèle (nombre de réservoirs et de solutés, formulation des processus) est contraint par les observations disponibles ou des connaissances expertes (*Hrachowitz et al.*, 2014) que *Kavetski et al.* (2011) qualifient par ailleurs de « complexité identifiable ».

L'appréciation de la performance d'un modèle simulant à la fois débit et qualité de l'eau oblige à réfléchir à des méthodes d'évaluation adaptées. En effet, la performance d'un modèle est généralement évaluée à l'aide d'une métrique (une fonction objectif) qui reflète le degré de similitude entre une variable simulée et une variable observée (*Dawson et al.*, 2007). Ces métriques permettent d'évaluer quantitativement et objectivement la capacité d'un modèle à reproduire le fonctionnement d'un des aspects du système. La modélisation multi-élémentaire impose d'évaluer les performances du modèle pour plusieurs éléments (la performances globale) par le biais de fonction multi-objectifs (*Birkel et al.*, 2014; *Hrachowitz et al.*, 2014; *Moriasi et al.*, 2015; *Ritter and Muñoz-Carpena*, 2013). Le choix des composantes d'une fonction multi-objectifs est crucial dans la démarche de calibration car celles-ci doivent représenter un maximum d'aspects du système modélisé, l'enjeu étant d'éviter d'utiliser des composantes antagonistes qui complique la recherche de jeux de paramètres satisfaisants (*Bennett et al.*, 2013).

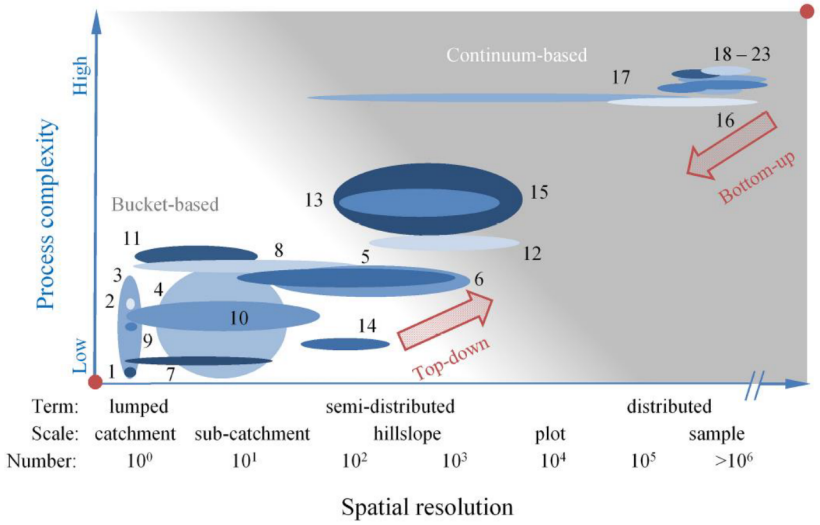

1: unit hydrograph (*Sherman*, 1932)
2: HBV (*Bergstrom*, 1992)
3: SUPERFLEX (*Fenicia et al.*, 2011)
4: FLEX-Topo (*Gharari et al.*, 2014)
5: mhM (*Samaniego et al.*, 2010)
6: mhM-topo (*Nijzink et al.*, 2016)
7: SWAT (*Arnold et al.*, 1998)
8: NWS-Sacramento (*Burnash*, 1995)
9: GR4J (*Perrin et al.*, 2003a)
10: HYPE (*Lindström et al.*, 2010)
11: VIC (*Liang et al.*, 1994)
12: TOPMODEL (*Beven and Kirkby*, 1979)
13: CRHM (*Pomeroy et al.*, 2007)
14: TACD (*Uhlenbrook et al.*, 2004)
15: WASIM-ETH (*Schulla and Jasper*, 1998)
16: DHSVM (*Wigmosta et al.*, 1994)
17: MIKE-SHE (*Refsgaard and Storm*, 1990)
18: PARFLOW (*Kollet and Maxwell*, 2008)
19: CATFLOW (*Zehe et al.*, 2001)
20: HYDRUS-3D (*Šimůnek et al.*, 2008)
21: CATHY (*Camporese et al.*, 2010)
22: HydroGeoSphere (*Jones et al.*, 2006)
23: PIHM (*Qu and Duffy*, 2007)

Figure 15 Répartition schématique de différentes approches de modélisation selon un gradient de discrétisation spatiale et de complexité des processus représentés. Source : Hrachowitz and Clark (2017)

2.5. English summary of the material and methods

In this thesis, we used data from a research observatory dedicated to the environment: the AgrHyS observatory. Among the numerous observatories of the critical zone belonging to the French network OZCAR and the European network on Ecosystems Research eLTER, the agro-hydrological observatory AgrHyS focuses on the relationships between agriculture and water quality. The specificities of the AgrHyS obsevatory are: (1) a river fed by a shallow groundwater, (2) an intensive agricultural activity associating polyculture and breeding, (3) a temperate oceanic climate (Fovet et al., 2018). The Kervidy-Naizin watershed is one of the study sites of the AgrHys observatory. It is a 5-km² agricultural headwatershed, where measurement of flow and major anions concentrations were initiated in the early 1990ies. Since 2000 the monitoring of water quality was extended with a daily frequency and to the concentrations of dissolved organic and inorganic carbon, and since 2007 to the concentrations of reactive and total phosphorus. A weather station located 1 km east of the watershed outlet recorded the weather conditions (precipitation, temperature, wind speed, global radiation) and a network of 12 piezometers where the shallow groundwater level and concentrations are recorded. These data are accessible on the Internet: https://www6.inra.fr/ore_agrhys_eng/Data.

The chapter describes also the overall approach. It follows a general learning framework where the first step is an analysis of the datasets from the observatory which lead to the formulation of hypotheses about the catchment functioning within a perceptual model, and then their translation into the equations of a conceptual model. The study of time series relies on several methods of data analysis and exploration (Lloyd et al., 2014) to identify the long-term, multi-year, seasonal and event-driven relationships between the variables. The hypothesis resulting from these analyses are used in the development of a conceptual model to identify the water pathways and the sources of the elements at the scale of the catchment compartments. We review the several models developed on the Kervidy-Naizin catchment for one of the three elements studied (NO_3, DOC and SRP). The heterogeneity between these previous developments and their differences in represented processes and corresponding representations make difficult the integration of the other elements whereas a global and multi-element approach appears relevant and parsimonious.

3. Analyses des séries temporelles C, N, P et variables hydro-climatiques

L'objectif de ce premier travail est de proposer un schéma perceptuel qui synthétise les relations entre climat et concentrations en DOC, NO_3 et SRP à l'exutoire du bassin versant de Kervidy-Naizin à partir de l'analyse des séries de données journalières de plus de 15 ans. Ce travail a donné lieu à la publication d'un article dans la revue *Water Resources Research* (*Strohmenger et al.*, 2020) qui constitue l'essentiel du chapitre pour lequel un résumé étendu en français est ici proposé.

3.1. Résumé de l'article

Les dynamiques de variations des concentrations en DOC, NO_3 et SRP dans le cours d'eau sont le fruit d'interactions entre facteurs du milieu, facteurs hydrologiques et anthropiques dont il est complexe de distinguer les effets. Les variations temporelles des concentrations ont été étudiés à plusieurs échelles temporelles : à long terme en lien avec les changements climatiques (*Monteith et al.*, 2007; *Worrall and Burt*, 2007), et anthropiques et en particulier agricoles (*Aquilina et al.*, 2012; *Dupas et al.*, 2018); à l'échelle pluriannuelle avec un effet des années sèches et humides, ou des cycles d'années plus ou moins humides/chaudes en lien avec les cycles climatiques tels que la *North Atlantic Oscillation* (*Gascuel-Odoux et al.*, 2010; *Mellander et al.*, 2018); à l'échelle annuelle, en lien avec les saisonnalités hydrologique et biogéochimique (*Abbott et al.*, 2018; *Aubert et al.*, 2013c) ; et à l'échelle évènementielle de la crue, en lien avec le régime des évènements pluie-débit (*Bowes et al.*, 2015; *Lambert et al.*, 2013; *Outram et al.*, 2014). Cependant, les études des liens entre climat et qualité de l'eau s'appuient rarement sur des jeux de données multiéléments et sont souvent focalisées sur une seule échelle temporelle. Or, on peut attendre des réponses différentes selon les origines et natures des éléments, par exemple le DOC est présumé sensible au réchauffement, NO_3 et SRP sont d'origine directement agricole et donc présumés sensibles au changements d'activités humaines. Cet article présente l'analyse des coévolutions des variables hydro-climatiques et des concentrations en DOC, NO_3 et SRP à l'aide de méthodes spécifiques aux différentes échelles temporelles pour répondre à plusieurs questions : quelles sont les coévolutions des variables hydro-climatiques à long terme ? Quel est l'impact des variations interannuelles du climat sur la saisonnalité des concentrations ? Quelles sont les conditions hydro-climatiques favorables aux concentrations extrêmes dans le cours d'eau ?

Cette étude s'appuie sur les 16 ans de données journalières acquises sur le petit bassin versant agricole de Kervidy-Naizin (Observatoire AgrHyS, OZCAR). Les évolutions sur 16 années (échelle long terme) ont été analysées à l'aide des tests de Mann-Kendall et de Theil Sen. Le test de Mann-Kendall permet d'identifier la présence d'une tendance dans une série temporelle, alors que le test de Theil Sen en calcule la pente médiane. Ces tendances ont été calculées deux fois pour chaque variable : (i) sur la période globale entre 2002 et 2017 ; (ii) pendant les différentes périodes hydrologiques (recharge, hautes eaux, récession et sèche) basées sur le débit du cours d'eau. La saisonnalité des variables a été analysée à l'aide d'une décomposition en séries de Fourier (en une combinaison de fonctions périodiques) pour identifier les synchronies/asynchronies de ces cyclicités annuelles moyennes entre 2002 et 2017, ainsi que pour identifier les éventuelles corrélations de leurs amplitudes et déphasages annuels. Les concentrations extrêmes journalières ont été analysées par une approche probabiliste des distributions des conditions

hydro-climatiques associées aux concentrations maximums et minimums en DOC, NO_3 et SRP, en écoulement de base et en écoulement de crue.

Les résultats issus de l'analyse à long terme montrent des tendances à l'augmentation de la température (principalement en période sèche) et de l'humidité du bassin versant (pendant la période humide) des concentrations en DOC (en période humide et en récession), à la diminution pour les concentrations en NO_3 et SRP. Les variables du débit et des piézomètres ne montrent pas de tendance globale mais affichent une augmentation pendant la période humide et une diminution pendant les périodes de recharge et de récession. Les analyses de saisonnalités montrent des cycles réguliers pour la température et le rayonnement global (maximas en juillet et juin, respectivement), alors que ces cycles sont plus bruités pour la pluie et le vent (maximas en octobre et février, respectivement). La cyclicité moyenne du débit montre un maximum au mois de février, synchronisé avec celle des piézomètres de haut de versant. Les piézomètres de bas de versant affichent un palier de saturation de février jusqu'à juin. Les saisonnalités moyennes du DOC et du NO_3 sont nettement opposées avec des maximas en octobre et en mai, respectivement. L'analyse de corrélation des amplitudes et déphasages annuels ne montre pas de relations claire entre une variable hydro-climatique et chimique. Les analyses journalières des conditions hydro-climatiques associées aux concentrations extrêmes montrent que l'humidité du bassin est la variable la plus influente sur les concentrations en DOC, NO_3 et SRP. La température ne semble pas influencer les concentrations extrêmes journalières. Les conditions favorables aux concentrations maximums en NO_3 sont souvent associées aux concentrations minimum en DOC. Les concentrations maximums de SRP ne sont visibles que lors d'épisodes hydrologiques extrêmes avec forte pluie, piézomètres saturés et débit très élevé.

L'opposition du DOC et NO_3 à toutes les échelles suggèrent des mécanismes communs entre ces deux éléments. La diminution du NO_3 à long terme est imputée aux changements opérés dans les systèmes agricoles, tamponnés par l'inertie du bassin versant. L'augmentation de la concentration en DOC à long terme peut être expliquée par la diminution des réactions de dénitrification en lien avec la diminution du NO_3 ou l'augmentation de la contribution des zones sources de carbone provoquée par l'extension des zones humides. Un autre mécanisme pouvant augmenter les concentrations en DOC et diminuer celles en NO_3 serait l'augmentation du ruissellement de surface occasionnée par la modification du régime de pluie. Les oppositions entre les concentrations en DOC et NO_3, à l'échelle saisonnière et en période de crue sont le résultat de contributions relatives de plusieurs compartiments du bassin versant, chacun présentant des compositions et caractéristiques hydrodynamiques spécifiques. Ces contributions relatives, principalement des eaux souterraines (riches en NO_3) et de zone riparienne (riche en DOC), sont contrôlées la connectivité hydrologique avec le cours d'eau, elle-même contrôlée par les battements de la nappe. Les concentrations en SRP présentent des dynamiques plus singulières qui répondent aux conditions anoxiques favorables à la dissolution du phosphore en bas de versant saturé ainsi qu'à des processus de mobilisation du SRP depuis le lit du cours d'eau et la zone hyporhéïque.

En conclusion, le climat local semble évoluer vers une saisonnalité plus contrastée des conditions hydrologiques du bassin versant (saison humide plus humide) qui montrent à leur tour, une influence sur les dynamiques des concentrations des solutés dans le cours d'eau. Les précipitations et les conditions d'humidités sont les moteurs principaux des variations de concentrations dans le cours d'eau à l'échelle saisonnière et évènementielle. En effet, ces deux paramètres déterminent la connectivité hydrologique des compartiments sources, ainsi que les réactions biogéochimiques qui en dépendent. Sur le long terme, la qualité de l'eau semble davantage contrôlée par des facteurs anthropiques, alors que les dynamiques infra-annuelles dépendent principalement des précipitations.

3.2. Multi-temporal relationships between the hydro-climate and exports of carbon, nitrogen and phosphorus in a small agricultural watershed

L. Strohmenger[1], O. Fovet[1], N. Akkal-Corfini[1], R. Dupas[1], P. Durand[1], M. Faucheux[1], G. Gruau[2], Y. Hamon[1], A. Jaffrezic[1], C. Minaudo[3], P. Petitjean[2], C. Gascuel-Odoux[1]

[1] UMR SAS, INRAE, AGROCAMPUS OUEST, 35000 Rennes, France

[2] OSUR, Géosciences Rennes, CNRS, UMR 6118, Campus de Beaulieu, 35042 Rennes, France

[3] Physics of Aquatic Systems Laboratory, EPFL, Lausanne, Switzerland

Key Points

- Analysis of 16 years of daily hydro-climatic and water chemistry variables in a 5 km² agricultural watershed
- Opposite temporal patterns for nitrate and DOC, independent of SRP variations, at inter-annual, seasonal and event time scales
- Agricultural pressures and climate drive long-term trends, while watershed wetness controls shorter-term variations

Abstract

Agriculture affects the biogeochemical cycles of carbon, nitrogen and phosphorus, leading to a deterioration of surface water quality. The increasing magnitude of climate change raises questions about potential additional or mitigating effects of climate change on this deterioration. One way to understand these potential effects is to cross-analyze the dynamics of nutrient concentrations and hydro-climatic variables at multiple time scales. Here, we used a 16-year dataset, from a 5 km² agricultural watershed in France with a temperate oceanic climate, that contains a daily record of nutrient concentrations and hydro-climatic variables from 2002-2017. We calculated Mann-Kendall and Theil-Sen tests, Fourier transforms, and daily hydro-climatic distributions associated with extreme stream concentrations to investigate long-term trends, seasonal dynamics and their inter-annual variations, and the daily time scale, respectively. Dynamics of dissolved organic carbon (DOC) and nitrate (NO_3) concentrations displayed opposite patterns at the three temporal scales, while soluble reactive phosphorus concentrations showed decoupled dynamics, related more to extreme hydrological events. Climate and past agricultural changes seem to have a synergetic effect that leads to long-term NO_3 decrease and DOC increase. Precipitation and, to a greater extent, watershed wetness controlled seasonal and event-driven dynamics.

1. Introduction

Assessing water quality and its evolution is a major issue for society in the context of global change (*Nickus et al.*, 2010). Effects of climate on water quality have often been studied for large rivers, since rivers concentrate most long-term water quality time series. However, it is difficult to disentangle hydrological and biogeochemical effects in the terrestrial and aquatic compartments of watersheds from observations in large rivers (*Marzadri et al.*, 2017). Studies of small rivers or streams are more likely to reveal effects of climate change on nutrient mobilization dynamics in watersheds, but these studies remain relatively rare (*Ford et al.*, 2018). These dynamics result from complex interactions between the watershed structure (e.g. geology, topography, soils) and anthropogenic and hydroclimatic drivers (*Basu et al.*, 2010; *Davis et al.*, 2014; *Dick et al.*, 2015). Climate influences surface water chemistry via both hydrological and biogeochemical mechanisms (*Bartolai et al.*, 2015; *Delpla et al.*, 2009; *Green et al.*, 2014; *Marshall and Randhir*, 2008; *Ockenden et al.*, 2017; *Stuart et al.*, 2011). Indeed, climate drives the hydrological budget and flow paths and thus mobilization of chemical elements and their residence times. In addition, climate also influences biogeochemical reactions that depend on temperature and wetness (*Covino*, 2017; *Salmon-Monviola et al.*, 2013; *Stuart et al.*, 2011; *Whitehead et al.*, 2009). The response of water quality to climate change is thus likely to differ among chemical elements depending on their sources and mobilization pathways, and on their sensitivity to climate vs. local anthropogenic drivers. Therefore, integrated approaches that study multiple elements are required to understand and predict the future of water quality in agricultural areas. For instance, dissolved organic carbon (DOC) is assumed to be more sensitive to temperature (*Delpla et al.*, 2009; *Singh et al.*, 2016) but less sensitive to agriculture than nitrates (NO_3) or soluble reactive P (SRP) (*Bennett et al.*, 2001; *Galloway and Cowling*, 2002). NO_3 and SRP also have different sources and mobilization processes (*Basu et al.*, 2011; *Bowes et al.*, 2015; *Thomas et al.*, 2016).

The reported effects of climate on C, N and P concentrations depend on the element and the temporal scale:

1. Over periods longer than a decade, considered here to be “long-term”, available water-quality time series cover mainly North of America and Europe. Several trends in these time series have been observed. Increases in DOC concentration (*Monteith et al.*, 2007; *Worrall and Burt*, 2007) are usually attributed to climate warming and global (pH, deposition) changes. Decreases in NO_3 (*Aquilina et al.*, 2012; *Dupas et al.*, 2018a; *Howden et al.*, 2010; *Monteith et al.*, 2000) and SRP (*Bowes et al.*, 2011; *Dupas et al.*, 2018b; *Minaudo et al.*, 2015) concentrations are attributed to changes in agricultural and household pressures or hydro-climatic changes.

2. Over shorter periods (a few years), climate cycles occur in a succession of wet and cold years followed by dry and warm years, related to the North Atlantic Oscillation in Northern Europe. Several studies have identified responses of stream concentrations of NO_3 and SRP to these cycles (*Gascuel-Odoux et al.*, 2010; *Loecke et al.*, 2017; *Mellander et al.*, 2018; *Monteith et al.*, 2000).

3. At the annual scale, seasonal variations in weather induce strong seasonality in hydrology and biogeochemistry, leading to seasonal variations in stream concentrations (*Abbott et al.*, 2018; *Aubert et al.*, 2013; *Halliday et al.*, 2012; *Martin et al.*, 2004; *Mulholland and Hill*, 1997). For headwaters controlled by a shallow water table, water table fluctuation is the main driver of dissolved C, N and P seasonality (*Musolff et al.*, 2015; *Newcomer et al.*, 2018; *Van Meter et al.*). Indeed, it controls the connectivity between solute sources (e.g. in soils or

groundwater) and the stream, as well as soil moisture, which influences biogeochemical processes such as reduction and mineralization.

4. Finally, the precipitation regime is the main driver of the storm regime, which is responsible for most export of DOC (*Lambert et al.*, 2013; *Morel et al.*, 2009) and SRP (*Bowes et al.*, 2015; *Dupas et al.*, 2015c; *Outram et al.*, 2014), while storm-flow usually dilutes NO_3 concentrations (*Bowes et al.*, 2015; *Oeurng et al.*, 2010).

Few studies have investigated water quality response to local climatic conditions considering i) multiple elements (*Michalak*, 2016; *Singh et al.*, 2016; *Whitehead et al.*, 2009) with contrasting sources, mobilization and reactivity, such as DOC, NO_3 and SRP; and ii) several temporal scales (from one day to decades). Such studies require high-frequency multi-element sampling in small-scale watersheds over a long period (>10 years). We developed an approach to perform such an analysis to address the following questions:

- Are there measurable changes in climatic, hydrological and concentration variables?
- How do changes in annual weather/water regimes influence seasonal variations in concentrations?
- How do changes in extreme conditions, such as storm events and droughts, influence stream concentrations?

We analyzed the co-variability of climatic variables and DOC, NO_3, and SRP stream-water concentrations by comparing (1) their long-term trends over a 16-year period, (2) the synchrony of average and inter-annual seasonal patterns, and (3) daily hydro-climatic conditions associated with low and high concentrations for different hydrological regimes, using a suitable method for each temporal scale. We used an original daily dataset for 2002-2017 from an Environmental Research Observatory (ERO) containing daily meteorological and hydrological variables, as well as DOC, NO_3 and SRP stream-water concentrations. This dataset was well suited to conduct an analysis that addressed the criteria of length (>10 years), frequency (<1 week), and multiple elements (C, N and P).

2. Methods

2.1. Study site

The Kervidy-Naizin study site is a 4.9 km² agricultural headwater located in western France that has been instrumented since the 1970s for long-term observations (Figure A 1). This research watershed belongs to the ERO AgrHyS (ERO of response times in Agro-Hydro-Systems https://www6.inra.fr/ore_agrhys_eng/, (*Fovet et al.*, 2018b; *Gascuel-Odoux et al.*, 2018)). It is one of the French Critical Zone Observatories (OZCAR) (*Gaillardet et al.*, 2018).

The draining headwater stream is the Coët Dan, is a second Strahler order intermittent stream with high discharge periods from November-April and completely dry periods (no flow) from July-October. The mean ± standard deviation of annual runoff was 296 ± 150 mm for 2002-2017. The climate is temperate oceanic, with mean annual temperature of 11.2 ± 0.6°C and mean annual precipitation of 810 ± 180 mm. Precipitation varies seasonally throughout the year, with higher precipitation from October-February (mean monthly precipitation of 92 ± 31 mm) and lower precipitation from March-July (mean monthly precipitation of 50 ± 14 mm).

The Kervidy-Naizin watershed is mostly flat with a maximum slope <5% and elevation that ranges from 98-140 m above sea level. The bedrock is composed of impermeable Brioverian schists with pyrite (FeS_2), above which a locally fractured layer of schists is buried under 1-30 m of weathered material and silty loam soils.

Land use is characterized by intensive mixed-farming, with 91% of the watershed area under agriculture that grows crops used for animal feed, primarily maize (silage or grain) and grasslands. The main crop rotations are maize-winter wheat or barley and maize-grasslands, which leads to a watershed area dominated by maize (36%), cereals (32%) and grasslands (13%) according to farm surveys performed in 2008 and 2013, and to annual land-use surveys (*Casal et al.*, 2019; *Viaud et al.*, 2018). The watershed has a high livestock density (ca. 5 livestock units.ha^{-1}), composed of cattle, pigs and poultry (*Casal et al.*, 2019).

Agricultural production intensified during the 1970s, leading to an increase in mineral N, P and livestock organic matter (OM) inputs (*Cheverry*, 1998). Following environmental policies in the 1990s (European Union Nitrates Directive, and national implementations), agricultural practices changed to reduce nutrient inputs, which decreased the most from 1998-2008. From 1993-2000, the first Management Plan for Agricultural Pollution (the French "Plan de Maitrise des Pollutions d'Origine Agricole") targeted the standardization of livestock buildings and improvement of manure storage. The Second Management Plan (2001-2008) imposed fertilization management plans, optimization of grazing strategies, mandatory soil coverage and manure processing. From 2008-2017, agricultural management and land use likely continued to evolve, but to a lesser extent. Local farm surveys performed before 1995 led to estimates of annual soil N surplus (mineral + organic inputs – crop exportations) of ca. 150-200 kg N.ha^{-1}.y^{-1} (*Cheverry*, 1998). Farm surveys performed in 2008 and 2013 led to estimates of the average annual surplus over the studied period (2002-2017) of 100 kg N.ha^{-1}.y^{-1} (*Casal et al.*, 2019) and 13 kg P.ha^{-1}.y^{-1} (*Dupas et al.*, 2015b).

Previous studies highlighted a strong annual pattern in the dynamics of hydrological and chemical elements in the Kervidy-Naizin watershed (*Aubert et al.*, 2013). Analysis of seasonal and annual means and variances emphasized a sequence of four hydrological periods during the water year associated with different flow paths and shallow groundwater fluctuations: (1) rising of base flow, (2) high base flow, (3)

recession of base flow and (4) dry (*Dupas et al.*, 2015a; *Humbert et al.*, 2015). Tracer experiments and multi-compartment monitoring for 1-2 years each indicated that this sequence controlled biogeochemical processes (*Aubert et al.*, 2013; *Dupas et al.*, 2015a; *Fovet et al.*, 2018a; *Humbert et al.*, 2015; *Lambert et al.*, 2013), mobilization of biogeochemical elements (*Lambert et al.*, 2013) and transport mechanisms during storm events (*Aubert et al.*, 2013; *Dupas et al.*, 2015a; *Fovet et al.*, 2018a). DOC and SRP exports were found to be controlled by the hydrological connectivity of wetland soils with the stream (*Dupas et al.*, 2015a; *Humbert et al.*, 2015), while NO_3 export was related to contribution from the groundwater reservoir during high-base-flow and recession periods (*Molenat et al.*, 2002). No synthetic study has yet been performed to analyze and compare concentrations of C, N and P, and their synchrony or asynchrony with climate drivers, using the same method for a given temporal scale. In addition, the longer dataset used in the present study allows for assessment of whether the previous findings are consistent over the years and analysis of trends.

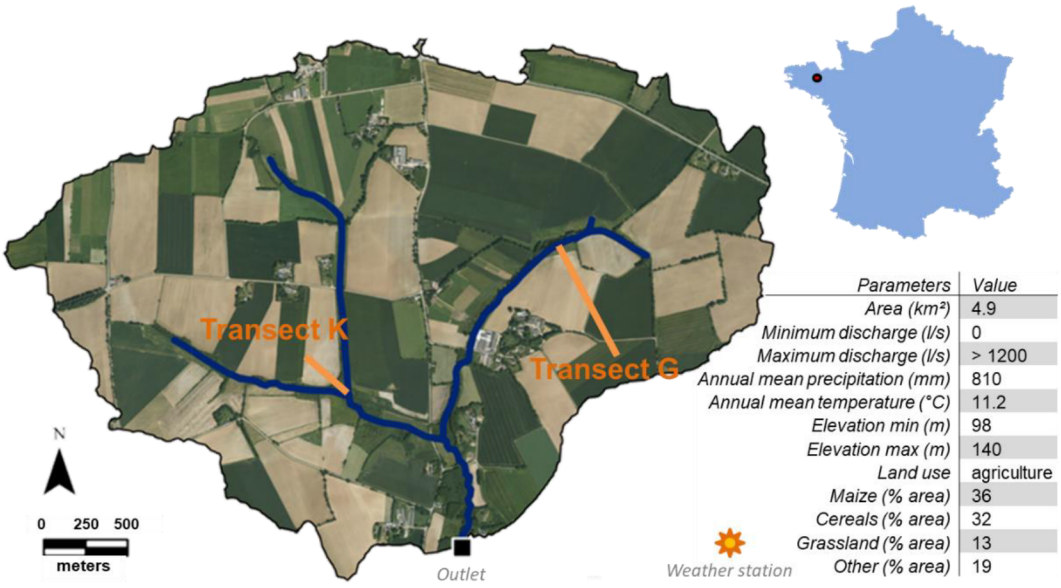

Figure A 1. Aerial photograph of the Kervidy-Naizin watershed, showing the locations of the stream and transects K and G.

2.2. Solute monitoring

Stream water was sampled manually every day at ca. 17:00 at the outlet station. Samples were filtered in the field (pore size: 0.22 µm for C and anions and 0.45 µm for P analyses) and stored in the dark at 4°C in propylene bottles. Analyses were performed within two weeks of sampling. NO_3, chloride (Cl) and sulfate (SO_4) concentrations were measured by ionic chromatography (DIONEX DX 100, *ISO 10304* (1995), precision: 2.5%). Quantification and detection limits were respectively 0.23 and 0.77 $mg.l^{-1}$ for Cl, 0.54 and 1.79 for NO_3 and 0.42 and 1.40 for SO_4). Total and dissolved inorganic carbon (TDC, DIC) concentrations were measured using a carbon analyzer (Shimadzu TOC 5050A, *Petitjean et al.* (2004), precision: 0.5 $mg.l^{-1}$). DOC was estimated as TDC minus DIC (precision: 0.7 $mg.l^{-1}$). Quantification and detection limits were respectively 0.31 and 0.41 $mg.l^{-1}$ for DIC and 0.23 and 0.31 for DOC. SRP concentration was measured by

colorimetric analysis after reaction with ammonium molybdate (*ISO 15681* (2005); (*Murphy and Riley*, 1962), precision: 5%, quantification and detection limits: 0.045 and 0.035 mg.l^{-1}, respectively). SRP concentrations were determined every three days from 2007-2015 and daily thereafter; thus, the corresponding time series are shorter. This study focused on DOC, NO_3 and SRP dynamics. SO_4 and Cl were also included because of their common source with DOC and NO_3, respectively, and thus their contribution to interpretation of C, N and P variations. The laboratories are engaged in proficiency testing programs of BIPEA (https://www.bipea.org/).

2.3. Hydro-climate

We used daily records of meteorological, hydrological and chemical variables monitored in the Kervidy-Naizin watershed from October 2001 to September 2017. The daily meteorological data were obtained from a weather station (Cimel Enerco 516i), located 1 km east of the outlet, that recorded precipitation (rain rate, RR), air temperature (AirTemp), global radiation (GR) and wind speed (Wind) each hour. Potential evapotranspiration (PET) was calculated using the Penman equation (*Penman*, 1956).

Water table level was measured every 15 minutes in 10 piezometers along two transects, G and K (Figure A 1), by Orpheus OTT pressure probes. Stream level was recorded at the outlet every minute by a float-operated shaft-encoder level sensor (Thalimedes OTT), then converted to stream flow using a rating curve (*Carluer*, 1998) (Supporting Information S1). We calculated a daily mean level from these records.

To characterize watershed wetness, we calculated the Antecedent Precipitation Index (API) (*Osborn and Lane*, 1969), which is calculated for each day *t* based on the precipitation during previous days (Eq. 1).

$$API(t) = \sum_{i=0}^{t} RR(t-i).exp^{-ik} \qquad (1)$$

where *k* is the decreasing rate of the previous day's contribution (contributions < 5% were ignored).

We tested a wide range for values for *k* and set it so that API integrated the precipitation of eight previous days, which had the highest correlation with DOC and NO_3 concentrations. These variables are described in Supporting Information S2.

2.4. Trend detection

The 16-year trends (hereafter, "long-term trends") were estimated for each variable and then compared to identify co-evolutions. We used Mann-Kendall and Theil-Sen (TS) tests to identify trends and to quantify their magnitudes, respectively (*He et al.*, 2015; *Lloyd et al.*, 2014; *Srinivas et al.*, 2020; *Ye and Kameyama*, 2020). The Mann-Kendall score reflects the probability of a trend in the dataset, while the TS slope (unit.year^{-1}) is the median slope of a variable over the study period (2002-2017).

Unlike linear regression based on the least squares approach, the TS method is unaffected by potential outliers in the data. These tests were performed for all variables twice: within the complete time series and within different hydrological periods. These periods were divided slightly differently than those in previous studies of this watershed to ensure that a dry period and wet period were defined every year. The periods were defined using dry and wet thresholds set to the 10^{th} and 75^{th} percentiles, respectively, of the complete time series in flowing conditions. Because the dry period contained no-flow periods that lacked concentration data, trends were calculated from the three wettest periods only.

2.5. Fourier transform and seasonal signal analysis

At the seasonal scale, the objective was to describe each variable's average pattern throughout each year from 2002-2017, to assess the synchrony between water quality variables and hydro-climatic variables, and then compare the inter-annual variability in these seasonal patterns. We used a Fourier transform to analyze the seasonality in time series. Compared to previous analyses that aggregated data (by month or season) or used variograms (*Aubert et al.*, 2013), Fourier transformation of these datasets allowed the magnitude and timing of dominant cyclic patterns in the data to be identified (*Kędra et al.*, 2016). A discrete Fourier transform reproduces a signal with a combination of cosine and sine functions of several wavelengths (Eq. 2).

$$\begin{cases} F(t) = C + \sum_{n=1}^{12} A_n \cos(w_n t) + B_n \sin(w_n t) \\ w = \frac{2\pi}{T} \end{cases} \quad (2)$$

where *F(t)* is the Fourier series on day *t*, *C* a constant offset, *n* the harmonic number, A_n and B_n the amplitudes of cosine and sine, respectively, w_n the pulsatance of the n^{th} harmonic, and *T* the longest wavelength.

We used 12 harmonics for this study: the longest harmonic wavelength was set to twice the length of the time series (32 years), and the next 11 harmonic wavelengths were set to half that of the previous harmonic (Eq. 3).

$$w_n = 2 \times w_{n-1} \quad (3)$$

Harmonics of wavelength >1 year were considered to reproduce the inter-annual trend of the signal, while those with wavelength ≤1 year were used to reproduce intra-annual variations. To assess the variability in this seasonal pattern among years, two characteristics were used for each variable: annual amplitude and the maximum-value phase. The Fourier series were fitted to minimize the sum of the residual between observed and calculated signals using the least-squares method, leading to calibrated amplitudes of the cosine and sine functions for each wavelength. Seasonality of the signals was assessed using two harmonics with pulsatance equal to 365 and 182.5 days. Amplitudes and phase shifts were calculated for each hydrological year individually. Year-to-year deviations from the average seasonal

patterns were studied to identify, for instance, whether years with higher amplitudes of temperature were associated with higher amplitudes of concentrations, or whether early peaks of precipitation were associated with early peaks of concentration. A correlation matrix shows these potential correlations between amplitudes and phase shifts.

2.6. Effect of inter-annual dry periods

The control of dry-period length on solute concentrations was investigated by comparing annual discharge-weighted concentration of the solutes to the length of the dry period. For each year, this period corresponded to a water table level in the downslope piezometer of transect K that was deeper than 30 cm, and thus to the period when soil C and P wetland sources were disconnected from the stream (*Humbert et al.*, 2015).

2.7. Analysis of conditions associated with the highest and lowest concentrations

For the complete time series, we compared the co-occurrence of the lowest and highest daily concentrations with those of the hydro-climatic variables. Base-flow and storm-flow conditions were analyzed separately. We split the dataset into base-flow and storm-event conditions, based on differences in flow (*Aubert et al.*, 2013). Storm events were identified when an increase in discharge exceeded 15 $l.s^{-1}$ for 10 min. Then, discharge at peak flow was identified. The last value of discharge greater than the initial discharge determined the end of the storm event. Any day with a storm event, regardless of duration, was itself considered to be a storm event. Discharge intensity for each storm event was calculated as peak flow minus base flow, the latter being assumed to equal the initial discharge before the event.

To focus on co-occurrence of the highest and lowest concentrations, and to compare variables with different variances and non-normal distributions, we calculated a contingency table of the variables classified. First, we split each hydro-climatic variable into five quantiles (classes, Supporting Information S3). For RR, its many zero values (53%) (days without precipitation) were allocated to class 1. Then, a subset of the rainy days (RR>0 mm) was subdivided into four classes based on its quartiles. Next, we calculated a 5 × 5 contingency table for each pair of X (concentration) and Y (hydro-climatic variable) variables. The i^{th} row and j^{th} column of the contingency table corresponded to the number of days when X was in class i and Y was in class j. Then, the contingency table was converted into a table of relative frequency of occurrence by dividing each cell of row i by the sum of days in that class Xi. Finally, these tables were plotted as a histogram for each concentration and each flow regime. Special focus was given to the distribution of classes X1 (lowest concentrations) and X5 (highest concentrations). Equal distribution of Xi among the classes of Y would suggest little relationship between Xi and Y. For a strong positive relationship between X and Y, a high probability of association was expected between X1 and Y1 or between X5 and Y5, while for a strong negative relationship between X and Y, a high probability of association was expected between X1 and Y5 or X5 and Y1.

All analyses were performed using MATLAB® software (2019a).

3. Results

3.1. Trends over 16 years

Table A 1 summarizes trends for each variable for the entire study period and for hydrological periods (recharge, wet and recession), while Supporting Information S4 provides plots of time series and long-term trends. We focus the results and interpretation on the trends detected and their directions rather than their magnitude because of differences in units and the difficulty in normalizing trends of variables whose average was close to zero (e.g. water table levels in the downslope area frequently close to soil surface).

The Mann-Kendall test detected positive trends for API and AirTemp. The overall positive trend for API (0.02 mm.year^{-1}) was driven most likely by a positive trend during the wet period, while the overall positive trend for AirTemp (0.04°C.year^{-1}) was driven mostly by a stronger positive trend during the recession period (0.12°C.year^{-1}) despite having a negative trend during the recharge period (-0.13°C.year^{-1}). GR showed a negative trend during the recharge period and a positive one during the wet period. A slight overall negative trend was detected for Wind, with higher slopes during the recession and recharge periods.

Discharge and most piezometers had low or null slopes for overall trends but a negative trend during recharge and recession periods and positive trends during wet periods. Thus, the hydrology was characterized by winters becoming wetter and summers becoming drier. For discharge, the increase during the wet period (1.5 l.s^{-1}.year^{-1}) was higher than the decreases during the recharge and recession periods (-0.4 and -0.31 l.s^{-1}.year^{-1}, respectively). The magnitude of overall and seasonal trends varied greatly among piezometers, likely because of differences in their locations (the maximum limited by the soil surface in downslope locations) and depths (4-8 m), which sometimes limited the ability to capture the entire recession.

DOC and SO_4 concentrations showed overall positive trends (0.034 and 0.096 mg.l^{-1}.year^{-1}, respectively), while Cl, NO_3 and SRP concentrations showed overall negative trends (-0.44, -1.2 and -0.0013 mg.l^{-1}.year^{-1}, respectively). We observed positive trends for DOC concentrations for the wet and recession periods, while SO_4 concentrations instead had positive trends for the recharge and recession periods. NO_3 and Cl concentrations showed negative trends during all three hydrological periods.

Table A 1 Long-term trends calculated from 2002-2017 on the Kervidy-Naizin watershed. Overall trends are based on the complete time series. Hydrological periods' trends focus on three periods identified for hydrological activity of the watershed. Trend value is the annual Theil-Sen slope, which bold when Mann-Kendall test is significant (p-value<0.05). Rain rate>0 (RR+), global radiation (GR), potential evapotranspiration (PET), bottomland piezometer (PG1, PK1), upland piezometer (PG6, PK4), daily discharge (Qd) and 8-day Antecedent Precipitation Index (API8)

Trend	DOC (mg l^{-1} yr^{-1})	NO_3 (mg l^{-1} yr^{-1})	SRP (mg l^{-1} yr^{-1})	Cl (mg l^{-1} yr^{-1})	SO_4 (mg l^{-1} yr^{-1})	RR (mm yr^{-1})	RR+ (mm yr^{-1})	GR (j cm^{-2} yr^{-1})	Temp (°C yr^{-1})	Wind (m s^{-1} yr^{-1})	PET (mm yr^{-1})	RR-PET (mm yr^{-1})
Overall	**3.4E-02**	**-1.2E+00**	**-1.3E-03**	**-4.4E-01**	**9.6E-02**	**0.0E+00**	**0.0E+00**	1.1E+00	**4.3E-02**	**-2.1E-02**	0.0E+00	0.0E+00
Recharge	4.7E-02	**-1.2E+00**	**-2.6E-03**	**-2.3E-01**	**4.2E-01**	0.0E+00	0.0E+00	**-1.1E+01**	**-1.3E-01**	**-2.6E-02**	**0.0E+00**	**2.6E-02**
Wet	**3.5E-02**	**-1.5E+00**	-2.8E-05	**-5.2E-01**	**6.2E-02**	**0.0E+00**	0.0E+00	**5.3E+00**	0.0E+00	**-2.1E-02**	0.0E+00	**1.7E-02**
Recession	**3.9E-02**	**-1.2E+00**	**-1.1E-03**	**-3.8E-01**	**1.1E-01**	0.0E+00	0.0E+00	4.2E+00	**1.2E-01**	**-2.5E-02**	9.1E-03	0.0E+00

Trend	PG1 (mm yr^{-1})	PG2 (mm yr^{-1})	PG3 (mm yr^{-1})	PG4 (mm yr^{-1})	PG5 (mm yr^{-1})	PG6 (mm yr^{-1})	PK1 (mm yr^{-1})	PK2 (mm yr^{-1})	PK3 (mm yr^{-1})	PK4 (mm yr^{-1})	Qd (l s^{-1} yr^{-1})	API8 (mm yr^{-1})
Overall	9.2E-01	**-2.6E+00**	**6.6E+00**	-6.5E+00	**-1.3E+01**	3.9E+00	**-7.0E+00**	1.2E+00	2.6E+00	5.2E+00	**0.0E+00**	**2.1E-02**
Recharge	1.5E+00	**-1.1E+01**	**8.5E+00**	**2.4E+01**	-4.1E+00	-	**-7.8E+00**	-3.7E+00	**-3.6E+01**	-5.3E+00	**-4.0E-01**	1.5E-03
Wet	**1.0E+01**	**8.7E+00**	**1.2E+01**	**2.1E+01**	**2.1E+01**	**2.8E+01**	**-1.9E+00**	**1.3E+01**	**9.7E+00**	**7.8E+00**	**1.5E+00**	**9.6E-02**
Recession	**-3.3E+00**	**-2.3E+00**	**2.9E+00**	**-2.3E+01**	**-2.9E+01**	**-2.8E+01**	**-8.2E+00**	6.7E-01	**-7.1E+00**	**-1.3E+01**	**-3.1E-01**	8.7E-03

3.2. Seasonality

3.2.1.Average seasonal patterns

The Fourier series' accordance with the data was high for water table levels, stream discharge, GR, AirTemp, PET and NO_3 ($r>0.6$); medium for DOC and SRP concentrations ($r=0.47$ and 0.37, respectively, Supporting Information S5) and low for RR, Wind and API ($r<0.35$, Supporting Information S5). AirTemp and GR showed a clearly periodic seasonal cycle, while Wind and RR showed noisier cycles (Figure A 2, Supporting Information S6). Discharge dynamics showed a fast rising limb from October to January/February, followed by a slow recession until the end of the hydrological year. The seasonal signal of upslope piezometers (PK4 and PG5) was similar to that of discharge, while signals of downslope piezometers (PK1 and PG1) had a more rectangular shape. DOC, SO_4 and Cl concentrations peaked in October and November, at the beginning of the hydrological year, then decreased until April/May, and finally rose until the end of the hydrological year. NO_3 showed an opposite pattern to DOC, since NO_3 concentration was lowest at the beginning of the hydrological year, rose until the end of the wet period in March/April, and then slowly decreased until the end of the hydrological year. SRP showed a more complex pattern, with two peaks: its concentration decreased from October-December and then peaked first during the wet period in January/February and then again during the dry period in September.

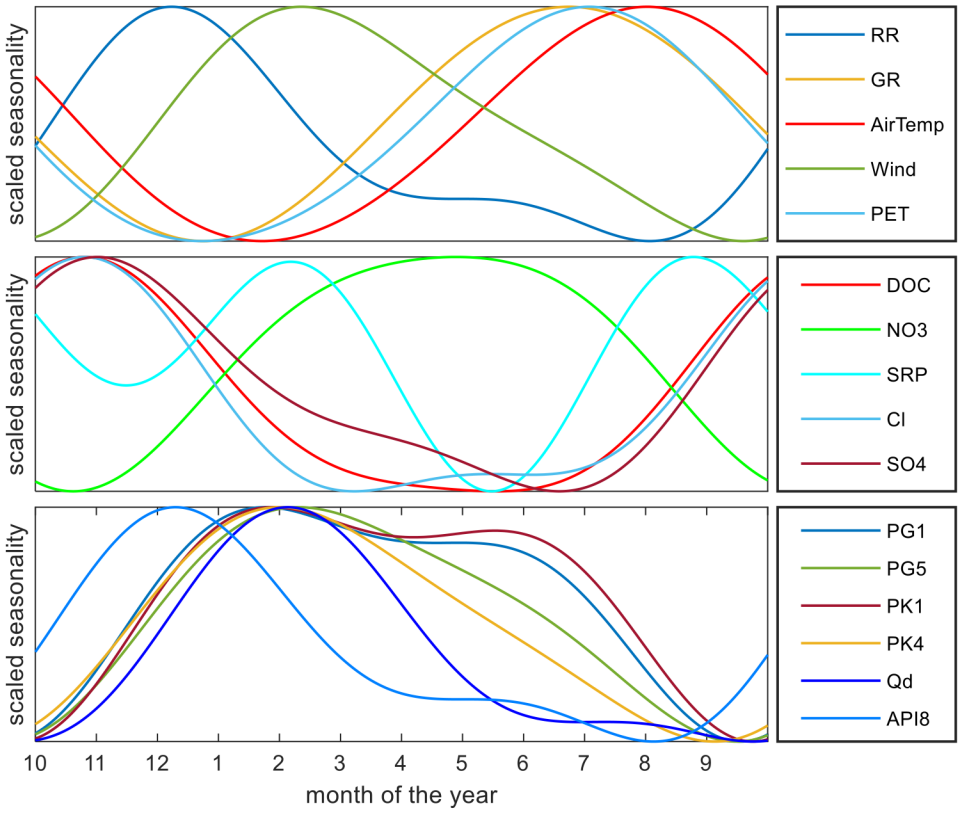

Figure A 2. Seasonal patterns of all variables identified by Fourier transforms (two harmonics) for (top panel) rain rate (RR), global radiation (GR), potential evapotranspiration (PET), (middle panel) DOC, NO_3, SRP, Cl and SO_4 concentrations, (bottom panel) bottomland piezometer (PG1, PK1), upland piezometer (PG6, PK4), daily discharge (Qd) and Antecedent Precipitation Index (API).

GR and AirTemp peaked in June and July, respectively, while RR and Wind peaked within wider temporal windows, from November to mid-February and January-March, respectively (Figure A 3). The water table in the downslope domain (PG1 and PK1) peaked from December-February, slightly before discharge peaked, while in the upslope domain, water table levels peaked from January-February Discharge peaked from mid-January to the beginning of March. DOC, SO_4 and Cl concentrations peaked in autumn from the beginning of October to the end of November at the onset of increased discharge. Then, because of its two annual peaks, SRP peaked in September and January. Finally, NO_3 concentrations peaked six months after the other solutes did, from the end of March to the end of May.

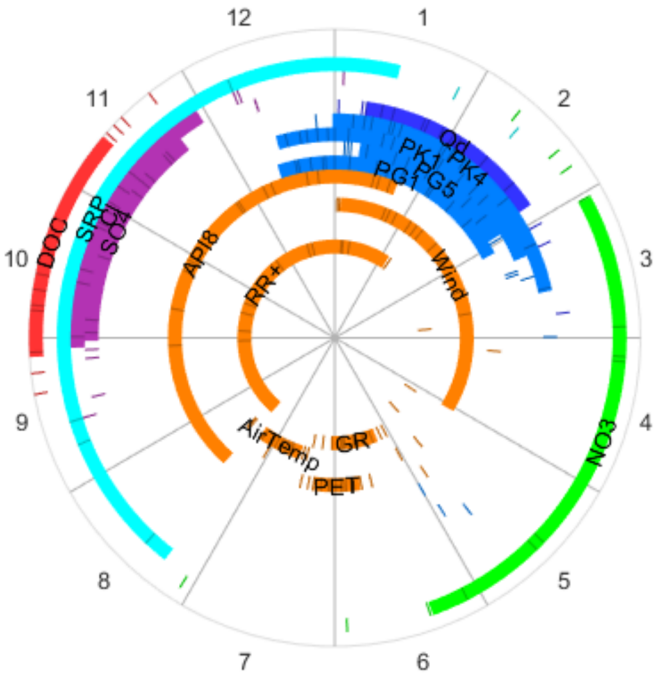

Figure A 3. Variability in dates of seasonal peaks of dissolved organic carbon (DOC), nitrate (NO_3), soluble reactive phosphorus (SRP), discharge (Qd), bottomland piezometer (PG1, PK1), upland piezometer (PG5, PK4), air temperature (AirTemp), wind speed, global radiation (GR), rain rate (RR), and Antecedent Precipitation Index (API). Numbers outside the circle correspond to months. Colored lines are the day of year of the peak amplitude of the seasonality for each hydrological year. The filled area is the mean day of year ± 1 standard deviation of the peak's annual seasonality.

3.2.2.Inter-annual variations

The seasonal amplitude (Table A 1) of DOC was positively correlated with those of RR, PET, bottomland piezometers (PG1, PK1) and SO_4. The seasonal amplitude of SRP was positively correlated with those of bottomland piezometers (PG1, PK1), GR and Cl and negatively correlated with that of Wind. The seasonal amplitude of NO_3 showed low correlations with those of all other variables.

The seasonal phase shift (Table A 3) of maximum DOC showed stronger positive correlation with the maxima of bottomland piezometers (PG1, PK1), SO_4 and Cl. The seasonal phase shift of maximum NO_3

was positively correlated mostly with that of RR. The seasonal phase shift of maximum SRP was positively correlated with the maxima of RR, upland and bottomland piezometers, discharge, Cl and SO_4. Stronger correlations found for SRP may have been due to its shorter time series.

Table A 2 Correlation matrix of the ranks of annual amplitudes of the seasonality identified by two-harmonic Fourier transforms. Rain rate (RR), global radiation (GR), potential evapotranspiration (PET), bottomland piezometer (PG1, PK1), upland piezometer (PG6, PK4), daily discharge (Qd) and 8-day Antecedent Precipitation Index (API8). Bold values exceed 0.40.

Variable	DOC	NO_3	SRP	Cl	SO_4	RR	GR	AirT.	Wind	PET	PG1	PG5	PK1	PK4	Qd	API8
DOC	**1.00**	0.33	0.17	-0.18	**0.65**	**0.46**	0.28	-0.20	-0.22	**0.41**	**0.46**	0.03	**0.48**	0.11	-0.20	**0.47**
NO_3	0.33	**1.00**	-0.36	-0.13	0.31	0.26	0.00	0.04	0.01	-0.03	-0.01	-0.12	0.16	0.00	-0.01	0.26
SRP	0.17	-0.36	**1.00**	**0.51**	0.03	0.11	**0.43**	-0.28	**-0.55**	0.18	**0.62**	**0.49**	**0.59**	**0.48**	0.35	0.11
RR	**0.46**	0.26	0.11	0.32	0.21	**1.00**	0.24	0.05	0.24	0.37	0.28	**0.50**	0.24	**0.73**	**0.58**	**0.99**
GR	0.28	0.00	**0.43**	-0.39	0.21	0.24	**1.00**	**0.59**	-0.32	**0.91**	**0.65**	0.20	**0.56**	0.04	-0.12	0.21
AirTemp	-0.20	0.04	-0.28	-0.03	0.07	0.05	**0.59**	**1.00**	-0.14	**0.57**	**0.41**	0.20	0.29	-0.05	-0.04	0.03
PET	**0.41**	-0.03	0.18	-0.25	0.36	0.37	**0.91**	**0.57**	-0.08	**1.00**	**0.69**	0.25	**0.54**	0.14	-0.11	0.36
Qd	-0.20	-0.01	0.35	**0.56**	-0.36	**0.58**	-0.12	-0.04	0.26	-0.11	-0.15	**0.54**	-0.22	**0.84**	**1.00**	**0.59**
API8	**0.47**	0.26	0.11	0.35	0.19	**0.99**	0.21	0.03	0.26	0.36	0.25	**0.49**	0.21	**0.73**	**0.59**	**1.00**

Table A 3 Correlation matrix of the ranks of annual phase shifts of the seasonality identified by two-harmonic Fourier transforms. Rain rate (RR), global radiation (GR), potential evapotranspiration (PET), bottomland piezometer (PG1, PK1), upland piezometer (PG6, PK4), daily discharge (Qd) and 8-day Antecedent Precipitation Index (API8). Bold values exceed 0.40.

Variable	DOC	NO_3	SRP	Cl	SO_4	RR	GR	AirT.	Wind	PET	PG1	PG5	PK1	PK4	Qd	API8
DOC	**1.00**	0.29	**0.44**	**0.54**	**0.56**	0.19	0.03	-0.35	0.05	0.21	**0.41**	0.34	**0.42**	0.14	0.26	0.17
NO_3	0.29	**1.00**	**0.48**	0.31	0.27	**0.49**	0.20	-0.16	-0.07	0.09	0.10	0.16	0.12	0.18	0.25	**0.48**
SRP	**0.44**	**0.48**	**1.00**	**0.79**	**0.78**	**0.51**	0.24	0.03	-0.30	0.19	**0.55**	**0.66**	**0.63**	**0.68**	**0.62**	**0.51**
RR	0.19	**0.49**	**0.51**	-0.17	0.13	**1.00**	-0.01	-0.07	-0.39	-0.01	-0.12	-0.04	-0.08	0.18	0.09	**1.00**
GR	0.03	0.20	0.24	0.19	-0.07	-0.01	**1.00**	0.21	-0.07	**0.91**	-0.14	-0.15	-0.17	-0.24	-0.21	0.01
AirTemp	-0.35	-0.16	0.03	-0.16	-0.01	-0.07	0.21	**1.00**	0.00	0.22	0.12	0.05	0.08	-0.11	-0.15	-0.05
PET	0.21	0.09	0.19	0.13	-0.07	-0.01	**0.91**	0.22	-0.06	**1.00**	-0.06	-0.08	-0.10	-0.22	-0.15	0.00
Qd	0.26	0.25	**0.62**	0.31	**0.44**	0.09	-0.21	-0.15	-0.04	-0.15	**0.59**	**0.83**	**0.64**	**0.86**	**1.00**	0.07
API8	0.17	**0.48**	**0.51**	-0.19	0.13	**1.00**	0.01	-0.05	**-0.43**	0.00	-0.12	-0.05	-0.08	0.19	0.07	**1.00**

Mean discharge-weighted concentrations of DOC increased and SRP decreased as the length of the preceding dry period increased (r=0.68 and -0.49, respectively), while that of NO_3 was unaffected by dry-period length (r=-0.09) (Figure A 4). This relationship remained scattered for SRP.

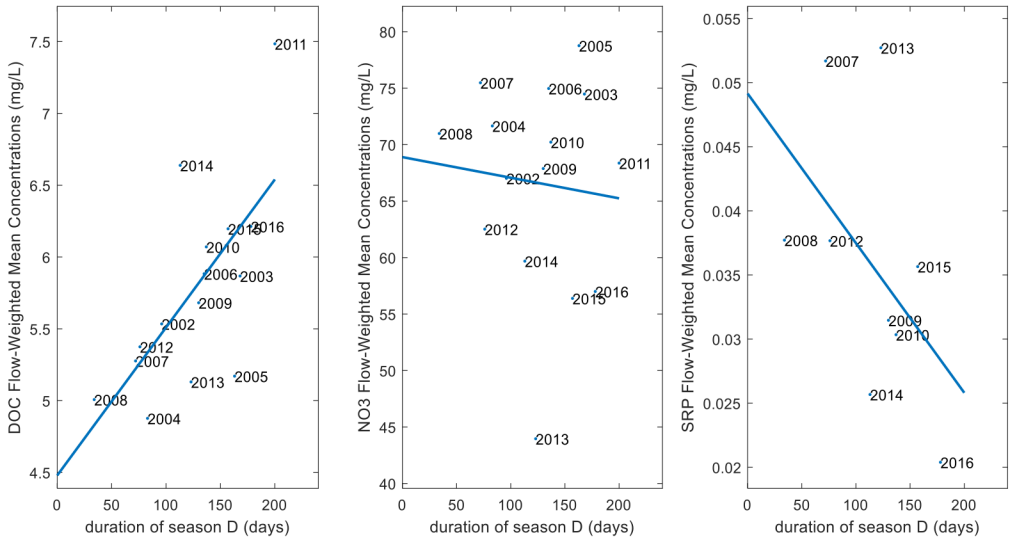

Figure A 4 Discharge weighted-mean dissolved organic carbon (DOC) (left), nitrate (NO_3) (middle) and soluble reactive phosphorus (SRP) (right) concentrations as a function of the duration of the dry period (season D), during which the stream is disconnected from the surface soil horizon. Note that fewer years were available for SRP than DOC and NO_3.

3.3. Highest and lowest concentrations

As detailed below, the main associations with the extreme concentrations detected differed by hydrological regime, with less co-occurrence of the highest/lowest concentrations and hydroclimatic variables for base-flow than storm-flow conditions. The highest and lowest DOC and SRP were frequently associated with the same conditions, unlike NO_3. Generally, extreme concentrations of DOC, NO_3 and SRP were associated mainly with extreme RR and API, rather than with extreme AirTemp or Wind.

3.3.1.Base-flow conditions

The highest DOC and SRP concentrations and lowest NO_3 concentrations co-occurred with the highest API class, and vice-versa. The highest NO_3 and DOC concentrations co-occurred with the lowest AirTemp classes, and the highest DOC concentrations co-occurred with the lowest GR and PET classes (Figure A 5, Supporting Information S7). The highest NO_3 concentrations co-occurred with the highest classes of discharge and piezometric levels, while the highest DOC and SRP concentrations showed no trend among classes of discharge or piezometry (Figure A 5).

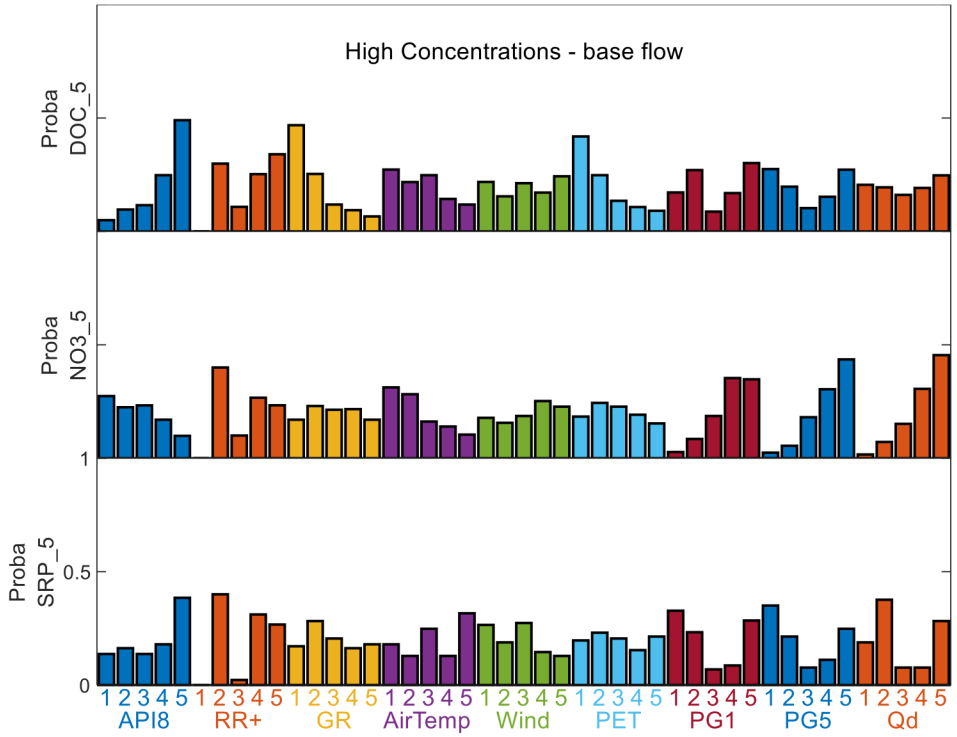

Figure A 5 Distributions of hydrological and meteorological classes for the highest concentrations of dissolved organic carbon (DOC), nitrate (NO_3) and soluble reactive phosphorus (SRP) during base flow. Rain rate >0 (RR+), global radiation (GR), air temperature (AirTemp), potential evapotranspiration (PET), bottomland piezometer (PG1), upland piezometer (PG5), daily discharge (Qd) and Antecedent Precipitation Index (API).

3.3.2.Storm-flow conditions

On days with a storm event, the occurrence of the highest DOC and SRP concentrations and the lowest NO_3 concentrations increased with the class of API, RR and, to some extent, Wind (Figure A 6), and vice-versa (Supporting Information S8), such as for base flow. Note that the days with storm events were expected to be windier. The lowest DOC and SRP concentrations co-occurred with the highest classes of GR and PET, while the lowest NO_3 concentrations co-occurred with the lowest classes of GR and PET (Figure A 6). The highest SRP concentrations co-occurred only with highest class of daily discharge and piezometric levels, but the highest SRP and DOC concentrations and the lowest NO_3 concentrations co-occurred with the highest classes of storm-flow peak discharge (Figure A 6, Supporting Information S8).

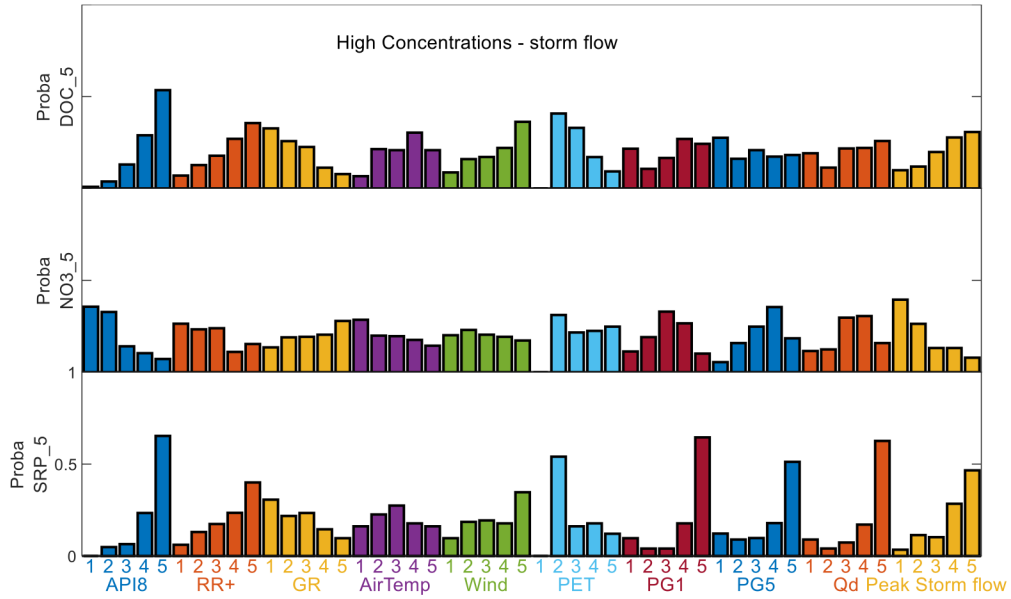

Figure A 6 Distributions of hydrological and meteorological classes for the highest concentrations of dissolved organic carbon (DOC), nitrate (NO_3) and soluble reactive phosphorus (SRP) during storm flow. Rain rate >0 (RR+), global radiation (GR), air temperature (AirTemp), potential evapotranspiration (PET), bottomland piezometer (PG1), upland piezometer (PG5), daily discharge (Qd) and Antecedent Precipitation Index (API).

4. Discussion

4.1. Comparison of C, N and P temporal patterns

4.1.1.Opposite DOC and NO_3 patterns from daily to decadal scales

Looking at the three temporal scales, a major result is the opposite DOC and NO_3 dynamics, highlighting that both solutes are controlled by common mechanisms (*Heppell et al.*, 2017; *Koenig et al.*, 2017; *Taylor and Townsend*, 2010; *Weigand et al.*, 2017). The long-term decrease in NO_3 and increase in DOC can be explained by several non-exclusive factors. The decrease in NO_3 is likely a result of past reduction of agricultural pressures that led to a decrease in NO_3 storage in the watershed. In piezometers, groundwater NO_3 concentrations were observed to decrease from a mean of 109.5 ± 38.5 mg NO_3 l^{-1} in 2000 to 59.3 ± 30.8 mg NO_3 l^{-1} in 2018 along transect K. Despite relatively constant agricultural N input during the study period, the amounts of N input likely decreased the most from 1998-2008, due to environmental regulations. The observation that Cl concentrations, also influenced by fertilization practices (*Aubert et al.*, 2013; *Hrachowitz et al.*, 2015), decreased supports the idea of stock depletion after the past reduction of agricultural pressures. In addition, *Goodale et al.* (2005) suggested that the long-term decrease in stream NO_3 concentrations observed in forested streams in the White Mountains of New Hampshire, USA, could be related to the increase in DOC concentrations, due to either increased denitrification or N immobilization in soils or sediments. In the Kervidy-Naizin agricultural ecosystem, N availability is far higher than that in semi-natural ecosystems, but similar relationships are expected. *Salmon-Monviola et al.* (2013), in a modeling study of the Kervidy-Naizin watershed, predicted an increase in denitrification under climate change scenarios, not only in wetlands but also in upland areas. In upland, areas of denitrification expanded because of greater NO_3 availability due to more mineralization (temperature effect) and less leaching (precipitation effect). In near-stream wetlands, both warming and increased frequency of aerobic-anaerobic cycles increased denitrification rates due to greater variability in precipitation. Thus, climate may help explain the NO_3 trend through a combination of favorable conditions of temperature and water supply, which also influenced the release of DOC driven by reductive reactions (*Grybos et al.*, 2009), since these mechanisms are interrelated in time and space. In addition, the increase in winter flow and storm-event frequency, which would increase surface runoff and overland flow, rich in DOC and poor in NO_3, could also partly explain the long-term decrease in NO_3 concentrations and increase in DOC concentrations (*Mellander et al.*, 2018). Storm-event frequency varied greatly from 2002-2017 and seemed to increase slightly during the study period (TS slope: 0.54 storm events per year), though the sample size (n=16) was too small to extract a significant trend according to the Mann-Kendall test. Finally, like DOC concentrations, SO_4 concentrations increased slightly, which could be explained either by partial re-oxidation of the sulfur stored in organic-rich riparian soil (*Eimers et al.*, 2007) during winter flow periods or by a slightly increased contribution of SO_4-rich deep groundwater to the stream (*Morel et al.*, 2009).

The seasonal opposition observed between DOC and NO_3 resulted in part from the mixing of three end-member compartments with different water transmissivities and concentrations (*Fovet et al.*, 2015; *Molenat et al.*, 2002; *Ruiz et al.*, 2002). Indeed, in the Kervidy-Naizin watershed, surface soil horizons and near-stream areas have higher OM contents and lower NO_3 concentrations than deeper water or upslope areas (*Aubert et al.*, 2013). Maximum DOC (Cl and SO_4) and minimum NO_3 concentrations occurred in autumn, when downslope soils (DOC-rich, NO_3-poor) contributed more water to streams than hillslope groundwater did. As the water table rose during autumn, DOC and NO_3 concentrations decreased and increased, respectively, because the contribution from upland groundwater (ca. 1.5 mg DOC l^{-1} (*Morel*, 2009) and 90 mg NO_3 l^{-1} (*Aubert et al.*, 2013)) increased. During low flow in summer, DOC and NO_3

concentrations continued to increase and decrease, respectively, while deep groundwater supplied nearly all water to the stream. Thus, some production/mobilization processes associated with NO_3 consumption and DOC production are likely to occur in near-stream or in-stream areas during this period (*Arango et al.*, 2007; *Barnes and Raymond*, 2010; *Bernhardt and Likens*, 2002). DOC concentrations peaked under wet or storm-flow conditions, when NO_3 concentrations were lowest. In contrast, NO_3 concentrations peaked under high-water-table and drier conditions, when DOC concentrations were lowest. This opposition between maxima and minima of daily DOC and NO_3 concentrations can also be interpreted as the result of relative mixing contributions. These contributions of soil-surface riparian flows, DOC-rich and NO_3-poor, and upslope groundwater flows, NO_3-rich and DOC-poor (*Aubert et al.*, 2013), vary more during storm flow than base flow, which explains the clearer co-occurrences for the first regime.

Thus, at all three temporal scales, the hydrological mechanisms involved are the relative mixing of hydrological flow paths (*Heppell et al.*, 2017; *Weigand et al.*, 2017) that express opposite vertical or lateral spatial gradients of C and N sources via variations in their hydrological connectivity (*Covino*, 2017) (Figure A 7). The biogeochemical processes invoked involve connections between N and C cycles. They include soil mineralization of OM, denitrification and immobilization by heterotrophic microbes in near- or in-stream areas rich in OM (*Boano et al.*, 2014) and NO_3 reduction associated with Fe redox transformations in soils that can lead to DOC and SRP release into the soil solution (*Grybos et al.*, 2009; *Gu et al.*, 2019) (Figure A 7). Near-stream and in-stream areas include the water column, streambed and hyporheic zone, though our data did not allow us to identify which one was the most reactive. The location of C and N sources depends on biogeochemical properties and agricultural pressures. In return, hydrological connectivity influences not only the transport, but also the cycling and transformation, of C and nutrients through the watershed (*Covino*, 2017). This opposition between DOC and NO_3 dynamics suggests that changes in temperature, wetness or hydrological flow paths are likely to drive changes in both concentrations but also in their seasonal and event dynamics, with opposite responses of DOC and NO_3, and thus greater response of stream DOC:NO_3 ratios.

4.1.2.Singularity of SRP dynamics

Long-term trends in P concentration were difficult to interpret since the corresponding time series were shorter and varied in frequency (every 3 days at first, then daily). Several studies on larger watersheds also reported a decreasing trend in SRP concentrations, related mainly to a decrease in the number of point sources (*Bowes et al.*, 2011; *Minaudo et al.*, 2015). This trend was not expected, since the studied watershed contains only a few farms, which have individual septic tanks.

SRP concentration showed two distinct peaks of seasonality. Timing of the first peak (in February) was correlated with the timing of annual peaks in water table level, after a period of soil water saturation. This first peak occurred when the water table reaches the surface soil horizons enriched in P (*Dupas et al.*, 2015a; *Gu et al.*, 2017). Soil water monitoring emphasized an increase in SRP concentration after ca. 1-2 months of soil saturation (*Dupas et al.*, 2015a; *Gu et al.*, 2017). Long periods of soil saturation and warmer temperatures may increase mobilization of SRP adsorbed on soil aggregates due to reduction of soil Fe-oxyhydroxides (*Dupas et al.*, 2015b; *Dupas et al.*, 2016; *Gu et al.*, 2018; *Gu et al.*, 2019; *Gu et al.*, 2017) (Figure A 7). This mechanism cannot account for the second peak, in summer, since the surface soil horizons were no longer saturated nor hydrologically connected to the stream at that time. This second peak was most likely due to in-stream processes that involved either P mineralization or release from streambed sediments and the hyporheic zone (*Boano et al.*, 2014).

From field and experimental studies, a release of DOC into soil solutions under anoxic conditions was also emphasized and related primarily to the increase in pH caused by reduction reactions (*Grybos et al.*, 2009). Thus, a winter increase in stream DOC concentration similar to the first peak in SRP was expected. However, no such increase was observed in the present time-series, which might suggest consumption of DOC between riparian sources and the stream, or preferential adsorption on DOC on the soil solid phase at the riparian soil-stream interface (*Boano et al.*, 2014).

Maximum daily SRP concentrations during storm days was driven by rain-discharge events and the hydrological state of the watershed (highest values of daily RR, API, discharge and piezometric level), which was similar for DOC concentrations. Maximum daily SRP concentrations during base flow showed little relationship with hydro-climatic variable classes except API, which might have been due to the nature of the processes that mobilize SRP, such as surface and subsurface flow that occur only during hydrological events.

4.2. Climatic drivers of stream concentration dynamics

The trend analysis showed a small overall increase in AirTemp but stable precipitation and GR, in accordance with findings of *Borg and Sundbom* (2014) and *Oni et al.* (2013) in western Europe. Nonetheless, the magnitude of the mean increase in AirTemp (<0.04°C.year^{-1}) was much lower than annual thermal fluctuations (8.11°C). It also suggested that climate change would influence primarily the seasonal distribution of hydro-climatic variations, which is likely to intensify both wet and dry periods, in line with previous studies (*Chang et al.*, 2001; *Gombault et al.*, 2015; *Salmon-Monviola et al.*, 2013; *Wang et al.*, 2018), or increase storm-event frequency (not significant). Disentangling the human (agricultural) and climatic drivers of concentration trends was not possible here, but their respective effects appeared to be synergistic. The seasonally opposite variations in precipitation and PET control the recharge of shallow groundwater, which delivers 80-90% of stream flow (*Aubert et al.*, 2013; *Lambert et al.*, 2013; *Molenat et al.*, 2002). High precipitation and low PET in autumn fills the water table, which then feeds the stream. The average pattern of hydrological seasonality identified by the Fourier series agrees with knowledge about water cycles in temperate watersheds dominated by a shallow water table (*Miguez-Macho and Fan*, 2012). The lengths of the four hydrological periods (recharge, wet, recession and dry) showed significant inter-annual variability, although the time series (16 years from 2002-2017) was too short to reveal a significant trend (Supporting Information S9). Changes in these hydrological periods could be a major driver of changes in water quality (Figure A 7).

The fact that the stream in the Kervidy-Naizin watershed dries out completely almost every summer for up to four months is a strong feature of its seasonal functioning. Intermittence has been shown to influence microbial processes due to rewetting of accumulated material in the dry channel (*Covino*, 2017; *Datry et al.*, 2018), which is likely to influence C emissions from streams significantly (*Marcé et al.*, 2018), especially in temperate climates. The increase in dry-period frequency is also likely to increase mobilization of P from the land during rewetting events (*Forber et al.*, 2017). The positive effect of dry-period length on mean annual DOC concentration of the following hydrological year confirms the same observation during a shorter period by *Humbert et al.* (2015). Its negative effect on SRP concentration was unexpected, however, because we assumed that it had the same relationship as it did with DOC. Indeed, SRP and DOC are assumed to have the same riparian origin in this watershed and are also known to respond to alternating wet and dry periods (*Gu et al.*, 2018). Given the difficulty in capturing stream concentrations at the very beginning of the rewetting, special sampling effort focused on this period could

help understand effects of dry-period length on biogeochemical cycles better. Rapid immobilization of SRP released during rewetting by being consumed or adsorbed on bed sediments may contribute to the lack of a positive relationship between SRP concentration and dry-period length.

The response of daily concentrations differed between base-flow and storm-flow periods. For instance, peak NO_3 concentrations were associated with the highest base flow, while minimum NO_3 concentrations were associated with the highest storm flow. The opposite dynamics of NO_3 vs. DOC and SRP concentrations were amplified during storm flow. *Vautard and Yiou* (2009) highlighted an increase in the amount of precipitation per event but no increase in the number of events in western Europe. In the study site, the number of events increased non-significantly, but changes in the intensity of storm events could influence storm-flow extremes, since peak storm discharge was associated with the highest SRP and DOC concentrations and lowest NO_3 concentrations.

Of all variables, API had the most influence at all temporal scales, regardless of the flow conditions or solute, with similar dynamics with DOC and SRP concentrations, and opposite dynamics with NO_3 concentrations. API is a proxy of both soil wetness, which controls biogeochemical transformation of soil nutrients, and of the relative contribution of surface water flows in the watershed (*Newcomer et al.*, 2018) (Figure A 7).

To extend the analysis over climatic gradients, the methodological approach developed in this study could be applied to other observatories of the critical zone. These observatories can monitor multi-element concentrations with sufficient temporal frequency to investigate storm dynamics that are key for several elements (e.g. P) and seasonal cycles that can help understand the processes that control solute sources, mobilization and transfer and thus help reveal their responses to changing climatic regimes (*Koenig et al.*, 2017).

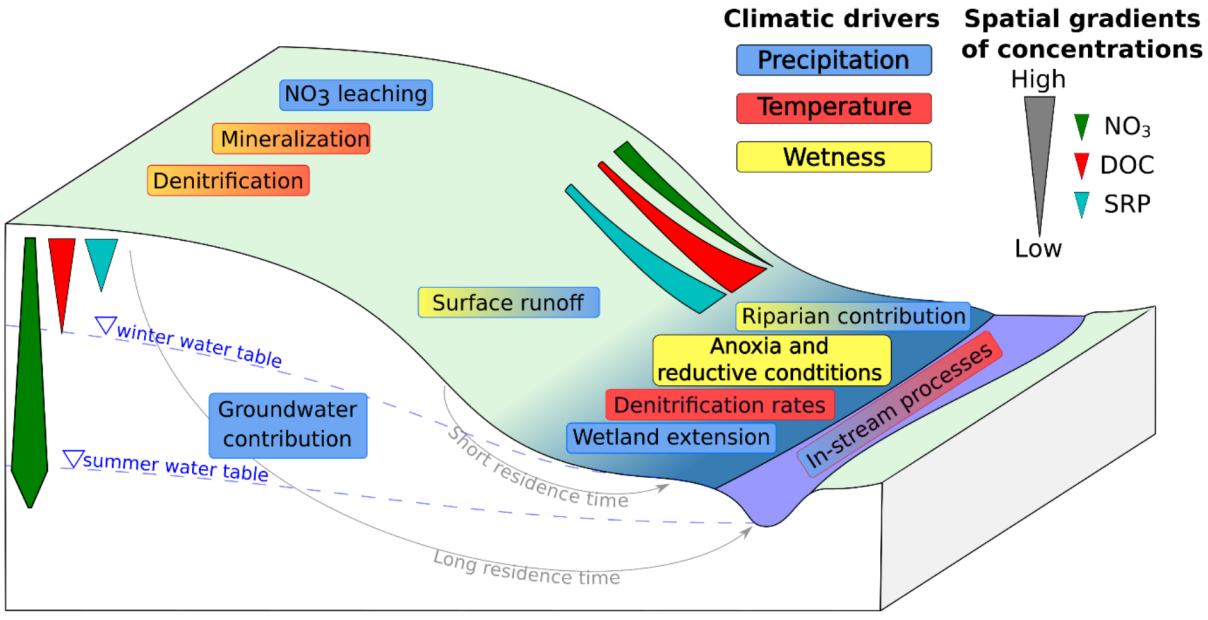

Figure A 7 Conceptual model of climate controls on C, N and P processes and export at the hillslope scale

5. Conclusions

To identify effects of climate drivers on solute concentrations, we analyzed the co-evolution of hydro-climatic variables and DOC, NO_3 and SRP concentrations with a set of methods adapted to different temporal scales of interest. Benefiting from research observatories that collect large amounts of environmental data, the analysis was based on a 16-year time series of daily data from a temperate agro-hydrological observatory dominated by a shallow water table.

Over the 16 years, the climate trends identified were increases in air temperature and hydrological contrast among seasons (wetter winters and drier summers). The length of hydrological periods varied but showed no significant trend, and the number of storm events seemed to increase (non-significant). As reported for other watersheds, water-quality trends were identified: NO_3 concentrations decreased, while DOC concentrations increased. Climate and past agricultural changes seem to have a synergistic effect on long-term responses of stream-water concentrations, by combining more intense winter water export and biogeochemical reactions with lower agriculture pressure.

For the three solutes, the dynamics of stream-water concentrations among seasons and events are more sensitive to dynamics of precipitation and hydrological variables than to those of air temperature or global radiation. The main driving variable is a proxy of watershed wetness (API). In overall, the water-quality response appears to vary less than hydro-climatic variables do, which may be related to legacy stocks in this watershed or to the fact that the climate remains temperate, despite its detected trends.

The integrated analysis of DOC, NO_3 and SRP highlighted the opposition of dynamics of DOC and NO_3 concentrations due to opposition in their spatial sources and opposite effects of biogeochemical processes that act at all of these temporal scales. In contrast, the dynamics of SRP concentrations at the outlet were decoupled from those of DOC and NO_3 concentrations, since SRP concentrations were controlled more by storms and wetness conditions. The set of methods developed would be useful for other observatories worldwide for similar types of data, offering an important perspective for regional or global analyses based on small networks of research observatories.

Acknowledgments, Samples and Data

The French National Research Institute for Agriculture, Food and Environment (INRAE) and the Bretagne Region co-funded the doctoral program of L.S. The AgrHyS Observatory is supported by INRAE (UMR SAS (2010), *Observatoire de Recherche en Environnement sur les Agro-Hydrosystèmes (ORE AgrHyS),* INRAE. https://doi.org/10.15454/1.5499682911557678e12). All AgrHyS data are available on the Internet: https://www6.inra.fr/ore_agrhys_eng/Data. Carbon and anion concentrations were measured at the Géosciences Rennes laboratory. We thank Laurence Carteaux and Nicolas Gilliet for the phosphorus analyses performed at the UMR SAS laboratory. We are grateful to Jean-Paul Guillard for his precious help with sampling on the Kervidy-Naizin watershed over the years and to all the farmers of Naizin-Évellys for hosting our observations, sampling and surveys.

References

Abbott, B. W., F. Moatar, O. Gauthier, O. Fovet, V. Antoine, and O. Ragueneau (2018), Trends and seasonality of river nutrients in agricultural catchments: 18years of weekly citizen science in France, Sci Total Environ, 624, 845-858.

Aquilina, L., A. Poszwa, C. Walter, V. Vergnaud, A.-C. Pierson-Wickmann, and L. Ruiz (2012), Long-term effects of high nitrogen loads on cation and carbon riverine export in agricultural catchments, Environmental science & technology, 46(17), 9447-9455.

Arango, C. P., J. L. Tank, J. L. Schaller, T. V. Royer, M. J. Bernot, and M. B. David (2007), Benthic organic carbon influences denitrification in streams with high nitrate concentration, Freshwater Biology, 52(7), 1210-1222.

Aubert, A. H., et al. (2013), Solute transport dynamics in small, shallow groundwater-dominated agricultural catchments: insights from a high-frequency, multisolute 10 yr-long monitoring study, Hydrology and Earth System Sciences, 17(4), 1379-1391.

Barnes, R. T., and P. A. Raymond (2010), Land-use controls on sources and processing of nitrate in small watersheds: insights from dual isotopic analysis, Ecol. Appl., 20(7), 1961-1978.

Bartolai, A. M., L. He, A. E. Hurst, L. Mortsch, R. Paehlke, and D. Scavia (2015), Climate change as a driver of change in the Great Lakes St. Lawrence River basin, *J. Gt. Lakes Res.*, *41*, 45-58.

Basu, N. B., S. E. Thompson, and P. S. C. Rao (2011), Hydrologic and biogeochemical functioning of intensively managed catchments: A synthesis of top-down analyses, *Water Resources Research*, *47*(10).

Basu, N. B., G. Destouni, J. W. Jawitz, S. E. Thompson, N. V. Loukinova, A. Darracq, S. Zanardo, M. Yaeger, M. Sivapalan, and A. Rinaldo (2010), Nutrient loads exported from managed catchments reveal emergent biogeochemical stationarity, *Geophys. Res. Lett.*, *37*(23).

Bennett, E. M., S. R. Carpenter, and N. F. Caraco (2001), Human impact on erodable phosphorus and eutrophication: a global perspective: increasing accumulation of phosphorus in soil threatens rivers, lakes, and coastal oceans with eutrophication, *BioScience*, *51*(3), 227-234.

Bernhardt, E. S., and G. E. Likens (2002), Dissolved organic carbon enrichment alters nitrogen dynamics in a forest stream, *Ecology*, *83*(6), 1689-1700.

Boano, F., J. W. Harvey, A. Marion, A. I. Packman, R. Revelli, L. Ridolfi, and A. Wörman (2014), Hyporheic flow and transport processes: Mechanisms, models, and biogeochemical implications, *Reviews of Geophysics*, *52*(4), 603-679.

Borg, H., and M. Sundbom (2014), Long-term trends of water chemistry in mountain streams in Sweden - slow recovery from acidification, *Biogeosciences*, *11*(1), 173-184.

Bowes, M., H. Jarvie, S. J. Halliday, R. Skeffington, A. Wade, M. Loewenthal, E. Gozzard, J. Newman, and E. Palmer-Felgate (2015), Characterising phosphorus and nitrate inputs to a rural river using high-frequency concentration–flow relationships, *Sci. Total Environ.*, *511*, 608-620.

Bowes, M., J. Smith, C. Neal, D. Leach, P. Scarlett, H. Wickham, S. Harman, L. Armstrong, J. Davy-Bowker, and M. Haft (2011), Changes in water quality of the River Frome (UK) from 1965 to 2009: Is phosphorus mitigation finally working?, *Sci. Total Environ.*, *409*(18), 3418-3430.

Carluer, N. (1998), Vers une modélisation hydrologique adaptée à l'évaluation des pollutions diffuses: prise en compte du réseau anthropique. Application au bassin versant de Naizin (Morbihan), Paris 6.

Casal, L., P. Durand, N. Akkal-Corfini, C. Benhamou, F. Laurent, J. Salmon-Monviola, S. Ferrant, A. Probst, J.-L. Probst, and F. Vertès (2019), Reduction of stream nitrate concentrations by land management in contrasted landscapes, *Nutrient Cycling in Agroecosystems*, *114*(1), 1-17.

Chang, H., B. M. Evans, and D. R. Easterling (2001), THE EFFECTS OF CLIMATE CHANGE ON STREAM FLOW AND NUTRIENT LOADING 1, *JAWRA Journal of the American Water Resources Association*, *37*(4), 973-985.

Cheverry, C. (1998), *Agriculture intensive et qualité des eaux*, Editions Quae.

Covino, T. (2017), Hydrologic connectivity as a framework for understanding biogeochemical flux through watersheds and along fluvial networks, *Geomorphology*, *277*, 133-144.

Datry, T., et al. (2018), A global analysis of terrestrial plant litter dynamics in non-perennial waterways, *Nat. Geosci.*, *11*(7), 497-503.

Davis, C. A., A. S. Ward, A. J. Burgin, T. D. Loecke, D. A. Riveros-Iregui, D. J. Schnoebelen, C. L. Just, S. A. Thomas, L. J. Weber, and M. A. St Clair (2014), Antecedent moisture controls on stream nitrate flux in an agricultural watershed, *J. Environ. Qual.*, *43*(4), 1494-1503.

Delpla, I., A. V. Jung, E. Baures, M. Clement, and O. Thomas (2009), Impacts of climate change on surface water quality in relation to drinking water production, *Environ Int*, *35*(8), 1225-1233.

Dick, J., D. Tetzlaff, C. Birkel, and C. Soulsby (2015), Modelling landscape controls on dissolved organic carbon sources and fluxes to streams, *Biogeochemistry*, *122*(2-3), 361-374.

Dupas, R., C. Gascuel-Odoux, N. Gilliet, C. Grimaldi, and G. Gruau (2015a), Distinct export dynamics for dissolved and particulate phosphorus reveal independent transport mechanisms in an arable headwater catchment, *Hydrological Processes*, *29*(14), 3162-3178.

Dupas, R., C. Minaudo, G. Gruau, L. Ruiz, and C. Gascuel-Odoux (2018a), Multidecadal Trajectory of Riverine Nitrogen and Phosphorus Dynamics in Rural Catchments, *Water Resources Research*, *54*(8), 5327-5340.

Dupas, R., J. Tittel, P. Jordan, A. Musolff, and M. Rode (2018b), Non-domestic phosphorus release in rivers during low-flow: Mechanisms and implications for sources identification, *Journal of Hydrology*, *560*, 141-149.

Dupas, R., G. Gruau, S. Gu, G. Humbert, A. Jaffrezic, and C. Gascuel-Odoux (2015b), Groundwater control of biogeochemical processes causing phosphorus release from riparian wetlands, *Water Res*, *84*, 307-314.

Dupas, R., R. Tavenard, O. Fovet, N. Gilliet, C. Grimaldi, and C. Gascuel-Odoux (2015c), Identifying seasonal patterns of phosphorus storm dynamics with dynamic time warping, *Water Resources Research*, *51*(11), 8868-8882.

Dupas, R., J. Salmon-Monviola, K. J. Beven, P. Durand, P. M. Haygarth, M. J. Hollaway, and C. Gascuel-Odoux (2016), Uncertainty assessment of a dominant-process catchment model of dissolved phosphorus transfer, *Hydrology and Earth System Sciences*, *20*(12), 4819-4835.

Eimers, M. C., S. A. Watmough, J. M. Buttle, and P. J. Dillon (2007), Drought-induced sulphate release from a wetland in south-central Ontario, *Environ. Monit. Assess.*, *127*(1-3), 399-407.

Forber, K. J., M. C. Ockenden, C. Wearing, M. J. Hollaway, P. D. Falloon, R. Kahana, M. L. Villamizar, J. G. Zhou, P. J. Withers, and K. J. Beven (2017), Determining the effect of drying time on phosphorus solubilization from three agricultural soils under climate change scenarios, *J. Environ. Qual.*, *46*(5), 1131-1136.

Ford, W. I., K. King, and M. R. Williams (2018), Upland and in-stream controls on baseflow nutrient dynamics in tile-drained agroecosystem watersheds, *Journal of Hydrology*, *556*, 800-812.

Fovet, O., L. Ruiz, M. Faucheux, J. Molénat, M. Sekhar, F. Vertès, L. Aquilina, C. Gascuel-Odoux, and P. Durand (2015), Using long time series of agricultural-derived nitrates for estimating catchment transit times, *Journal of Hydrology*, *522*, 603-617.

Fovet, O., et al. (2018a), Seasonal variability of stream water quality response to storm events captured using high-frequency and multi-parameter data, *Journal of Hydrology*, *559*, 282-293.

Fovet, O., et al. (2018b), AgrHyS: An Observatory of Response Times in Agro-Hydro Systems, *Vadose Zone J.*, *17*(1).

Gaillardet, J., et al. (2018), OZCAR: The French Network of Critical Zone Observatories, *Vadose Zone J.*, *17*(1).

Galloway, J. N., and E. B. Cowling (2002), Reactive nitrogen and the world: 200 years of change, *AMBIO: A Journal of the Human Environment*, *31*(2), 64-72.

Gascuel-Odoux, C., P. Aurousseau, P. Durand, L. Ruiz, and J. Molenat (2010), The role of climate on inter-annual variation in stream nitrate fluxes and concentrations, *Sci Total Environ*, *408*(23), 5657-5666.

Gascuel-Odoux, C., O. Fovet, G. Gruau, L. Ruiz, and P. Merot (2018), Evolution of scientific questions over 50 years in the Kervidy-Naizin catchment: from catchment hydrology to integrated studies of biogeochemical cycles and agroecosystems in a rural landscape, *Cuadernos de Investigación Geográfica*, *44*(2), 535-555.

Gombault, C., M.-F. Sottile, F. F. Ngwa, C. A. Madramootoo, A. R. Michaud, I. Beaudin, and M. Chikhaoui (2015), Modelling climate change impacts on the hydrology of an agricultural watershed in southern Québec, *Canadian Water Resources Journal/Revue canadienne des ressources hydriques*, *40*(1), 71-86.

Goodale, C. L., J. D. Aber, P. M. Vitousek, and W. H. McDowell (2005), Long-term decreases in stream nitrate: successional causes unlikely; possible links to DOC?, *Ecosystems*, *8*(3), 334-337.

Green, C. T., B. A. Bekins, S. J. Kalkhoff, R. M. Hirsch, L. Liao, and K. K. Barnes (2014), Decadal surface water quality trends under variable climate, land use, and hydrogeochemical setting in Iowa, USA, *Water Resources Research*, *50*(3), 2425-2443.

Grybos, M., M. Davranche, G. Gruau, P. Petitjean, and M. Pédrot (2009), Increasing pH drives organic matter solubilization from wetland soils under reducing conditions, *Geoderma*, *154*(1-2), 13-19.

Gu, S., G. Gruau, F. Malique, R. Dupas, P. Petitjean, and C. Gascuel-Odoux (2018), Drying/rewetting cycles stimulate release of colloidal-bound phosphorus in riparian soils, *Geoderma*, *321*, 32-41.

Gu, S., G. Gruau, R. Dupas, P. Petitjean, Q. Li, and G. Pinay (2019), Respective roles of Fe-oxyhydroxide dissolution, pH changes and sediment inputs in dissolved phosphorus release from wetland soils under anoxic conditions, *Geoderma*, *338*, 365-374.

Gu, S., G. Gruau, R. Dupas, C. Rumpel, A. Creme, O. Fovet, C. Gascuel-Odoux, L. Jeanneau, G. Humbert, and P. Petitjean (2017), Release of dissolved phosphorus from riparian wetlands: Evidence for complex interactions among hydroclimate variability, topography and soil properties, *Sci. Total Environ.*, *598*, 421-431.

Halliday, S. J., A. J. Wade, R. A. Skeffington, C. Neal, B. Reynolds, P. Rowland, M. Neal, and D. Norris (2012), An analysis of long-term trends, seasonality and short-term dynamics in water quality data from Plynlimon, Wales, *Sci. Total Environ.*, *434*, 186-200.

He, T., Y. Lu, Y. Cui, Y. Luo, M. Wang, W. Meng, K. Zhang, and F. Zhao (2015), Detecting gradual and abrupt changes in water quality time series in response to regional payment programs for watershed services in an agricultural area, *Journal of Hydrology*, *525*, 457-471.

Heppell, C. M., A. Binley, M. Trimmer, T. Darch, A. Jones, E. Malone, A. L. Collins, P. J. Johnes, J. E. Freer, and C. E. M. Lloyd (2017), Hydrological controls on DOC: nitrate resource stoichiometry in a lowland, agricultural catchment, southern UK, *Hydrology and Earth System Sciences*, *21*(9), 4785-4802.

Howden, N., T. Burt, F. Worrall, M. Whelan, and M. Bieroza (2010), Nitrate concentrations and fluxes in the River Thames over 140 years (1868–2008): are increases irreversible?, *Hydrological Processes*, *24*(18), 2657-2662.

Hrachowitz, M., O. Fovet, L. Ruiz, and H. H. G. Savenije (2015), Transit time distributions, legacy contamination and variability in biogeochemical 1/f(alpha) scaling: how are hydrological response dynamics linked to water quality at the catchment scale?, *Hydrological Processes*, *29*(25), 5241-5256.

Humbert, G., A. Jaffrezic, O. Fovet, G. Gruau, and P. Durand (2015), Dry-season length and runoff control annual variability in stream DOC dynamics in a small, shallow groundwater-dominated agricultural watershed, *Water Resources Research*, *51*(10), 7860-7877.

ISO 10304, N. (1995), Determination of dissolved fluoride, chloride, nitrite, orthophosphate, bromide, nitrate, and sulfate ions, using liquid chromatography of ions, edited by AFNOR.

ISO 15681, N. (2005), Determination of orthophosphates and total phosphorus contents by flow analysis (FIA and CFA), edited by AFNOR.

Kędra, M., Ł. Wiejaczka, and K. Wesoły (2016), The role of reservoirs in shaping the dominant cyclicity and energy of mountain river flows, *River Res. Appl.*, *32*(4), 561-571.

Koenig, L. E., M. D. Shattuck, L. E. Snyder, J. D. Potter, and W. H. McDowell (2017), Deconstructing the Effects of Flow on DOC, Nitrate, and Major Ion Interactions Using a High-Frequency Aquatic Sensor Network, *Water Resources Research*, *53*(12), 10655-10673.

Lambert, T., A. C. Pierson-Wickmann, G. Gruau, A. Jaffrezic, P. Petitjean, J. N. Thibault, and L. Jeanneau (2013), Hydrologically driven seasonal changes in the sources and production mechanisms of dissolved organic carbon in a small lowland catchment, *Water Resources Research*, *49*(9), 5792-5803.

Lloyd, C., J. Freer, A. Collins, P. Johnes, and J. Jones (2014), Methods for detecting change in hydrochemical time series in response to targeted pollutant mitigation in river catchments, *Journal of Hydrology*, *514*, 297-312.

Loecke, T. D., A. J. Burgin, D. A. Riveros-Iregui, A. S. Ward, S. A. Thomas, C. A. Davis, and M. A. S. Clair (2017), Weather whiplash in agricultural regions drives deterioration of water quality, *Biogeochemistry*, *133*(1), 7-15.

Marcé, R., B. Obrador, L. Gómez-Gener, N. Catalán, M. Koschorreck, M. I. Arce, G. Singer, and D. von Schiller (2018), Emissions from dry inland waters are a blind spot in the global carbon cycle, *Earth-science reviews*, *188*, 240-248.

Marshall, E., and T. Randhir (2008), Effect of climate change on watershed system: a regional analysis, *Clim. Change*, *89*(3-4), 263-280.

Martin, C., L. Aquilina, C. Gascuel-Odoux, J. Molenat, M. Faucheux, and L. Ruiz (2004), Seasonal and interannual variations of nitrate and chloride in stream waters related to spatial and temporal patterns of groundwater concentrations in agricultural catchments, *Hydrological Processes*, *18*(7), 1237-1254.

Marzadri, A., M. M. Dee, D. Tonina, A. Bellin, and J. L. Tank (2017), Role of surface and subsurface processes in scaling N2O emissions along riverine networks, *Proceedings of the National Academy of Sciences*, *114*(17), 4330-4335.

Mellander, P. E., P. Jordan, M. Bechmann, O. Fovet, M. M. Shore, N. T. McDonald, and C. Gascuel-Odoux (2018), Integrated climate-chemical indicators of diffuse pollution from land to water, *Sci Rep*, *8*(1), 944.

Michalak, A. M. (2016), Study role of climate change in extreme threats to water quality, *Nature News*, *535*(7612), 349-350.

Miguez-Macho, G., and Y. Fan (2012), The role of groundwater in the Amazon water cycle: 1. Influence on seasonal streamflow, flooding and wetlands, *Journal of Geophysical Research: Atmospheres*, *117*(D15).

Minaudo, C., M. Meybeck, F. Moatar, N. Gassama, and F. Curie (2015), Eutrophication mitigation in rivers: 30 years of trends in spatial and seasonal patterns of biogeochemistry of the Loire River (1980–2012), *Biogeosciences*, *12*(8), 2549-2563.

Molenat, J., C. Gascuel-Odoux, P. Davy, P. Durand, and G. Gruau (2002), Nitrate export from an agricultural basin: control mechanisms and nitrate residence times, *International Association of Hydrological Sciences, Publication*(273), 273-278.

Monteith, D. T., C. Evans, and B. Reynolds (2000), Are temporal variations in the nitrate content of UK upland freshwaters linked to the North Atlantic Oscillation?, *Hydrological Processes*, *14*(10), 1745-1749.

Monteith, D. T., et al. (2007), Dissolved organic carbon trends resulting from changes in atmospheric deposition chemistry, *Nature*, *450*(7169), 537-540.

Morel, B. (2009), Transport de carbone organique dissous dans un bassin versant agricole à nappe superficielle, Agrocampus - Ecole nationale supérieure d'agronomie de Rennes.

Morel, B., P. Durand, A. Jaffrezic, G. Gruau, and J. Molenat (2009), Sources of dissolved organic carbon during stormflow in a headwater agricultural catchment, *Hydrological Processes*, *23*(20), 2888-2901.

Mulholland, P. J., and W. R. Hill (1997), Seasonal patterns in streamwater nutrient and dissolved organic carbon concentrations: Separating catchment flow path and in-stream effects, *Water Resources Research*, *33*(6), 1297-1306.

Murphy, J., and J. P. Riley (1962), A modified single solution method for the determination of phosphate in natural waters, *Analytica chimica acta*, *27*, 31-36.

Musolff, A., C. Schmidt, B. Selle, and J. H. Fleckenstein (2015), Catchment controls on solute export, *Advances in Water Resources*, *86*, 133-146.

Newcomer, M. E., S. S. Hubbard, J. H. Fleckenstein, U. Maier, C. Schmidt, M. Thullner, C. Ulrich, N. Flipo, and Y. Rubin (2018), Influence of hydrological perturbations and riverbed sediment characteristics on hyporheic zone respiration of CO2 and N2, *Journal of Geophysical Research: Biogeosciences*, *123*(3), 902-922.

Nickus, U., K. Bishop, M. Erlandsson, C. D. Evans, M. Forsius, H. Laudon, D. M. Livingstone, D. Monteith, and H. Thies (2010), Direct impacts of climate change on freshwater ecosystems, *Climate change impacts on freshwater ecosystems*, 38-64.

Ockenden, M. C., M. J. Hollaway, K. J. Beven, A. Collins, R. Evans, P. Falloon, K. J. Forber, K. Hiscock, R. Kahana, and C. Macleod (2017), Major agricultural changes required to mitigate phosphorus losses under climate change, *Nature communications*, *8*(1), 161.

Oeurng, C., S. Sauvage, and J.-M. Sánchez-Pérez (2010), Temporal variability of nitrate transport through hydrological response during flood events within a large agricultural catchment in south-west France, *Sci. Total Environ.*, *409*(1), 140-149.

Oni, S. K., M. N. Futter, K. Bishop, S. J. Kohler, M. Ottosson-Lofvenius, and H. Laudon (2013), Long-term patterns in dissolved organic carbon, major elements and trace metals in boreal headwater catchments: trends, mechanisms and heterogeneity, *Biogeosciences*, *10*(4), 2315-2330.

Osborn, H., and L. Lane (1969), Precipitation-runoff relations for very small semiarid rangeland watersheds, *Water Resources Research*, *5*(2), 419-425.

Outram, F. N., C. Lloyd, J. Jonczyk, C. M. Benskin, F. Grant, M. Perks, C. Deasy, S. Burke, A. L. Collins, and J. Freer (2014), High-frequency monitoring of nitrogen and phosphorus response in three rural catchments to the end of the 2011–2012 drought in England, *Hydrology and Earth System Sciences*, *18*(9), 3429-3448.

Penman, H. L. (1956), Estimating evaporation, *Eos, Transactions American Geophysical Union*, *37*(1), 43-50.

Petitjean, P., O. Henin, and G. Gruau (2004), *Dosage du carbone organique dissous dans les eaux douces naturelles. Intérêt, Principe, Mise en Oeuvre et Précautions Opératoires*.

Ruiz, L., S. Abiven, C. Martin, P. Durand, V. Beaujouan, and J. Molenat (2002), Effect on nitrate concentration in stream water of agricultural practices in small catchments in Brittany : II. Temporal variations and mixing processes, *Hydrology and Earth System Sciences*, *6*(3), 507-513.

Salmon-Monviola, J., P. Moreau, C. Benhamou, P. Durand, P. Merot, F. Oehler, and C. Gascuel-Odoux (2013), Effect of climate change and increased atmospheric CO2 on hydrological and nitrogen cycling in an intensive agricultural headwater catchment in western France, *Clim. Change*, *120*(1-2), 433-447.

Singh, N. K., W. M. Reyes, E. S. Bernhardt, R. Bhattacharya, J. L. Meyer, J. D. Knoepp, and R. E. Emanuel (2016), Hydro-climatological influences on long-term dissolved organic carbon in a mountain stream of the southeastern United States, *J. Environ. Qual.*, *45*(4), 1286-1295.

Srinivas, R., A. P. Singh, K. Dhadse, and C. Garg (2020), An evidence based integrated watershed modelling system to assess the impact of non-point source pollution in the riverine ecosystem, *J. Clean Prod.*, *246*, 17.

Stuart, M., D. Gooddy, J. Bloomfield, and A. Williams (2011), A review of the impact of climate change on future nitrate concentrations in groundwater of the UK, *Sci. Total Environ.*, *409*(15), 2859-2873.

Taylor, P. G., and A. R. Townsend (2010), Stoichiometric control of organic carbon-nitrate relationships from soils to the sea, *Nature*, *464*(7292), 1178-1181.

Thomas, Z., B. Abbott, O. Troccaz, J. Baudry, and G. Pinay (2016), Proximate and ultimate controls on carbon and nutrient dynamics of small agricultural catchments, *Biogeosciences*, *13*(6), 1863-1875.

Van Meter, K. J., S. Chowdhury, D. K. Byrnes, and N. B. Basu (2019), Biogeochemical asynchrony: Ecosystem drivers of seasonal concentration regimes across the Great Lakes Basin, *Limnol. Oceanogr.*, *n/a*(n/a).

Vautard, R., and P. Yiou (2009), Control of recent European surface climate change by atmospheric flow, *Geophys. Res. Lett.*, *36*(22).

Viaud, V., P. Santillàn-Carvantes, N. Akkal-Corfini, C. Le Guillou, N. C. Prévost-Bouré, L. Ranjard, and S. Menasseri-Aubry (2018), Landscape-scale analysis of cropping system effects on soil quality in a context of crop-livestock farming, *Agriculture, ecosystems & environment*, *265*, 166-177.

Wang, L. L., D. C. Flanagan, Z. G. Wang, and K. A. Cherkauer (2018), Climate Change Impacts on Nutrient Losses of Two Watersheds in the Great Lakes Region, *Water*, *10*(4), 442.

Weigand, S., et al. (2017), Spatiotemporal Analysis of Dissolved Organic Carbon and Nitrate in Waters of a Forested Catchment Using Wavelet Analysis, *Vadose Zone J.*, *16*(3).

Whitehead, P. G., R. L. Wilby, R. W. Battarbee, M. Kernan, and A. J. Wade (2009), A review of the potential impacts of climate change on surface water quality, *Hydrological Sciences Journal*, *54*(1), 101-123.

Worrall, F., and T. Burt (2007), Trends in DOC concentration in Great Britain, *Journal of Hydrology*, *346*(3-4), 81-92.

Ye, F., and S. Kameyama (2020), Long-term spatiotemporal changes of 15 water-quality parameters in Japan: An exploratory analysis of countrywide data during 1982–2016, *Chemosphere*, *242*, 125245.

4. Modélisation des dynamiques infra-annuelles

L'ambition de ce chapitre est de progresser par la traduction du schéma perceptuel du fonctionnement du bassin versant en schéma conceptuel modélisé numériquement (cf. chapitre II), et ainsi de pouvoir tester les principales hypothèses formulées sur les sources et la mobilisation du DOC et du NO_3. Le SRP n'a pas été retenu dans ce premier exercice de modélisation pour plusieurs raisons : les dynamiques des concentrations en SRP sont très liées aux évènements de crue, or la représentation des crues nécessite un pas de temps infra-journalier; la durée de la série temporelle du SRP est plus courte que pour les autres variables ; la représentation de l'opposition des dynamiques du DOC et le NO_3 à toutes les échelles temporelles (cf. chapitre III) semblait déjà suffisamment complémentaires pour caractériser le fonctionnement du bassin versant.

Le modèle présenté ici est le fruit d'une mobilité de trois mois effectuée sous la responsabilité de Markus Hrachowitz à TU Delft, au Pays-Bas. Ce chapitre est présenté sous forme d'article préparé pour une soumission dans la revue scientifique *Science of the total environment*.

4.1. Résumé de l'article

L'analyse de données a confirmé que les dynamiques des concentrations dans le cours d'eau sont le fruit d'interactions complexes entre système agricole et processus hydrologiques dont les effets diffèrent selon l'échelle temporelle. De plus, ces analyses ont mis en évidence le contraste entre les sources et voies de transfert du DOC et du NO_3 reflétées par l'opposition nette des dynamiques de leurs concentrations dans le cours d'eau. Les principaux modèles de transfert de NO_3 et DOC actuellement proposés dans la littérature (SWAT, TNT2, INCA, HYPE) en reproduisent les dynamiques séparément, parfois dans des routines indépendantes du modèle hydrologique. Ces modèles (semi-)distribués sont souvent sous-contraints au regard du nombre de paramètres nécessaires pour les calibrer. C'est pourquoi une partie de la communauté de modélisateurs hydro-chimique s'oriente vers des approches plus parcimonieuses, notamment vers des modèles conceptuels globaux, dits « à réservoirs » avec des formalismes de processus hydro-biogéochimiques plus empiriques. Ces modèles offrent l'avantage de mettre en évidence les processus émergents à l'échelle d'un bassin versant, en plus de reposer sur un nombre plus restreint de paramètres. L'intégration de séries temporelles de concentration dans le processus de calibration d'un modèle apporte des contraintes supplémentaires sur les chemins d'écoulement de l'eau, qui peut, et c'est notre hypothèse, augmenter le réalisme du modèle proposé, d'autant plus si les solutés pris en compte présentent des dynamiques contrastées tels que le DOC et le NO_3. Ce cadre est par ailleurs choisi car la question n'est pas celle des changements des pressions, qui sont nécessairement à spatialiser, mais celui du climat qui contraint globalement le bassin versant.

L'approche développée vise donc à exploiter la richesse des séries temporelles de concentrations pour mieux contraindre le modèle hydrologique, pour identifier les processus essentiels pour reproduire les dynamiques annuelles et évènementielles du débit et des concentrations en DOC et NO_3 dans le cours d'eau. Nous avons donc développé un modèle simple, fondé sur l'hypothèse de mélange de deux sources de solutés contribuant au cours d'eau pour en reproduire les dynamiques saisonnières et évènementielles. Nous avons également analysé l'évolution des paramètres hydrologiques entre une calibration basée sur

le débit uniquement et une calibration basée sur débits et les concentrations dans le but d'évaluer les effets des contraintes apportées par les variables des concentrations.

D'autre part, si le modèle est effectivement mieux contraint par les séries des concentrations, sa calibration devrait permettre de confirmer nos connaissances sur les sources et chemins d'écoulement de l'eau et des solutés dans le bassin versant.

Les simulations s'appuient sur les séries temporelles journalières de pluie, évaporation potentielle, débit et concentrations en DOC et NO_3 issues du jeu de données du bassin versant de Kervidy-Naizin (Observatoire AgrHyS, OZCAR). Nous avons développé un modèle conceptuel, basé sur une approche FLEX proposée par (*Fenicia et al.*, 2006). Ce modèle est composé de trois réservoirs : un compartiment insaturé, que l'on peut assimiler à la zone insaturée des versants, un compartiment saturé et lent, que l'on peut assimiler à la nappe et un compartiment rapide, que l'on peut assimiler à un mélange entre les écoulements préférentiels et la zone riparienne. Les concentrations en DOC et NO_3 sont présumées constantes dans les deux réservoirs sources qui contribuent directement au cours d'eau (lent et rapide). La performance du modèle a été évaluée de deux façons pour en discuter les différences : d'abord par une fonction objectif des erreurs sur le débit, ensuite par une fonction multi-objectifs intégrant les qualités de simulations du débit et des concentrations. La calibration des 11 paramètres a été effectuée par la méthode de Monte-Carlo (10^7 itérations) pendant la période 2012-2017. L'intervalle de confidence des simulations a été estimé par la méthode GLUE (*Beven and Binley*, 1992).

Les simulations produites par ce modèle reproduisent bien les dynamiques annuelles et évènementielles du débit et des concentrations en DOC et NO_3 après calibration avec la fonction multi-objectifs. L'analyse des composantes de cette fonction multi-objectifs soulève une compétition entre la qualité de simulation hydrologique et la qualité de simulation chimique. En effet, les meilleures simulations de concentrations ne sont pas associées au meilleures simulations hydrologiques. Contrairement à nos attentes, l'incertitude des paramètres hydrologiques a plutôt augmenté lors de la calibration multi-objectifs, par comparaison à la calibration hydrologique. La calibration visant un compromis entre performance sur les débits et concentrations conduit à une contribution relative plus importante des eaux profondes au débit du cours d'eau.

Cet exercice de modélisation tend à supporter l'idée que les oppositions entre DOC et NO_3 à l'échelle annuelle et évènementielle sont principalement contrôlées par la distribution spatiale de leurs sources respectives où les temps de résidence de l'eau sont contrastés. La principale source de NO_3 se situe dans le réservoir souterrain (nappe d'altérite), dont l'écoulement est lent et saisonnier alors que la principale source de DOC se situe dans le réservoir riparien dont la réponse hydrologique est rapide et soutient l'écoulement en crue. A noter, une sous-estimation constante du NO_3 lors de la phase de validation (période de 2004-2012) très probablement liée à l'épuisement du stock de NO_3 hérité des activités agricoles. Suite à la calibration multi-objectifs, la réponse hydrologique du réservoir riparien est plus rapide mais conduit à moins de flux, la pluie étant davantage dirigée vers la recharge de la nappe.

Ce modèle basé sur des hypothèses simples réussi à reproduire les dynamiques infra-annuelles du débit et des concentrations en DOC et NO_3, et il parait désormais pertinent de le tester dans des conditions différentes du contexte agricole intensif caractéristique du bassin versant de Kervidy-Naizin sans doute marqué, plus qu'ailleurs, par des stockages hérités de l'activité agricole.

4.2. Modelling of the opposite infra-annual dynamics of NO_3 and DOC concentrations in an agricultural headwater stream based on simple reservoirs assumptions

L. Strohmenger[1], O. Fovet1, M. Hrachowitz[2], J. Salmon-Monviola[1], C. Gascuel-Odoux[1]

[1] UMR SAS, INRAE, Institut Agro, 35 000 Rennes, France

[2] Department of Water Management, Faculty of Civil Engineering and Geosciences, Delft University of Technology, Delft, Netherlands

Key Points

- Mixing hypothesis based of two end-members with constant concentrations succeeds at reproducing seasonal and storm event dynamics of discharge, DOC and NO_3 concentrations.
- Including DOC and NO_3 concentrations for the calibration step changed relative distribution of water flows within the catchment.
- The dynamics of stream concentrations of DOC and NO_3 are primarily driven by water flow paths through groundwater (NO_3 rich) and riparian zone (DOC rich).
- Long-term dynamics require more complex representation of DOC and NO_3 cycling.

Abstract

Agriculture disturbs the biogeochemical cycles of major elements, leading to the alteration of elemental stoichiometry in surface stream waters with potential impacts on their ecosystems. However, catchment hydrological models and water quality models remain yet relatively disconnected. Multi-element conceptual modelling appears as a relevant and parsimonious approach for building hydro-chemical models and linking hydrological and water quality catchment processes. The opposition observed between DOC and NO_3 spatio-temporal patterns also make them a relevant couple of elements for constraining the hydrological transport pathways within catchments. Our purpose was to develop a simple conceptual model able to reproduce the infra-annual dynamics (seasonal and event-driven) of stream flow, DOC and NO_3 concentrations. We used the FLEX modelling framework and data from a small headwater agricultural catchment (AgrHyS observatory). The model consists in three reservoirs: an unsaturated reservoir, a slow reservoir representing the groundwater and a fast reservoir representing the riparian zone. The sources of DOC and NO_3 are assumed to behave as infinite storages with a fixed concentrations in each reservoir contributing to the stream. Stream concentrations are then supposed to result from the simple mixing of the slow and fast reservoirs. The model reasonably reproduced the annual and storm event dynamics of the discharge, DOC and NO_3 concentrations in the stream suggesting that the dynamics of concentrations were indeed primarily driven by the dynamics of mixing between water flow paths through groundwater (NO_3 rich and DOC poor) and through the riparian zone (DOC rich and NO_3 poor). The relative contribution of the slow reservoir to the stream is higher in the hydro-chemical model than in a hydrological model that would not take into account the concentrations but the hydro-chemical model also shows higher uncertainty on the hydrological parameters. The legacy storage of NO_3 resulting from past N fertilization excess in the studied catchment makes the assumption that main NO_3 and DOC sources behave as infinite pools at the scale of several years. Nevertheless, reproducing the long-term trends on solutes concentration would require more complex representations of the biogeochemical processes.

1. Introduction

Stream nutrient concentrations result from complex interactions between the physiographic characteristics of a catchment, anthropogenic and hydroclimatic conditions, biogeochemical processes and hydrological connectivity (*Basu et al.*, 2010; *Davis et al.*, 2014; *Dick et al.*, 2015). Past intensification of agriculture over the 20th century resulted in large nutrient legacy storages in catchments (*Basu et al.*, 2011; *Dupas et al.*, 2018; *Haygarth et al.*, 2014; *Hrachowitz et al.*, 2015) and losses to surface water in Europe (*Bouraoui and Grizzetti*, 2011; *Graeber et al.*, 2012; *Howden et al.*, 2011) and elsewhere (*Alexander and Smith*, 2006; *Bartsch et al.*, 2013; *Smith et al.*, 2013). Such losses can result in alteration of stoichiometry responsible for the degradation of water bodies (*Borah et al.*, 2002; *Fuss et al.*, 2017; *Lee et al.*, 2000). Reducing their transfer from lands to streams requires knowledge about their sources, transport and transformation processes (*Dusek et al.*, 2019; *Ford et al.*, 2018; *Pettersson et al.*, 2001).

Models can be used to test hypotheses about physical and biogeochemical processes governing the transfer and transformation of water and solutes (*Birkel et al.*, 2017; *Dusek et al.*, 2019; *Pettersson et al.*, 2001; *Trevisan et al.*, 2019). Perceptual and conceptual modelling of these processes are crucial steps of the learning frameworks in catchment sciences, such as described by *Dunn et al.* (2008) and *Beven* (2011). Because states cannot be directly observed and properties cannot be measured everywhere within a catchment, the model requires calibration of at least some of the parameters (Hrachowitz and Clark, 2017) using comparison metrics between model outputs and observations time series.

A better use of the chemistry time series, such as stream concentrations in chemical elements, besides the stream-flow (i.e. coupling biogeochemical and hydrological cycles) for the parameters calibration should improve the realism of hydrological models (*Birkel et al.*, 2017; *Fovet et al.*, 2015; *Hrachowitz et al.*, 2013a; *Pettersson et al.*, 2001; *Woodward et al.*, 2013). Authors usually distinguished three conceptual water components within a catchment: surface, vadose, and groundwater hydrology, each component associated to the following water flow paths: surface runoff, subsurface runoff and baseflow respectively (e.g. *Addiscott and Mirza* (1998)). These components differ in terms of chemical composition, water transit times and flow velocity (e.g. *Aubert et al.* (2013b)). Thus, the relative water fluxes contributions of multiple individual flow paths have an influence on the chemical composition of a river (*Woodward and Stenger*, 2018). These relative contributions vary in time (*Hrachowitz et al.*, 2013b), according to precipitation and catchment wetness that determine the infra-annual variations (seasonal, storm and inter-storm conditions) of solute concentration in the river (*Zuecco et al.*, 2016). Using time series of multiple elements may provide further insights on the relative contributions and on the dynamics of the different water flow paths. Therefore, they may also increase the confidence on models parameters and the realism of our perception of the catchment behavior. This is particularly true if the spatial distribution and the stream concentration dynamics of these elements are well contrasted (*Shafii et al.*, 2019; *Shrestha et al.*, 2013; *Woodward and Stenger*, 2018) such as it is frequently the case for DOC and NO_3 (*Taylor and Townsend*, 2010). Previous studies, for example showed that the seasonal variation of Dissolved Organic Carbon (DOC) and nitrate (NO_3) are related to the water table fluctuation in groundwater-fed catchments (*Abbott et al.*, 2018; *Aubert et al.*, 2013b; *Strohmenger et al.*, 2020; *Thomas et al.*, 2016). In contrast, short-term variations of DOC and NO_3 have been linked to the activation of subsurface and surface flow paths during storm events and the consequent mobilization of DOC-rich and NO_3 poor riparian soils, especially the surface layers (*Bernal et al.*, 2002; *Bowes et al.*, 2015; *Fovet et al.*, 2018a; *Outram et al.*, 2014; *Strohmenger et al.*, 2020).

Several (semi-)distributed process-based hydrological models reproduce both NO_3 and DOC stream concentrations such as SWAT (*Arnold et al.*, 1998), TNT2 (*Beaujouan et al.*, 2002), INCA (*Whitehead*

et al., 1998), or HYPE (*Lindström et al.*, 2010). They account for different biogeochemical processes or for the same processes, using different formalisms (see e.g. *Ferrant et al.* (2011)). These (semi-)distributed approaches usually aimed at dynamically following the spatial evolution of a solute within the catchment explicitly considering differences in land use, agricultural practices or climate conditions. These models typically treat NO_3 and DOC separately in distinct routines or even in different versions of the model leading to different representations depending on the element, and are applicable on medium to large catchment area. As highlighted by *Beven* (2001), the particularity of distributed models is that parameter values can potentially be different for every element in the spatial discretization (grid or hydrological response unit), meaning that a very high number of parameter values must be specified (*Kelleher et al.*, 2017). The limited information in observed data sets available for constraining these parameters may lead to equifinality (*Beven and Binley*, 1992; *Beven and Freer*, 2001), which is not specific to distributed models though.

Recently, one can notice a renewed interest for more lumped and more conceptual hydrological and biogeochemical models "with parsimonious and more abstract representations of the processes" at the catchment scale (*Hrachowitz and Clark*, 2017). *Xu et al.* (2012), *Seibert et al.* (2009) and *Musolff et al.* (2016) expressed the loads of DOC or total organic carbon and NO_3 with respect to groundwater storage only. *Birkel et al.* (2014), *Fovet et al.* (2015) and *Woodward and Stenger* (2018) successfully applied catchment-scale conceptual models to simulate stream loads of DOC or NO_3.

However, catchment hydrological models and water quality models at the catchment scale remain yet mainly disconnected, as highlighted and detailed in the overview by Hrachowitz et al. (2016), and such disconnection increases again between various water quality models that consider different chemical elements of the water quality.

The purpose of this study was therefore to develop a conceptual model able to reproduce multi-elemental hydro-chemical stream signatures. We selected as such signatures the infra-annual dynamics of stream flow and stream DOC and NO_3 concentrations due to their opposite dynamic. We hypothesized that:

i) it was possible to reproduce the infra-annual (at seasonal and storm-event scales) dynamics of DOC and NO_3 concentrations in the stream using only the mixing of two compartments characterized by contrasted hydrological reactivity and chemistry according to the assumptions from previous studies (*Strohmenger et al.*, 2020).

ii) the hydrological behavior would change when integrating the water quality into the model. Therefore, we expected the hydrological parameter sets to be different when calibrating only a hydrological model using stream flow and when calibrating the complete model using both stream flow and concentrations, and their uncertainty too.

The results of this study may provide a contribution to the development of a more integrated understanding of catchments and will constitute a first step in strengthening the link between catchment-scale hydrological and water quality models.

2. Methods

2.1. Study site

The Kervidy-Naizin catchment is located in the Brittany region, Western France (48°N; 2°5'W, Figure B 1) and part of the AgrHyS Critical Zone Observatory (*Fovet et al.*, 2018b). This 5-km² headwater catchment is dominated by intensive agricultural activities (*Viaud et al.*, 2018). Land use is characterized by intensive mixed cropping-farming, with maize, cereals and grasslands, and a high indoor livestock density. The topography is relatively flat, the elevation ranges from 98-140 m above sea level. Soils are Cambisols and Luvisols with silty loam texture (FAO classification (*WRB*, 2006)). The parent material is made of impermeable Brioverian schists and above it a fissured and fracture layer mantled by weathered layer from 1 to 30 m deep (*Molénat et al.*, 2005). The climate is temperate oceanic, with an average annual temperature of 11.2 ± 0.6°C (mean ± standard deviation). Average annual precipitation reaches 810 ± 180 mm yr^{-1}. The outlet is a second Strahler order intermittent stream (frequently dry between July-October) with average runoff of 296 ± 150 mm yr^{-1}. Within the landscape, DOC and NO_3 accumulate rather in wetlands soils and groundwater, respectively (*Aubert et al.*, 2013b; *Strohmenger et al.*, 2020).

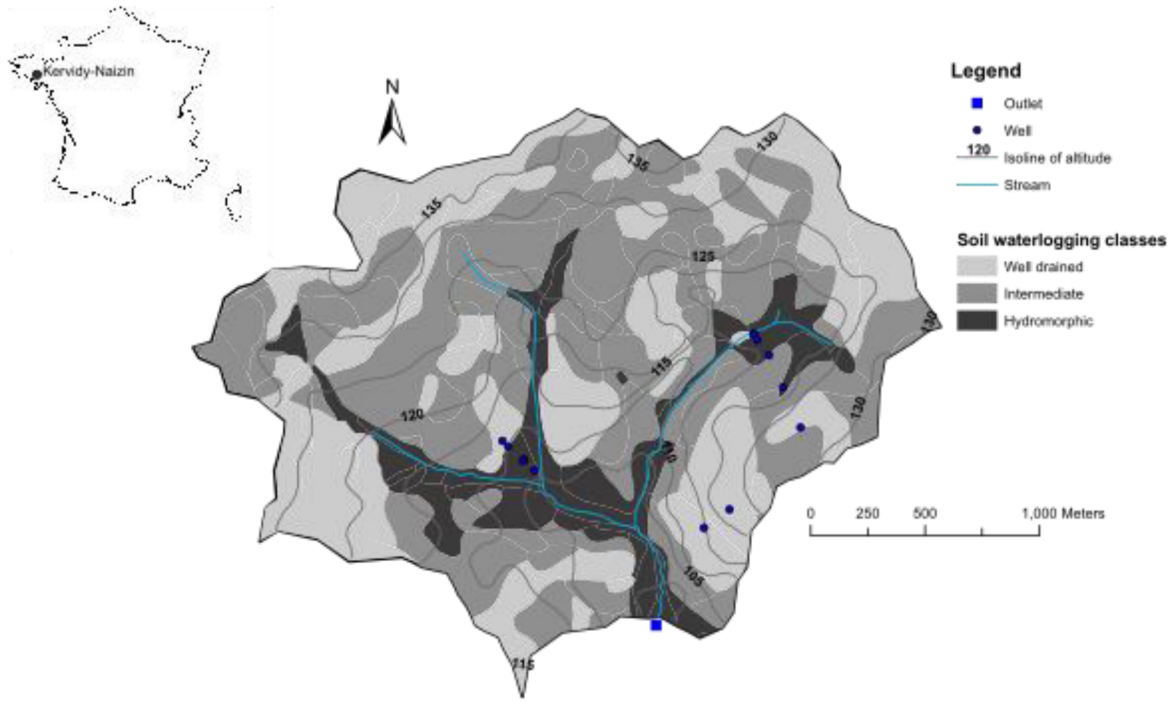

Figure B 1 Map of the Kervidy-Naizin catchment (Brittany, France, source : Aubert et al. (2013a))

2.2. Data monitoring

We used daily aggregated meteorological and streamflow's measurements collected from 2002-2017. Precipitation, air temperature, global radiation and wind speed were recorded hourly by a

weather station (Cimel Enerco 516i) located 1 km east of the outlet. Potential evapotranspiration (PET) was calculated using the Penman equation (*Penman*, 1956). Stream level was recorded at the outlet of the catchment every minute by a *float*-operated *shaft-encoder* level sensor (Thalimedes OTT), then converted to stream flow using a rating curve (*Carluer*, 1998).

Stream water was sampled manually every day at ca. 17:00 at the outlet station. Samples were filtered in the field (pore size: 0.22 µm) and stored in the dark at 4°C in propylene bottles. Analyses were performed within two weeks of sampling. NO_3 concentrations were measured by ionic chromatography (DIONEX DX 100, *ISO 10304* (1995), precision: 2.5%). DOC was estimated as total dissolved carbon minus dissolved inorganic carbon using a carbon analyzer (Shimadzu TOC 5050A, *Petitjean et al.* (2004), precision on DOC: 0.7 mg l^{-1}).

3. Model description

3.1. Model structure

We used a simple semi-distributed hydrological model based on the FLEX model family (*Fenicia et al.*, 2006) for simulating the hydrological fluxes. We have chosen the model structure following the approach proposed by *Hrachowitz et al.* (2014). The selected model structure (Figure B 2) comprises three reservoirs, very similar to the conceptual model of *Birkel et al.* (2010): the unsaturated reservoir (SU), the slow responding reservoir (SS) and the fast responding reservoir (SF). Conceptually, the SU, SS and SF reservoirs represent the unsaturated root-zone of the hillslopes, the groundwater and the riparian compartments within the catchment, respectively. The water fluxes via SF reservoir are interpreted as preferential and overland flows (Q_F), the fluxes from SU to SS represent the infiltration and groundwater recharge (R_{SS}), and the fluxes from SS to stream as the base flow sustained by shallow groundwater (Q_S).

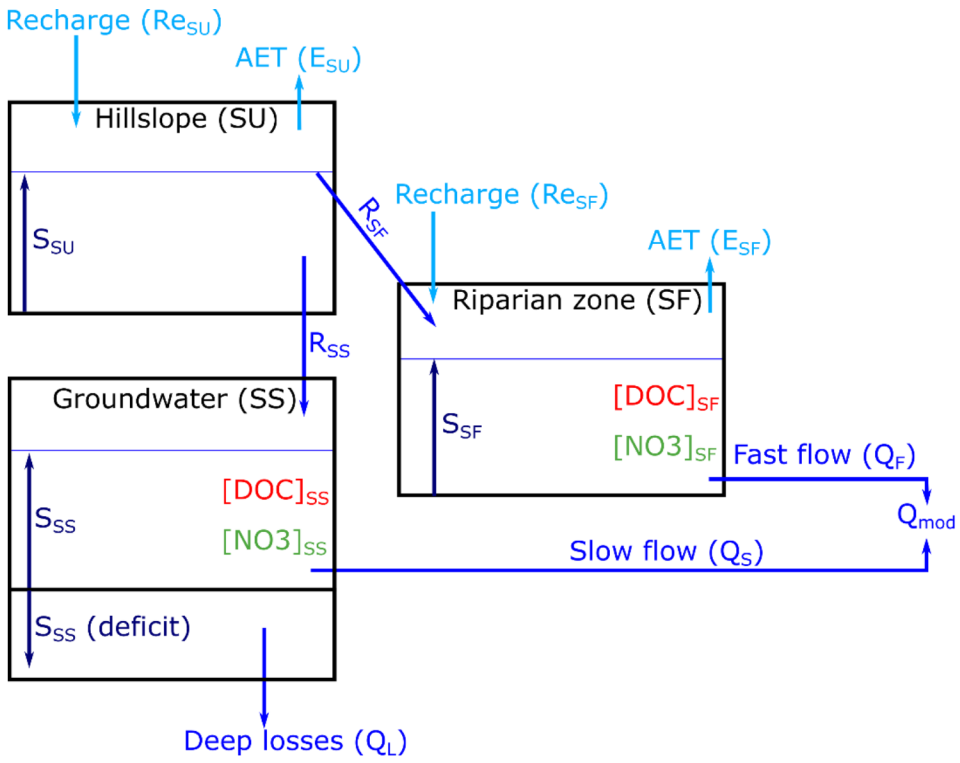

Figure B 2 Conceptual diagram of the hydro-chemical model. S_i is the water storage in the i^{th} reservoir.

The rainfall-runoff model (Figure B 2) used daily rainfall P [mm] and PET [mm] to model daily specific discharge [mm d^{-1}] at the outlet. The hillslope runoff coefficient (Cr) depends of the volume of actual water stored in SU (Table B 1). We used SU_{cr} as a power of 10 in order to allow for a uniform distribution of <1 and >1 exponent of the S_U water saturation (logarithmic and exponential relationship between Cr and saturation, respectively).

Table B 1 Water balance and flux equations used in the model.

Reservoir	Process	Flux Equations	Units
S_U	Recharge	$Re_{S_U} = S_{U\,surface} P$	L d^{-1}
	Runoff coefficient	$Cr = \left(\frac{S_{S_U}}{S_{U_{capacity}}}\right)^{10^{SU_{cr}}} \leq 1$	-
	Runoff	$Ru = CrP$	L d^{-1}
	Recharge from S_U to S_S	$R_{S_S} = RuSU_{cp}$	L d^{-1}
	Runoff from S_U to S_F	$R_{S_F} = Ru\,(1 - SU_{cp})$	L d^{-1}
	Evaporation	$E_{S_U} = SU_{surface} PET \leq S_{S_U}$	L d^{-1}
	Water balance	$dS_{S_U} = Re_{S_U} - Ru - E_{S_U}$	L d^{-1}
S_S	Slow Flow	$Q_S = k_{S_S} S_{S_S}$	L d^{-1}
	Water balance	$dS_{S_S} = R_{S_S} - Q_S - Q_L$	L d^{-1}
	Solute flux to stream	$F_{S_S} = Q_S C_{S_S}$	mg
S_F	Recharge from rain	$Re_{S_F} = S_{F\,surface} P$	L d^{-1}
	Fast flow	$Q_F = k_{S_F} S_{S_F}$	L d^{-1}
	Evaporation	$E_{S_F} = SF_{surface} PET \leq S_{S_F}$	L d^{-1}
	Water balance	$dS_{S_F} = Re_{S_F} - E_{S_F} - Q_F$	L d^{-1}
	Solute flux to stream	$F_{S_F} = Q_F C_{S_F}$	mg
Stream	Total discharge	$Q_{mod} = Q_S + Q_F$	L d^{-1}
	Solute concentration	$C_{stream} = \frac{F_{S_S} + F_{S_F}}{Q_S + Q_F}$	mg l^{-1}

The produced hillslope runoff is redistributed among S_F and S_S reservoirs according to SU_{cp} parameter. Remaining water in S_U reservoir is available for evapotranspiration (E_{S_U}, Figure B 2).

The slow reservoir (S_S, Figure B 2) receives water flow from the hillslope runoff. This reservoir S_S slowly drains into the stream flow (Q_s, Figure B 2) following a linear storage-discharge relationship controlled by the parameter k_{S_S} (Table B 2) if the actual S_S water storage is positive. Indeed, a storage deficit in the S_S reservoir is possible in the model structure (Figure B 2) and this deficit must be filled to enable the activation of the slow flow from S_S in order to reproduce the no-flow period at the outlet during summer. We attributed a constant draining flow from S_S reservoir (Q_L, Table B 2) that reproduces the deep losses from shallow groundwater.

The fast reservoir (S_F, Figure B 2) receives water from the hillslope runoff and some direct rainfall. S_F reservoir rapidly drains (Q_F, Figure B 2) into the stream following a linear storage-discharge relationship controlled by the parameter k_{S_F} (Table B 2). Remaining water in S_F reservoir is available for evapotranspiration (E_{S_F}, Figure B 2).

The total modelled stream discharge (Q_{mod}) is the sum of the slow and fast contributions from S_S and S_F, respectively (Figure B 2).

*Table B 2 Uninformed prior parameter distributions and descriptions of the parameters of the hydro-chemical model. * $SF_{surface}$ is calculated as 1 – $SU_{surface}$, thus it is not a calibrated parameter.*

parameter	Prior range of parameter		unit	description
$SU_{surface}$	0,7	1,0	% catchment size	Surface of the hillslope reservoir
$SU_{capacity}$	1,0	500,0	L	Maximum storage of the unsaturated reservoir
SU_{cr}	-1,0	1,0	-	Controls the hillslope runoff generation
SU_{Cp}	0,0	1,0	%	% of hillslope runoff into fast reservoir
k_{Ss}	0,0	0,1	$.d^{-1}$	storage coefficient of slow reservoir
k_{Sf}	0,1	1,0	$.d^{-1}$	storage coefficient of fast reservoir
Q_L	0,0	1,0	$L\ d^{-1}$	deep losses from groundwater
$SF_{surface}$*	0,0	0,3	% catchment size	1 - $SU_{surface}$
SS_{DOC}	0	30	$mg\ l^{-1}$	DOC concentration in slow reservoir
SS_{NO3}	0	100	$mg\ l^{-1}$	NO_3 concentration in slow reservoir
SF_{DOC}	0	30	$mg\ l^{-1}$	DOC concentration in fast reservoir
SF_{NO3}	0	100	$mg\ l^{-1}$	NO_3 concentration in fast reservoir

3.2. Chemical model

An objective of the model was to assess if a simple model based on hydrological contributions and two different sources of the solutes can reproduce the DOC and NO_3 temporal patterns of stream concentrations. We assumed that the fast and slow reservoirs are the main sources of DOC and NO_3, respectively. Fast reservoir represents riparian soils and generates the surface water flow paths contributions to stream which have been identified as the main source of DOC, and to contribute mainly during storm flows (*Lambert et al.*, 2014; *Morel et al.*, 2009). Slow reservoir represents the shallow groundwater, which receives NO_3 leaching from the unsaturated reservoir and generates the subsurface water flow paths contributions to stream which dominate the base flow and the export of NO_3 (*Aubert et al.*, 2013b; *Molénat et al.*, 2008). Thus, we set different and fixed DOC and NO_3 concentrations in SF and Ss reservoirs, so that there is no need to specify concentration in SU (Figure B 1). Using fixed concentrations, we assumed that both reservoirs acted like infinite pools of solutes. Because of the larger supply of DOC from riparian organic soils (*Humbert et al.*, 2015; *Lambert et al.*, 2013), and because of the legacy mass storage of NO_3 connected to stream via groundwater (*Basu et al.*, 2010; *Molénat et al.*, 2008), these compartments, indeed, behave like an infinite source of DOC and NO_3, respectively. We defined the prior range of values of the solutes concentration based on the observed 2002-2017 time series (Table B 2).

The daily stream concentration of a solute is the result of the mixing of two end members: the slow and fast flow components where we assume the complete mixing of the solutes (Table B 1). We assumed no process to occur in the stream because we do not have information to evaluate such processes and to discriminate them from the mixing processes. This assumption seems reasonable regarding that the study site is a small headwater catchment with short distance (up to 2 km) from the spring to the outlet (*Morel et al.*, 2009).

3.3. Performance metrics and model calibration

We used the Kling–Gupta efficiency score (KGE, *Gupta et al.* (2009)) to assess the goodness of fit between the modelled and the observed times (Equation 1).

$$KGE_X = \sqrt{(r-1)^2 + (\alpha-1)^2 + (\beta-1)^2} \quad (1)$$

$$r = corr(X_{obs}, X_{sim}) \quad \alpha = \frac{\sigma_{sim}}{\sigma_{obs}} \qquad \beta = \frac{\mu_{sim}}{\mu_{obs}}$$

Where μ and σ are the mean and standard deviation of observed and simulated time series *X* which can be stream flow or concentrations variables. KGE ranges from 0-infinity, optimal parameter sets tends to minimize the KGE score.

The solute concentration depends greatly on the quality of the discharge simulation (Figure B 3) and solutes time series, which contains missing value for the dry period. For these reasons we chose to compute the solute KGE score by excluding the simulated and observed concentrations couple at any time t when the relative error between observed and simulated discharge is higher than 0.5 (Equation 2).

$$ER(t) = \frac{|Q_{obs}(t) - Q_{sim}(t)|}{Q_{obs}(t)} \quad (2)$$

Where *ER(t)* is the relative error on discharge at time *t*. In addition, we computed a *cover estimator* (in %) as the ratio of the number of days with simulated concentration and observed concentration. We computed the cover estimator in order to penalize good solute KGE score obtained on a very few couples of simulated-observed DOC or NO_3 concentration (i.e. with high ER on the discharge, Equation 3).

$$KGE_{solute} = KGE(C_{obs}, C_{sim}) + 1 - cover\ estimator \quad (3)$$

Where KGE_{solute} is the KGE score of DOC or NO_3 simulation adjusted with the *cover estimator*. We assessed the overall goodness of fit (KGE_{global}) of the model as the Euclidian distance of the equally weighted KGE scores of discharge, DOC and NO_3 (Equation 4).

$$KGE_{global} = \sqrt{KGE_Q^2 + KGE_{DOC}^2 + KGE_{NO3}^2} \quad (4)$$

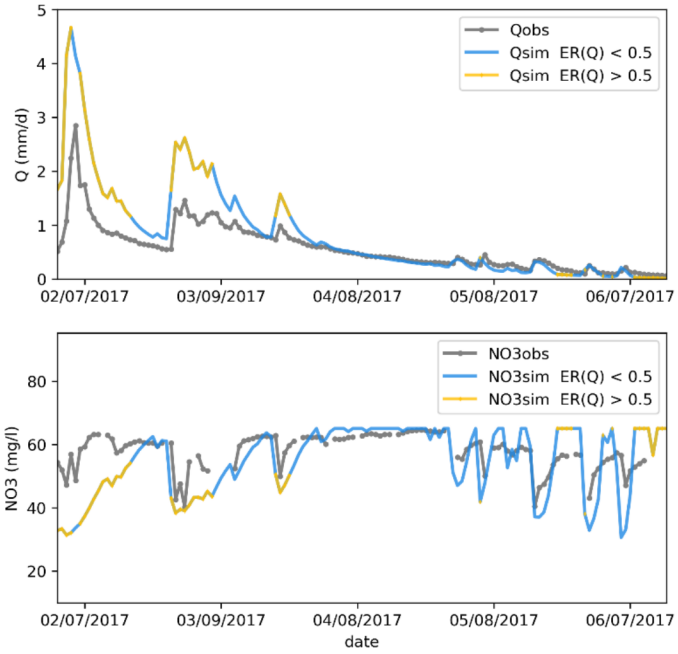

Figure B 3 Periods of evaluation of the concentrations KGE are represented by the blue lines when the relative error on discharge is <0.5.

We used the global likelihood uncertainty estimation (GLUE, *Beven and Binley* (1992)) to estimate parameters values and uncertainties. The calibration period was set to 2013-2017, after a 2 years warmup period, whereas the period 2002-2012 was used as model test period. We conducted a Monte Carlo random sampling strategy (10^7 iterations) with uniform prior parameter distributions between the ranges shown in Table B 2. The parameter sets from prior distribution are assessed in terms of some likelihood measure relative to the observations. We used an inversed normalized KGE_{global} so that the objective function value increases with increasing goodness of fit of the simulations (Equation 5).

$$OF^i = \frac{\sum_n KGE^n}{KGE^i} \quad (5)$$

Where OF^i is the inverse normalized *KGE* of the i^{th} parameter set simulation, and *n* the total number of parameter sets used to estimate the uncertainty. We retained the 1000 best simulations (0.01%) as acceptable or "behavioral" parameters sets (*Beven and Freer*, 2001). Calibrated values and associated uncertainty were estimated using the median value of the acceptable range and the 10^{th}-90^{th} confidence intervals. We conducted twice such calibration: one for the hydrological parameters only using the KGE_Q and one for all the parameters using the KGE_{global}.

4. Results

4.1. Modelled discharge and concentrations

Overall, the model succeeded at reproducing discharge and solutes time-series (Figure B 4) after calibrating using the KGE_{global}. The KGE scores of the median simulation were for the calibration and validation periods respectively: 0.18 and 0.23 for discharge; 0.61 and 0.78 for DOC; 0.72 and 0.91 for NO_3. The model performs similarly during calibration period and test period (2008-2012, Figure B 4) except for NO_3 which showed a constant bias error with an overall underestimation of about 10 mg l^{-1} during the test period.

The modelled discharge reproduced well the seasonal observed dynamics among the recharge, wet and recession periods. Daily peaks of discharge associated to storm events were very well captured during the wet period and slightly overestimated for the recharge and recession periods. Even though the modelled discharge was often equal to zero during the dry period, thus capturing the main feature of base flow during this period, the model generated storm-events flow responses that were unobserved on the measured discharge for this period. The confidence intervals of the modelled stream flow were narrow and included the observed data most of the time (Figure B 4).

The model well reproduced the opposition of DOC and NO_3 stream dynamics at seasonal and storm-event time-scales (Figure B 4). In the fall season, median simulated concentrations were above 10 mg l^{-1} of DOC and below 40 mg l^{-1} of NO_3. They decreased during the rewetting period to less than 5 mg l^{-1} of DOC and increased up to more than 70 mg l^{-1} of NO_3, remained at these levels during the wet and recession periods. At the end of the recession period, they slightly increased to ca. 5 mg l^{-1} of DOC and decreased to ca. 40 mg l^{-1} of NO_3. The storm event dynamics of the solutes were also well reproduced. Concentrations increased by ca. 5 mg l^{-1} of DOC and decreased by ca. 20 mg l^{-1} of NO_3 during storm event, though the increases of DOC were slightly underestimated at the beginning of the rewetting period and overestimated at the end of the recession period. Dilutions of the simulated NO_3 during storm event were often slightly underestimated in comparison with observed NO_3 storm dilutions. The confidence intervals of the modelled concentrations included the observed data most of the time, and were relatively narrow for DOC and wider for NO_3 concentration that display higher uncertainty (Figure B 4).

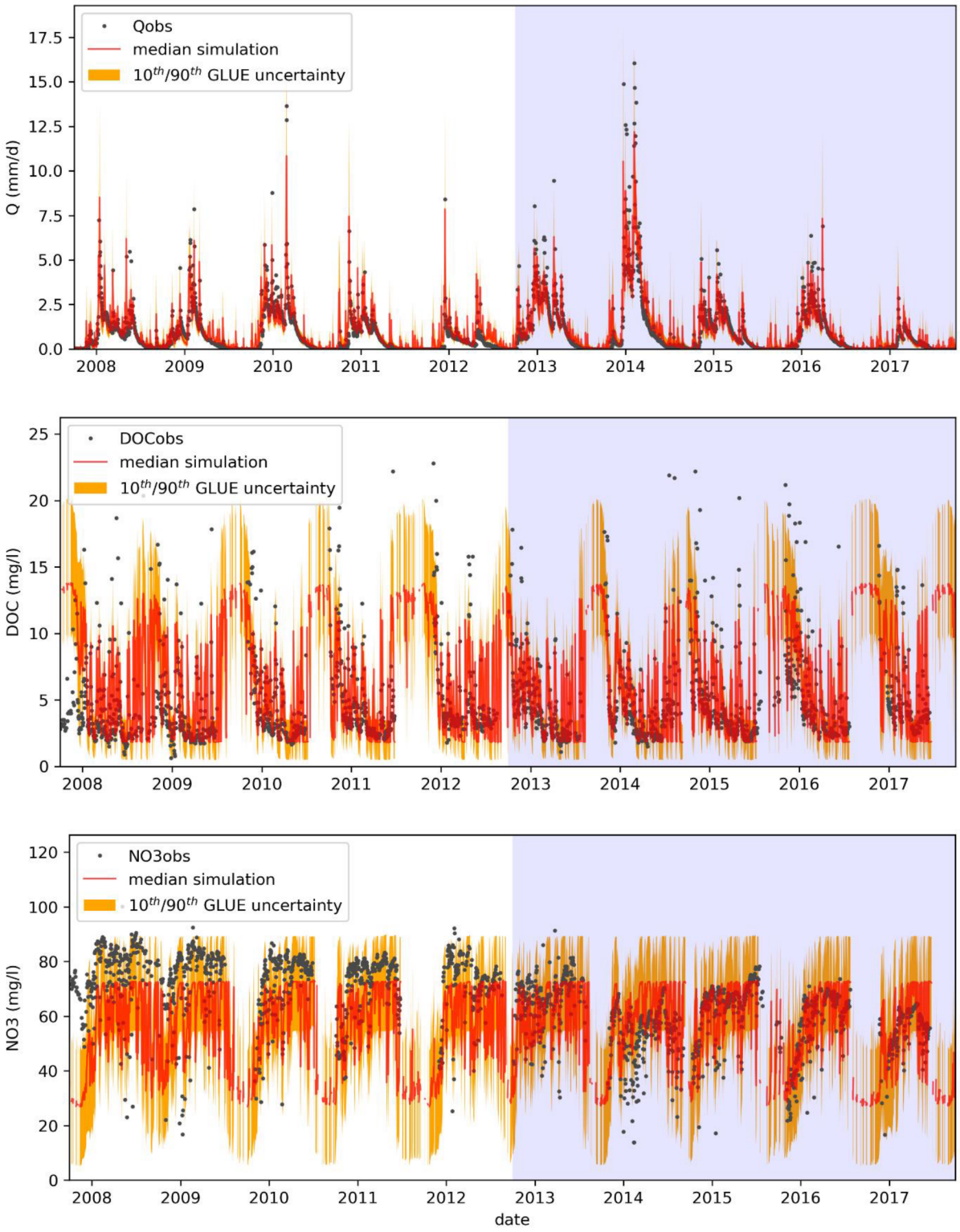

Figure B 4 Observed (grey dots), median (red line), and 10th/90th confidence intervals (orange area) of the modelled times series of Q, DOC and NO_3 after calibrating with the global KGE objective function. Shaded area (2013-2017) covers the calibrations period while the white area covers the test period.

4.2. Hydrological versus hydro-chemical performances

Discharge simulations reached lower KGE scores than solute KGE scores (Figure B 5). The minimum KGE scores after 10^7 simulations were 0.05, 0.5 and 0.6 for Q, DOC and NO_3, respectively. The best simulations (lower KGE scores) of DOC (KGE between 0.5-0.7) and NO_3 (KGE between 0.6-0.8) were associated to good (but not best) simulations of the discharge (KGE between 0.08-0.2).

Increasing the KGE score of the discharge (from 0.05 to 0.1) decreased the KGE scores of DOC (from 1.0 to 0.6) and NO_3 (from 0.8 to 0.6). Further increase of the discharge KGE (from 0.1 to ca. 0.3) did not change solutes KGE scores. Finally, increasing the KGE score of the discharge (over 0.3) increased the KGE score of the solutes.

The 1000 best simulations based on the global performance (Figure B 5) were associated to a wide range of performance of the simulated discharge (0.07-0.7) and to solutes KGE from 0.5-1.0 (purple area, Figure B 5). The best NO_3 KGE scores were compatible with the best DOC KGE scores (Figure B 5).

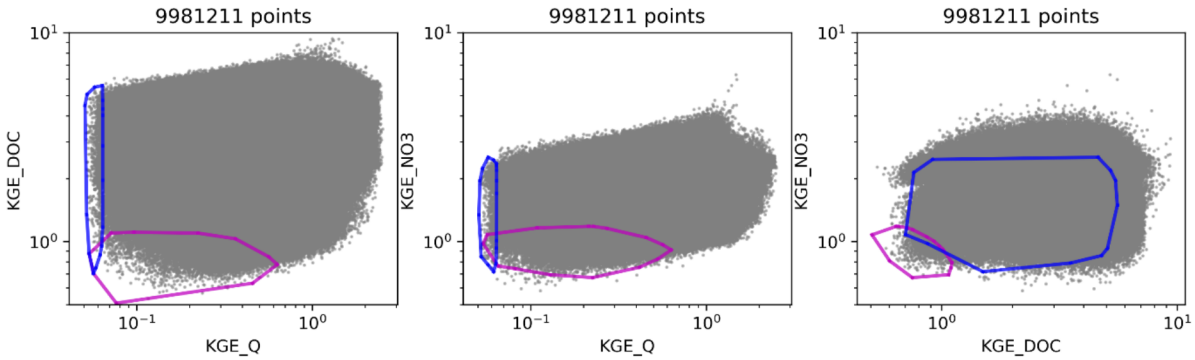

Figure B 5 Log scaled dotty plots of the KGE scores after 10^7 simulations. The circled areas include the 1000 best simulations based on discharge only (KGE_Q, blue), and overall (KGE_{global}, purple) performance metrics.

4.3. Parameters

The DOC concentrations were lower in the Ss reservoir than in the Sf reservoir with a median value (10^{th}/90^{th} quantiles) of 2.5 (0.5/6.9) mg l^{-1} and 12.8 (6.5/21.3) mg l^{-1}, respectively (Table B 3). The NO_3 concentrations were higher in the Ss reservoir than in the Sf reservoir with 71.6 (39.5/92.8) mg l^{-1} and 32.3 (7.2/65) mg l^{-1}, respectively.

The calibration of the model with the global objective function tended to increase uncertainties on hydrological parameters in comparison with the hydrological objective function (Table B 3) except for Su_{cp} that controls the redistribution of hillslope runoff between the riparian zone and the groundwater.

The calibration of the model with the global objective function also changed the median value of the behavioral parameters sets (Table B 3). The surface of the hillslope slightly decreased (i.e. surface of the riparian zone increased) but its storage capacity (S_{Su}) increased a little. Parameters that control the flowrates of Ss (k_{Ss}) and Sf (K_{Sf}) reservoirs slightly decreased and increased, respectively. Deep losses remained almost identical between pure hydrological and global calibration.

*Table B 3 Estimated median parameters values (and 10th-90th confidence intervals) after calibration with pure hydrological (KGE_Q) and global (KGE_{global}) objective functions. * $SF_{surface}$ is calculated as 1 – $SU_{surface}$, thus it is not a calibrated parameter*

parameter	*KGE_Q*	*KGE_global*	*unit*
$SU_{surface}$	0.93 (0.82 - 0.99)	0.90 (0.76 - 0.98)	% of catchment size
$SU_{capacity}$	178.51 (109.77 - 227.51)	212.25 (62.74 - 422.38)	L
SU_{Cr}	0.49 (0.18 - 0.85)	-0.03 (-0.76 - 0.72)	-
SU_{Cp}	0.31 (0.08 - 0.88)	0.21 (0.05 - 0.50)	%
k_{SS}	0.06 (0.04 - 0.09)	0.04 (0.01 - 0.08)	$.d^{-1}$
K_{SF}	0.24 (0.13 - 0.49)	0.51 (0.20 - 0.86)	$.d^{-1}$
$SF_{surface}$	0.07 (0.01 - 0.18)	0.10 (0.02 - 0.24)	% of catchment size
Q_L	0.17 (0.04 - 0.44)	0.20 (0.03 - 0.62)	$L\ d^{-1}$
SS_{NO3}		70.97 (39.64 - 92.72)	$mg\ l^{-1}$
SS_{DOC}		2.52 (0.56 - 6.88)	$mg\ l^{-1}$
SF_{NO3}		30.90 (6.73 - 64.37)	$mg\ l^{-1}$
SF_{DOC}		12.79 (6.51 - 21.39)	$mg\ l^{-1}$

4.4. Water budgets

For the 1000 best simulations based on the KGE_Q only, the modelled evapo-transpiration was of 480 mm yr^{-1} in average (Figure B 6) with 463 and 17 mm yr^{-1} from SU and SF reservoir, respectively. The modelled annual runoff at the outlet was 364 mm yr^{-1} in average with 53.0 % from SS (193 mm yr^{-1}) and 47.0% from SF (171 mm yr^{-1}) reservoirs, and the annual deep losses from the SS reservoir approximated 57 mm yr^{-1} (15.7% of annual runoff).

When calibrated on KGE_{global}, the simulated evaporation-transpiration from SU were lower (416 mm yr^{-1}) and similar for SF (18 mm yr^{-1}, Figure B 6). Runoff increased up to 398 mm yr^{-1}, with higher contributions from SS (242 mm yr^{-1}, 60.8%) and lower from SF (156 mm yr^{-1}, 39.2%). Deep losses slightly increased to 61 mm yr^{-1}.

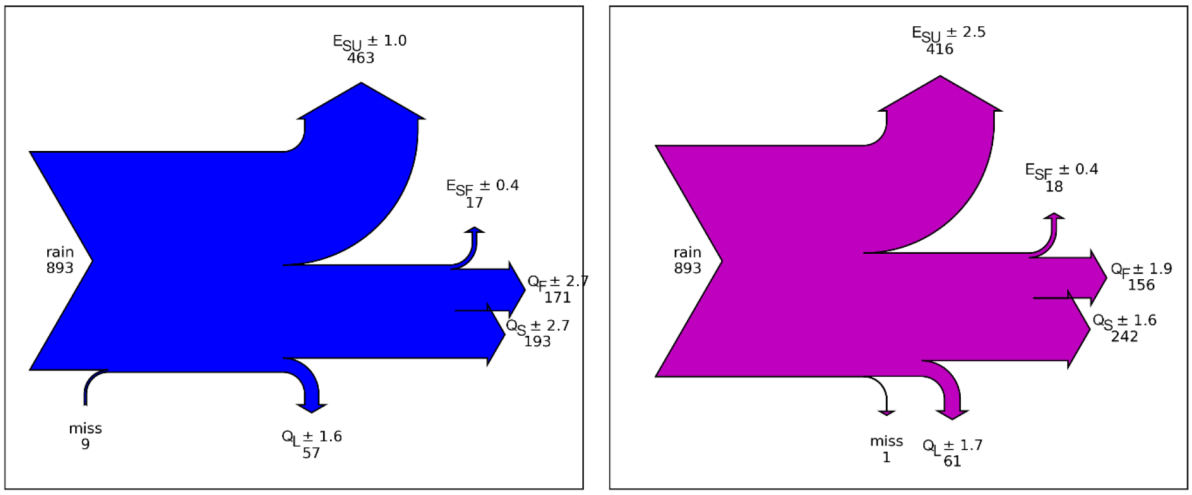

Figure B 6 Average annual water budgets ± standard error (mm yr^{-1}) for the 1000 best simulations based on (a) KGE_Q, (b) KGE_{global}. "Miss" is the balance between outflows and inflows.

5. Discussion

5.1. Reproducing DOC and NO_3 dynamics using a simple mixing model

The results suggest that a simple model with three reservoirs is a plausible conception of the study catchment to simultaneously explain the seasonal, storm and inter-storm dynamics of Q, DOC and NO_3. The main source of NO_3 within the catchment was modelled in the slow reservoir that represent more or less the groundwater compartment with a calibrated constant concentration of ca. 70 mg l^{-1}, while the fast reservoir that can be assimilated to the riparian compartment was calibrated to ca. 30 mg l^{-1} (Table B 3). Conversely, the main source of DOC of our calibrated model was the slow reservoir (*Casson et al.*, 2019; *Dick et al.*, 2015; *Morel et al.*, 2009) with a calibrated concentration of ca. 13 mg l^{-1} in S_F reservoir versus ca. 3 mg l^{-1} in S_S reservoir (Table B 3). These calibrated concentrations were consistent with DOC and NO_3 observed concentrations of 1.2 and 91.7 mg l^{-1} respectively in deep groundwater, and 19.8 and 6.7 mg l^{-1} respectively in wetland for the 2000-2010 period on the same catchment (*Aubert et al.*, 2013b). The hierarchy and order of magnitude of concentrations observed into groundwater versus riparian wetland are similar to those of concentration calibrated into slow reservoir versus fast reservoir.

The high amount of NO_3 stored in groundwater originates from past agricultural activities on the catchment (*Aubert et al.*, 2013b; *Basu et al.*, 2010; *Dupas et al.*, 2018; *Molénat et al.*, 2008; *Strohmenger et al.*, 2020). The N-surplus generated by excessive organic fertilization leached and accumulated into the vadose zone and the groundwater. The low NO_3 concentration in the riparian zone is explained by heterotrophic denitrification that can occur in this compartment under anoxic conditions when the water table reaches the soil surface (*Bell et al.*, 2015; *Casson et al.*, 2019; *Montreuil et al.*, 2010; *Oehler et al.*, 2009). Conversely, measured DOC concentration in groundwater was low (*Aubert et al.*, 2013b), whereas high amount of DOC was found in the riparian soils, which depict high soil organic matter content, especially in the surface layers where DOC produced from microbial biomass decay or leaf decomposition can accumulate (*Birkel et al.*, 2014; *Humbert et al.*, 2015; *Morel et al.*, 2009). The differences of hydrological reactivity and chemical composition between those two conceptual reservoirs, that we can relate to groundwater and riparian zone, allowed to reproduce the contrasting dynamics of the DOC and NO_3 stream concentrations. The S_S reservoir, which is NO_3 rich and DOC poor, contributes to the base flow, controlling the seasonal patterns of concentrations when the water table is hydrologically connected to the stream. The S_F reservoir, which is DOC rich and NO_3 poor, contributes mostly during storm events, driving the fast increases (decreases) of DOC (NO_3) stream concentrations, in comparison with the inter-storm days.

Even though the model succeeded quite well at reproducing seasonal and storm dynamics, we can underline that the simulated NO_3 showed constant underestimation of the concentrations for the validation period and wider confidence intervals than the discharge and the DOC concentrations. This underestimation is likely due to the long-term trend on NO_3 time series. This multi-annual trend has been related to the reduction of agricultural N-surplus which occurred mainly between 1998 and 2008 and induced a delayed decrease in groundwater concentration, thus in stream concentrations (*Dupas et al.*, 2018; *Strohmenger et al.*, 2020). Our model, focused on infra-annual dynamics, and the use of a constant parameter for groundwater concentration does not allow to reproduce such long-term trend. Hence, to model inter-annual dynamics of NO_3, one need to consider the inter-annual dynamics of NO_3 in the groundwater. This could be achieved as a first approach by a fitted trend S_S concentration with respect to time. Another approach would be to explicitly represent the Nitrogen net inputs, transport and fate through the three reservoirs.

Other authors also proposed such simple mixing assumptions for DOC modelling at larger scale with landscape-mixing model (e.g. *Ågren et al.* (2014) or at similar scales (e.g. *Boyer et al.* (1996)). In the literature, the concentrations of hydrological reservoirs are also often represented as a function of temperature and moisture as these factors control the principal biogeochemical processes influencing DOC and NO_3. Temperature and water saturation level both increase the apparent production of DOC via solubilization and desorption (e.g. *Birkel et al.* (2014) and *Birkel et al.* (2020)) and the denitrification rate of NO_3 (e.g *Birkel et al.* (2014). As a first investigation, we tested the interest of adding such temperature and moisture effect using linear functions of air temperature, reservoir storage, or both in the slow and fast reservoirs but without significant improvement of the model performances according to the KGE_{global} scores (results not shown).

5.2. Benefits of the global calibration for better constraining the hydrological model

The global calibration, taking into account of the concentrations in stream, changed the distribution of water flows within the catchment in comparison with the hydrological calibration. The increased median values of $SF_{surface}$ and k_{SF} (Table B 3) suggest that the global calibration lead to faster flowrate in the S_F reservoir. Thus, simulations of the solutes dynamics are optimized with more contrasted hydrological reactivity for S_S and S_F reservoirs. The decrease of Q_F (Figure B 6) implies that the S_F reservoir received less water from the S_U reservoir (E_{SF} remained the same). Indeed, the ratio of hillslope runoff from S_U to S_F (SU_{cp} parameter, Table B 3) decreased with the global calibration. Thus, the model that takes account of the solutes concentrations suggests that the hillslope contributes more to vertical flows (i.e. groundwater recharge) than horizontal flows (i.e. hillslope runoff, preferential flows) in comparison with the hydrological model calibrated on stream flow time series only. Furthermore, this exhibits the need to improve the formulation of transit times and water flow paths. Representing and calibrating explicitly the transit times within the reservoirs could improve the model. *Rinaldo et al.* (2015) proposed a tool to simulate the distribution of water ages of a reservoir outflow using the storage selection functions (SAS-functions). SAS functions have been used with success in studies such as *Harman* (2015) and *Benettin et al.* (2017) for the simulation of isotopes dynamics and Cl concentration in stream, respectively.

Unlike we expected, the parameters uncertainties (Table B 3) increased in overall when calibrating with the global objective function (KGE_{global}) compared to the hydrological objective function (KGE_Q). Therefore, the simulated concentrations were less sensitive to hydrological parameters than we expected and adding concentration time series in the objective function lead to more overall equifinality.

5.3. Relevance of the model and perspectives for studying climate effects on water quality

The model showed higher uncertainties and residual for the rewetting and recession periods than for the wet period (Figure B 4). In addition, the model overestimated the NO_3 concentration for extreme hydrological years such as 2014 (wet) and 2017 (dry, Figure B 4). Our results suggest that the catchment behavior may change in time. *Morel et al.* (2009) and *Davis et al.* (2014) found that DOC and NO_3 exports varied according to pre-event hydrological conditions. *Outram et al.* (2016) found that dry antecedent conditions temporally increased nitrate-N exports in following storm events.

The fact that such a simple model with constant concentrations is able to reproduce infra-annual dynamics of DOC and NO_3 raises questions about its capacity to anticipate the effects of climate change

on water quality (*Strohmenger et al.*, 2020). Before that, one can firstly question the transposability of the model in other contexts than the Kervidy-Naizin catchment, where the past N-surplus lead to important legacy storage of NO_3 in groundwater and where DOC supply is large in the riparian zone, allowing for assuming the main NO_3 and DOC sources behave as infinite pools at least over several years. Indeed, our study showed that physical transport and flow paths are the main drivers of the annual and storm event dynamics of NO_3 and DOC stream concentration (*Godsey et al.*, 2009). In such chemostatic case, the assumption of constant concentration parameters in each reservoir appears to be relevant to test the effect of precipitation regime and evaporation due to climate change, and the consequent catchment wetness and water flows paths, in order to predict the dynamics of DOC and NO_3 concentrations in the stream. It would be relevant to test such simple model in a gradient of catchments with diverse legacy or natural ecosystem storages.

6. Conclusions

We developed a simple model to identify the main drivers of the annual and DOC and NO_3 stream concentrations in a small headwater agricultural catchment. The model consists in three reservoirs: an unsaturated reservoir representing root and vadose zones of the hillslope, a slow reservoir representing the groundwater and a fast reservoir representing the riparian zone and the preferential flows. The modelled stream concentrations of DOC and NO_3 are represented as the result of the mixing of two end members: the fast and slow reservoirs.

The model reasonably reproduced the annual and storm event dynamics of the discharge, DOC and NO_3 concentrations in the stream, suggesting that the main drivers of those dynamics were indeed the transport of DOC and NO_3, and the differences in hydrological reactivity and in chemistry composition between the two compartments. The main source of stream DOC was the fast reservoir with a calibrated concentration of 13 mg l^{-1}, while the main source of stream NO_3 was the slow reservoir with a calibrated concentration of 70 mg l^{-1}. Using multi-objective function including observed daily DOC and NO_3 concentrations for calibrating the model parameters lead to higher relative contribution of the slow reservoir to the stream but increased the uncertainty on the hydrological parameters. Nevertheless, reproducing the long-term trends on solutes concentration would require more complex representations of the biogeochemical processes.

The legacy storage of NO_3 resulting from past N fertilization excess in the studied catchment makes the assumption that main NO_3 and DOC sources behave as infinite valuable at the scale of several years. Nevertheless, reproducing the long-term trends on solutes concentration would require more complex representations of the biogeochemical processes.

Acknowledgments, Samples and Data

The French National Research Institute for Agriculture, Food and Environment (INRAE) and the Region Bretagne co-funded the doctoral program of L.S. who also benefited from a grant for a mobility in TU Delft funded by the Universite Bretagne Loire and the Region Bretagne. The AgrHyS Observatory is supported by INRAE (UMR SAS (2010), *Observatoire de Recherche en Environnement sur les Agro-Hydrosystèmes (ORE AgrHyS),* INRAE. https://doi.org/10.15454/1.5499682911557678e12). All AgrHyS data are available on the Internet: https://www6.inra.fr/ore_agrhys_eng/Data. Carbon and anion concentrations were measured at the Géosciences Rennes laboratory. We are grateful to Jean-Paul Guillard for his precious help with sampling on the Kervidy-Naizin catchment over the years and to all the farmers of Naizin-Évellys for hosting our observations, sampling and surveys.

References

Abbott, B. W., F. Moatar, O. Gauthier, O. Fovet, V. Antoine, and O. Ragueneau (2018), Trends and seasonality of river nutrients in agricultural catchments: 18years of weekly citizen science in France, Sci Total Environ, 624, 845-858, doi: 10.1016/j.scitotenv.2017.12.176.

Addiscott, T. M., and N. A. Mirza (1998), Modelling contaminant transport at catchment or regional scale, Agric. Ecosyst. Environ., 67(2-3), 211-221, doi: 10.1016/s0167-8809(97)00120-5.

Ågren, A., I. Buffam, D. Cooper, T. Tiwari, C. Evans, and H. Laudon (2014), Can the heterogeneity in stream dissolved organic carbon be explained by contributing landscape elements?, Biogeosciences, 11(4), 1199-1213.

Alexander, R. B., and R. A. Smith (2006), Trends in the nutrient enrichment of US rivers during the late 20th century and their relation to changes in probable stream trophic conditions, Limnol. Oceanogr., 51(1part2), 639-654.

Arnold, J. G., R. Srinivasan, R. S. Muttiah, and J. R. Williams (1998), Large area hydrologic modeling and assessment part I: model development 1, JAWRA Journal of the American Water Resources Association, 34(1), 73-89.

Aubert, A. H., C. Gascuel-Odoux, and P. Merot (2013a), Annual hysteresis of water quality: A method to analyse the effect of intra- and inter-annual climatic conditions, Journal of Hydrology, 478, 29-39, doi: 10.1016/j.jhydrol.2012.11.027.

Aubert, A. H., et al. (2013b), Solute transport dynamics in small, shallow groundwater-dominated agricultural catchments: insights from a high-frequency, multisolute 10 yr-long monitoring study, Hydrology and Earth System Sciences, 17(4), 1379-1391, doi: 10.5194/hess-17-1379-2013.

Bartsch, S., S. Peiffer, C. L. Shope, S. Arnhold, J.-J. Jeong, J.-H. Park, J. Eum, B. Kim, and J. H. Fleckenstein (2013), Monsoonal-type climate or land-use management: Understanding their role in the mobilization of nitrate and DOC in a mountainous catchment, Journal of hydrology, 507, 149-162.

Basu, N. B., S. E. Thompson, and P. S. C. Rao (2011), Hydrologic and biogeochemical functioning of intensively managed catchments: A synthesis of top-down analyses, Water Resources Research, 47(10), doi: 10.1029/2011WR010800.

Basu, N. B., G. Destouni, J. W. Jawitz, S. E. Thompson, N. V. Loukinova, A. Darracq, S. Zanardo, M. Yaeger, M. Sivapalan, and A. Rinaldo (2010), Nutrient loads exported from managed catchments reveal emergent biogeochemical stationarity, Geophys. Res. Lett., 37(23), doi: 10.1029/2010GL045168.

Beaujouan, V. r., P. Durand, L. Ruiz, P. Aurousseau, and G. Cotteret (2002), A hydrological model dedicated to topography-based simulation of nitrogen transfer and transformation: rationale and application

to the geomorphology- denitrification relationship, Hydrological Processes, 16(2), 493-507, doi: 10.1002/hyp.327.
Bell, N., R. A. C. Cooke, T. Olsen, M. B. David, and R. Hudson (2015), Characterizing the Performance of Denitrifying Bioreactors during Simulated Subsurface Drainage Events, J. Environ. Qual., 44(5), 1647-1656, doi: 10.2134/jeq2014.04.0162.
Benettin, P., C. Soulsby, C. Birkel, D. Tetzlaff, G. Botter, and A. Rinaldo (2017), Using SAS functions and high-resolution isotope data to unravel travel time distributions in headwater catchments, Water Resources Research, 53(3), 1864-1878.
Bernal, S., A. Butturini, and F. Sabater (2002), Variability of DOC and nitrate responses to storms in a small Mediterranean forested catchment, Hydrology and Earth System Sciences Discussions, 6(6), 1031-1041.
Beven, K. (2001), How far can we go in distributed hydrological modelling?
Beven, K., and A. Binley (1992), The future of distributed models: model calibration and uncertainty prediction, Hydrological processes, 6(3), 279-298.
Beven, K., and J. Freer (2001), Equifinality, data assimilation, and uncertainty estimation in mechanistic modelling of complex environmental systems using the GLUE methodology, Journal of hydrology, 249(1-4), 11-29.
Beven, K. J. (2011), Rainfall-runoff modelling: the primer, John Wiley & Sons.
Birkel, C., C. Soulsby, and D. Tetzlaff (2014), Integrating parsimonious models of hydrological connectivity and soil biogeochemistry to simulate stream DOC dynamics, Journal of Geophysical Research: Biogeosciences, 119(5), 1030-1047.
Birkel, C., T. Broder, and H. Biester (2017), Nonlinear and threshold-dominated runoff generation controls DOC export in a small peat catchment, Journal of Geophysical Research-Biogeosciences, 122(3), 498-513, doi: 10.1002/2016jg003621.
Birkel, C., D. Tetzlaff, S. Dunn, and C. Soulsby (2010), Towards a simple dynamic process conceptualization in rainfall–runoff models using multi-criteria calibration and tracers in temperate, upland catchments, Hydrological Processes: An International Journal, 24(3), 260-275.
Birkel, C., C. Duvert, A. Correa, N. C. Munksgaard, D. T. Maher, and L. B. Hutley (2020), Tracer-Aided Modeling in the Low-Relief, Wet-Dry Tropics Suggests Water Ages and DOC Export Are Driven by Seasonal Wetlands and Deep Groundwater, Water Resources Research, 56(4), e2019WR026175.
Borah, D. K., M. Demissie, and L. L. Keefer (2002), AGNPS-based assessment of the impact of BMPs on nitrate-nitrogen discharging into an Illinois water supply lake, Water Int., 27(2), 255-265, doi: 10.1080/02508060208686999.
Bouraoui, F., and B. Grizzetti (2011), Long term change of nutrient concentrations of rivers discharging in European seas, Sci. Total Environ., 409(23), 4899-4916.
Bowes, M., H. Jarvie, S. J. Halliday, R. Skeffington, A. Wade, M. Loewenthal, E. Gozzard, J. Newman, and E. Palmer-Felgate (2015), Characterising phosphorus and nitrate inputs to a rural river using high-frequency concentration–flow relationships, Sci. Total Environ., 511, 608-620, doi: 10.1016/j.scitotenv.2014.12.086.
Boyer, E. W., G. M. Hornberger, K. E. Bencala, and D. McKnight (1996), Overview of a simple model describing variation of dissolved organic carbon in an upland catchment, Ecological Modelling, 86(2-3), 183-188.
Carluer, N. (1998), Vers une modélisation hydrologique adaptée à l'évaluation des pollutions diffuses: prise en compte du réseau anthropique. Application au bassin versant de Naizin (Morbihan), Paris 6.
Casson, N. J., M. C. Eimers, S. A. Watmough, and M. C. Richardson (2019), The role of wetland coverage within the near-stream zone in predicting of seasonal stream export chemistry from forested headwater catchments, Hydrological Processes, 33(10), 1465-1475, doi: 10.1002/hyp.13413.

Davis, C. A., A. S. Ward, A. J. Burgin, T. D. Loecke, D. A. Riveros-Iregui, D. J. Schnoebelen, C. L. Just, S. A. Thomas, L. J. Weber, and M. A. St Clair (2014), Antecedent moisture controls on stream nitrate flux in an agricultural watershed, J. Environ. Qual., 43(4), 1494-1503, doi: 10.2134/jeq2013.11.0438.

Dick, J., D. Tetzlaff, C. Birkel, and C. Soulsby (2015), Modelling landscape controls on dissolved organic carbon sources and fluxes to streams, Biogeochemistry, 122(2-3), 361-374, doi: 10.1007/s10533-014-0046-3.

Dunn, S. M., J. Freer, M. Weiler, M. J. Kirkby, J. Seibert, P. F. Quinn, G. Lischeid, D. Tetzlaff, and C. Soulsby (2008), Conceptualization in catchment modelling: simply learning?, Hydrological Processes, 22(13), 2389-2393, doi: 10.1002/hyp.7070.

Dupas, R., C. Minaudo, G. Gruau, L. Ruiz, and C. Gascuel-Odoux (2018), Multidecadal Trajectory of Riverine Nitrogen and Phosphorus Dynamics in Rural Catchments, Water Resources Research, 54(8), 5327-5340, doi: 10.1029/2018wr022905.

Dusek, J., M. Dohnal, T. Vogel, A. Marx, and J. A. Barth (2019), Modelling multiseasonal preferential transport of dissolved organic carbon in a shallow forest soil: Equilibrium versus kinetic sorption, Hydrological Processes, 33(22), 2898-2917.

Fenicia, F., H. H. G. Savenije, P. Matgen, and L. Pfister (2006), Is the groundwater reservoir linear? Learning from data in hydrological modelling, Hydrology and Earth System Sciences, 10(1), 139-150, doi: 10.5194/hess-10-139-2006.

Ferrant, S., F. Oehler, P. Durand, L. Ruiz, J. Salmon-Monviola, E. Justes, P. Dugast, A. Probst, J. L. Probst, and J. M. Sanchez-Perez (2011), Understanding nitrogen transfer dynamics in a small agricultural catchment: Comparison of a distributed (TNT2) and a semi distributed (SWAT) modeling approaches, Journal of Hydrology, 406(1-2), 1-15, doi: 10.1016/j.jhydrol.2011.05.026.

Ford, W. I., K. King, and M. R. Williams (2018), Upland and in-stream controls on baseflow nutrient dynamics in tile-drained agroecosystem watersheds, Journal of Hydrology, 556, 800-812, doi: 10.1016/j.jhydrol.2017.12.009.

Fovet, O., L. Ruiz, M. Faucheux, J. Molénat, M. Sekhar, F. Vertès, L. Aquilina, C. Gascuel-Odoux, and P. Durand (2015), Using long time series of agricultural-derived nitrates for estimating catchment transit times, Journal of Hydrology, 522, 603-617, doi: 10.1016/j.jhydrol.2015.01.030.

Fovet, O., et al. (2018a), Seasonal variability of stream water quality response to storm events captured using high-frequency and multi-parameter data, Journal of Hydrology, 559, 282-293, doi: 10.1016/j.jhydrol.2018.02.040.

Fovet, O., et al. (2018b), AgrHyS: An Observatory of Response Times in Agro-Hydro Systems, Vadose Zone J., 17(1), doi: 10.2136/vzj2018.04.0066.

Fuss, T., B. Behounek, A. J. Ulseth, and G. A. Singer (2017), Land use controls stream ecosystem metabolism by shifting dissolved organic matter and nutrient regimes, Freshwater Biology, 62(3), 582-599, doi: 10.1111/fwb.12887.

Godsey, S. E., J. W. Kirchner, and D. W. Clow (2009), Concentration–discharge relationships reflect chemostatic characteristics of US catchments, Hydrological Processes: An International Journal, 23(13), 1844-1864.

Graeber, D., J. Gelbrecht, M. T. Pusch, C. Anlanger, and D. von Schiller (2012), Agriculture has changed the amount and composition of dissolved organic matter in Central European headwater streams, Sci. Total Environ., 438, 435-446.

Gupta, H. V., H. Kling, K. K. Yilmaz, and G. F. Martinez (2009), Decomposition of the mean squared error and NSE performance criteria: Implications for improving hydrological modelling, Journal of hydrology, 377(1-2), 80-91.

Harman, C. J. (2015), Time-variable transit time distributions and transport: Theory and application to storage-dependent transport of chloride in a watershed, Water Resources Research, 51(1), 1-30.

Haygarth, P. M., H. P. Jarvie, S. M. Powers, A. N. Sharpley, J. J. Elser, J. Shen, H. M. Peterson, N.-I. Chan, N. J. Howden, and T. Burt (2014), Sustainable phosphorus management and the need for a long-term perspective: The legacy hypothesis, edited, ACS Publications

Howden, N. J. K., T. P. Burt, S. A. Mathias, F. Worrall, and M. J. Whelan (2011), Modelling long-term diffuse nitrate pollution at the catchment-scale: Data, parameter and epistemic uncertainty, Journal of Hydrology, 403(3-4), 337-351, doi: 10.1016/j.jhydrol.2011.04.012.

Hrachowitz, M., and M. P. Clark (2017), HESS Opinions: The complementary merits of competing modelling philosophies in hydrology, Hydrol. Earth Syst. Sci, 21(8), 3953-3973.

Hrachowitz, M., O. Fovet, L. Ruiz, and H. H. G. Savenije (2015), Transit time distributions, legacy contamination and variability in biogeochemical 1/f(alpha) scaling: how are hydrological response dynamics linked to water quality at the catchment scale?, Hydrological Processes, 29(25), 5241-5256, doi: 10.1002/hyp.10546.

Hrachowitz, M., H. Savenije, T. Bogaard, D. Tetzlaff, and C. Soulsby (2013a), What can flux tracking teach us about water age distribution patterns and their temporal dynamics?, Hydrology and Earth System Sciences.

Hrachowitz, M., O. Fovet, L. Ruiz, T. Euser, S. Gharari, R. Nijzink, J. Freer, H. H. G. Savenije, and C. Gascuel-Odoux (2014), Process consistency in models: The importance of system signatures, expert knowledge, and process complexity, Water Resources Research, 50(9), 7445-7469, doi: 10.1002/2014wr015484.

Hrachowitz, M., P. Benettin, B. M. van Breukelen, O. Fovet, N. J. K. Howden, L. Ruiz, Y. van der Velde, and A. J. Wade (2016), Transit timesthe link between hydrology and water quality at the catchment scale, Wiley Interdiscip. Rev.-Water, 3(5), 629-657, doi: 10.1002/wat2.1155.

Hrachowitz, M., et al. (2013b), A decade of Predictions in Ungauged Basins (PUB)a review, Hydrol. Sci. J.-J. Sci. Hydrol., 58(6), 1198-1255, doi: 10.1080/02626667.2013.803183.

Humbert, G., A. Jaffrezic, O. Fovet, G. Gruau, and P. Durand (2015), Dry-season length and runoff control annual variability in stream DOC dynamics in a small, shallow groundwater-dominated agricultural watershed, Water Resources Research, 51(10), 7860-7877, doi: 10.1002/2015wr017336.

ISO 10304, N. (1995), Determination of dissolved fluoride, chloride, nitrite, orthophosphate, bromide, nitrate, and sulfate ions, using liquid chromatography of ions, edited by AFNOR

Kelleher, C., B. McGlynn, and T. Wagener (2017), Characterizing and reducing equifinality by constraining a distributed catchment model with regional signatures, local observations, and process understanding, Hydrology and Earth System Sciences, 21(7), 3325.

Lambert, T., A. C. Pierson-Wickmann, G. Gruau, A. Jaffrezic, P. Petitjean, J. N. Thibault, and L. Jeanneau (2013), Hydrologically driven seasonal changes in the sources and production mechanisms of dissolved organic carbon in a small lowland catchment, Water Resources Research, 49(9), 5792-5803, doi: 10.1002/wrcr.20466.

Lambert, T., A.-C. Pierson-Wickmann, G. Gruau, A. Jaffrézic, P. Petitjean, J.-N. Thibault, and L. Jeanneau (2014), DOC sources and DOC transport pathways in a small headwater catchment as revealed by carbon isotope fluctuation during storm events.

Lee, K. Y., T. R. Fisher, T. E. Jordan, D. L. Correll, and D. E. Weller (2000), Modeling the hydrochemistry of the Choptank River Basin using GWLF and Arc/Info: 1. Model calibration and validation, Biogeochemistry, 49(2), 143-173, doi: 10.1023/a:1006375530844.

Lindström, G., C. Pers, J. Rosberg, J. Strömqvist, and B. Arheimer (2010), Development and testing of the HYPE (Hydrological Predictions for the Environment) water quality model for different spatial scales, Hydrology research, 41(3-4), 295-319.

Molénat, J., C. Gascuel-Odoux, P. Davy, and P. Durand (2005), How to model shallow water-table depth variations: the case of the Kervidy-Naizin catchment, France, Hydrological Processes: An International Journal, 19(4), 901-920.

Molénat, J., C. Gascuel-Odoux, L. Ruiz, and G. Gruau (2008), Role of water table dynamics on stream nitrate export and concentration in agricultural headwater catchment (France), Journal of Hydrology, 348(3-4), 363-378.

Montreuil, O., P. Merot, and P. Marmonier (2010), Estimation of nitrate removal by riparian wetlands and streams in agricultural catchments: effect of discharge and stream order, Freshwater Biology, 55(11), 2305-2318.

Morel, B., P. Durand, A. Jaffrezic, G. Gruau, and J. Molenat (2009), Sources of dissolved organic carbon during stormflow in a headwater agricultural catchment, Hydrological Processes, 23(20), 2888-2901, doi: 10.1002/hyp.7379.

Musolff, A., C. Schmidt, M. Rode, G. Lischeid, S. M. Weise, and J. H. Fleckenstein (2016), Groundwater head controls nitrate export from an agricultural lowland catchment, Advances in Water Resources, 96, 95-107, doi: 10.1016/j.advwatres.2016.07.003.

Nijzink, R. C., L. Samaniego, J. Mai, R. Kumar, S. Thober, M. Zink, D. Schäfer, H. H. Savenije, and M. Hrachowitz (2016), The importance of topography-controlled sub-grid process heterogeneity and semi-quantitative prior constraints in distributed hydrological models, Hydrol. Earth Syst. Sci, 20(3), 1151-1176.

Oehler, F., P. Durand, P. Bordenave, Z. Saadi, and J. Salmon-Monviola (2009), Modelling denitrification at the catchment scale, Sci. Total Environ., 407(5), 1726-1737.

Outram, F. N., R. J. Cooper, G. Sünnenberg, K. M. Hiscock, and A. A. Lovett (2016), Antecedent conditions, hydrological connectivity and anthropogenic inputs: Factors affecting nitrate and phosphorus transfers to agricultural headwater streams, Sci. Total Environ., 545, 184-199.

Outram, F. N., C. Lloyd, J. Jonczyk, C. M. Benskin, F. Grant, M. Perks, C. Deasy, S. Burke, A. L. Collins, and J. Freer (2014), High-frequency monitoring of nitrogen and phosphorus response in three rural catchments to the end of the 2011–2012 drought in England, Hydrology and Earth System Sciences, 18(9), 3429-3448, doi: 10.5194/hess-18-3429-2014.

Penman, H. L. (1956), Estimating evaporation, Eos, Transactions American Geophysical Union, 37(1), 43-50, doi: 10.1029/TR037i001p00043.

Petitjean, P., O. Henin, and G. Gruau (2004), Dosage du carbone organique dissous dans les eaux douces naturelles. Intérêt, Principe, Mise en Oeuvre et Précautions Opératoires.

Pettersson, A., B. Arheimer, and B. Johansson (2001), Nitrogen concentrations simulated with HBV-N: New response function and calibration strategy - Paper presented at the Nordic Hydrological Conference (Uppsala, Sweden June, 2000), Nord. Hydrol., 32(3), 227-248.

Rinaldo, A., P. Benettin, C. J. Harman, M. Hrachowitz, K. J. McGuire, Y. Van Der Velde, E. Bertuzzo, and G. Botter (2015), Storage selection functions: A coherent framework for quantifying how catchments store and release water and solutes, Water Resources Research, 51(6), 4840-4847.

Seibert, J., T. Grabs, S. Köhler, H. Laudon, M. Winterdahl, and K. Bishop (2009), Linking soil-and stream-water chemistry based on a Riparian Flow-Concentration Integration Model, Hydrology and earth system sciences, 13(12), 2287-2297.

Shafii, M., J. R. Craig, M. L. Macrae, M. C. English, S. L. Schiff, P. Van Cappellen, and N. B. Basu (2019), Can Improved Flow Partitioning in Hydrologic Models Increase Biogeochemical Predictability?, Water Resources Research.

Shrestha, R. R., K. Osenbrück, and M. Rode (2013), Assessment of catchment response and calibration of a hydrological model using high-frequency discharge–nitrate concentration data, Hydrology Research, 44(6), 995-1012.

Smith, A. P., A. W. Western, and M. C. Hannah (2013), Linking water quality trends with land use intensification in dairy farming catchments, Journal of Hydrology, 476, 1-12.

Strohmenger, L., O. Fovet, N. Akkal-Corfini, R. Dupas, P. Durand, M. Faucheux, G. Gruau, Y. Hamon, A. Jaffrezic, and C. Minaudo (2020), Multi-temporal relationships between the hydro-climate and exports of carbon, nitrogen and phosphorus in a small agricultural watershed, Water Resources Research, e2019WR026323.

Taylor, P. G., and A. R. Townsend (2010), Stoichiometric control of organic carbon-nitrate relationships from soils to the sea, Nature, 464(7292), 1178-1181, doi: 10.1038/nature08985.

Thomas, Z., B. Abbott, O. Troccaz, J. Baudry, and G. Pinay (2016), Proximate and ultimate controls on carbon and nutrient dynamics of small agricultural catchments, Biogeosciences, 13(6), 1863-1875, doi: 10.5194/bg-13-1863-2016.

Trevisan, D., C. Giguet-Covex, P. Sabatier, P. Quetin, and F. Arnaud (2019), Coupling indicators and lumped-parameter modeling to assess suspended matter and soluble phosphorus losses, Sci. Total Environ., 650, 3027-3040, doi: 10.1016/j.scitotenv.2018.09.392.

Viaud, V., P. Santillàn-Carvantes, N. Akkal-Corfini, C. Le Guillou, N. C. Prévost-Bouré, L. Ranjard, and S. Menasseri-Aubry (2018), Landscape-scale analysis of cropping system effects on soil quality in a context of crop-livestock farming, Agriculture, ecosystems & environment, 265, 166-177, doi: 10.1016/j.agee.2018.06.018.

Whitehead, P., E. Wilson, D. Butterfield, and K. Seed (1998), A semi-distributed integrated flow and nitrogen model for multiple source assessment in catchments (INCA): Part II—application to large river basins in south Wales and eastern England, Sci. Total Environ., 210, 559-583.

Woodward, S. J. R., and R. Stenger (2018), Bayesian chemistry-assisted hydrograph separation (BACH) and nutrient load partitioning from monthly stream phosphorus and nitrogen concentrations, Stochastic Environmental Research and Risk Assessment, 32(12), 3475-3501, doi: 10.1007/s00477-018-1612-3.

Woodward, S. J. R., R. Stenger, and V. J. Bidwell (2013), Dynamic analysis of stream flow and water chemistry to infer subsurface water and nitrate fluxes in a lowland dairying catchment, Journal of Hydrology, 505, 299-311, doi: 10.1016/j.jhydrol.2013.07.044.

WRB, I. W. G. (2006), World reference base for soil resources, edited, pp. 1-128, Food and Agriculture Organization (FAO) Rome, Italy

Xu, N., J. E. Saiers, H. F. Wilson, and P. A. Raymond (2012), Simulating streamflow and dissolved organic matter export from a forested watershed, Water Resources Research, 48, 18, doi: 10.1029/2011wr011423.

Zuecco, G., D. Penna, M. Borga, and H. J. van Meerveld (2016), A versatile index to characterize hysteresis between hydrological variables at the runoff event timescale, Hydrological Processes, 30(9), 1449-1466, doi: 10.1002/hyp.10681.

5. Discussion générale et perspectives

Ce cinquième chapitre vise à croiser les travaux développés dans les chapitres 3 et 4 et à aborder plusieurs sujets de discussion et d'ouverture vers des pistes d'amélioration et d'utilisation du modèle développé. D'une part, il est question de poursuivre plus en détail l'analyse des simulations produites par le modèle (Figure B 4, chapitre 4) et d'en tester la capacité à reproduire les signatures saisonnières et à long terme, ainsi que l'opposition entre DOC et NO_3 observée sur les des signaux mesurés (chapitre 3). D'autre part, les limites du modèle sont abordées pour proposer des pistes d'améliorations qui font l'objet de développement en cours sur la modélisation des concentrations en solutés. Sont également abordés les options et contraintes de l'intégration du phosphore. Enfin les implications de ce travail en terme d'écologie aquatique dans une perspective d'approche intégrées des ressources en eaux concluent ce chapitre.

5.1. Comparaison des signatures hydro-chimiques simulées et observées

Le modèle a produit des chroniques journalières simulées de débit et de concentration en DOC et en NO_3 dans le cours d'eau. Ces chroniques simulées peuvent être analysées au même titre que les chroniques observées pour en extraire les signatures à long terme et saisonnières. Ces signatures ont été obtenues par l'application des mêmes méthodes que celles présentées dans le chapitre 3. Pour rappel, ces méthodes sont les tests de Mann Kendall et Theil Sen pour évaluer les tendances sur le long terme, et la décomposition en série de Fourier pour identifier les motifs saisonniers moyens. Les données utilisées pour ces analyses sont les médianes des simulations acceptables retenues par la méthode GLUE (chapitre 4).

5.1.1. Evolution long terme des variables simulées

Les tendances à long terme des concentrations simulées de DOC et de NO_3 ne sont pas significatives d'après le test de Mann Kendall, contrairement aux concentrations observées qui affichent une augmentation des concentrations en DOC et une diminution des concentrations en NO_3 (Table 1). En revanche le débit simulé présente un très faible tendance à l'augmentation du débit de l'ordre de 4.10^{-3} $mm.d^{-1}.yr^{-1}$, alors que le débit observé n'en présente pas.

L'absence de tendance long terme pour les concentrations simulées était attendue car aucune tendance sur les entrées ou sur les mécanismes de production et de consommation n'est représenté dans le modèle, la reproduction de tendance long-terme n'étant pas un objectif de la modélisation. Cela dit, l'incapacité du modèle (dans son état de développement actuel) à reproduire les évolutions à long terme des concentrations suggère que ces tendances observées ne sont pas liées à une évolution des contributions relatives d'eau d'origine souterraine et superficielle au débit du cours d'eau. Ces résultats corroborent un peu plus l'hypothèse de l'influence du stock de NO_3 hérité des pratiques agricoles dans le passé sur les dynamiques à long terme des concentrations en NO_3 dans le cours d'eau. L'évolution des concentrations en DOC, en miroir à celles des concentrations de NO_3 mais de pente relative plus modérée (+0.7% versus -1.7% des moyennes de DOC et NO_3 par an, respectivement), serait donc liée à des

mécanismes biogéochimiques couplant DOC et NO_3, en particulier les situations réductrices (favorables à la dénitrification et à la dissolution réductive de la MO) et la production de biomasse (consommant du N minéral et produisant de la MO).

Table 1 Tendances long termes des variables simulées et observées. Les tendances significative (p-value < 0.05 pour le teste de Mann Kendall) sont représentées en gras.

	DOC $mg.l^{-1}.yr^{-1}$	*NO_3* $mg.l^{-1}.yr^{-1}$	*Q* $mm.d^{-1}.yr^{-1}$
observed	**3,4E-02**	**-1,2E+00**	**0,0E+00**
simulated	-3,7E-03	2,4E-02	**4,0E-03**

5.1.2. Saisonnalité des variables simulées

Les motifs saisonniers des séries de Fourier des variables simulées et observées sont très proches (Figure 16). Les périodes de maximum du débit et de NO_3 simulés sont synchrones avec celles des signaux observés au mois de février et de mai, respectivement. La période de concentration maximum du DOC simulé, en octobre, est déphasée d'un mois environ avec celle du DOC observé, en novembre. Les motifs saisonniers simulés épousent bien les motifs observés pour les trois variables, même si quelques déphasages apparaissent lors des périodes de fin de récession et de reprise d'écoulement de mai à novembre.

Ces résultats suggèrent que le fonctionnement saisonnier du bassin versant et les contributions des zones sources de DOC et de NO_3 sont bien reproduits par le modèle. Toutefois, les périodes de hautes eaux et de récessions, soutenues par le débit de base d'origine souterraine, sont bien reproduites alors que des divergences sont visibles pour les périodes d'assec et de reprise d'écoulement. Le décalage de la concentration maximale de DOC simulée est sans doute lié en grande partie à la divergence entre débits simulés et observés à cette période automnale. Les divergences entre débits simulés et observés entre juillet et octobre s'expliquent par les contributions ponctuelles du compartiment rapide du modèle lors d'évènements pluvieux, alors que le débit observé est nul et ne répond plus aux pluies pendant l'assec. Le déphasage du débit lors de la reprise de l'écoulement en octobre suggère qu'un mécanisme manque dans le modèle, qui peut être lié à un déficit en eaux sous-estimé en été, ou à l'évolution des coefficients de vidange des réservoirs variables selon leurs taux de remplissage (avec un réservoir inactif quand il est peu rempli et dont la réactivité hydrologique augmente avec le stock d'eau). Ces divergences entre variables simulées et observées soulignent la nécessité d'un travail spécifique pour affiner la conceptualisation du fonctionnement des cours d'eau intermittents.

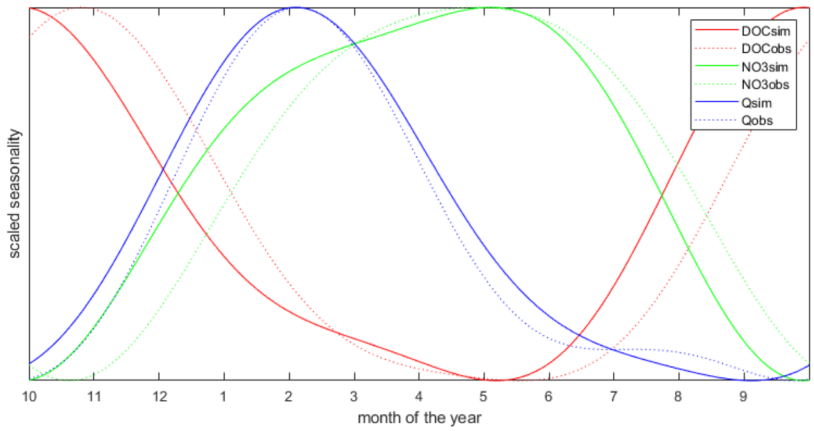

Figure 16 Saisonnalités moyennes des variables simulées et observées, identifiées par les composantes de périodes de retours de 365 et 183.5j des séries de Fourier.

5.1.3. Oppositions du DOC et du NO_3

L'anti-corrélation entre les concentrations en DOC et NO_3 est bien représentée sur les simulations (Figure 16 et Figure 17). Elle est cependant plus exprimée sur les simulations que sur les observations (Figure 17), d'une part en raison des concentrations fixées dans les deux compartiments contributifs au cours d'eau dans le modèle, ce qui a pour effet de caricaturer l'opposition entre DOC et NO_3, et d'autre part par l'absence de tendance long terme dans les séries simulées, ce qui conduit à une relation beaucoup plus linéaire sur les simulations. L'anti-corrélation entre DOC et NO_3 simulée est davantage superposée aux données observées pendant la période de calibration (2012-2017) que pendant la période de validation (2004-2012). On peut également remarquer que le modèle reproduit mal le bruit observé autour de cette anti-corrélation, peut être en raison de processus biogéochimiques (processus in-stream, dépendance des concentrations à la température) non représentés dans la version actuelle du modèle.

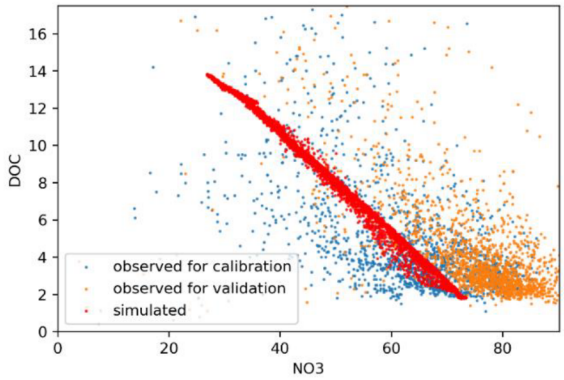

Figure 17 Concentrations ($mg.l^{-1}$) journalières en DOC versus concentrations en NO_3 simulées et observées pendant les périodes de calibration et validation.

5.2. Les limites du modèle

5.2.1. Corrélation entre simulations et observations

Dans l'ensemble, les variables simulées par le modèle sont corrélées avec les données journalières observées (Figure 18). Cependant, les simulations du DOC sont plutôt surestimées par rapport aux observations, particulièrement pour les faibles concentrations en DOC observées alors qu'à l'inverse, les concentrations en NO_3 sont fréquemment sous-estimées. Ces observations confirment que si le simple mélange de deux sources de solutés suffit pour reproduire les traits principaux des dynamiques des concentrations, d'autres compartiments et/ou processus réactifs contribuent sans doute à ces dynamiques.

On peut également remarquer un effet de palier pour les concentrations faibles en DOC simulées (2 $mg.l^{-1}$) et pour les concentrations fortes en NO_3 simulées (70 $mg.L^{-1}$). Ces valeurs de concentrations correspondent à la paramétrisation obtenue pour le réservoir lent : les écoulements simulés sont alors alimentés par le réservoir souterrain uniquement. Ces écoulements ont lieu pendant les périodes de basses eaux, à faible débit, lorsque les vitesses d'écoulement sont favorables à des processus in-stream qui ne sont pas formulés dans le modèle actuel. Enfin, le décalage du nuage de points du NO_3 entre les périodes de validation et de calibration illustre une fois de plus la tendance long terme du NO_3 mesurée mais pas simulée. Aussi, les corrélations entre NO_3 simulés et observés affichent des pentes identiques entre les deux périodes. Ainsi, l'épuisement progressif du stock de NO_3 hérité entraine une diminution conjointe des faibles et fortes valeurs de concentrations, ce qui tend à confirmer que les dynamiques infra-annuelles de concentration du NO_3 dans le cours d'eau résultent en premier lieu de phénomènes de dilution du NO_3 d'origine souterraine par un écoulement plus rapide et plus superficiel.

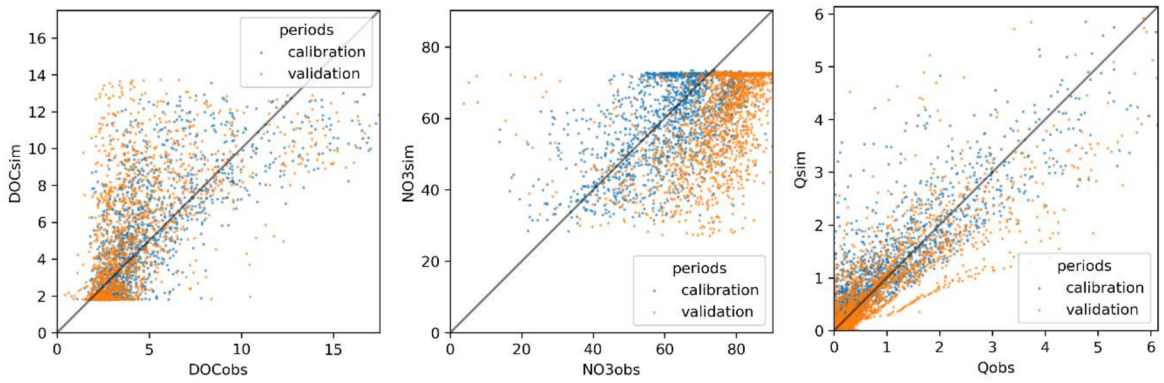

Figure 18 Scatter plot des variables simulées versus variables observées pour les périodes de calibration (point bleu) et validation (point orange)

5.2.2. Distributions des variables simulées et observées

Les variables simulées évoluent globalement dans la même gamme de variation que les variables observées (Figure 18 et Figure 19), ce qui conforte l'idée que les valeurs de concentrations calibrées sont cohérentes avec la réalité. Les asymétries des distributions des valeurs sont globalement respectées avec des occurrences plus nombreuses pour les valeurs faibles pour le DOC et le débit, et inversement, des occurrences plus nombreuses pour les valeurs élevées de NO_3. Ces résultats nous montrent que le modèle est capable de reproduire des distributions cohérentes pour les trois variables.

Si les distributions du débit simulé coïncident très bien avec celles du débit observé, celles des concentrations simulées présentent néanmoins quelques différences avec les distributions des concentrations observées. En effet, les asymétries du DOC et du NO_3 simulés sont très exagérées avec des pics de distribution très resserrés au niveau des concentrations très faibles et très élevées pour le DOC et le NO_3, respectivement. De plus, les valeurs élevées de DOC simulées et les valeurs faibles de NO_3 simulées sont également surreprésentées (les distributions observées étant plus asymptotiques pour ces gammes de valeurs) et sont probablement la conséquence des écoulements simulés en été et alimentés exclusivement pas le réservoir rapide, pendant les assecs lorsque le débit est censé être nul. Les limites de l'approche « end-member » du modèle se reflètent donc dans les distributions presque bimodales affichées par les concentrations simulées.

Enfin, la distribution du NO_3 observées en période de calibration est décalée vers des valeurs inférieures en comparaison avec la période de validation, alors que les distributions du NO_3 simulées sont identiques pour les deux périodes. Cela reflète une fois de plus la tendance long terme observée sur le NO_3 et non reproduite par le modèle.

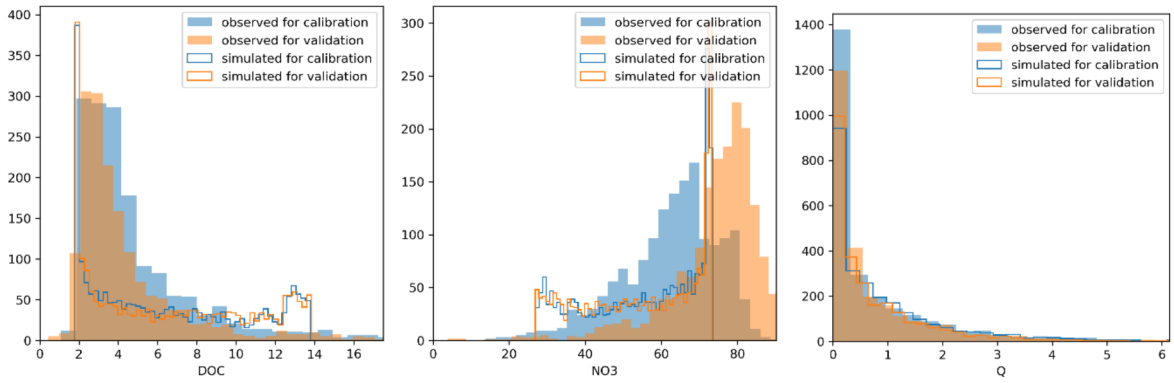

Figure 19 Distributions des variables observées et simulées pendant les périodes de calibration et de simulation.

5.2.1. Intégration du phosphore dans le modèle

La série temporelle des concentrations en phosphore n'a pas été intégrée pour les raisons évoquées en introduction du chapitre 4. Cependant, la complexité des processus liés au transport du SRP représente une source de contraintes, donc d'informations supplémentaires sur le fonctionnement du bassin versant. Ces contraintes sont de nature hydrologique et physico-chimique. En effet, l'analyse de données à mis en évidence que l'export de SRP est principalement visible lors d'évènements hydrologiques de crue, de manière accentuée lorsque l'humidité du bassin versant et les niveaux de nappe élevés sont associés à un évènement pluvieux de forte intensité. Ainsi, l'intégration du SRP dans ce modèle offre une opportunité de raffiner la représentation des fluctuations de nappe en bas de versant, les processus de ruissellement de surface et par conséquent la genèse des écoulements de crue. *Dupas et al.* (2015a) ont mis en évidence une évolution saisonnière des mécanismes de mobilisation du SRP avec le rôle de la nappe de base de versant pour la mobilisation lors des crues d'automne et surtout d'hiver, et des processus de mobilisation relevant plutôt de l'érosion pour les crues de printemps. Une sélection des évènements à reproduire pourrait donc s'avérer utile. La représentation plus fine des dynamiques de concentrations en crue est limitée par le pas de temps journalier du modèle, les crues ayant une durée moyenne de l'ordre de 12 heures sur le bassin de Kervidy-Naizin. Des données de concentration en phosphore à des pas de temps sub-journaliers sont disponibles sur l'observatoire : soit à l'échelle des crues, toutes les 10 à 20 minutes, grâce au préleveur automatique qui a permis d'échantillonner une sélection de crues chaque année depuis l'automne 2007, soit en continu toutes les 30 minutes, grâce à un analyseur in situ de phosphore en fonctionnement depuis avril 2016, mesurant le TRP, i.e. le phosphore total réactif, sans qu'il y ait filtration de l'échantillon à 0.45 µm. La stratégie qui pourrait être mise en œuvre pour exploiter le potentiel de ces jeux de données infra-journaliers dans la modélisation serait de calibrer non pas des concentrations mais des flux journaliers de phosphore réactif, en calculant les flux observés à partir des données à haute résolution temporelle, au moins pour les jours en crue, comme proposé par (*Dupas et al.*, 2016).

5.3. Evolutions préconisées pour le modèle et en cours d'étude

5.3.1. Concentrations dynamiques dans les sources

Les comparaisons entre variables simulées et observées ont mis en évidence que l'approche de type end-member à deux compartiments, bien que permettant de reproduire l'essentiel des dynamiques du débit et des concentrations à l'exutoire, pourrait être révisée dans le but d'améliorer les simulations.

Un premier axe d'amélioration envisageable serait d'augmenter le pas de temps de la simulation, ce qui pourrait également permettre la simulation du transport du phosphore, cela dit, les données mesurées des concentrations disponibles sont essentiellement journalières et ne permettent donc pas d'évaluer les variables simulées à un pas de temps plus fin. Les données acquises à hautes fréquentes depuis quelques années permettront à l'avenir de développer de telles approches.

Un autre axe d'amélioration du modèle serait d'exprimer les concentrations des réservoirs en fonction de la quantité d'eau qu'il contient (*Eklof et al.*, 2015; *Musolff et al.*, 2016; *Seibert et al.*, 2009; *Xu et al.*, 2012) dans le but de reproduire les effets de processus physico-chimiques ou biogéochimiques de mobilisation des éléments. En effet, la quantité d'eau dans un réservoir, et plus particulièrement dans le réservoir riparien car plus sujet à saturation, a une influence sur les conditions physico-chimiques du milieu, et par conséquent sur les processus de désorption du carbone (*Grybos et al.*, 2009), et de dénitrification du NO_3 (*Bell et al.*, 2015; *Casson et al.*, 2019). Le niveau d'eau peut également refléter l'extension spatiale de la nappe qui contrôle la connectivité hydrologique entre des zones sources de solutés avec le cours d'eau.

Les concentrations en solutés dans les réservoirs peuvent également être exprimées en fonction de la température (*Birkel et al.*, 2014; *Dunn et al.*, 2013; *Kasurinen et al.*, 2016). En effet, les cinétiques de réaction des processus biogéochimiques tels que la minéralisation, la production de biomasse, la dénitrification peuvent dépendre de la température du milieu (*Casson et al.*, 2019; *Kasurinen et al.*, 2016; *Laudon et al.*, 2012).

5.3.2. Stocks de solutés et temps de transit dans les réservoirs

L'approche end-member telle qu'utilisée par le modèle ne permet pas de simuler l'évolution des quantités de solutés présentes dans les différents compartiments, ni les flux d'éléments entre ces compartiments. Pour ce faire, il serait nécessaire de simuler explicitement les stocks de solutés et leurs transferts entre les différents compartiments du modèle tel que proposée par (*Birkel et al.*, 2014) pour le DOC par exemple. Les variations de stocks de solutés seraient alors soumises à des mécanismes de production, de consommation et de mobilisation. Ces mécanismes, de natures biogéochimiques et physico-chimiques, sont contrôlés par la température et les conditions hydriques dans les réservoirs.

Cette approche proposerait une représentation un peu plus physique des processus s'appliquant aux solutés et permettrait de tenir compte des apports d'origine anthropique (surplus de NO_3). Les fonctions de production, consommation et mobilisation feraient alors intervenir aussi directement les variables climatiques (température, niveau de remplissage des réservoirs) et permettraient donc de tester de manière théorique mais plus approfondie l'effet de scénarios climatiques (*Salmon-Monviola et al.*,

2013). Une telle structure permettrait également d'évaluer en quoi la représentation des éléments chimiques comme le DOC, le NO_3 et éventuellement le SRP permet de contraindre les temps de transit de l'eau dans les réservoirs et donc l'âge de l'eau dans le cours d'eau. En effet, le cours d'eau est composée d'un mélange d'eaux de différents âges selon les contributions relatives des différentes sources et les trajets d'écoulement (*Benettin et al.*, 2017). Ces trajets d'écoulement ainsi que les temps de résidence associés déterminent les interactions possibles entre l'eau et les éléments chimiques ou biologiques des milieux poreux traversés, donc la composition chimique de l'eau. Le temps de résidence de l'eau dans un modèle conceptuel peut être formulé à l'aide de *StorAge Selection functions* (SAS-function), concept proposé par *Rinaldo et al.* (2015). Les *SAS-functions* permettent en effet de paramétrer la distribution des âges de l'eau des flux sortants des différents réservoirs, et donc la distribution des âges de l'eau dans chaque réservoir, à l'aide de deux paramètres par flux (Figure 20). Les chroniques de concentration en DOC et NO_3 représentent donc une opportunité pour contraindre les distributions de l'âge des eaux en provenance de différents compartiments qui alimentent le cours d'eau. Ces développements sont actuellement en cours de réalisation en collaboration avec J. Salmon-Monviola.

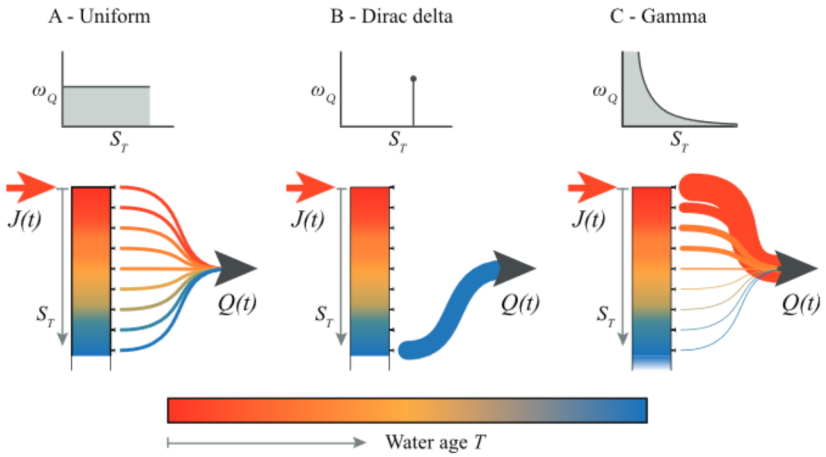

Figure 20 Schéma conceptuel du fonctionnement de la fonction SAS pour 3 distributions: A) uniforme, B) eau ancienne uniquement, C) préférence pour les eaux jeunes, d'après Harman (2015)

5.4. Etudier les effets du climat sur la qualité de l'eau : implications et extrapolations de l'étude

5.4.1. Le modèle pour étudier les effets du climat : pertinence et limites

L'approche générale de la thèse était de mobiliser des jeux de données issus d'un observatoire de la zone critique pour étudier l'effet du climat sur la qualité chimique de l'eau (*Senhorst and Zwolsman*, 2005; *Whitehead et al.*, 2009). Le climat du site étudié est tempéré avec des variations temporelles des températures qui restent dans une gamme modérée malgré le réchauffement global, contrairement à des régions où les températures avoisinent déjà des gammes extrêmes pour les réactions biologiques ou chimiques (*Han et al.*, 2010) (*Bélanger et al.*, 2006) et où les formes de précipitations sont directement sensibles au réchauffement (neige …). Ainsi, beaucoup d'études sur le climat se focalisent sur les zones les plus vulnérables et sur son évolution : arides, semi-arides, tropicales, boréales (*Futter et al.*, 2008; *Lutz et al.*, 2016; *Rogora et al.*, 2003). Il semble important d'étudier ces questions dans les zones tempérées également (*Merot et al.*, 2014), qui sont par ailleurs largement concernées par des problèmes de qualité de l'eau (*Michalak*, 2016) car favorables à l'activité agricole et où les évolutions climatiques sont plus subtiles.

Dans ce contexte, aucune réponse directe des concentrations à la température n'a pu être identifiée. En revanche la sensibilité des concentrations aux flux et aux stocks d'eau dans le bassin versant est bien identifiée. Considérer un jeu de données multi-élémentaire a été effectivement intéressant, notamment parce que les 3 éléments choisis ici sont mobilisés via des compartiments et des voies d'écoulement différents (*Crossman et al.*, 2014). La spécificité du SRP est de présenter une dynamique de concentrations essentiellement reliées aux évènements de crues, tandis que sa concentration en écoulement de base fluctue dans un niveau proche du bruit du signal. L'étude des dynamiques de NO_3 et de DOC a montré leur opposition à toute les échelles de temps, opposition attribuée notamment à des sources localisées dans des compartiments différents et dont les réponses au climat, en particulier aux précipitations, obéissent à des dynamiques différentes, comme appuyé par le modèle proposé.

La longueur des séries disponibles sur l'observatoire AgrHyS est tout juste adaptée à l'étude des tendances : 17 années pour les chroniques de DOC et NO_3 dans le cours d'eau et 10 années pour le SRP. Notons que des données plus anciennes étaient disponibles pour NO_3 et débit uniquement, à des fréquences un peu différentes. L'évolution des concentrations dans le cours d'eau n'est détectable que depuis quelques années, ce qui était une nouveauté importante de l'analyse proposée ici par rapport aux travaux antérieurs (*Aubert et al.*, 2013c; *Dupas et al.*, 2015a; *Humbert et al.*, 2015). Les plus longues chroniques de concentrations disponibles sur les observatoires de ce type sont de l'ordre de 25 à 35 années (*Ponnou-Delaffon et al.*, 2020; *Tallec et al.*, 2013) (*Pierret et al.*, 2019). Aucun de ces 3 observatoires ne dispose de chroniques long terme pour C, N et P en raisons des questions de recherches et des éléments qui y sont associées.

Les stocks « hérités » de N et de P liés à l'activité agricole, identifiés dans le bassin de Kervidy-Naizin comme contrôlant les flux, ne sont pas forcément généralisables aux contextes forestiers, ou à des contextes hydrologiques différents. C'est pourquoi il parait intéressant de modéliser d'autres éléments en transposant le modèle à d'autres sites d'étude. Par exemple, les séries d'observation des flux de sédiments fins pourraient être utiles pour mieux contraindre les écoulements superficiels et les dynamiques de crue, alors que des éléments majeurs comme le calcium ou le sodium (produits de l'altération de la roche mère) pourraient mieux contraindre les écoulement plus profonds. Aussi, l'intégration de traceurs inertes de

l'eau tels que les isotopes stables ($H/^2H$, $^{16}O/^{18}O$), ou encore le chlorure, en contexte non agricole, apporterait de nouvelles contraintes sur les temps de résidence, en particulier pour calibrer les fonctions SAS et les âges de l'eau à l'exutoire.

Les réseaux de surveillance de la qualité de l'eau disposent aujourd'hui également de chroniques de plusieurs décennies (*Burt et al.*, 2014; *Dupas et al.*, 2018; *Minaudo et al.*, 2015; *Worrall et al.*, 2015) à des pas de temps généralement mensuelles, et sur des bassins versant beaucoup plus grands où il est plus difficile de relier la signature de l'exutoire aux processus de transferts à travers les paysages, car s'ajoutent des processus de transfert dans le réseau hydrographique, en plus des mélanges entre bassins versant. Les discontinuités hydrologiques, la présence de communes et de rejets de traitements marquent souvent les dynamiques de ces trois éléments.

5.4.2. Ce qu'il manque pour simuler des scénarios climatiques

Dans le cadre du modèle proposé, l'influence du climat sur les concentrations est directe, de par l'effet des précipitations et de leur distribution saisonnière sur les contributions relatives des compartiments, et indirecte, de par l'effet de la température sur les processus d'évapotranspiration. Ces effets peuvent se manifester à l'échelle pluriannuelle, saisonnière et de la crue. Pour tester de manière théorique l'effet de scénarios climatiques, les développements proposés en 5.3.2 sont à privilégier, en particulier pour intégrer des fonctions de productions, consommation et mobilisation des éléments faisant explicitement intervenir les variables climatiques comme la température (*Laudon et al.*, 2012) et l'humidité (*Forber et al.*, 2017), assimilée au niveau de remplissage des réservoirs. L'amélioration de la représentation des processus à l'étiage (*Giuntoli et al.*, 2013; *Pal et al.*, 2015; *Thirel et al.*, 2015) et en particulier en assec pourrait aussi s'avérer d'une grande influence sur les prédictions du modèle.

Pour utiliser le modèle afin de tester l'effet de scénarios climatiques, il serait nécessaire de disposer de scénarios de forçages climatiques locaux pertinents. Cela suppose de régionaliser les scénarios issus des modèles climatiques globaux qui nécessitent une correction pour les échelles spatiales plus fines (*Blanke et al.*, 2016; *Hadjikakou et al.*, 2011; *Salmon-Monviola et al.*, 2013). Les méthodes de désagrégation spatiale peuvent, d'une part, altérer la cohérence physique entre les variables, et d'autre part, les sorties des modèles climatiques globaux ne sont pas toujours réalistes, en particulier le timing des évènements de pluies intenses ou la fonte du manteau neigeux en fonction du relief local. Si le modèle global capture bien la tendance moyenne de l'évolution d'une variable, il n'en capture pas forcément la totalité des aspects. En particulier, la prédiction des pluies extrêmes s'est souvent révélée sensible à la méthode de désagrégation spatiale appliquée aux sorties du modèle climatique (*Ekström et al.*, 2018). Or d'après nos résultats, les concentrations vont être particulièrement sensibles non pas aux variations moyennes mais bien à l'évolution de la distribution des précipitations et de la séquence des évènements pluie-débit (*Strohmenger et al.*, 2020). En effet, le total des précipitations annuelles ne permet pas de projeter la réponse des concentrations en soluté dans le cours d'eau, car c'est en réalité la distribution des pluies au cours de l'année qui gouverne leur mobilisation. Une année humide avec des pluies distribuées de manière homogène dans le temps sera favorable aux écoulement verticaux par infiltration qui participent à la recharge lente de l'aquifère profond, ce dernier contribuant au débit de base de la rivière. Les concentrations seront donc élevées en NO_3 et faibles en DOC, du moins les premières années. A l'inverse, le même cumul de précipitation annuel concentré sur des épisodes pluvieux intenses lors de courtes périodes activera davantage les écoulements horizontaux et donc favorisera la contribution de

sources riches en DOC et faibles en NO_3 au débit du cours d'eau (*Green et al.*, 2014) (Green et al., 2014). La saisonnalité des écoulements est fortement liée à celle de l'évapotranspiration, aussi l'influence non pas seulement de la température mais également de la concentration atmosphérique en CO_2 sur ces flux est importante. Cette influence se traduit par un effet direct sur la conductance stomatique et donc la transpiration des plantes et par un effet indirect sur la croissance de la biomasse, en particulier des cultures, et donc leur transpiration (*Salmon-Monviola et al.*, 2013). L'évolution de la concentration atmosphérique en CO_2 paraît donc importante à intégrer dans les scénarios climatiques et la manière dont le modèle est capable d'en tenir compte.

Par ailleurs, de telles simulations ne permettraient d'explorer qu'une partie des évolutions car les activités agricoles, et plus généralement les facteurs anthropiques et écologiques du bassin versant ne sont pas figés dans le temps et évolueront aussi en fonction des conditions climatiques.

5.4.3. Lier qualité chimique et écologique des milieux aquatiques

Les effets du changement climatique sur les écosystèmes aquatiques se focalisent souvent sur les effets directs de la température et sur les effets indirects de la disponibilité en eau (*Woodward et al.*) mais ces derniers vont se combiner aux effets indirects de l'évolution de la qualité de l'eau qui répond aux effets du climat et des pressions humaines (*Oliver et al.*, 2017). Dans cette étude, le choix des trois éléments C, N et P était cohérent avec les menaces écologiques liées à des bouleversements trophiques, ces trois éléments étant fondamentaux pour les organismes vivants (*Finzi et al.*, 2011).

L'étude des couplages biogéochimiques de ces trois éléments (production primaire, respiration, minéralisation…) était en dehors du sujet de la thèse, néanmoins l'analyse des co-évolutions de ces trois éléments dans les cours d'eau permet de projeter quelques conséquences de l'évolution de la qualité de l'eau et de ses dynamiques sur les communautés aquatiques et leur réseau trophique à partir des ratios élémentaires ou stœchiométriques, ici C/N/P. Ces ratios stœchiométriques n'ont pas été abordés par les travaux présentés, on peut cependant supposer que l'activité métabolique du cours d'eau va varier saisonnièrement en fonction des variations des conditions de lumière et de température mais aussi de la stœchiométrie du cours d'eau : avec un ratio C/N fort à l'automne, qui diminue jusqu'à un minimum hivernal avant de ré-augmenter au printemps. On peut également s'interroger sur les effets des évènements de crue sur cette activité métabolique (*Bernal et al.*, 2019) avec des ratios C/N fortement augmentés et des ratios N/P fortement diminués au cours des crues. Sur le long-terme, on peut projeter :

- Qu'étant donnée l'opposition du DOC et du NO_3, l'évolution long-terme du ratio C/N sera amplifiée par rapport aux évolutions de chaque élément. Puisque la concentration en DOC augmente et celle en NO_3 diminue, ce ratio aura tendance à augmenter fortement.
- Que l'évolution du régime des évènements de crues associées à du ruissellement de surface affectera la fréquence des variations significatives des ratios C/N et N/P, puisque ceux-ci sont fortement augmenté et diminué, respectivement, lors des crues.

5.5. English summary of the discussion chapter

This chapter aims to link the methods and the results from chapters 3 and 4, to suggest several improvements of the model, and to discuss some application perspectives. We analyzed the simulated time series to identify long-term and seasonal signature using the methods described in chapter 3. The model did not reproduce the long-term trend of concentrations, this was expected because no trend on inputs or on production and consumption mechanisms were represented in the model. The mean seasonal patterns of the simulated and observed variables were very close, suggesting that the seasonal functioning of the catchment area and the contributions of DOC and NO_3 source areas were well reproduced by the model. However, some differences between simulated and observed variables during dry periods may suggest the need for specific work to improve the conceptualization of the functioning of intermittent rivers.

The model represented an opposition of DOC and NO_3 concentrations as observed although this opposition was a little exaggerated due to the use of constant concentrations values, and also by the lack of long-term trend in the NO_3 simulated series. The model was also able of reproducing asymmetries in the distributions of DOC and NO_3 concentrations, consistently with the observed data. However, the peaks of the simulated distributions were too narrow in comparison with the observations, which reflects the limitations of the end-member approach with constant concentrations. In addition, the frequent overestimations of DOC and underestimations of NO_3 suggested that other reactive processes or sources may contribute to variations of the stream concentrations.

We discuss the difficulties and opportunities of adding phosphorus in the model, it would bring more constraints on hydrological and physico-chemical functioning, and may improve the representation of downslope water table fluctuations and on the surface runoff processes that generate storm event. Other discussed perspectives for improving the model are:

- *To compute the concentrations in reservoirs as a function of temperature and water storage*
- *To explicitly simulate the mass of solutes in the compartments. The apparent production and transformation of the elements within the reservoirs would be controlled by the temperature and wetness conditions.*
- *As a complement to the modeling of solute storages in reservoirs, solute time series may be used to constrain the parameters of StorAge Selection-functions, thus to simulate water age distributions.*

We did not identify effect of temperature on solutes concentrations under the temperate oceanic climate of the Kervidy-Naizin catchment, likely because the temperature ranges remained moderate for biogeochemical reactions despite its long-term increase. Temperature indirectly influences the dynamics of solute concentrations through evapotranspiration that controls the catchment wetness. Indeed, solutes concentrations are more controlled by the seasonal distribution of precipitation and evapotranspiration than by their annual values. Thus, the regional seasonal distribution of the climatic variables is a key feature to predict with the climate model in order to predict climate effect on solutes concentrations in the river.

6. Conclusion

Les objectifs de cette thèse étaient d'étudier les dynamiques des concentrations en Carbone, Azote et Phosphore dissous dans un cours d'eau en contexte agricole, pour comparer les dynamiques de ces trois éléments d'origine et de nature hétérogènes, en terme de synchronie à plusieurs échelles temporelles, et pour identifier et comparer les effets du climat sur ces dynamiques.

Le travail s'est appuyé sur les données d'observations acquises dans le cadre de l'ORE AgrHyS, sur le bassin versant de Kevidy-Naizin, une tête de bassin versant agricole de 5 km², situé en Bretagne, France. Les chroniques disponibles sur ce site d'étude couvrent la période de 2002 à 2017 avec des données à minima journalières météorologiques (précipitation, température, rayonnement, vent), hydrologiques (débit, niveaux piézométriques) et sur la composition chimique de l'eau (concentrations en DOC, NO_3 et SRP). La longueur et la fréquence de ce jeu de données ont permis dans un premier volet, d'en faire une analyse à long terme, saisonnière et évènementielle. Chacune de ces échelles temporelles a été étudiée à l'aide d'une méthode appropriée :

- Les évolutions sur 16 ans ont été analysées à l'aide des tests de Mann-Kendall et de Theil Sen pour identifier les tendances à long-terme.
- La saisonnalité des variables a été analysée à l'aide d'une décomposition en séries de Fourier pour identifier les synchronies/asynchronies des cyclicités annuelles moyennes.
- Les concentrations extrêmes journalières ont été analysées par une approche probabiliste pour identifier les conditions hydroclimatiques associées aux concentrations maximums et minimums en DOC, NO_3 et SRP.

Les résultats montrent une évolution du climat local vers une saisonnalité plus contrastée des conditions hydrologiques qui se répercute sur les dynamiques des concentrations des solutés dans le cours d'eau. En effet, les précipitations et l'indice d'humidité du bassin (estimé par le cumul de précipitations sur une semaine) ont été identifiées comme les principaux moteurs des variations de concentrations dans le cours d'eau à l'échelle saisonnière et évènementielle. Ces deux variables contrôlent la connectivité hydrologique des sources de solutés avec le cours d'eau, ainsi que les réactions biogéochimiques qui les affectent. Sur le long terme, la qualité de l'eau semble davantage répondre aux facteurs anthropiques, en particulier par l'activité agricole et notamment la fertilisation.

Les dynamiques des concentrations en DOC et en NO_3 présentent des oppositions pour les trois échelles temporelles, suggérant des mécanismes communs entre ces deux éléments. A long-terme, les concentrations en NO_3 et en SRP diminuent alors que la concentration du DOC augmente. Les diminutions des concentrations en NO_3 et SRP à long terme sont imputées essentiellement aux changements opérés dans les systèmes agricoles, avec une inertie liée aux temps de réponse du bassin versant qui temporisent cependant cette diminution. Les hypothèses pour expliquer l'augmentation long-terme de la concentration en DOC sont une réduction des différents processus en conditions réductrices dans les zones ripariennes (comme la dénitrification en lien avec la diminution du NO_3), ou l'augmentation de la contribution des zones sources de carbone suite à la modification du régime de précipitation. Les saisonnalités moyennes des concentrations en DOC et du NO_3 sont nettement opposées avec des pics de concentration pendant les mois d'octobre et de mai, respectivement et deux pics de concentration du SRP en décembre et février. Cette opposition entre DOC et NO_3, également visible en période de crue, est le résultat de contributions hydrologiques aux compositions en DOC et NO_3 opposées (riche en DOC et pauvre en NO_3 ou vice versa) et dont les contributions relatives au cours d'eau changent au cours des

saisons et selon que le bassin est en crue ou non. On identifie notamment deux compartiments : un compartiment souterrain riche en NO_3 et un compartiment plus superficiel riche en DOC. Les concentrations en SRP sont découplées de celles du DOC et du NO_3, le SRP répondant davantage à l'échelles évènementielles et aux conditions anoxiques en bas de versant saturé, favorables à la dissolution du phosphore.

Les résultats de ces analyses ont permis de produire ce schéma perceptuel du fonctionnement du bassin versant à partir duquel dans un second volet, un modèle hydro-chimique conceptuel et global a été développé. Ce modèle avait pour ambition de reproduire les dynamiques saisonnière et évènementielle du débit et des concentrations en DOC et NO_3 à l'exutoire du bassin versant, à un pas de temps journalier. Les concentrations journalières en DOC et en NO_3 observées à l'exutoire du bassin versant de Kervidy-Naizin ont donc été mobilisées pour apporter des contraintes supplémentaires sur la représentation des chemins d'écoulement de l'eau dans le modèle. Un modèle simple, basé sur une hypothèse de mélange entre deux réservoirs sources aux réponses hydrologiques et aux compositions chimiques contrastées a permis de reproduire les dynamiques infra-annuelles principales observées pour le débit et les concentrations en DOC et NO_3.

Ces résultats tendent à conforter que les oppositions entre DOC et NO_3 à l'échelle annuelle et évènementielle sont liées et principalement contrôlées par les mélanges entre chemins d'écoulement de l'eau dans deux compartiments : le compartiment souterrain (nappe superficielle majoritairement située dans les altérite), dont l'écoulement est lent et saisonnier, qui représente la principale source de NO_3, et le compartiment riparien, dont la réponse hydrologique est rapide, représente la principale source de DOC. Les tendances à long-terme, n'ont pu être reproduites par ce modèle. En particulier sur la concentration en NO_3, pour laquelle la tendance est la plus importante, ceci nécessiterait de représenter un épuisement du stock hérité des activités agricoles historiques.

Plusieurs pistes en cours de développement ont été proposées pour faire évoluer le modèle : la première vise à modéliser des concentrations dynamiques dans les compartiments en fonction des conditions d'humidité et de température qui contrôlent les processus biogéochimiques; la seconde vise à simuler explicitement l'évolution de stocks de solutés en fonction des processus biogéochimiques faisant intervenir les variables climatiques (température, humidité), des entrées agricoles en NO_3 pour le réservoir SU, et des transferts entre les différents compartiments en utilisant la modélisation des temps de résidence et âges de l'eau par des fonctions-de StorAge Selection.

Il parait intéressant transposer ce modèle à d'autres sites observatoires, en utilisant éventuellement d'autres éléments tels que les flux de sédiments fins pour mieux contraindre les écoulements superficiels et les dynamiques de crue, ou les produits de l'altération de la roche mère et mieux contraindre ainsi les écoulements superficiels et profonds. Le manque de données de ce type reste un frein majeur à toute tentative de transposition. L'utilisation du modèle en simulation pour tester l'effet du climat sur la qualité de l'eau nécessite de disposer de scénarios de forçages climatiques régionalisés, notamment sur les distributions saisonnières et évènementielles des précipitations et de l'évapotranspiration de référence auxquelles l'état hydrique du bassin et donc les mobilisations de DOC et NO_3 sont sensibles. Ce travail reste à faire, notamment sur le modèle en cours de développement, pour analyser ces effets qui comporteront, quoiqu'il en soit, de fortes incertitudes d'ordre climatique, hydrologique et biogéochimique.

Références

Abbott, B. W., F. Moatar, O. Gauthier, O. Fovet, V. Antoine, and O. Ragueneau (2018), Trends and seasonality of river nutrients in agricultural catchments: 18years of weekly citizen science in France, *Sci Total Environ*, *624*, 845-858, doi: 10.1016/j.scitotenv.2017.12.176.

Aquilina, L., A. Poszwa, C. Walter, V. Vergnaud, A.-C. Pierson-Wickmann, and L. Ruiz (2012), Long-term effects of high nitrogen loads on cation and carbon riverine export in agricultural catchments, *Environmental science & technology*, *46*(17), 9447-9455, doi: 10.1021/es301715t.

Arnold, J. G., R. Srinivasan, R. S. Muttiah, and J. R. Williams (1998), Large area hydrologic modeling and assessment part I: model development 1, *JAWRA Journal of the American Water Resources Association*, *34*(1), 73-89.

Aubert, A. (2013), Analyse des motifs temporels d'une chronique décennale haute-fréquence de qualité de l'eau dans un observatoire agro-hydrologique, AGROCAMPUS OUEST.

Aubert, A. H., C. Gascuel-Odoux, and P. Merot (2013a), Annual hysteresis of water quality: A method to analyse the effect of intra- and inter-annual climatic conditions, *Journal of Hydrology*, *478*, 29-39, doi: 10.1016/j.jhydrol.2012.11.027.

Aubert, A. H., R. Tavenard, R. Emonet, A. de Lavenne, S. Malinowski, T. Guyet, R. Quiniou, J. M. Odobez, P. Merot, and C. Gascuel-Odoux (2013b), Clustering flood events from water quality time series using Latent Dirichlet Allocation model, *Water Resources Research*, *49*(12), 8187-8199, doi: 10.1002/2013wr014086.

Aubert, A. H., et al. (2013c), Solute transport dynamics in small, shallow groundwater-dominated agricultural catchments: insights from a high-frequency, multisolute 10 yr-long monitoring study, *Hydrology and Earth System Sciences*, *17*(4), 1379-1391, doi: 10.5194/hess-17-1379-2013.

Bartley, R., W. J. Speirs, T. W. Ellis, and D. K. Waters (2012), A review of sediment and nutrient concentration data from Australia for use in catchment water quality models, *Marine pollution bulletin*, *65*(4-9), 101-116.

Basu, N. B., P. Jindal, K. E. Schilling, C. F. Wolter, and E. S. Takle (2012), Evaluation of analytical and numerical approaches for the estimation of groundwater travel time distribution, *Journal of Hydrology*, *475*, 65-73.

Basu, N. B., G. Destouni, J. W. Jawitz, S. E. Thompson, N. V. Loukinova, A. Darracq, S. Zanardo, M. Yaeger, M. Sivapalan, and A. Rinaldo (2010), Nutrient loads exported from managed catchments reveal emergent biogeochemical stationarity, *Geophys. Res. Lett.*, *37*(23), doi: 10.1029/2010GL045168.

Beaujouan, V., P. Durand, and L. Ruiz (2001), Modelling the effect of the spatial distribution of agricultural practices on nitrogen fluxes in rural catchments, *Ecological modelling*, *137*(1), 93-105.

Beaujouan, V. r., P. Durand, L. Ruiz, P. Aurousseau, and G. Cotteret (2002), A hydrological model dedicated to topography-based simulation of nitrogen transfer and transformation: rationale and application to the geomorphology- denitrification relationship, *Hydrological Processes*, *16*(2), 493-507, doi: 10.1002/hyp.327.

Bélanger, S., H. Xie, N. Krotkov, P. Larouche, W. F. Vincent, and M. Babin (2006), Photomineralization of terrigenous dissolved organic matter in Arctic coastal waters from 1979 to 2003: Interannual variability and implications of climate change, *Glob. Biogeochem. Cycle*, *20*(4).

Bell, N., R. A. C. Cooke, T. Olsen, M. B. David, and R. Hudson (2015), Characterizing the Performance of Denitrifying Bioreactors during Simulated Subsurface Drainage Events, *J. Environ. Qual.*, *44*(5), 1647-1656, doi: 10.2134/jeq2014.04.0162.

Bende-Michl, U., K. Verburg, and H. P. Cresswell (2013), High-frequency nutrient monitoring to infer seasonal patterns in catchment source availability, mobilisation and delivery, *Environ. Monit. Assess.*, *185*(11), 9191-9219.

Benettin, P., C. Soulsby, C. Birkel, D. Tetzlaff, G. Botter, and A. Rinaldo (2017), Using SAS functions and high-resolution isotope data to unravel travel time distributions in headwater catchments, *Water Resources Research*, *53*(3), 1864-1878.

Benhamou, C., J. Salmon-Monviola, P. Durand, C. Grimaldi, and P. Merot (2013), Modeling the interaction between fields and a surrounding hedgerow network and its impact on water and nitrogen flows of a small watershed, *Agric. Water Manage.*, *121*, 62-72.

Bennett, N. D., B. F. Croke, G. Guariso, J. H. Guillaume, S. H. Hamilton, A. J. Jakeman, S. Marsili-Libelli, L. T. Newham, J. P. Norton, and C. Perrin (2013), Characterising performance of environmental models, *Environmental Modelling & Software*, *40*, 1-20.

Bergstrom, S. (1992), The HBV model-its structure and applications.

Bernal, S., A. Lupon, W. M. Wollheim, F. Sabater, S. Poblador, and E. Martí (2019), Supply, demand, and in-stream retention of dissolved organic carbon and nitrate during storms in Mediterranean forested headwater streams, *Frontiers in Environmental Science*, *7*, 60.

Beven, K., and A. Binley (1992), The future of distributed models: model calibration and uncertainty prediction, *Hydrological processes*, *6*(3), 279-298.

Beven, K. J., and M. J. Kirkby (1979), A physically based, variable contributing area model of basin hydrology/Un modèle à base physique de zone d'appel variable de l'hydrologie du bassin versant, *Hydrological Sciences Journal*, *24*(1), 43-69.

Birkel, C., C. Soulsby, and D. Tetzlaff (2014), Integrating parsimonious models of hydrological connectivity and soil biogeochemistry to simulate stream DOC dynamics, *Journal of Geophysical Research: Biogeosciences*, *119*(5), 1030-1047.

Birkel, C., D. Tetzlaff, S. Dunn, and C. Soulsby (2010), Towards a simple dynamic process conceptualization in rainfall–runoff models using multi-criteria calibration and tracers in temperate, upland catchments, *Hydrological Processes: An International Journal*, *24*(3), 260-275.

Blanke, J. H., M. Lindeskog, J. Lindström, and V. Lehsten (2016), Effect of climate data on simulated carbon and nitrogen balances for Europe, *Journal of Geophysical Research: Biogeosciences*, *121*(5), 1352-1371.

Bowes, M., H. Jarvie, S. J. Halliday, R. Skeffington, A. Wade, M. Loewenthal, E. Gozzard, J. Newman, and E. Palmer-Felgate (2015), Characterising phosphorus and nitrate inputs to a rural river using high-frequency concentration–flow relationships, *Sci. Total Environ.*, *511*, 608-620, doi: 10.1016/j.scitotenv.2014.12.086.

Bowes, M. J., W. A. House, R. A. Hodgkinson, and D. V. Leach (2005), Phosphorus–discharge hysteresis during storm events along a river catchment: the River Swale, UK, *Water Res.*, *39*(5), 751-762.

Burnash, R. (1995), The NWS river forecast system-catchment modeling, *Computer models of watershed hydrology*, 311-366.

Burns, D. A., B. A. Pellerin, M. P. Miller, P. D. Capel, A. J. Tesoriero, and J. M. Duncan (2019), Monitoring the riverine pulse: Applying high-frequency nitrate data to advance integrative understanding of biogeochemical and hydrological processes, *Wiley Interdiscip. Rev.-Water*, *6*(4), 24, doi: 10.1002/wat2.1348.

Burt, T., N. Howden, and F. Worrall (2014), On the importance of very long-term water quality records, *Wiley Interdisciplinary Reviews: Water*, *1*(1), 41-48.

Buysse, P., C. R. Flechard, Y. Hamon, and V. Viaud (2016), Impacts of water regime and land-use on soil CO 2 efflux in a small temperate agricultural catchment, *Biogeochemistry*, *130*(3), 267-288.

Camporese, M., C. Paniconi, M. Putti, and S. Orlandini (2010), Surface-subsurface flow modeling with path-based runoff routing, boundary condition-based coupling, and assimilation of multisource observation data, *Water Resources Research*, *46*(2).

Cann, C. (1998), Evolution de l'agriculture et de sa pression polluante sur le bassin et en Bretagne, *Agriculture intensive et qualité des eaux, Inra Editions*, 25-40.

Carluer, N. (1998), Vers une modélisation hydrologique adaptée à l'évaluation des pollutions diffuses: prise en compte du réseau anthropique. Application au bassin versant de Naizin (Morbihan), Paris 6.

Casal, L., P. Durand, N. Akkal-Corfini, C. Benhamou, F. Laurent, J. Salmon-Monviola, and F. Vertes (2018), Optimal location of set-aside areas to reduce nitrogen pollution: a modelling study, *The Journal of Agricultural Science*, *156*(9), 1090-1102.

Casson, N. J., M. C. Eimers, S. A. Watmough, and M. C. Richardson (2019), The role of wetland coverage within the near-stream zone in predicting of seasonal stream export chemistry from forested headwater catchments, *Hydrological Processes*, *33*(10), 1465-1475, doi: 10.1002/hyp.13413.

Chaplot, V., and C. Walter (2003), Subsurface topography to enhance the prediction of the spatial distribution of soil wetness, *Hydrological processes*, *17*(13), 2567-2580.

Chaplot, V., C. Walter, and P. Curmi (2003), Testing quantitative soil-landscape models for predicting the soil hydromorphic index at a regional scale, *Soil science*, *168*(6), 445-454.

Cheverry, C. (1998), *Agriculture intensive et qualité des eaux*, Editions Quae.

Crave, A., and C. Gascuel-Odoux (1997), The influence of topography on time and space distribution of soil surface water content, *Hydrological processes*, *11*(2), 203-210.

Cross, W. F., J. M. Hood, J. P. Benstead, A. D. Huryn, and D. Nelson (2015), Interactions between temperature and nutrients across levels of ecological organization, *Glob. Change Biol.*, *21*(3), 1025-1040.

Crossman, J., M. Futter, P. G. Whitehead, E. Stainsby, H. Baulch, L. Jin, S. Oni, R. L. Wilby, and P. Dillon (2014), Flow pathways and nutrient transport mechanisms drive hydrochemical sensitivity to climate change across catchments with different geology and topography, *Hydrology & Earth System Sciences*, *18*(12).

Davranche, M., M. Grybos, G. Gruau, M. Pédrot, A. Dia, and R. Marsac (2011), Rare earth element patterns: A tool for identifying trace metal sources during wetland soil reduction, *Chemical Geology*, *284*(1-2), 127-137.

Davranche, M., A. Dia, M. Fakih, B. Nowack, G. Gruau, G. Ona-nguema, P. Petitjean, S. Martin, and R. Hochreutener (2013), Organic matter control on the reactivity of Fe (III)-oxyhydroxides and associated As in wetland soils: A kinetic modeling study, *Chemical Geology*, *335*, 24-35.

Dawson, C. W., R. J. Abrahart, and L. M. See (2007), HydroTest: a web-based toolbox of evaluation metrics for the standardised assessment of hydrological forecasts, *Environmental Modelling & Software*, *22*(7), 1034-1052.

de Lavenne, A., H. Boudhraâ, and C. Cudennec (2015), Streamflow prediction in ungauged basins through geomorphology-based hydrograph transposition, *Hydrology Research*, *46*(2), 291-302.

Denis, M., L. Jeanneau, P. Petitjean, A. Murzeau, M. Liotaud, L. Yonnet, and G. Gruau (2017), New molecular evidence for surface and sub-surface soil erosion controls on the composition of stream DOM during storm events.

Dettling, M. (2013), Applied time series analysis, *Applied time series analysis*.

Dick, J., D. Tetzlaff, C. Birkel, and C. Soulsby (2015), Modelling landscape controls on dissolved organic carbon sources and fluxes to streams, *Biogeochemistry*, *122*(2-3), 361-374, doi: 10.1007/s10533-014-0046-3.

Drouet, J.-L., S. Duretz, P. Durand, P. Cellier, and S. Reis (2012), Modelling the contribution of short-range atmospheric and hydrological transfers to nitrogen fluxes, budgets and indirect emissions in rural landscapes, *Biogeosciences*, *9*(5).

Dunn, S. M., L. Johnston, C. Taylor, H. Watson, Y. Cook, and S. J. Langan (2013), Capability and limitations of a simple grid-based model for simulating land use influences on stream nitrate concentrations, *Journal of Hydrology*, *507*, 110-123, doi: 10.1016/j.jhydrol.2013.10.016.

Dunn, S. M., J. Freer, M. Weiler, M. J. Kirkby, J. Seibert, P. F. Quinn, G. Lischeid, D. Tetzlaff, and C. Soulsby (2008), Conceptualization in catchment modelling: simply learning?, *Hydrological Processes*, *22*(13), 2389-2393, doi: 10.1002/hyp.7070.

Dupas, R. (2015), Identification et modélisation des processus à l'origine des transferts de phosphore dissous dans un bassin versant agricole, Rennes, Agrocampus Ouest.

Dupas, R., C. Gascuel-Odoux, N. Gilliet, C. Grimaldi, and G. Gruau (2015a), Distinct export dynamics for dissolved and particulate phosphorus reveal independent transport mechanisms in an arable headwater catchment, *Hydrological Processes*, *29*(14), 3162-3178, doi: 10.1002/hyp.10432.

Dupas, R., C. Minaudo, G. Gruau, L. Ruiz, and C. Gascuel-Odoux (2018), Multidecadal Trajectory of Riverine Nitrogen and Phosphorus Dynamics in Rural Catchments, *Water Resources Research*, *54*(8), 5327-5340, doi: 10.1029/2018wr022905.

Dupas, R., M. Delmas, J.-M. Dorioz, J. Garnier, F. Moatar, and C. Gascuel-Odoux (2015b), Assessing the impact of agricultural pressures on N and P loads and eutrophication risk, *Ecological Indicators*, *48*, 396-407, doi: 10.1016/j.ecolind.2014.08.007.

Dupas, R., G. Gruau, S. Gu, G. Humbert, A. Jaffrezic, and C. Gascuel-Odoux (2015c), Groundwater control of biogeochemical processes causing phosphorus release from riparian wetlands, *Water Res*, *84*, 307-314, doi: 10.1016/j.watres.2015.07.048.

Dupas, R., R. Tavenard, O. Fovet, N. Gilliet, C. Grimaldi, and C. Gascuel-Odoux (2015d), Identifying seasonal patterns of phosphorus storm dynamics with dynamic time warping, *Water Resources Research*, *51*(11), 8868-8882, doi: 10.1002/2015wr017338.

Dupas, R., J. Salmon-Monviola, K. J. Beven, P. Durand, P. M. Haygarth, M. J. Hollaway, and C. Gascuel-Odoux (2016), Uncertainty assessment of a dominant-process catchment model of dissolved phosphorus transfer, *Hydrology and Earth System Sciences*, *20*(12), 4819-4835, doi: 10.5194/hess-20-4819-2016.

Durand, P. (2004), Simulating nitrogen budgets in complex farming systems using INCA: calibration and scenario analyses for the Kervidy catchment (W. France).

Ebeling, P., R. Kumar, M. Weber, L. Knoll, J. Fleckenstein, and A. Musolff (2020), Archetypes and Controls of Riverine Nutrient Export Across German Catchments.

Ecrepont, S. (2019), Analyse des effets d'échelle, d'organisation spatiale et de structuration géomorphologique pour la modélisation des débits et de flux hydrochimiques en bassins non jaugés, Rennes 1.

Eklof, K., A. Kraus, M. Futter, J. Schelker, M. Meili, E. W. Boyer, and K. Bishop (2015), Parsimonious Model for Simulating Total Mercury and Methylmercury in Boreal Streams Based on Riparian Flow Paths and Seasonality, *Environmental Science & Technology*, *49*(13), 7851-7859, doi: 10.1021/acs.est.5b00852.

Ekström, M., E. D. Gutmann, R. L. Wilby, M. R. Tye, and D. G. Kirono (2018), Robustness of hydroclimate metrics for climate change impact research, *Wiley Interdisciplinary Reviews: Water*, *5*(4), e1288.

Fenicia, F., D. Kavetski, and H. H. G. Savenije (2011), Elements of a flexible approach for conceptual hydrological modeling: 1. Motivation and theoretical development, *Water Resources Research*, *47*, 13, doi: 10.1029/2010wr010174.

Fenicia, F., H. H. G. Savenije, P. Matgen, and L. Pfister (2006), Is the groundwater reservoir linear? Learning from data in hydrological modelling, *Hydrology and Earth System Sciences*, *10*(1), 139-150, doi: 10.5194/hess-10-139-2006.

Finzi, A. C., A. T. Austin, E. E. Cleland, S. D. Frey, B. Z. Houlton, and M. D. Wallenstein (2011), Responses and feedbacks of coupled biogeochemical cycles to climate change: examples from terrestrial ecosystems, *Frontiers in Ecology and the Environment*, *9*(1), 61-67.

Flechard, C., E. Nemitz, R. Smith, D. Fowler, A. Vermeulen, A. Bleeker, J. Erisman, D. Simpson, L. Zhang, and Y. Tang (2011), Dry deposition of reactive nitrogen to European ecosystems: a comparison of inferential models across the NitroEurope network, *Atmos. Chem. Phys.*, *11*(6), 2703-2728.

Forber, K. J., M. C. Ockenden, C. Wearing, M. J. Hollaway, P. D. Falloon, R. Kahana, M. L. Villamizar, J. G. Zhou, P. J. Withers, and K. J. Beven (2017), Determining the effect of drying time on phosphorus solubilization from three agricultural soils under climate change scenarios, *J. Environ. Qual.*, *46*(5), 1131-1136, doi: 10.2134/jeq2017.04.0144.

Ford, W. I., K. King, and M. R. Williams (2018), Upland and in-stream controls on baseflow nutrient dynamics in tile-drained agroecosystem watersheds, *Journal of Hydrology*, *556*, 800-812, doi: 10.1016/j.jhydrol.2017.12.009.

Fovet, O., A. Jaffrézic, G. Gruau, and P. Durand (2013), Soil control on the spatial variability of DOC concentration in headwater catchments: a comprehensive modeling approach to the annual dynamics of stream DOC concentration.

Fovet, O., L. Ruiz, M. Faucheux, J. Molénat, M. Sekhar, F. Vertès, L. Aquilina, C. Gascuel-Odoux, and P. Durand (2015), Using long time series of agricultural-derived nitrates for estimating catchment transit times, *Journal of Hydrology*, *522*, 603-617, doi: 10.1016/j.jhydrol.2015.01.030.

Fovet, O., et al. (2018), AgrHyS: An Observatory of Response Times in Agro-Hydro Systems, *Vadose Zone J.*, *17*(1), doi: 10.2136/vzj2018.04.0066.

Fu, B., W. S. Merritt, B. F. Croke, T. R. Weber, and A. J. Jakeman (2019), A review of catchment-scale water quality and erosion models and a synthesis of future prospects, *Environmental modelling & software*, *114*, 75-97.

Futter, M., M. Starr, M. Forsius, and M. Holmberg (2008), Modelling the effects of climate on long-term patterns of dissolved organic carbon concentrations in the surface waters of a boreal catchment, *Hydrology and Earth System Sciences*, *12*(2), 437-447.

Gaillardet, J., et al. (2018), OZCAR: The French Network of Critical Zone Observatories, *Vadose Zone J.*, *17*(1), doi: 10.2136/vzj2018.04.0067.

Gascuel-Odoux, C., P. Aurousseau, P. Durand, L. Ruiz, and J. Molenat (2010), The role of climate on inter-annual variation in stream nitrate fluxes and concentrations, *Sci Total Environ*, *408*(23), 5657-5666, doi: 10.1016/j.scitotenv.2009.05.003.

Gascuel-Odoux, C., O. Fovet, G. Gruau, L. Ruiz, and P. Merot (2018), Evolution of scientific questions over 50 years in the Kervidy-Naizin catchment: from catchment hydrology to integrated studies of biogeochemical cycles and agroecosystems in a rural landscape, *Cuadernos de Investigación Geográfica*, *44*(2), 535-555, doi: 10.18172/cig.3383.

Gascuel, C., M. Weiler, and J. Molenat (2010), Effect of the spatial distribution of physical aquifer properties on modelled water table depth and stream discharge in a headwater catchment.

Gharari, S., M. Hrachowitz, F. Fenicia, H. Gao, and H. Savenije (2014), Using expert knowledge to increase realism in environmental system models can dramatically reduce the need for calibration, *Hydrology & Earth System Sciences*, *18*(12).

Giuntoli, I., B. Renard, J.-P. Vidal, and A. Bard (2013), Low flows in France and their relationship to large-scale climate indices, *Journal of Hydrology*, *482*, 105-118.

Green, C. T., B. A. Bekins, S. J. Kalkhoff, R. M. Hirsch, L. Liao, and K. K. Barnes (2014), Decadal surface water quality trends under variable climate, land use, and hydrogeochemical setting in Iowa, USA, *Water Resources Research*, *50*(3), 2425-2443, doi: 10.1002/2013WR014829.

Grybos, M., M. Davranche, G. Gruau, P. Petitjean, and M. Pédrot (2009), Increasing pH drives organic matter solubilization from wetland soils under reducing conditions, *Geoderma*, *154*(1-2), 13-19, doi: 10.1016/j.geoderma.2009.09.001.

Gu, S., G. Gruau, F. Malique, R. Dupas, P. Petitjean, and C. Gascuel-Odoux (2018), Drying/rewetting cycles stimulate release of colloidal-bound phosphorus in riparian soils, *Geoderma*, *321*, 32-41, doi: 10.1016/j.geoderma.2018.01.015.

Gu, S., G. Gruau, R. Dupas, P. Petitjean, Q. Li, and G. Pinay (2019), Respective roles of Fe-oxyhydroxide dissolution, pH changes and sediment inputs in dissolved phosphorus release from wetland soils under anoxic conditions, *Geoderma*, *338*, 365-374, doi: 10.1016/j.geoderma.2018.12.034.

Gu, S., G. Gruau, R. Dupas, C. Rumpel, A. Creme, O. Fovet, C. Gascuel-Odoux, L. Jeanneau, G. Humbert, and P. Petitjean (2017), Release of dissolved phosphorus from riparian wetlands: Evidence for complex interactions among hydroclimate variability, topography and soil properties, *Sci. Total Environ.*, *598*, 421-431, doi: 10.1016/j.scitotenv.2017.04.028.

Guillemot, S., O. Fovet, C. Gascuel-Odoux, G. Gruau, A. Casquin, F. Curie, C. Minaudo, L. Strohmenger, and F. Moatar (2020), Spatio-temporal controls of CNP dynamics across headwater catchments of a temperate agricultural region from public data analysis, *Hydrology and Earth System Sciences Discussions*, 1-31.

Hadjikakou, M., P. G. Whitehead, L. Jin, M. Futter, P. Hadjinicolaou, and M. Shahgedanova (2011), Modelling nitrogen in the Yeşilirmak River catchment in Northern Turkey: impacts of future climate and environmental change and implications for nutrient management, *Sci. Total Environ.*, *409*(12), 2404-2418.

Han, C.-W., S.-G. Xu, J.-W. Liu, and J.-J. Lian (2010), Nonpoint-source nitrogen and phosphorus behavior and modeling in cold climate: A review, *Water Sci. Technol.*, *62*(10), 2277-2285.

Harman, C. J. (2015), Time-variable transit time distributions and transport: Theory and application to storage-dependent transport of chloride in a watershed, *Water Resources Research*, *51*(1), 1-30.

Haygarth, P. M., H. P. Jarvie, S. M. Powers, A. N. Sharpley, J. J. Elser, J. Shen, H. M. Peterson, N.-I. Chan, N. J. Howden, and T. Burt (2014), Sustainable phosphorus management and the need for a long-term perspective: The legacy hypothesis, edited, ACS Publications

He, B. N., J. T. He, L. Wang, X. W. Zhang, and E. P. Bi (2019), Effect of hydrogeological conditions and surface loads on shallow groundwater nitrate pollution in the Shaying River Basin: Based on least squares surface fitting model, *Water Res.*, *163*, 10, doi: 10.1016/j.watres.2019.114880.

Howarth, R., G. Billen, D. Swaney, A. Townsend, N. Jaworski, K. Lajtha, J. Downing, R. Elmgren, N. Caraco, and T. Jordan (1996), Riverine inputs of nitrogen to the North Atlantic Ocean: fluxes and human influences, *Biogeochemistry*, *35*, 75-139.

Howarth, R. W. (2008), Coastal nitrogen pollution: a review of sources and trends globally and regionally, *Harmful algae*, *8*(1), 14-20.

Howden, N. J., T. P. Burt, F. Worrall, S. Mathias, and M. J. Whelan (2011), Nitrate pollution in intensively farmed regions: What are the prospects for sustaining high-quality groundwater?, *Water Resources Research*, *47*(6).

Hrachowitz, M., and M. P. Clark (2017), HESS Opinions: The complementary merits of competing modelling philosophies in hydrology, *Hydrol. Earth Syst. Sci*, *21*(8), 3953-3973.

Hrachowitz, M., O. Fovet, L. Ruiz, and H. H. G. Savenije (2015), Transit time distributions, legacy contamination and variability in biogeochemical 1/f(alpha) scaling: how are hydrological response

dynamics linked to water quality at the catchment scale?, *Hydrological Processes*, *29*(25), 5241-5256, doi: 10.1002/hyp.10546.

Hrachowitz, M., H. Savenije, T. Bogaard, D. Tetzlaff, and C. Soulsby (2013), What can flux tracking teach us about water age distribution patterns and their temporal dynamics?, *Hydrology and Earth System Sciences*.

Hrachowitz, M., P. Benettin, B. M. van Breukelen, O. Fovet, N. J. K. Howden, L. Ruiz, Y. van der Velde, and A. J. Wade (2016), Transit timesthe link between hydrology and water quality at the catchment scale, *Wiley Interdiscip. Rev.-Water*, *3*(5), 629-657, doi: 10.1002/wat2.1155.

Hrachowitz, M., O. Fovet, L. Ruiz, T. Euser, S. Gharari, R. Nijzink, J. Freer, H. H. G. Savenije, and C. Gascuel-Odoux (2014), Process consistency in models: The importance of system signatures, expert knowledge, and process complexity, *Water Resources Research*, *50*(9), 7445-7469, doi: 10.1002/2014wr015484.

Humbert, G. (2015), Déterminisme hydro-climatique de la composition et du transfert des matières organiques dissoutes dans un bassin versant agricole.

Humbert, G., A. Jaffrezic, O. Fovet, G. Gruau, and P. Durand (2015), Dry-season length and runoff control annual variability in stream DOC dynamics in a small, shallow groundwater-dominated agricultural watershed, *Water Resources Research*, *51*(10), 7860-7877, doi: 10.1002/2015wr017336.

Humbert, G., T. B. Parr, L. Jeanneau, R. Dupas, P. Petitjean, N. Akkal-Corfini, V. Viaud, A.-C. Pierson-Wickmann, M. Denis, and S. Inamdar (2019), Agricultural Practices and Hydrologic Conditions Shape the Temporal Pattern of Soil and Stream Water Dissolved Organic Matter, *Ecosystems*, 1-19.

ISO 10304, N. (1995), Determination of dissolved fluoride, chloride, nitrite, orthophosphate, bromide, nitrate, and sulfate ions, using liquid chromatography of ions, edited by AFNOR

ISO 15681, N. (2005), Determination of orthophosphates and total phosphorus contents by flow analysis (FIA and CFA), edited by AFNOR

Jaffrézic, A., and P. Mérot (1998), Empirical modeling of the oxidoreduction potentiel variations in a hydromorphic organic soil, *Mineralogical Magazine*, *62*, 703-704.

Jeanneau, L., P. Buysse, M. Denis, G. Gruau, P. Petitjean, A. Jaffrézic, C. Flechard, and V. Viaud (2020), Water Table Dynamics Control Carbon Losses from the Destabilization of Soil Organic Matter in a Small, Lowland Agricultural Catchment, *Soil Systems*, *4*(1), 2.

Jones, J., E. Sudicky, A. E. Brookfield, and Y. J. Park (2006), An assessment of the tracer-based approach to quantifying groundwater contributions to streamflow, *Water Resources Research*, *42*(2).

Jordan, T. E., D. L. Correll, and D. E. Weller (1997), Relating nutrient discharges from watersheds to land use and streamflow variability, *Water resources research*, *33*(11), 2579-2590.

Kasurinen, V., K. Alfredsen, A. Ojala, J. Pumpanen, G. A. Weyhenmeyer, M. N. Futter, H. Laudon, and F. Berninger (2016), Modeling nonlinear responses of DOC transport in boreal catchments in Sweden, *Water Resources Research*, *52*(7), 4970-4989.

Kavetski, D., F. Fenicia, and M. P. Clark (2011), Impact of temporal data resolution on parameter inference and model identification in conceptual hydrological modeling: Insights from an experimental catchment, *Water Resources Research*, *47*(5).

Kolbe, T., J. Marcais, Z. Thomas, B. W. Abbott, J. R. de Dreuzy, P. Rousseau-Gueutin, L. Aquilina, T. Labasque, and G. Pinay (2016), Coupling 3D groundwater modeling with CFC-based age dating to classify local groundwater circulation in an unconfined crystalline aquifer, *Journal of Hydrology*, *543*, 31-46, doi: 10.1016/j.jhydrol.2016.05.020.

Kollet, S. J., and R. M. Maxwell (2008), Demonstrating fractal scaling of baseflow residence time distributions using a fully-coupled groundwater and land surface model, *Geophys. Res. Lett.*, *35*(7).

Lambert, T., A. C. Pierson-Wickmann, G. Gruau, A. Jaffrezic, P. Petitjean, J. N. Thibault, and L. Jeanneau (2013), Hydrologically driven seasonal changes in the sources and production mechanisms of dissolved organic carbon in a small lowland catchment, *Water Resources Research*, *49*(9), 5792-5803, doi: 10.1002/wrcr.20466.

Lambert, T., A.-C. Pierson-Wickmann, G. Gruau, A. Jaffrézic, P. Petitjean, J.-N. Thibault, and L. Jeanneau (2014), DOC sources and DOC transport pathways in a small headwater catchment as revealed by carbon isotope fluctuation during storm events.

Lapointe, B. E., P. J. Barile, and W. R. Matzie (2004), Anthropogenic nutrient enrichment of seagrass and coral reef communities in the Lower Florida Keys: discrimination of local versus regional nitrogen sources, *Journal of Experimental Marine Biology and Ecology*, *308*(1), 23-58.

Laudon, H., J. Buttle, S. K. Carey, J. McDonnell, K. McGuire, J. Seibert, J. Shanley, C. Soulsby, and D. Tetzlaff (2012), Cross-regional prediction of long-term trajectory of stream water DOC response to climate change, *Geophys. Res. Lett.*, *39*, 6, doi: 10.1029/2012gl053033.

Le Guillou, C., N. Chemidlin Prévost-Bouré, B. Karimi, N. Akkal-Corfini, S. Dequiedt, V. Nowak, S. Terrat, S. Menasseri-Aubry, V. Viaud, and P. A. Maron (2019), Tillage intensity and pasture in rotation effectively shape soil microbial communities at a landscape scale, *MicrobiologyOpen*, *8*(4), e00676.

Lefrançois, J. (2007), Dynamiques et origines des matières en suspension sur de petits bassins versants agricoles sur schiste.

Liang, X., D. P. Lettenmaier, E. F. Wood, and S. J. Burges (1994), A simple hydrologically based model of land surface water and energy fluxes for general circulation models, *Journal of Geophysical Research: Atmospheres*, *99*(D7), 14415-14428.

Lindström, G., C. Pers, J. Rosberg, J. Strömqvist, and B. Arheimer (2010), Development and testing of the HYPE (Hydrological Predictions for the Environment) water quality model for different spatial scales, *Hydrology research*, *41*(3-4), 295-319.

Lintern, A., J. A. Webb, D. Ryu, S. Liu, D. Waters, P. Leahy, U. Bende-Michl, and A. W. Western (2018), What Are the Key Catchment Characteristics Affecting Spatial Differences in Riverine Water Quality?, *Water Resources Research*, *54*(10), 7252-7272, doi: 10.1029/2017wr022172.

Lloyd, C., J. Freer, A. Collins, P. Johnes, and J. Jones (2014), Methods for detecting change in hydrochemical time series in response to targeted pollutant mitigation in river catchments, *Journal of Hydrology*, *514*, 297-312.

Loecke, T. D., A. J. Burgin, D. A. Riveros-Iregui, A. S. Ward, S. A. Thomas, C. A. Davis, and M. A. S. Clair (2017), Weather whiplash in agricultural regions drives deterioration of water quality, *Biogeochemistry*, *133*(1), 7-15, doi: 10.1007/s10533-017-0315-z.

Lutz, S. R., S. Mallucci, E. Diamantini, B. Majone, A. Bellin, and R. Merz (2016), Hydroclimatic and water quality trends across three Mediterranean river basins, *Sci. Total Environ.*, *571*, 1392-1406.

Mellander, P. E., P. Jordan, M. Bechmann, O. Fovet, M. M. Shore, N. T. McDonald, and C. Gascuel-Odoux (2018), Integrated climate-chemical indicators of diffuse pollution from land to water, *Sci Rep*, *8*(1), 944, doi: 10.1038/s41598-018-19143-1.

Merot, P., S. Corgne, D. Delahaye, P. Desnos, V. Dubreuil, C. Gascuel, J.-L. Giteau, A. Joannon, H. Quenol, and J.-B. Narcy (2014), Évaluation, impacts et perceptions du changement climatique dans le Grand Ouest de la France métropolitaine: le projet CLIMASTER, *Cahiers Agricultures*, *23*(2), 96-107 (101).

Mérot, P., A. Crave, C. Gascuel-Odoux, and S. Louhala (1994), Effect of saturated areas on backscattering coefficient of the ERS 1 synthetic aperture radar: First results, *Water Resources Research*, *30*(2), 175-179.

Michalak, A. M. (2016), Study role of climate change in extreme threats to water quality, *Nature News*, *535*(7612), 349-350, doi: 10.1038/535349a.

Minaudo, C., M. Meybeck, F. Moatar, N. Gassama, and F. Curie (2015), Eutrophication mitigation in rivers: 30 years of trends in spatial and seasonal patterns of biogeochemistry of the Loire River (1980–2012), *Biogeosciences*, *12*(8), 2549-2563, doi: 10.5194/bg-12-2549-2015.

Minaudo, C., R. Dupas, C. Gascuel-Odoux, V. Roubeix, P. A. Danis, and F. Moatar (2019), Seasonal and event-based concentration-discharge relationships to identify catchment controls on nutrient export regimes, *Advances in Water Resources*, *131*, 11, doi: 10.1016/j.advwatres.2019.103379.

Molénat, J., and C. Gascuel-Odoux (2002), Modelling flow and nitrate transport in groundwater for the prediction of water travel times and of consequences of land use evolution on water quality, *Hydrological Processes*, *16*(2), 479-492.

Molénat, J., C. Gascuel-Odoux, P. Davy, and P. Durand (2005), How to model shallow water-table depth variations: the case of the Kervidy-Naizin catchment, France, *Hydrological Processes: An International Journal*, *19*(4), 901-920.

Molénat, J., C. Gascuel-Odoux, L. Ruiz, and G. Gruau (2008), Role of water table dynamics on stream nitrate export and concentration in agricultural headwater catchment (France), *Journal of Hydrology*, *348*(3-4), 363-378.

Molénat, J., P. Durand, C. Gascuel-Odoux, P. Davy, and G. Gruau (2002), Mechanisms of nitrate transfer from soil to stream in an agricultural watershed of French Brittany, *Water, air, and soil pollution*, *133*(1-4), 161-183.

Monteith, D. T., C. Evans, and B. Reynolds (2000), Are temporal variations in the nitrate content of UK upland freshwaters linked to the North Atlantic Oscillation?, *Hydrological Processes*, *14*(10), 1745-1749, doi: 10.1002/1099-1085(200007)14:10<1745::AID-HYP116>3.0.CO;2-O.

Monteith, D. T., et al. (2007), Dissolved organic carbon trends resulting from changes in atmospheric deposition chemistry, *Nature*, *450*(7169), 537-540, doi: 10.1038/nature06316.

Morel, B. (2009), Transport de carbone organique dissous dans un bassin versant agricole à nappe superficielle, Agrocampus - Ecole nationale supérieure d'agronomie de Rennes.

Morel, B., P. Durand, A. Jaffrezic, G. Gruau, and J. Molenat (2009), Sources of dissolved organic carbon during stormflow in a headwater agricultural catchment, *Hydrological Processes*, *23*(20), 2888-2901, doi: 10.1002/hyp.7379.

Moriasi, D. N., M. W. Gitau, N. Pai, and P. Daggupati (2015), Hydrologic and water quality models: Performance measures and evaluation criteria, *Transactions of the ASABE*, *58*(6), 1763-1785.

Musolff, A., C. Schmidt, M. Rode, G. Lischeid, S. M. Weise, and J. H. Fleckenstein (2016), Groundwater head controls nitrate export from an agricultural lowland catchment, *Advances in Water Resources*, *96*, 95-107, doi: 10.1016/j.advwatres.2016.07.003.

Nijzink, R. C., L. Samaniego, J. Mai, R. Kumar, S. Thober, M. Zink, D. Schäfer, H. H. Savenije, and M. Hrachowitz (2016), The importance of topography-controlled sub-grid process heterogeneity and semi-quantitative prior constraints in distributed hydrological models, *Hydrol. Earth Syst. Sci*, *20*(3), 1151-1176.

Oehler, F. (2006), Mesure de la dénitrification et modélisation spatialisée des flux d'azote à l'échelle d'un petit bassin versant d'élevage, Rennes, Agrocampus Ouest.

Oliver, T. H., S. Gillings, J. W. Pearce-Higgins, T. Brereton, H. Q. Crick, S. J. Duffield, M. D. Morecroft, and D. B. Roy (2017), Large extents of intensive land use limit community reorganization during climate warming, *Glob. Change Biol.*, *23*(6), 2272-2283.

Outram, F. N., C. Lloyd, J. Jonczyk, C. M. Benskin, F. Grant, M. Perks, C. Deasy, S. Burke, A. L. Collins, and J. Freer (2014), High-frequency monitoring of nitrogen and phosphorus response in three rural catchments to the end of the 2011–2012 drought in England, *Hydrology and Earth System Sciences*, *18*(9), 3429-3448, doi: 10.5194/hess-18-3429-2014.

Pal, I., E. Towler, and B. Livneh (2015), How can we better understand low river flows as climate changes, *Eos (Washington. DC)*, *96*.

Perrin, C., C. Michel, and V. Andréassian (2001), Does a large number of parameters enhance model performance? Comparative assessment of common catchment model structures on 429 catchments, *Journal of hydrology*, *242*(3-4), 275-301.

Perrin, C., C. Michel, and V. Andréassian (2003a), Improvement of a parsimonious model for streamflow simulation, *Journal of hydrology*, *279*(1-4), 275-289.

Perrin, C., C. Michel, and V. Andreassian (2003b), Improvement of a parsimonious model for streamflow simulation, *Journal of Hydrology*, *279*(1-4), 275-289, doi: 10.1016/s0022-1694(03)00225-7.

Petitjean, P., O. Henin, and G. Gruau (2004), *Dosage du carbone organique dissous dans les eaux douces naturelles. Intérêt, Principe, Mise en Oeuvre et Précautions Opératoires*.

Pettersson, A., B. Arheimer, and B. Johansson (2001), Nitrogen concentrations simulated with HBV-N: New response function and calibration strategy - Paper presented at the Nordic Hydrological Conference (Uppsala, Sweden June, 2000), *Nord. Hydrol.*, *32*(3), 227-248.

Pierret, M.-C., D. Viville, E. Dambrine, S. Cotel, and A. Probst (2019), Twenty-five year record of chemicals in open field precipitation and throughfall from a medium-altitude forest catchment (Strengbach-NE France): An obvious response to atmospheric pollution trends, *Atmospheric Environment*, *202*, 296-314.

Pomeroy, J., D. Gray, T. Brown, N. Hedstrom, W. Quinton, R. Granger, and S. Carey (2007), The cold regions hydrological model: a platform for basing process representation and model structure on physical evidence, *Hydrological Processes: An International Journal*, *21*(19), 2650-2667.

Ponnou-Delaffon, V., A. Probst, V. Payre-Suc, F. Granouillac, S. Ferrant, A.-S. Perrin, and J.-L. Probst (2020), Long and short-term trends of stream hydrochemistry and high frequency surveys as indicators of the influence of climate change, agricultural practices and internal processes (Aurade agricultural catchment, SW France), *Ecological Indicators*, *110*, 105894.

Potter, P., N. Ramankutty, E. M. Bennett, and S. D. Donner (2010), Characterizing the spatial patterns of global fertilizer application and manure production, *Earth Interactions*, *14*(2), 1-22.

Pourret, O., A. Dia, M. Davranche, G. Gruau, O. Hénin, and M. Angee (2007), Organo-colloidal control on major-and trace-element partitioning in shallow groundwaters: confronting ultrafiltration and modelling, *Appl. Geochem.*, *22*(8), 1568-1582.

Qu, Y., and C. J. Duffy (2007), A semidiscrete finite volume formulation for multiprocess watershed simulation, *Water Resources Research*, *43*(8).

Refsgaard, J. C., and B. Storm (1990), Construction, calibration and validation of hydrological models, in *Distributed hydrological modelling*, edited, pp. 41-54, Springer.

Richard, G., P. Stengel, G. Lemaire, P. Cellier, and E. Valceschini (2018), *Une agronomie pour le XXIe siècle*, éditions Quae.

Rinaldo, A., P. Benettin, C. J. Harman, M. Hrachowitz, K. J. McGuire, Y. Van Der Velde, E. Bertuzzo, and G. Botter (2015), Storage selection functions: A coherent framework for quantifying how catchments store and release water and solutes, *Water Resources Research*, *51*(6), 4840-4847.

Ringard, J., M. Chiriaco, S. Bastin, and F. Habets (2019), Recent trends in climate variability at the local scale using 40 years of observations: the case of the Paris region of France, *Atmos. Chem. Phys.*, *19*(20), 13129–13155.

Ritter, A., and R. Muñoz-Carpena (2013), Performance evaluation of hydrological models: Statistical significance for reducing subjectivity in goodness-of-fit assessments, *Journal of Hydrology*, *480*, 33-45.

Rogora, M., R. Mosello, and S. Arisci (2003), The effect of climate warming on the hydrochemistry of alpine lakes, *Water, Air, and Soil Pollution*, *148*(1-4), 347-361.

Ruiz, L., S. Abiven, C. Martin, P. Durand, V. Beaujouan, and J. Molenat (2002a), Effect on nitrate concentration in stream water of agricultural practices in small catchments in Brittany : II. Temporal variations and mixing processes, *Hydrology and Earth System Sciences*, *6*(3), 507-513, doi: 10.5194/hess-6-507-2002.

Ruiz, L., S. Abiven, P. Durand, C. Martin, F. Vertes, and V. Beaujouan (2002b), Effect on nitrate concentration in stream water of agricultural practices in small catchments in Brittany: I. Annual nitrogen budgets.

Salmon-Monviola, J. (2017), Modélisation agro-hydrologique spatialement distribuée pour évaluer les impacts des changements climatique et agricole sur la qualité de l'eau.

Salmon-Monviola, J., P. Moreau, C. Benhamou, P. Durand, P. Merot, F. Oehler, and C. Gascuel-Odoux (2013), Effect of climate change and increased atmospheric CO2 on hydrological and nitrogen cycling in an intensive agricultural headwater catchment in western France, *Clim. Change*, *120*(1-2), 433-447, doi: 10.1007/s10584-013-0828-y.

Samaniego, L., R. Kumar, and S. Attinger (2010), Multiscale parameter regionalization of a grid-based hydrologic model at the mesoscale, *Water Resources Research*, *46*(5).

Schilling, K. E., and J. Spooner (2006), Effects of watershed-scale land use change on stream nitrate concentrations, *J. Environ. Qual.*, *35*(6), 2132-2145.

Schulla, J., and K. Jasper (1998), Modellbeschreibung WaSiM-ETH, *ETH Zürich*.

Seibert, J., T. Grabs, S. Köhler, H. Laudon, M. Winterdahl, and K. Bishop (2009), Linking soil-and stream-water chemistry based on a Riparian Flow-Concentration Integration Model, *Hydrology and earth system sciences*, *13*(12), 2287-2297.

Senhorst, H., and J. Zwolsman (2005), Climate change and effects on water quality: a first impression, *Water Sci. Technol.*, *51*(5), 53-59.

Sherman, L. K. (1932), Streamflow from rainfall by the unit-graph method, *Eng. News Record*, *108*, 501-505.

Shrestha, R. R., K. Osenbrück, and M. Rode (2013), Assessment of catchment response and calibration of a hydrological model using high-frequency discharge–nitrate concentration data, *Hydrology Research*, *44*(6), 995-1012.

Šimůnek, J., M. T. van Genuchten, and M. Šejna (2008), Development and applications of the HYDRUS and STANMOD software packages and related codes, *Vadose Zone J.*, *7*(2), 587-600.

Strohmenger, L., O. Fovet, N. Akkal-Corfini, R. Dupas, P. Durand, M. Faucheux, G. Gruau, Y. Hamon, A. Jaffrezic, and C. Minaudo (2020), Multi-temporal relationships between the hydro-climate and exports of carbon, nitrogen and phosphorus in a small agricultural watershed, *Water Resources Research*, e2019WR026323.

Tallec, G., P. Ansart, A. Guérin, N. Derlet, N. Pourette, A. Guenne, O. Delaigue, H. Boudhraâ, and C. Loumagne (2013), L'Orgeval, un observatoire long terme pour l'environnement: caractéristiques du bassin et variables mesurées, edited, Editions Quae

Tavakoly, A. A., F. Habets, F. Saleh, Z. L. Yang, C. Bourgeois, and D. R. Maidment (2019), An integrated framework to model nitrate contaminants with interactions of agriculture, groundwater, and surface water at regional scales: The STICS-EauDyssee coupled models applied over the Seine River Basin, *Journal of Hydrology*, *568*, 943-958, doi: 10.1016/j.jhydrol.2018.11.061.

Temnerud, J., J. Seibert, M. Jansson, and K. Bishop (2007), Spatial variation in discharge and concentrations of organic carbon in a catchment network of boreal streams in northern Sweden, *Journal of Hydrology*, *342*(1-2), 72-87.

Thirel, G., V. Andréassian, C. Perrin, J.-N. Audouy, L. Berthet, P. Edwards, N. Folton, C. Furusho, A. Kuentz, and J. Lerat (2015), Hydrology under change: an evaluation protocol to investigate how

hydrological models deal with changing catchments, *Hydrological Sciences Journal*, *60*(7-8), 1184-1199.

Thomas, Z., B. Abbott, O. Troccaz, J. Baudry, and G. Pinay (2016), Proximate and ultimate controls on carbon and nutrient dynamics of small agricultural catchments, *Biogeosciences*, *13*(6), 1863-1875, doi: 10.5194/bg-13-1863-2016.

Thompson, S., N. Basu, J. Lascurain, A. Aubeneau, and P. Rao (2011), Relative dominance of hydrologic versus biogeochemical factors on solute export across impact gradients, *Water Resources Research*, *47*(10).

Uhlenbrook, S., S. Roser, and N. Tilch (2004), Hydrological process representation at the meso-scale: the potential of a distributed, conceptual catchment model, *Journal of Hydrology*, *291*(3-4), 278-296.

Viaud, V., P. Merot, and J. Baudry (2004), Hydrochemical buffer assessment in agricultural landscapes: from local to catchment scale, *Environ. Manage.*, *34*(4), 559-573.

Viaud, V., P. Durand, P. Merot, E. Sauboua, and Z. Saadi (2005), Modeling the impact of the spatial structure of a hedge network on the hydrology of a small catchment in a temperate climate, *Agric. Water Manage.*, *74*(2), 135-163.

Viaud, V., P. Santillàn-Carvantes, N. Akkal-Corfini, C. Le Guillou, N. C. Prévost-Bouré, L. Ranjard, and S. Menasseri-Aubry (2018), Landscape-scale analysis of cropping system effects on soil quality in a context of crop-livestock farming, *Agriculture, ecosystems & environment*, *265*, 166-177, doi: 10.1016/j.agee.2018.06.018.

Vongvixay, A., C. Grimaldi, R. Dupas, O. Fovet, F. Birgand, N. Gilliet, and C. Gascuel-Odoux (2018), Contrasting suspended sediment export in two small agricultural catchments: Cross-influence of hydrological behaviour and landscape degradation or stream bank management, *Land Degradation & Development*, *29*(5), 1385-1396.

Walter, C., and P. Curmi (1998), Les sols du bassin versant du Coët-Dan: organisation, variabilité spatiale et cartographie, *Agriculture intensive et qualité des eaux*, 85.

Wang, L., A. Butcher, M. Stuart, D. Gooddy, and J. Bloomfield (2013), The nitrate time bomb: a numerical way to investigate nitrate storage and lag time in the unsaturated zone, *Environ. Geochem. Health*, *35*(5), 667-681.

Wen, H., J. Perdrial, B. W. Abbott, S. Bernal, R. Dupas, S. E. Godsey, A. Harpold, D. Rizzo, K. Underwood, and T. Adler (2020), Temperature controls production but hydrology regulates export of dissolved organic carbon at the catchment scale, *Hydrology and Earth System Sciences*, *24*(2), 945-966.

Whitehead, P. G., R. L. Wilby, R. W. Battarbee, M. Kernan, and A. J. Wade (2009), A review of the potential impacts of climate change on surface water quality, *Hydrological Sciences Journal*, *54*(1), 101-123, doi: 10.1623/hysj.54.1.101.

Wigmosta, M. S., L. W. Vail, and D. P. Lettenmaier (1994), A distributed hydrology-vegetation model for complex terrain, *Water resources research*, *30*(6), 1665-1679.

Woodward, G., D. M. Perkins, and L. E. Brown Climate change and freshwater ecosystems: impacts across.

Woodward, S. J. R., R. Stenger, and V. J. Bidwell (2013), Dynamic analysis of stream flow and water chemistry to infer subsurface water and nitrate fluxes in a lowland dairying catchment, *Journal of Hydrology*, *505*, 299-311, doi: 10.1016/j.jhydrol.2013.07.044.

Worrall, F., and T. Burt (2007), Trends in DOC concentration in Great Britain, *Journal of Hydrology*, *346*(3-4), 81-92, doi: 10.1016/j.jhydrol.2007.08.021.

Worrall, F., N. J. Howden, and T. P. Burt (2015), Time series analysis of the world's longest fluvial nitrate record: evidence for changing states of catchment saturation, *Hydrological Processes*, *29*(3), 434-444.

WRB, I. W. G. (2006), World reference base for soil resources, edited, pp. 1-128, Food and Agriculture Organization (FAO) Rome, Italy

Xu, N., J. E. Saiers, H. F. Wilson, and P. A. Raymond (2012), Simulating streamflow and dissolved organic matter export from a forested watershed, *Water Resources Research*, *48*, 18, doi: 10.1029/2011wr011423.

Zehe, E., T. Maurer, J. Ihringer, and E. Plate (2001), Modeling water flow and mass transport in a loess catchment, *Physics and Chemistry of the Earth, Part B: Hydrology, Oceans and Atmosphere*, *26*(7-8), 487-507.

Zuecco, G., D. Penna, M. Borga, and H. J. van Meerveld (2016), A versatile index to characterize hysteresis between hydrological variables at the runoff event timescale, *Hydrological Processes*, *30*(9), 1449-1466, doi: 10.1002/hyp.10681.

Annexes

Supporting Information for: Multi-temporal relationships between the hydro-climate and exports of carbon, nitrogen and phosphorus in a small agricultural watershed

L. Strohmenger[1], O. Fovet[1], N. Akkal-Corfini[1], R. Dupas[1], P. Durand[1], M. Faucheux[1], G. Gruau[2], Y. Hamon[1], A. Jaffrezic[1], C. Minaudo[3], P. Petitjean[2], C. Gascuel-Odoux[1]

[1] UMR SAS, INRAE, AGROCAMPUS OUEST, 35000 Rennes, France

[2] OSUR, Géosciences Rennes, CNRS, UMR 6118, Campus de Beaulieu, 35042 Rennes, France

[3] Physics of Aquatic Systems Laboratory, EPFL, Lausanne, Switzerland

Corresponding author:

Laurent Strohmenger (Laurent.strohmenger@inrae.fr)

Ophélie Fovet (Ophélie.fovet@inrae.fr)

Contents of this file

Supplementary information on the discharge-rating curve at the outlet station

Water level at the outlet is measured using a Thalimedes OTT® shaft encoder (resolution: 0.001 m) every minute. The gauging station is composed of a rectangular notch, and the rating curve is calculated from three equations depending on the range of water level (Eqs. 1, 2, 3), as developed by Carluer et al. (1998). The weir crest is 350 mm.

For $350 < h \leq 708$ mm,

$$\begin{cases} Q = \alpha(\beta + \gamma.(h - 350)).((h - 350)/1000 + 0.001)^{1.5} \\ \alpha = 2962.6, \beta = 0.596, \gamma = 3.91\ 10^{-5} \end{cases} \quad (1)$$

For $708 < h \leq 916$ mm,

$$\begin{cases} Q = \alpha h^5 + \beta h^4 + \gamma h^3 + \delta h^2 + \varepsilon h + \varphi \\ \alpha = 1.84\ 10^{-10}, \beta = -5.40\ 10^{-7}, \gamma = 6.192\ 10^{-4}, \delta = -0.3443378, \varepsilon = 93.5411, \varphi = -9979.57 \end{cases} \quad (2)$$

For $916 < h \leq 925$ mm,

$$\begin{cases} Q = \alpha h^3 + \beta h^2 + \gamma h + \delta \\ \alpha = 4.70210\ 10^{-4}, \beta = -0.8297537, \gamma = 364.6229, \delta = 1770.909 \end{cases} \quad (3)$$

where Q is the water discharge in $l.s^{-1}$ and h the upstream water level from the river bed in mm.

The full rating curve is plotted in Figure S1 along with punctual h/Q measurements that are performed for verification.

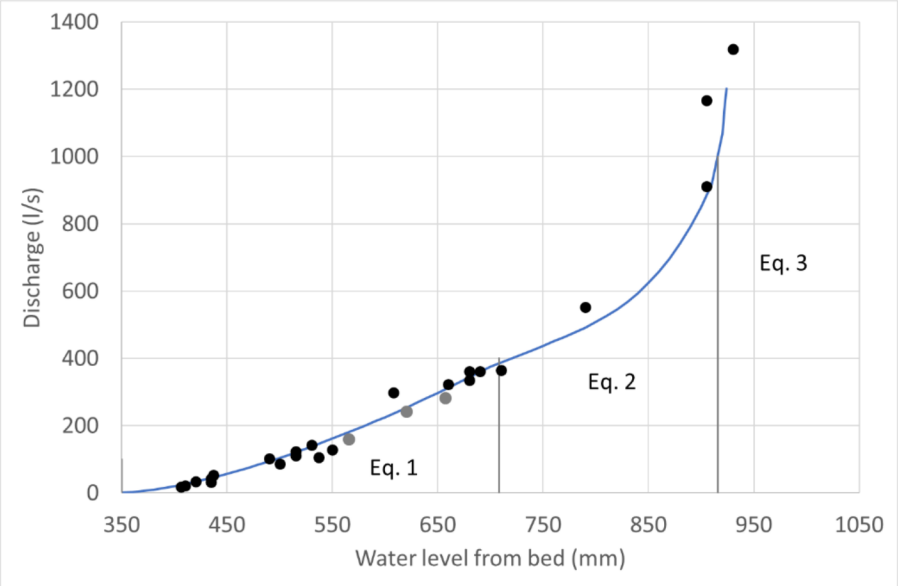

Figure S1. Flow-level rating curve at the outlet (blue line) and flow-level measurements (black and gray dots). Gray dots represent the most recent gaugings performed in winter 2019-2020.

Table S2. Concentration and hydro-climatic variables studied

Group	Name	Unit	Details	Measurement	Precision	Time step
Concentrations	DOC	(mg l^{-1})	Dissolved Organic Carbon	TDC - DOC	0.7 mg l^{-1}	1 day + storm
	DIC	(mg l^{-1})	Dissolved Inorganic Carbon	Carbon analyzer	0.5 mg l^{-1}	1 day + storm
	NO3	(mg l^{-1})	Nitrate	Chromatography	± 2.5%	1 day + storm
	SRP	(mg l^{-1})	Soluble Reactive Phosphorus	Colorimetry	± 5%	1 day + storm
	Cl	(mg l^{-1})	Chloride	Chromatography	± 2.5%	1 day + storm
	SO4	(mg l^{-1})	Sulfate	Chromatography	± 2.5%	1 day + storm
Climate	RR	mm	Rain Rate	Tipping bucket		1 hour
	RR+	mm	Rain Rate > 0 mm			
	GR	J cm^{-2}	Global Radiation	Weather station		1 hour
	AirTemp	°C	Air Temperature	Weather station		1 hour
	Wind	m s^{-1}	Wind Speed	Weather station		1 hour
	PET	mm	Penman Evapotranspiration			
	RR-PET	mm	Water balance			
Hydrology	PG1	mm	Water table depth	Pressure probe	± 2 mm	15 min
	PG2	mm	Water table depth	Pressure probe	± 2 mm	15 min
	PG3	mm	Water table depth	Pressure probe	± 2 mm	15 min
	PG4	mm	Water table depth	Pressure probe	± 2 mm	15 min
	PG5	mm	Water table depth	Pressure probe	± 2 mm	15 min
	PG6	mm	Water table depth	Pressure probe	± 2 mm	15 min
	PK1	mm	Water table depth	Pressure probe	± 2 mm	15 min
	PK2	mm	Water table depth	Pressure probe	± 2 mm	15 min
	PK3	mm	Water table depth	Pressure probe	± 2 mm	15 min
	PK4	mm	Water table depth	Pressure probe	± 2 mm	15 min
	Qd	l s^{-1}	Discharge	Floating sensor	± 1 mm	1 min
	API	mm	Sum of RR from t-8 days to t			
	StormEvent	-	1 if storm event, 0 if base flow			

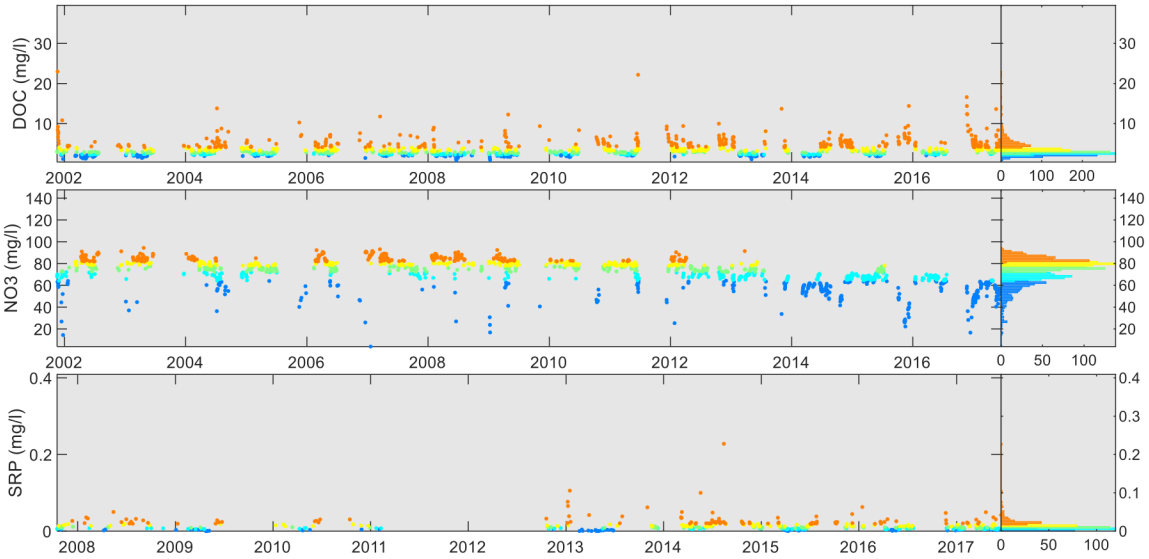

Figure S3. Time series and distribution of dissolved organic carbon (DOC), nitrate (NO_3) and soluble reactive phosphorus (SRP). Colors correspond to the 5 classes defined to examine co-occurrence of the highest (orange) and lowest (blue) concentrations (section 2.7 of the article).

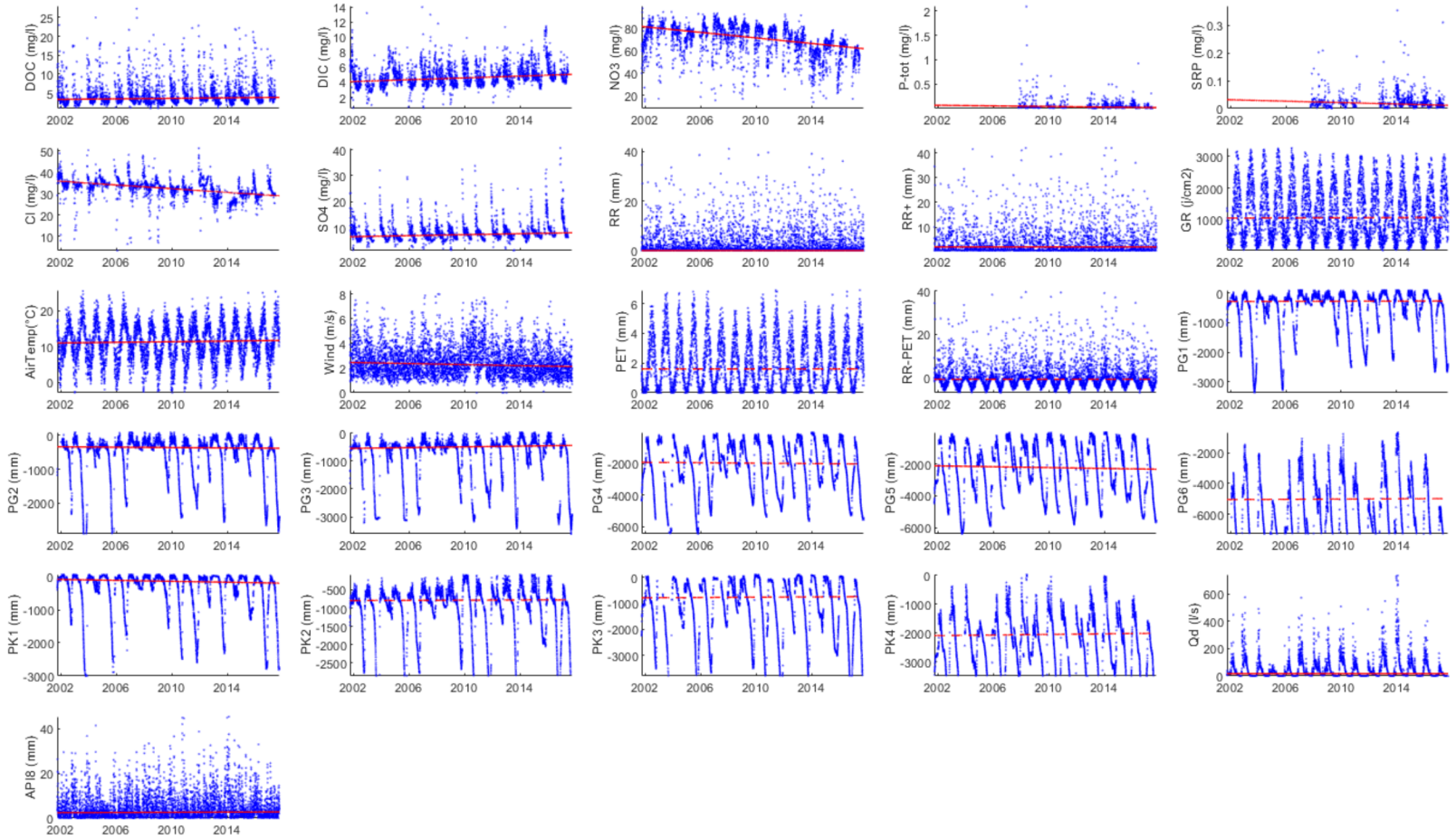

Figure S4. Time series (dots) and Theil-Sen slopes (solid red line if Mann-Kendall test is significant, dashed red line if not). Rain rate > 0 (RR+), global radiation (GR), air temperature (AirTemp), potential evapotranspiration (PET), bottomland piezometer (PG1, PK1), upland piezometer (PG5-6, PK4), daily discharge (Qd) and 8-day Antecedent Precipitation Index (API8).

Table S5. Correlation coefficient (r) and Nash-Sutcliffe model efficiency coefficient (NSE) between the Fourier series and the observed data. Rain rate (RR), global radiation (GR), potential evapotranspiration (PET), bottomland piezometer (PG1, PK1), upland piezometer (PG6, PK4), daily discharge (Qd) and Antecedent Precipitation Index (API).

Coefficient	DOC	DIC	NO_3	P-tot	SRP	Cl	SO4	RR	RR+	GR	AirTemp	Wind	PET
r	0,47	0,50	0,63	0,33	0,37	0,59	0,65	0,16	0,12	0,81	0,84	0,34	0,88
NSE	0,22	0,25	0,40	0,11	0,14	0,35	0,42	0,03	0,02	0,66	0,71	0,11	0,78

Coefficient	RR-PET	PG1	PG2	PG3	PG4	PG5	PG6	PK1	PK2	PK3	PK4	Qd	API8
r	0,39	0,82	0,78	0,81	0,87	0,89	0,73	0,79	0,78	0,85	0,79	0,63	0,28
NSE	0,15	0,68	0,62	0,65	0,76	0,79	0,54	0,63	0,61	0,72	0,62	0,39	0,08

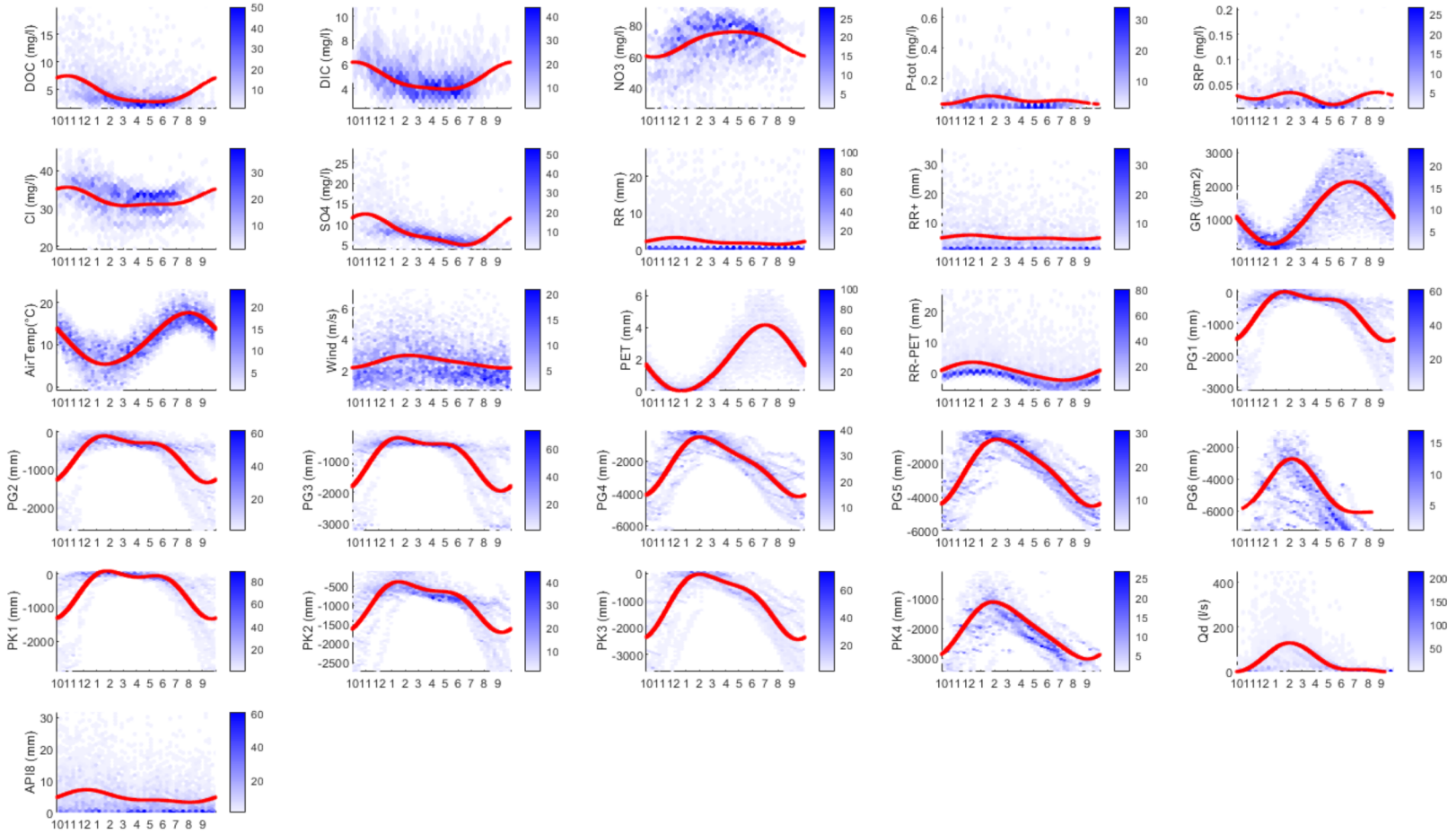

Figure S6. Mean annual cycles identified with Fourier transforms (red lines) and density plot (blue) for each concentration and hydro-climatic variable. Rain rate > 0 (RR+), global radiation (GR), air temperature (AirTemp), potential evapotranspiration (PET), bottomland piezometer (PG1, PK1), upland piezometer (PG5-6, PK4), daily discharge (Qd) and 8-day Antecedent Precipitation Index (API8).

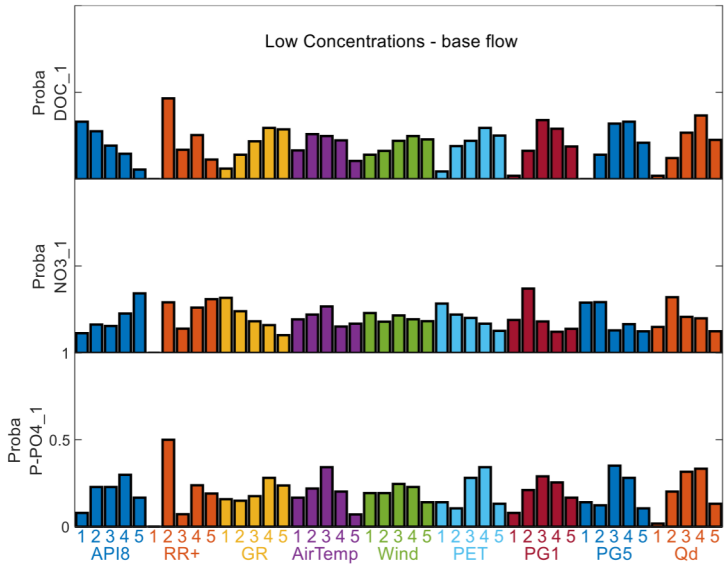

Figure S7. Distributions of hydrological and meteorological classes for the lowest concentrations of dissolved organic carbon (DOC), nitrate (NO_3) and soluble reactive phosphorus (P-PO_4) during base flow. Class 1 contains the lowest values, while class 5 contains the highest. Rain Rate > 0 (RR+), global radiation (GR), air temperature (AirTemp), potential evapotranspiration (PET), bottomland piezometer (PG1), upland piezometer (PG5), daily discharge (Qd) and 8-day Antecedent Precipitation Index (API8).

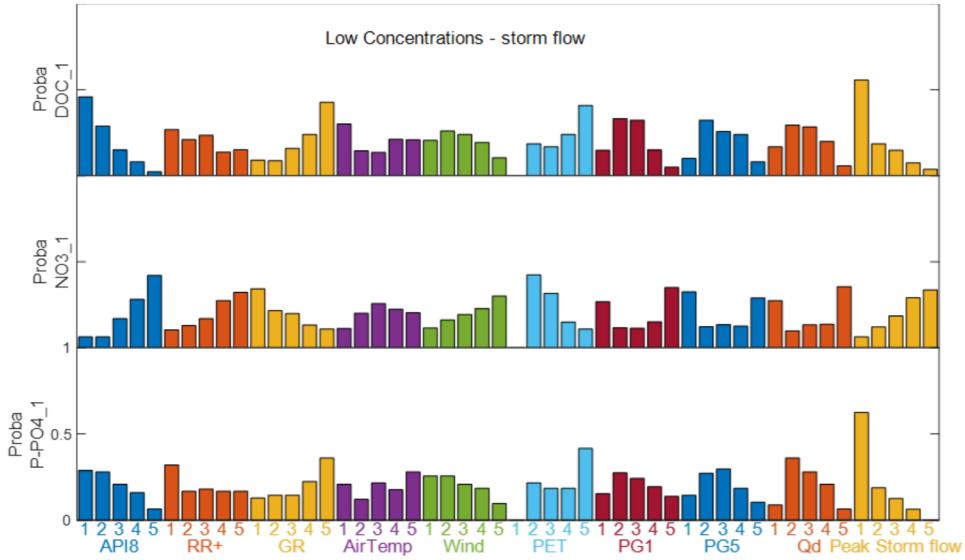

Figure S8. Distributions of hydrological and meteorological classes for the lowest concentrations of dissolved organic carbon (DOC), nitrate (NO_3) and soluble reactive phosphorus (P-PO_4) during storm flow. Class 1 contains the lowest values, while class 5 contains the highest. Rain rate >0 (RR+), global radiation (GR), air temperature (AirTemp), potential evapotranspiration (PET), bottomland piezometer (PG1), upland piezometer (PG5), daily discharge (Qd) and 8-day Antecedent Precipitation Index (API8).

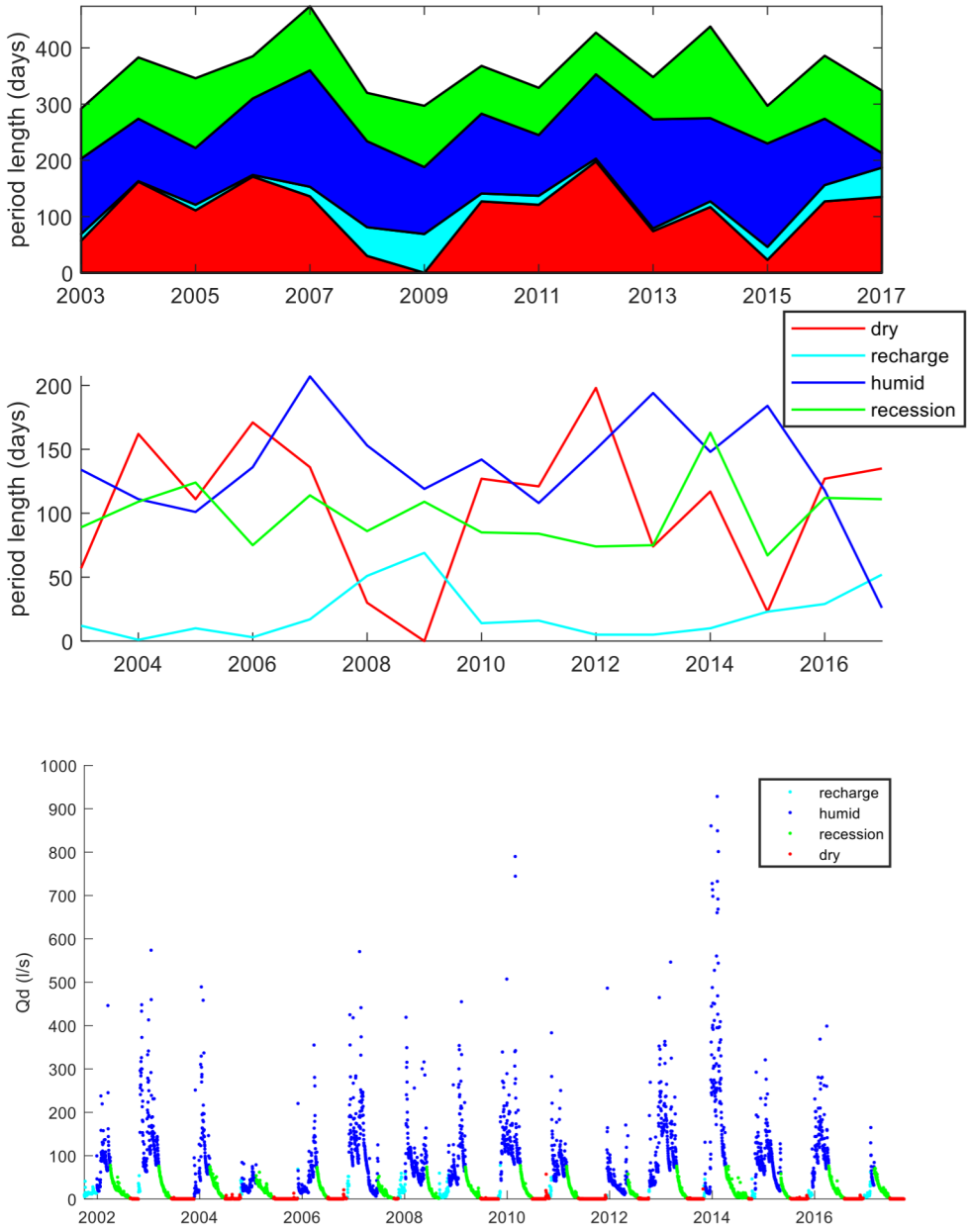

Figure S9. Cumulative and individual lengths of the four hydrological periods (recharge, wet, recession, dry) each year and daily discharge (Qd) during them

Spatio-temporal controls of C-N-P dynamics across headwater catchments of a temperate agricultural region from public data analysis

Stella Guillemot[1,2], Ophelie Fovet[1], Chantal Gascuel-Odoux[1], Gérard Gruau[3], Antoine Casquin[1], Florence Curie[2], Camille Minaudo[4], Laurent Strohmenger[1], and Florentina Moatar[5,2]
[1]INRAE, AGROCAMPUS OUEST/INSTITUT AGRO, UMR SAS, 35000 Rennes, France
[2]Université de Tours, EA 6293 GéHCO, 37200 Tours, France
[3]OSUR, Geosciences Rennes, CNRS, Université Rennes 1, 35000 Rennes, France
[4]EPFL, Physics of Aquatic Systems Laboratory, 1015 Lausanne, Switzerland
[5]INRAE, RIVERLY, 69625 Villeurbanne, France

Correspondence to: Ophelie Fovet (ophelie.fovet@inrae.fr)

Abstract. Characterizing and understanding spatial variability in water quality for a variety of chemical elements is an issue for present and future water resource management. However, most studies of spatial variability in water quality focus on a single element and rarely consider headwater catchments. Moreover, they assess few catchments and focus on annual means without considering seasonal variations. To overcome these limitations, we studied spatial variability and seasonal variation in dissolved C, N, and P concentrations at the scale of an intensively farmed region of France (Brittany). We analyzed 185 headwater catchments (from 5-179 km²) for which 10-year time series of monthly concentrations and daily stream flow were available from public databases. We calculated interannual loads, concentration percentiles, and seasonal metrics for each element to assess their spatial patterns and correlations. We then performed rank correlation analyses between water quality, human pressures, and soil and climate features. Results show that nitrate (NO_3) concentrations increased with increasing agricultural pressures and base flow contribution; dissolved organic carbon (DOC) concentrations decreased with increasing rainfall, base flow contribution, and topography; and soluble reactive phosphorus (SRP) concentrations showed weaker positive correlations with diffuse and point sources, rainfall and topography. An opposite pattern was found between DOC and NO_3: spatially, between their median concentrations, and temporally, according to their seasonal cycles. The annual maximum NO_3 concentration was in-phase with maximum flow when the base flow index was low, but this synchrony disappeared when flow flashiness was lower. The annual maximum SRP concentration occurred during the low-flow period in nearly all catchments. The approach shows that despite the relatively low frequency of public water quality data, such databases can provide consistent pictures of the spatio-temporal variability of water quality and of its drivers as soon as they contain a large number of catchments to compare and a sufficient length of concentration time series.

1 Introduction

As a condition for human health, food production, and ecosystem functions, water quality is recognized as "one of the main challenges of the 21st century" (FAO and WWC, 2015; UNESCO, 2015), and potential impacts of climate change on water quality are even more challenging (Whitehead et al., 2009). To better estimate and reduce human impact on water quality, water scientists are expected to provide integrated understanding of multiple pollutants (Cosgrove and Loucks, 2015). Eutrophication risks (Dodds and Smith, 2016) are considered the main factors that decrease the quality of surface water, according to objectives set by the European Union Water

Framework Directive. Mitigating the problem of eutrophication involves considering at least the three major elements: carbon (C), nitrogen (N), and phosphorus (P) (Le Moal et al., 2019).

Headwater catchments have been studied less than large rivers (Bishop et al., 2008), despite their influence on downstream water quality (Alexander et al., 2007; Barnes and Raymond, 2010; Bol et al., 2018) and higher spatial variability in their concentrations (Abbott et al., 2018a; Temnerud and Bishop, 2005). One reason for this is that most water quality monitoring networks coincide with the location of drinking-water production facilities, which explains why they focus on large rivers. Nonetheless, investigating spatial variability in upstream water quality is relevant for understanding what causes it to degrade, targeting locations with the greatest disturbances, and identifying which remediation policies would be most cost effective.

In non-agricultural headwater catchments, spatial variability in dissolved organic C (DOC) concentrations in streams has been related to topography, wetland coverage, and soil properties such as clay content or pH (Andersson and Nyberg, 2008; Brooks et al., 1999; Creed et al., 2008; Hytteborn et al., 2015; Temnerud and Bishop, 2005). Stream DOC concentrations and composition in agricultural and urbanized areas also generally differ greatly from those in semi-natural or pristine catchments (Graeber et al., 2012; Gücker et al., 2016). Over large gradients of human impact (e.g. from undisturbed to urban catchments), the cover of agricultural and urban land uses often appears as a key factor that explains differences in stream chemistry of C, N, and P species (e.g. Barnes and Raymond, 2010; Edwards et al., 2000; Mutema et al., 2015) and even silica (Onderka et al., 2012). Conversely, in more homogeneous catchments – e.g. mostly undisturbed (Mengistu et al., 2014) or mostly rural (Heppell et al., 2017; Lintern et al., 2018) – "natural" controls such as topography, geology, and flow paths are more frequently highlighted as the main factors that explain spatial variability in C, N and P.

Besides being spatially variable, C, N, and P concentrations also vary seasonally in streams and rivers (Aubert et al., 2013; Dawson et al., 2008; Duncan et al., 2015; Exner-Kittridge et al., 2016; Lambert et al., 2013), as does the composition of dissolved organic matter (Griffiths et al., 2011; Gücker et al., 2016). This seasonality can also be spatially structured. Several studies showed that the relative importance of catchment characteristics on water concentrations or loads varied by season because nutrient sources and biological and physico-chemical processes that influence nutrient mobilization and transfer in catchments (e.g. vegetation uptake, in-stream biomass production, denitrification) changed with the hydrological conditions (Ågren et al., 2007; Fasching et al., 2016; Gardner and McGlynn, 2009). Some variability in seasonal patterns of dissolved C, N, and/or P concentrations among headwater catchments has been reported (e.g. Van Meter et al., 2019; Abbott et al., 2018b; Duncan et al., 2015; Martin et al., 2004). Identifying these patterns is relevant from a management viewpoint as they may indicate changes in the locations of C, N, or P sources or their transfer pathways.

Thus, to date, analysis of spatial variability in water quality at the headwater scale:

1) is usually restricted to one element, although multi-element approaches are becoming more frequent (Edwards et al., 2000; Heppell et al., 2017; Lintern et al., 2018; Mengistu et al., 2014; Mutema et al., 2015),
2) is particularly rare for headwater catchments with similar human pressures (e.g. intensive farming), despite the high variability in water quality sometimes observed among them (e.g. Thomas et al. (2014)),
3) often uses mean annual values (concentration or load) to describe spatial variability in water quality among catchments, with little or no analysis of seasonal patterns (Ågren et al., 2007), and

4) is usually restricted to a few catchments: multiple-catchment studies are uncommon, despite their ability to identify dominant controlling factors better.

We studied the spatial variability and seasonal variation in water quality of 185 headwater catchments (from 5-179 km²) draining Brittany, an intensively farmed region of France. Our analysis focuses on dissolved C, N, and P concentrations as DOC, nitrate (NO_3), and soluble reactive P (SRP), respectively. We hypothesized that:

1) Human (i.e. rural and urban) pressures determine spatial variability in NO_3 and SRP concentrations, while soil and climate characteristics determine that in DOC and possibly SRP.
2) Seasonal variations in water quality provide information about spatial variability in biogeochemical sources and/or reactivity in catchments as a function of changes in water pathways and are correlated in part with spatial variability in concentrations and loads.

We selected headwater catchments for which relevant time series of DOC, NO_3, and SRP concentrations and stream flow were available (10 years of consecutive data measured at least monthly). In addition to estimating interannual loads, we calculated concentration metrics for each element to assess the spatial variability and temporal variation in water quality. Generalized Additive Models (GAMs) were applied to the time series to highlight average patterns of seasonal variation. Potential correlations between the water quality metrics and the geological, soil, climatic, hydrological, land cover, and human pressure characteristics of the corresponding headwater catchments were evaluated using rank correlation analyses.

2 Materials and Methods

2.1 Study area

Brittany is a 27,208 km² region in western France. Its bedrock is composed mainly of a crystalline substratum dominated by granite and schist (Supplement S1b). Its topography is moderate, with elevation ranging from 0-330 m a.s.l. Its climate is temperate oceanic, with precipitation ranging from 531 $mm.yr^{-1}$ in the east to 1070 $mm.yr^{-1}$ on the western coasts (regional median of 723.0 $mm.yr^{-1}$) (S1a), and a mean annual temperature of 12°C. The regional hydrographic network is dense, with a mean density of 1 $km.km^{-2}$. Its intensive agriculture has a strong influence on land use and agri-food production. Overall, 56.6% of the region was Utilized Agricultural Area (UAA) in 2017 (data from DREAL Bretagne, Brittany's Agency for Environment, Infrastructure, and Housing), which represented 6% of national UAA in 2016. Of total French production, Brittany produces 17.4% of milk and dairy products, 20% of pork products, and 17% of eggs and poultry (Brittany Chamber of Agriculture, 2016 data). At the canton (administrative district) scale, mean N and P surpluses are high and have high spatial variability (standard deviation (SD)): 50.01 ± 26.59 kg $N.ha^{-1}.yr^{-1}$ and 22.52 ± 12.66 kg $P.ha^{-1}.yr^{-1}$ (Supplement S1e,f). The region has a population of ca 3.3 million inhabitants (data 2017), some scattered throughout the region, and some concentrated in a few cities and near the coasts (Supplement S1c,d).

2.2 Stream data selection and headwater characteristics

Water quality data consisted of time series of DOC, NO_3, and SRP concentrations, extracted from two public monitoring networks – OSUR (Loire-Brittany Water Agency, 554 sites) and HYDRE/BEA (DREAL Bretagne, ca. 1964 sites), measured for regulatory monitoring, regional contracts, or specific programs. Concentrations were measured from grab samples. Headwater catchments were selected according to the following two criteria: (i)

independence, with no overlap of the drained areas of the water-quality stations selected, and (ii) availability of at least 80 measurements of DOC, NO_3, and SRP concentrations at the same station (after removing outliers, i.e. values > 200 mg $N.L^{-1}$ or 5 g $P.L^{-1}$) over 10 calendar years (2007-2016). We selected 185 stations (83% and 17% from OSUR and HYDRE/BEA, respectively) (hereafter, "concentration (C) stations"), which had mean frequencies of 12, 14, and 11 analyses per year for DOC, NO_3, and SRP, respectively.

Each C station was paired with a hydrometric station (Q). Observed daily streamflow data from the national hydrometric network (http://hydro.eaufrance.fr/) were used when draining headwater catchments for C and Q stations shared at least 80% of their areas (25% of cases). When observed Q data were not available, or at a frequency less than 320 measurements per year from 2007-2016 (75% of cases), discharge data were simulated using the GR4J model (Perrin et al., 2003). The headwater catchments selected and their associated C and Q stations were distributed throughout Brittany (Fig. 1).

The 185 headwater catchments selected cover ca. 32% of Brittany's area. Despite having a similar hydrographic context dominated by subsurface flow, the catchments have large differences in topography, geology, hydrology, and diffuse and point-source pressures of N and P. We used a set of catchment descriptors to quantify this variability (Table 1) (see Supplemental S2 for their statistical distribution). The descriptors selected included a set of spatial metrics for element sources (e.g. land use, pressure, soil contents) and for mobilization and retention processes (e.g. hydrology, climate, topography, geology, and soil properties).

The headwater catchments range in area from 5-179 km^2 (median of 38 km^2), and the density of each one's hydrographic network ranges from 0.47-1.49 $km.km^{-2}$ (median of 0.90 $km.km^{-2}$). Strahler stream order is 3 for 36% of the catchments, 2 for 18%, 4 for 17%, and 1 for 11%. Substrate composition is dominated by schists/micaschists (44%) or granites/gneisses (31%). In the topsoil horizon (0-30 cm), the soil organic C content varies greatly from 18.6-565.4 $g.kg^{-1}$ (median of 126.9 $g.kg^{-1}$), while the total P (Dyer method) content varies from 0.6-1.4 $g.kg^{-1}$ (median of 0.9 $g.kg^{-1}$). Land use is largely agricultural, although some catchments have high percentages of forested and urbanized areas. Riparian wetlands cover 12.3-36.3% of catchment area (median of 22.4%), forest covers 1.3-55.7% (median of 13.2%), pasture covers 10.3-46.7% (median of 25.6%), summer crops cover 6.5-50.3% (median of 27.8%), and winter crops cover 7.0-51.0% (median of 22.7%). The N and P surplus (potential diffuse agricultural sources) vary from 12.9-96.0 kg $N.ha^{-1}.yr^{-1}$ (median of 47.7) and 2.8-63.2 kg $P.ha^{-1}.yr^{-1}$ (median of 18.9), respectively. Urban areas cover 1.3-31.8% of the headwater catchments (median of 6%), with point-source input estimates ranging from 0-6.2 kg N. $ha^{-1}.yr^{-1}$ and 0-0.626 kg P. $ha^{-1}.yr^{-1}$. These data illustrate relative diversity in human pressures among the catchments despite a regional context of intensive agriculture. The daily mean flow (Qmean) varies from 4.8-24.5 $l.s^{-1}.km^{-2}$ (median of 10.8 $l.s^{-1}.km^{-2}$), the median of annual minimum of monthly flows (QMNA) varies from 0.2-5.9 $l.s^{-1}.km^{-2}$, and the flow flashiness index (W2), defined as the percentage of total discharge that occurs during the highest 2% of flows (Moatar et al., 2020), ranges from 10-28%.

2.3 Data analysis

2.3.1 Concentration and load metrics

To analyze spatial variability in DOC, NO_3, and SRP concentrations in streams, we calculated their 10^{th}, 50^{th}, and 90^{th} percentiles of concentration (C10, C50, and C90, respectively) for each headwater catchment from 2007-2016.

We also calculated the ratio of the coefficient of variation (CV) of mean concentration (CVc_{mean}) and to that of mean flow (CVq_{mean}) to compare spatial variabilities in concentrations and stream flow. We estimated interannual loads for a 10-year period (2007-2016), with 8-12 C-Q values per year. However, a 5-year period (2010-2014) was considered to analyze the spatial variability because it minimized data gaps (in C and Q time series) among all stations simultaneously.

To calculate interannual DOC, NO_3, and SRP loads for each headwater catchment, we tested different methods and selected the most suitable, depending on the reactivity of the element with flow. When C-Q relationships were relatively flat or diluted (NO_3) or slowly mobilized (DOC) during high flow (Q>Q50) , we used the discharge weighted concentration (DWC) method (Eq. 1), which estimates loads with lower uncertainties (Moatar and Meybeck, 2007; Raymond et al., 2013):

$$\mathrm{DWC} = \frac{\mathrm{k}}{\mathrm{A}} \times \frac{\sum_{\mathrm{i}=1}^{\mathrm{n}} \mathrm{C_i}\,\mathrm{Q_i}}{\sum_{\mathrm{i}=1}^{\mathrm{n}} \mathrm{Q_i}}\,\overline{\mathrm{Q}} \quad (1)$$

where DWC is the mean of annual loads ($kg.y^{-1}.ha^{-1}$), C_i is the instantaneous concentration ($mg.l^{-1}$), Q_i is the corresponding flow rate ($m^3.s^{-1}$), $\overline{Q}$ is the mean annual flow rate calculated from daily data ($m^3.s^{-1}$), A is the area of the headwater catchment (m^2), k is a conversion factor (31557.6), and n is the number of C-Q pairs per year.

The loads estimated by the DWC method were corrected for bias. Precisions were calculated from the number of samples (n), number of years, export regime exponent (b_{50high}), and W2 (Moatar et al., 2020).

To calculate SRP loads, regression methods were more suitable (because of strong concentration patterns when stream flow increases). We averaged the loads estimated by two regression methods developed by Raymond et al. (2013) – Integral Regression Curve (IRC) and Segmented Regression Curve (SRC) – both based on a regression between concentration and flow:

$$\mathrm{IRC} = \frac{\mathrm{k'}}{\mathrm{A}} \times \sum_{\mathrm{i}=1}^{\mathrm{n}} \mathrm{C_i Q_i} \quad (2)$$

$$\mathrm{SRC} = \frac{\mathrm{k'}}{\mathrm{A}} \times \left(\sum_{\mathrm{i}=1}^{\mathrm{n}} \mathrm{C_{inf} Q_i} + \sum_{\mathrm{i}=1}^{\mathrm{n}} \mathrm{C_{sup} Q_i}\right) \quad (3)$$

where IRC and SRC are the mean of annual loads ($kg.^{y-1}.ha^{-1}$); C_i, C_{sup}, and C_{inf} are instantaneous concentrations estimated by the regression curves ($mg.l^{-1}$); C_{sup} and C_{inf} are concentrations of flows above and below the median flow, respectively; and k' is a conversion factor (86.4).

2.3.2 Seasonal signal

Seasonal dynamics of discharge and solute concentrations were modeled using GAMs (Wood, 2017), which can estimate smoothed seasonal dynamics from time series (Musolff et al., 2017). The smoothing function was a cyclic cubic spline fitted to the month of the year (1-12); thus, the ends of the spline were forced to be equal, using the R package mgcv. We did not consider a long-term trend in the time series over the 10 years, for two reasons. First, significant long-term trends (according to Man-Kendall tests) had low amplitudes: mean Theil-Sen slopes ranged from -3% to 0% of the median concentration (while mean seasonal relative amplitudes exceeded 50%). Second,

performance of the GAMs did not increase significantly when a long-term trend was added: the mean adjusted coefficient of determination (Rsq) increased from 0.16 to 0.18 for DOC and from 0.30 to 0.40 for NO_3. We considered a seasonal dynamic to exist at Rsq ≥ 0.10.

Seasonal dynamics of the concentrations of the three solutes (DOC, NO_3, and SRP) and river discharge were then analyzed using five metrics calculated from the daily simulations of the GAMs. The first three were the annual amplitude (Ampli; i.e. annual maximum minus annual minimum), and the mean time in which annual maximum and minimum concentrations occurred (MaxPhase and MinPhase, respectively; in months from 1 January). The next was Ampli standardized by the corresponding mean concentration to compare the three solutes. The last metric was a seasonality index (SI), which measures the relative importance of summer (1 June to 31 July) concentrations compared to winter (15 January to 15 March) concentrations of an element, as follows (Eq. 4):

$$SI = \frac{C_{winter} - C_{summer}}{C_{winter} + C_{summer}} \quad (4)$$

where C_{winter} and C_{summer} are the mean of the GAM fitted at daily time step for winter and summer, respectively. Positive values of SI (near 1) indicate that $C_{winter} > C_{summer}$, while negative values (near -1) indicate that $C_{winter} < C_{summer}$. We considered that SI values close to 0 (from -0.1 to 0.1) indicated that C_{winter} equaled C_{summer}. The SI integrates both amplitude and phasing features of the seasonal signal.

2.3.2 Statistical analyses

To compare the concentration metrics of the elements, a multivariate analytical approach, principal component analysis (PCA), was performed for the 9 variables of concentration percentiles (C10, C50, and C90) of DOC, NO_3, and SRP for the dataset of 185 headwater catchments. To identify dominant drivers of spatial variability in concentration percentiles, seasonality, and loads of DOC, NO_3, and SRP, we calculated Spearman's rank correlation (r_s) between these water-quality metrics and the descriptors of the headwater catchments. We considered a rank correlation to be significant if the corresponding p-value was ≤ 0.05. All analyses were performed using R software (v. 3.6.1) with packages mgcv, hydroGOF, hydrostats, FactoMineR, tidyverse, lubridate, reshape2, plyr, ggcorrplot, and ggplot2 (Grolemund and Wickham, 2011; Le et al., 2008; Wickham, 2016, 2011; Wood, 2017; Zambrano-Bigiarini, 2020).

3 Results

3.1 Spatial variability in concentrations and loads

The C50 of the 185 headwater catchments ranged from 2-14.6 mg $C.l^{-1}$ for DOC, 0.9-15.8 mg $N.l^{-1}$ for NO_3, and 8-241 µg $P.l^{-1}$ for SRP (with 75% of the SRP C50 < 64 µg $P.l^{-1}$). The C50 displayed spatial gradients: rivers with DOC concentrations > 5 mg $C.l^{-1}$ were located in eastern Brittany, while the highest NO_3 concentrations were located on the west coast (Fig. 2). In contrast, the highest concentrations of SRP (C50 > 68 µg $P.l^{-1}$) were located in northern Brittany.

The two first axes of the PCA (Supplemental S3a) performed on the percentiles of DOC, NO_3, and SRP concentrations of the 185 headwater catchments explained 58% of the variance and revealed three important points. First, percentiles (C10, C50, or C90) were grouped by solute, showing that the spatial organization remained the same statistically regardless of the percentile. This illustrated the stability of spatial patterns, which were demonstrated by Abbott et al. (2018a) in Brittany, and confirmed by Dupas et al. (2019) in whole France. Second, there was a negative correlation between DOC and NO_3 concentrations (r_s = -0.58; Supplement S3b). Third, SRP concentrations had an orthogonal relation compared to DOC and NO_3 concentrations.

The ratios of mean concentration (CVc_{mean}) to mean flow (CVq_{mean}) were < 1 for DOC and NO_3 (Table 2), indicating that concentrations varied less in space than in flow, and vice-versa for SRP.

For DOC and NO_3, Ampli was not correlated significantly with C50, but it was with C90 (Fig. 3). For SRP, correlations between Ampli and the percentiles were high, with r_s > 0.85 for C50 and C90 (Fig. 3). The SI and phases were correlated more with C10 for DOC and NO_3 (negatively for SI and positively for the phases), and more with C90 for SRP (negatively, for SI only).

Mean (± 1 SD) interannual loads had high spatial variabilities – 20.71 ± 10.52 kg $C.ha^{-1}.yr^{-1}$ for DOC, 27.48 ± 18.51 kg $N.ha^{-1}.yr^{-1}$ for NO_3, and 0.315 ± 0.11 kg $P.ha^{-1}.yr^{-1}$ for SRP – which differed from those observed for concentrations (Fig. 2). Unsurprisingly, interannual loads of the three solutes were significantly ($p<0.001$) and strongly correlated with annual water fluxes (Pearson r = 0.88 for DOC, 0.90 for NO_3, and 0.75 for SRP). There were weak but significant positive correlations between mean interannual loads and seasonality indices (Ampli, SI) or C90 for DOC (Fig. 3). Mean interannual loads of NO_3 were significantly and positively correlated with C10 and C50, and negatively with its seasonality indices. The strongest significant correlation was found between mean interannual loads and concentration percentiles for SRP.

3.2 Characterization of concentrations seasonality

3.2.1 Performance of GAMS

Of the 185 catchments, GAMs were fitted for 159 for DOC concentrations, 168 for NO_3 concentrations, 162 for SRP concentrations, and 185 for discharge. The cases for which fitting was not possible corresponded to those with no seasonal cyclicity or with excessive interannual variability. The percentage of variance explained by the GAM varied by site and solute. Fitting performed best for NO_3, followed by SRP and then DOC: the means and SDs of the adjusted Rsq were 0.30 ± 0.18, 0.16 ± 0.11, and 0.22 ± 0.15 for NO_3, DOC, and SRP, respectively (Supplemental S4 and S5), and the percentages of catchment for which the fitted model had Rsq > 0.20 were 67%, 52% and 38%, respectively. Metrics calculated from monthly data differed only moderately from those calculated from sub-monthly data (Supplemental S6), which tended to validate the approach of using monthly data.

3.2.2 Types of seasonal cyclicity in DOC, NO_3, and SRP

Most of the catchments had a seasonal concentration cycle: 85%, 71%, 78%, and 100% for NO_3, DOC, SRP and discharge, respectively (Fig. 4). Means and SDs of the standardized Ampli were 0.59 ± 0.46 for NO_3, 0.53 ± 0.30 for DOC, 0.79 ± 0.14 for SRP, and 1.99 ± 0.38 for discharge. The distribution of the calculated seasonality indices is provided in Supplemental S7.

For all catchments, the annual phases for discharge were more stable than those for concentrations. The highest discharge period was centered on mid-February (winter) and the lowest discharge period on September. A strong gradient of hydrological dynamics was observed among catchments (Fig. 4). The highest W2 was associated with both severe low-flow discharge and many high discharge events. Values of Q_{mean}, BFI, W2, and QMNA clearly followed an east-west gradient (not shown). Because of similar seasonal discharge dynamics in all catchments, SI can be used to describe the seasonal dynamics of a concentration relative to those of discharge. When SI was positive, the concentration seasonality was in-phase with discharge; when negative, the concentration seasonality was out-of-phase with discharge (Fig. 4).

Most of the catchments had opposite dynamics for DOC and NO_3. For 90% of them, Pearson correlation between the daily GAM estimates of DOC and NO_3 was negative, and for 50% of the catchments, less than -0.79. The remaining 10% of catchments (15) had low Ampli of DOC and NO_3. The DOC and NO_3 concentrations had out-of-phase seasonal cycles, as shown by the negative correlation between SI and DOC or NO_3 for all catchments that had a significant seasonality in these concentrations (Fig. 5; $R^2 = 0.62$). We classified two types of catchments according to their seasonality in both DOC (MinPhase) and NO_3 (MaxPhase) concentrations and consistent with the SI (Fig. 5, Supplemental S7). NO_3 MaxPhase and DOC MinPhase that occurred before 1 May were classified as “in-phase” with discharge (Q), while those that occurred after were “out-of-phase” with Q. All catchments experienced high stability of the DOC MaxPhase and NO_3 MinPhase, which always occurred between July and December (Fig. 4, Supplemental S7).

The first type, “in-phase” (68% of the catchments with seasonality), had a NO_3 MaxPhase between October and May (Fig. 4, Supplemental S7) (i.e. high-flow period, in-phase with maximum discharge and usually with DOC MinPhase). For these catchments, the mean SI was positive for NO_3 (0.22 ± 0.19) and usually negative or null for DOC (0.00 ± 0.13). They tended to be located toward central Brittany and be associated with mesoscale catchments (mean of 52.6 ± 38.8 km²). They had large Ampli for NO_3 and low Ampli for DOC (mean relative Ampli of 0.83 ± 0.46, and 0.44 ± 0.23 for DOC) and relatively low C50 of NO_3 (means of 5.74 ± 2.46 mg $N.l^{-1}$ and 5.92 ± 2.00 mg $C.l^{-1}$).

The second type, “out-of-phase” (32% of the catchments with seasonality), had a DOC MinPhase and NO_3 MaxPhase between May and September (Fig. 4; Supplemental S7) (i.e. low-flow period, out-of-phase with maximum discharge). For most catchments, maximum NO_3 and minimum DOC concentrations occurred a mean of 1.85 months before minimum discharge or 5.5 months after maximum discharge, respectively. For these catchments, the mean SI was negative or null for NO_3 (-0.08 ± 0.06) and weakly positive for DOC (0.21 ± 0.10). These catchments were close to the coast and relatively small (mean of 31.4 ± 21.7 km²). The had smaller Ampli than “in-phase” catchments for NO_3, and higher Ampli for DOC (mean relative Ampli of 0.13 ± 0.13, and 0.74 ± 0.30 for DOC) and relatively high C50 of NO_3 (means of 8.27 ± 2.90 mg $N.l^{-1}$ and 5.00 ± 1.62 mg $C.l^{-1}$).

Some catchments had intermediate behavior between these two types (Figs. 4 and 5). Some had a plateau with maximum NO_3 and minimum DOC concentrations from winter to summer, while others showed two maxima for NO_3 or two minima for DOC (one synchronous with maximum discharge and another with minimum discharge). Other catchments also had maximum NO_3 synchronous with discharge, but minimum DOC after maximum discharge.

The seasonal dynamics of SRP were more stable than those of DOC and NO_3, but less stable than those of discharge. Thus, there was only one type of seasonality for SRP, which was out-of-phase with flow: MaxPhase SRP dominated in summer (mid-August ± 1.4 months), and MinPhase SRP dominated in late winter (March ± 1.2 months) (Fig. 4, Supplement S7), except for two catchments with maximum SRP in January-February.

3.3 Controlling factors of concentration percentiles and seasonality

The C50 of DOC was correlated significantly with 15 spatial variables and most strongly ($|r_s| \geq 0.4$) with topographic index, QMNA, and the other hydrological indices. The C50 of NO_3 was correlated significantly with 12 spatial variables, in particular diffuse agricultural sources ($r_s=0.68$ for the percentage of summer crops, $r_s>0.39$ for N and P surplus, and $r_s=0.48$ for soil erosion rate) and hydrological indices, through the base flow index (BFI) (positively) and W2 (negatively), (Table 3). The C50 of SRP was correlated significantly with more variables (18), but the correlations were slightly weaker. It correlated most strongly with soil P stock ($r_s=-0.40$), climate and hydrology (effective rainfall, Qmean, QMNA), elevation, and hydrographic network density. It had weaker positive correlations ($r_s<0.3$) with the soil erosion rate and domestic and agricultural pressures (urban percentage and P surplus).

Ampli and SI for DOC and NO_3 were correlated most with the hydrodynamic properties, followed by agricultural pressures (Fig. 6, Table 3). The catchments “in-phase” with discharge (i.e. positive SI-NO_3 and negative SI-DOC correlations) were associated with high hydrological reactivity (low BFI and high W2) and a low percentage of summer crops (Table 3). Conversely, catchments “out-of-phase” with discharge (i.e. negative SI-NO_3 and positive SI-DOC correlations) were associated with low hydrological reactivity (high BFI and QMNA, low W2) and a high percentage of summer crops.

Correlations of SI with catchment descriptors were weaker ($|r_s| \leq 0.4$) for SRP than for DOC and NO_3 because most catchments had the same seasonal pattern, with maximum SRP concentration during low flow. Catchments with the highest amplitudes of SRP concentration were associated with low QMNA and Q_{mean}, high W2, low effective rainfall, and low soil P stock. Interannual loads were correlated mainly with hydrological descriptors (positively with Qmean and QMNA, and negatively with W2) (Table 3). Interannual NO_3 loads were also correlated with the percentage of summer crops and soil TP content, while interannual SRP loads were correlated weakly with the percentage of summer crops, agricultural surplus, erosion, and point sources.

4 Discussion

4.1 Interpretation of the spatial opposition between DOC and NO_3

Spatial opposition between DOC and NO_3 concentrations has been reported for a wide range of ecosystems. Taylor and Townsend (2010) found a non-linear negative relationship between them for soils, groundwater, surface freshwater, and oceans, from global to local scales, and highlighted that this negative correlation prevails in disturbed ecosystems. Goodale et al. (2005) reported a similar negative correlation among 100 streams in the northeastern USA. Heppell et al. (2017) found that DOC and NO_3 concentrations were inversely correlated with the BFI in six reaches of the Hampshire Avon catchment (UK). Our contribution brings an original focus on this relationship in headwater catchments with high domestic and agricultural pressures. Taylor and Townsend (2010) interpreted this spatial opposition as a response of microbial processes (i.e. biomass production, nitrification, and denitrification) to the ratio of ambient DOC:NO_3, which controls NO_3 export/retention in catchments (see also Goodale et al. (2005)). In semi-natural ecosystems, high but poorly labile soil organic C pools were associated with lower N retention capacity and thus higher N leaching (Evans et al., 2006). Similarly, several studies (e.g. Hedin et al. (1998), Hill et al. (2000)) suggested that DOC supply limits in- and near-stream denitrification. In contrast, other studies claimed that N can influence loss of DOC from soils by altering substrate availability or/and microbial processing of soil organic matter (Findlay, 2005; Pregitzer et al., 2004). In our study, C50 were correlated with both BFI and QMNA, positively for NO_3 and negatively for DOC, which suggests that catchments strongly sustained by groundwater flow produced higher NO_3 and lower DOC concentrations, as reported in other rural catchments (e.g. Heppell et al., 2017). The C50 of NO_3 increased with agricultural pressures (percentage of summer crop, N surplus), as observed by Lintern et al. (2018), while that of DOC increased in flatter catchments, which is consistent with results of Mengistu et al. (2014) and Musolff et al. (2018).

This suggests that this spatial opposition between DOC and NO_3 results from the combination of heterogeneous human inputs, heterogeneous natural pools, and different physical and biogeochemical connections between C and N pools. In surface water, these heterogeneous sources are expressed to differing degrees depending on the catchment's hydrological behavior. When deep or slow flowpaths dominate, they store and release N via groundwater and mobilize little the sources rich in organic matter. When shallower and faster flowpaths dominate, they transport some of the N via compartments rich in organic matter, which causes N depletion and release of more DOC to the streams. The initial amounts of NO_3 along these flowpaths are a function of human pressures.

4.2 Interpretation of the temporal opposition between DOC and NO_3

The seasonal opposition between DOC and NO_3 concentration dynamics could be another manifestation of the spatial opposition between DOC and NO_3 sources, because the strength of the hydrological connection between sources and streams varies seasonally (e.g. Mulholland and Hill (1997), Weigand et al. (2017)). The direct contribution of biogeochemical reactions that connect DOC and NO_3 cycles may also vary seasonally (Mulholland and Hill, 1997; Plont et al., 2020). Indeed, temperature, wetness condition, and light availability influence rates of these organic matter reactions. In addition, the relative importance of the fluxes produced or consumed via these reactions appears clearer during the low-flow period, when the fluxes exported from the terrestrial ecosystem and delivered to the stream decrease. These reactions consume NO_3 (e.g. denitrification, biological uptake) and release (reductive dissolution) or produce (autotrophic production) DOC. Of the two seasonal NO_3-DOC cycles, the most

common in our datasets is thus maximum NO_3 in-phase with maximum discharge and minimum DOC, which has been reported in Brittany (Abbott et al., 2018b; Dupas et al., 2018) and elsewhere (Van Meter et al., 2019; Dupas et al., 2017; Halliday et al., 2012; Minaudo et al., 2015; Weigand et al., 2017). The main control of seasonal DOC-NO_3 cycles appears to be related to hydrological indices (expressed as BFI and W2). Hydrological flashiness reflects the relative importance of subsurface flow compared to deep base flow (Heppell et al., 2017); thus, low BFI (or high W2) would indicate higher connectivity with subsurface riparian sources and shorter transit times. This is consistent with results of Weigand et al. (2017), who observed higher seasonal amplitudes in DOC and NO_3 concentrations and stronger temporal anti-correlation between DOC and NO_3 concentrations in stream water dominated by subsurface runoff.

Our results are consistent with these previous results, while the correlations with catchment characteristics can provide some explanation. Catchments with low BFI have larger shallow flows and experience seasonal DOC-NO_3 cycles that are in-phase with flow and have higher NO_3 amplitudes. These cycles can be interpreted as the combination of several mechanisms:

1) Synchronization of NO_3-rich and DOC-poor groundwater contribution with maximum flow.
2) Large contribution of near-/in-stream biogeochemical processes at reduced low flows that decreases NO_3 concentration (e.g. NO_3 consumption by aquatic microorganisms, biofilms, and macrophytes).
3) Large DOC-rich riparian contribution throughout the year, but larger in autumn, when flow starts to increase, as described in detail in previous AgrHys Observatory studies (Aubert et al., 2013; Humbert et al., 2015).

In contrast, catchments with higher BFI have smaller shallow flows and experience mainly DOC and NO_3 cycles that are out-of-phase with flow and have lower amplitudes. These cycles can be attributed to the following:

1) More continuous groundwater contribution, combined with a decrease in agricultural pressures over time, which could increase NO_3 concentrations more in deeper groundwater than in shallower groundwater (Abbott et al., 2018b; Martin et al., 2004; Martin et al., 2006). This vertical gradient in groundwater supply could explain why NO_3 concentrations peaked during the annual discharge recession, which is sustained mainly by deep groundwater inputs.
2) Little contribution of near-/in-stream biogeochemical processes at reduced low flows due to larger inputs from groundwater, which maintains a relatively high minimum NO_3 concentration.
3) Contribution of DOC-rich riparian sources, mainly in autumn, that are smaller than those in in-phase catchments, again due to a predominantly deeper geometry of water circulation.

4.3 Interpretation of the spatial and temporal signature of SRP

The correlations between the C50 of SRP and geographic variables highlighted the importance of P sources (soil P stocks, followed by domestic and agricultural pressures) and surface flowpaths (e.g. hydrological indices, elevation, erosion risk). Similarly, analysis of regression models that predicted spatial variability in total P concentration of 102 rural catchments in Australia also indicated positive effects of human-modified land uses, natural land uses prone to soil erosion, mean P content of soils, and to a lesser extent, topography (Lintern et al., 2018). They always included the percentage of urban area, which suggests a considerable effect of sewage discharge, even at low levels of urbanization. The catchments analyzed in the present study have a homogeneous and relatively dense distribution of small villages but no large city, which seems to support this last hypothesis.

Sobota et al. (2011) studied spatial relationships among P inputs, land cover and mean annual concentrations of different forms of P in 24 catchments in California, USA. They found that P concentrations were significantly correlated with agricultural inputs and, to a lesser extent, agricultural land cover but not with estimates of sewage discharge.

The seasonality of SRP was generally the same in the region studied, and C50 and amplitudes were significantly correlated. A peak in seasonal SRP concentrations at low flow has been reported previously (Abbott et al., 2018b; Bowes et al., 2015; Dupas et al., 2018; Melland et al., 2012). It is interpreted as the result of a dominance of point sources diluted during high flow (Minaudo et al., 2019, 2015; Bowes et al., 2011) or of stream-bed sediment sources for which P release increases with temperature (Duan et al., 2012).

Correlation between spatial patterns of NO_3 and SRP was expected given the dominant agricultural origin of N and substantial agricultural origin of P, but it was not observed in all catchments. The C50 of NO_3 and SRP were high mainly on the northwestern coast, perhaps due to intensive vegetable production associated with a dominance of mineral fertilization (Lemercier et al., 2008). Elsewhere, a high proportion of allochthonous P in the topsoil results from livestock farming and manure application (Delmas et al., 2015). The P-retention capacity of soils (related to their Al, Ca, Fe, and clay contents) is also likely to increase spatial variability in the release of P from catchments (Delmas et al., 2015). Synchronous variations in SRP and DOC, such as those observed in small, completely agricultural headwater catchments without villages (Cooper et al., 2015; Dupas et al., 2015b; Gu et al., 2017), were not observed in the present set of catchments. We assume that synchronicity of SRP and DOC in small catchments depends on soil processes, such as reduction of soil Fe-oxyhydroxides in wetland zones (Gu et al., 2019), which are hidden by in-stream processes (P adsorption on streambed sediments) and downstream point-source inputs (especially P inputs) in the set of larger catchments studied.

Regarding the geographic data used as spatial descriptors, the region studied did not have a few dense urban centers but rather smaller domestic points scattered across the region, which is harder to characterize finely. Moreover, Brittany's coastlines may have higher population densities in spring and summer due to tourism. Refined estimates of domestic point sources and their seasonal variations would be useful in future analyses.

4.4 Hydrological vs. anthropogenic controls of spatial variability in water quality

Among the headwater catchments selected, the human pressures (agriculture for NO_3 and sewage water discharge for SRP) influenced the C50 and loads of NO_3 and SRP. However, the influence of hydrological descriptors on the spatial variability in their loads suggested a transport-limited behavior of these catchments (Basu et al., 2010). Nutrient load estimates had high uncertainties due to i) using modeled flow data when measurements were not available and ii) the frequency of concentration data (monthly), which is low for estimating nutrient loads (especially of P) (Raymond et al., 2013). Thus, these load estimates allowed only their relative spatial variation to be analyzed. Although land-use or agricultural pressure variables, in combination with rainfall and discharge variables, are good predictors of nutrient loads at larger scales (Dupas et al., 2015a; Grizzetti et al., 2005; Preston et al., 2011), the correlations with loads were lower in the set of headwater catchments selected. For NO_3, this can be explained by higher spatial variability (CVs) in water fluxes than in concentrations (Table 2), which can explain the dominance of hydrological fluxes in the spatial organization of nutrient loads. It may also suggest that the nutrient-surplus data at the local scale remained uncertain (Poisvert et al., 2017) or that at this scale, data on

agricultural practices would be more relevant, and that variability in concentration depends less on the magnitude of nutrient inputs than on their locations.

The catchments studied have clear seasonal dynamics in concentration, which is consist with previous observations (Minaudo et al., 2019; Abbott et al., 2018a). The seasonal pattern is controlled mainly by hydrological variables. It partly reflects the mixing of contrasting sources that are connected to streams by seasonally varying flowpaths with nutrients that are transferred vs. nutrients that are processed locally in hotspots (e.g. riparian buffer, stream water, stream sediments) or delivered over point sources. The seasonal NO_3-DOC pattern seemed to become somewhat homogenous among catchments larger than 100 km^2, where seasonal cycles with maximum NO_3 in-phase with flow seemed less common. This may be related to an increase in in-stream biological activity during summer as catchment size increases, enhanced by a lower stream water level and slower discharge (Minaudo et al., 2015). Therefore, the potential relationship between seasonal cycle type and catchment size should be studied over a wider range of catchment sizes and nested catchments to include variations along the hydrographic network.

5 Conclusion

To analyze spatial variability in water quality at a regional scale, we used an original dataset from public databases, little used by the scientific community, for the French region of Brittany with monthly measurements of water quality. The dataset selected covers 185 headwater and agricultural catchments monitored over a period sufficiently long (10 years) to allow the spatial (regional) variability and temporal (seasonal) variation in DOC, NO_3, and SRP concentrations to be analyzed. We described spatio-temporal variations in concentrations, loads, and seasonal patterns and analyzed their correlations with geographic variables (related to topography, hydro-climate, geology, soils, land uses, and human pressures). Our study showed the following:

1) Seasonal cycles of DOC and NO_3 concentrations are usually opposite from each other. Catchments with a low base-flow index exhibit maximum NO_3 in-phase with maximum flow, while those with a higher base-flow index exhibit maximum NO_3 after maximum flow. Both types exhibited maximum DOC in autumn, at the beginning of the annual increase in flow.
2) NO_3 concentrations increased as human pressures and base flow contribution increased. DOC concentrations decreased as rainfall, base flow contribution, and elevation increased. SRP concentrations showed weaker correlations with human pressures, rainfall, and hydrological and topographic variables.
3) Seasonal SRP cycles are synchronized in nearly all catchments that have a clear seasonal amplitude, with maximum SRP concentrations that occur during the summer low-flow period due to a decreased dilution capacity of point sources.

The spatial and temporal opposition between DOC and NO_3 concentrations likely results from a combination of heterogeneous human inputs and biogeochemical connection between these pools. The seasonal cycles in stream concentrations result from the mixing of water parcels that followed contrasting flowpaths, combined with high spatial variability in nutrient sources, local-scale biogeochemical processes, and point sources. As a perspective, we recommend further studies of multiple elements that are likely to show contrasting responses to diverse human pressures and to the retention/removal capacities of hydrosystems.

References

Abbott, B. W., Gruau, G., Zarnetske, J. P., Moatar, F., Barbe, L., Thomas, Z., Fovet, O., Kolbe, T., Gu, S., Pierson-Wickmann, A.-C., Davy, P., and Pinay, G.: Unexpected spatial stability of water chemistry in headwater stream networks, Ecol. Lett., 21, 296-308, https://doi.org/10.1111/ele.12897, 2018a.

Abbott, B. W., Moatar, F., Gauthier, O., Fovet, O., Antoine, V., and Ragueneau, O.: Trends and seasonality of river nutrients in agricultural catchments: 18 years of weekly citizen science in France, Sci. Total Environ., 624, 845-858, https://doi.org/10.1016/j.scitotenv.2017.12.176, 2018b.

Ågren, A., Buffam, I., Jansson, M., and Laudon, H.: Importance of seasonality and small streams for the landscape regulation of dissolved organic carbon export, J. Geophys. Res-Biogeo., 112, https://doi.org/10.1029/2006JG000381, 2007.

Alexander, R. B., Boyer, E. W., Smith, R. A., Schwarz, G. E., and Moore, R. B.: The Role of Headwater Streams in Downstream Water Quality, J Am Water Resour Assoc, 43, 41-59, 10.1111/j.1752-1688.2007.00005.x, 2007.

Andersson, J.-O. and Nyberg, L.: Spatial variation of wetlands and flux of dissolved organic carbon in boreal headwater streams, Hydrol. Process., 22, 1965-1975, https://doi.org/10.1002/hyp.6779, 2008.

Aubert, A. H., Gascuel-Odoux, C., Gruau, G., Akkal, N., Faucheux, M., Fauvel, Y., Grimaldi, C., Hamon, Y., Jaffrézic, A., Lecoz-Boutnik, M., Molénat, J., Petitjean, P., Ruiz, L., and Merot, P.: Solute transport dynamics in small, shallow groundwater-dominated agricultural catchments: insights from a high-frequency, multisolute 10 yr-long monitoring study, Hydrol. Earth Syst. Sci., 17, 1379-1391, https://doi.org/10.5194/hess-17-1379-2013, 2013.

Barnes, R. T. and Raymond, P. A.: Land-use controls on sources and processing of nitrate in small watersheds: insights from dual isotopic analysis, Ecol. Appl., 20, 1961-1978, https://doi.org/10.1890/08-1328.1, 2010.

Basu, N. B., Destouni, G., Jawitz, J. W., Thompson, S. E., Loukinova, N. V., Darracq, A., Zanardo, S., Yaeger, M., Sivapalan, M., Rinaldo, A., and Rao, P. S. C.: Nutrient loads exported from managed catchments reveal emergent biogeochemical stationarity, Geophys. Res. Lett., 37, https://doi.org/10.1029/2010GL045168, 2010.

Bishop, K., Buffam, I., Erlandsson, M., Fölster, J., Laudon, H., Seibert, J., and Temnerud, J.: Aqua Incognita: the unknown headwaters, Hydrol. Process., 22, 1239-1242, https://doi.org/10.1002/hyp.7049, 2008.

Bol, R., Gruau, G., Mellander, P.-E., Dupas, R., Bechmann, M., Skarbøvik, E., Bieroza, M., Djodjic, F., Glendell, M., Jordan, P., Van der Grift, B., Rode, M., Smolders, E., Verbeeck, M., Gu, S., Klumpp, E., Pohle, I., Fresne, M., and Gascuel-Odoux, C.: Challenges of reducing phosphorus based water eutrophication in the agricultural landscapes of northwest Europe, Front. Mar. Sci., 5, https://doi.org/10.3389/fmars.2018.00276, 2018.

Bowes, M. J., Jarvie, H. P., Halliday, S. J., Skeffington, R. A., Wade, A. J., Loewenthal, M., Gozzard, E., Newman, J. R., and Palmer-Felgate, E. J.: Characterising phosphorus and nitrate inputs to a rural river using high-frequency concentration–flow relationships, Sci. Total Environ., 511, 608-620, https://doi.org/10.1016/j.scitotenv.2014.12.086, 2015.

Bowes, M. J., Smith, J. T., Neal, C., Leach, D. V., Scarlett, P. M., Wickham, H. D., Harman, S. A., Armstrong, L. K., Davy-Bowker, J., Haft, M., and Davies, C. E.: Changes in water quality of the River Frome (UK) from 1965 to 2009: Is phosphorus mitigation finally working?, Sci. Total Environ., 409, 3418-3430, https://doi.org/10.1016/j.scitotenv.2011.04.049, 2011.

Brooks, P. D., McKnight, D. M., and Bencala, K. E.: The relationship between soil heterotrophic activity, soil dissolved organic carbon (DOC) leachate, and catchment-scale DOC export in headwater catchments, Water Resour. Res., 35, 1895-1902, https://doi.org/10.1029/1998WR900125, 1999.

Colmar, A., Walter, C., Le Bissonnais, Y., and Daroussin, J.: Démarche de validation régionale par avis d'experts du modèle MESALES d'estimation de l'aléa érosif, Etude et Gestion des Sols, 17, 19-32, 2010.

Cooper, R. J., Rawlins, B. G., Krueger, T., Lézé, B., Hiscock, K. M., and Pedentchouk, N.: Contrasting controls on the phosphorus concentration of suspended particulate matter under baseflow and storm event conditions in agricultural headwater streams, Sci. Total Environ., 533, 49-59, https://doi.org/10.1016/j.scitotenv.2015.06.113, 2015.

Cosgrove, W. J. and Loucks, D. P.: Water management: Current and future challenges and research directions, Water Resour. Res., 51, 4823-4839, https://doi.org/10.1002/2014WR016869, 2015.

Creed, I. F., Beall, F. D., Clair, T. A., Dillon, P. J., and Hesslein, R. H.: Predicting export of dissolved organic carbon from forested catchments in glaciated landscapes with shallow soils, Global Biogeochem. Cy., 22, https://doi.org/10.1029/2008GB003294, 2008.

Dawson, J. J. C., Soulsby, C., Tetzlaff, D., Hrachowitz, M., Dunn, S. M., and Malcolm, I. A.: Influence of hydrology and seasonality on DOC exports from three contrasting upland catchments, Biogeochemistry, 90, 93-113, https://doi.org/10.1007/s10533-008-9234-3, 2008.

Delmas, M., Saby, N., Arrouays, D., Dupas, R., Lemercier, B., Pellerin, S., and Gascuel-Odoux, C.: Explaining and mapping total phosphorus content in French topsoils, Soil Use Manage., 31, 259-269, https://doi.org/10.1111/sum.12192, 2015.

Dodds, W. K. and Smith, V. H.: Nitrogen, phosphorus, and eutrophication in streams, Inland Waters, 6, 155-164, DOI: 10.5268/IW-6.2.909, 2016.

Duan, S., Kaushal, S. S., Groffman, P. M., Band, L. E., and Belt, K. T.: Phosphorus export across an urban to rural gradient in the Chesapeake Bay watershed, J. Geophys. Res-Biogeo, 117, https://doi.org/10.1029/2011JG001782, 2012.

Duncan, J. M., Band, L. E., Groffman, P. M., and Bernhardt, E. S.: Mechanisms driving the seasonality of catchment scale nitrate export: Evidence for riparian ecohydrologic controls, Water Resour. Res., 51, 3982-3997, https://doi.org/10.1002/2015WR016937, 2015.

Dupas, R., Delmas, M., Dorioz, J.-M., Garnier, J., Moatar, F., and Gascuel-Odoux, C.: Assessing the impact of agricultural pressures on N and P loads and eutrophication risk, Ecol. Indic., 48, 396-407, https://doi.org/10.1016/j.ecolind.2014.08.007, 2015a.

Dupas, R., Gruau, G., Gu, S., Humbert, G., Jaffrézic, A., and Gascuel-Odoux, C.: Groundwater control of biogeochemical processes causing phosphorus release from riparian wetlands, Water Res., 84, 307-314, https://doi.org/10.1016/j.watres.2015.07.048, 2015b.

Dupas, R., Minaudo, C., and Abbott, B. W.: Stability of spatial patterns in water chemistry across temperate ecoregions, Environ. Res. Lett., 14, 074015, https://doi.org/10.1088/1748-9326/ab24f4, 2019.

Dupas, R., Minaudo, C., Gruau, G., Ruiz, L., and Gascuel-Odoux, C.: Multidecadal Trajectory of Riverine Nitrogen and Phosphorus Dynamics in Rural Catchments, Water Resour. Res., 54, 5327– 5340, https://doi.org/10.1029/2018WR022905, 2018.

Dupas, R., Musolff, A., Jawitz, J. W., Rao, P. S. C., Jäger, C. G., Fleckenstein, J. H., Rode, M., and Borchardt, D.: Carbon and nutrient export regimes from headwater catchments to downstream reaches, Biogeosciences, 14, 4391-4407, https://doi.org/10.5194/bg-14-4391-2017, 2017.

Edwards, A. C., Cook, Y., Smart, R., and Wade, A. J.: Concentrations of nitrogen and phosphorus in streams draining the mixed land-use Dee Catchment, north-east Scotland, J. Appl. Ecol., 37, 159-170, https://doi.org/10.1046/j.1365-2664.2000.00500.x, 2000.

Evans, C. D., Reynolds, B., Jenkins, A., Helliwell, R. C., Curtis, C. J., Goodale, C. L., Ferrier, R. C., Emmett, B. A., Pilkington, M. G., Caporn, S. J. M., Carroll, J. A., Norris, D., Davies, J., and Coull, M. C.: Evidence that Soil Carbon Pool Determines Susceptibility of Semi-Natural Ecosystems to Elevated Nitrogen Leaching, Ecosystems, 9, 453-462, https://doi.org/10.1007/s10021-006-0051-z, 2006.

Exner-Kittridge, M., Strauss, P., Blöschl, G., Eder, A., Saracevic, E., and Zessner, M.: The seasonal dynamics of the stream sources and input flow paths of water and nitrogen of an Austrian headwater agricultural catchment, Sci. Total Environ., 542, 935-945, https://doi.org/10.1016/j.scitotenv.2015.10.151, 2016.

FAO and WWC: Towards a water and food secure future: Critical perspectives for policy-makers, Food and Agriculture Organization of the United Nations (FAO) and the World Water Council (WWC) in support to the High Level Panel on Water for Food Security, Seventh World Water Forum in Daegu, South Korea, White paper, 76 pp., http://www.fao.org/3/a-i4560e.pdf, 2015.

Fasching, C., Ulseth, A. J., Schelker, J., Steniczka, G., and Battin, T. J.: Hydrology controls dissolved organic matter export and composition in an Alpine stream and its hyporheic zone, Limnol. Oceanogr., 61, 558-571, https://doi.org/10.1002/lno.10232, 2016.

Findlay, S. E.: Increased carbon transport in the Hudson River: unexpected consequence of nitrogen deposition?, Front. Ecol. Environ., 3, 133-137, https://doi.org/10.1890/1540-9295(2005)003[0133:ICTITH]2.0.CO;2, 2005.

Gardner, K. K. and McGlynn, B. L.: Seasonality in spatial variability and influence of land use/land cover and watershed characteristics on stream water nitrate concentrations in a developing watershed in the Rocky Mountain West: Human impacts on spatial N patterns, Water Resour. Res., 45, https://doi.org/10.1029/2008WR007029, 2009.

Goodale, C. L., Aber, J. D., Vitousek, P. M., and McDowell, W. H.: Long-term decreases in stream nitrate: successional causes unlikely; possible links to DOC?, Ecosystems, 8, 334-337, https://doi.org/10.1007/s10021-003-0162-8, 2005.

Graeber, D., Gelbrecht, J., Pusch, M. T., Anlanger, C., and von Schiller, D.: Agriculture has changed the amount and composition of dissolved organic matter in Central European headwater streams, Sci. Total Environ., 438, 435-446, https://doi.org/10.1016/j.scitotenv.2012.08.087, 2012.

Griffiths, N. A., Tank, J. L., Royer, T. V., Warrner, T. J., Frauendorf, T. C., Rosi-Marshall, E. J., and Whiles, M. R.: Temporal variation in organic carbon spiraling in Midwestern agricultural streams, Biogeochemistry, 108, 149-169, https://doi.org/10.1007/s10533-011-9585-z, 2011.

Grizzetti, B., Bouraoui, F., de Marsily, G., and Bidoglio, G.: A statistical method for source apportionment of riverine nitrogen loads, J. Hydrol., 304, 302-315, https://doi.org/10.1016/j.jhydrol.2004.07.036, 2005.

Grolemund, G. and Wickham, H.: Dates and Times Made Easy with lubridate, Journal of Statistical Software, 40, 1-25, DOI: 10.18637/jss.v040.i03, 2011.

Gu, S., Gruau, G., Dupas, R., Petitjean, P., Li, Q., and Pinay, G.: Respective roles of Fe-oxyhydroxide dissolution, pH changes and sediment inputs in dissolved phosphorus release from wetland soils under anoxic conditions, Geoderma, 338, 365-374, https://doi.org/10.1016/j.geoderma.2018.12.034, 2019.

Gu, S., Gruau, G., Dupas, R., Rumpel, C., Crème, A., Fovet, O., Gascuel-Odoux, C., Jeanneau, L., Humbert, G., and Petitjean, P.: Release of dissolved phosphorus from riparian wetlands: Evidence for complex interactions among hydroclimate variability, topography and soil properties, Sci. Total Environ., 598, 421-431, https://doi.org/10.1016/j.scitotenv.2017.04.028, 2017.

Gücker, B., Silva, R. C. S., Graeber, D., Monteiro, J. A. F., and Boëchat, I. G.: Urbanization and agriculture increase exports and differentially alter elemental stoichiometry of dissolved organic matter (DOM) from tropical catchments, Sci. Total Environ., 550, 785-792, https://doi.org/10.1016/j.scitotenv.2016.01.158, 2016.

Halliday, S. J., Wade, A. J., Skeffington, R. A., Neal, C., Reynolds, B., Rowland, P., Neal, M., and Norris, D.: An analysis of long-term trends, seasonality and short-term dynamics in water quality data from Plynlimon, Wales, Sci. Total Environ., 434, 186-200, https://doi.org/10.1016/j.scitotenv.2011.10.052, 2012.

Hedin, L. O., von Fischer, J. C., Ostrom, N. E., Kennedy, B. P., Brown, M. G., and Robertson, G. P.: Thermodynamic Constraints on Nitrogen Transformations and Other Biogeochemical Processes at Soil-Stream Interfaces, Ecology, 79, 684-703, DOI: 10.2307/176963, 1998.

Heppell, C. M., Binley, A., Trimmer, M., Darch, T., Jones, A., Malone, E., Collins, A. L., Johnes, P. J., Freer, J. E., and Lloyd, C. E. M.: Hydrological controls on DOC : nitrate resource stoichiometry in a lowland, agricultural catchment, southern UK, Hydrol. Earth Syst. Sc., 21, 4785-4802, https://doi.org/10.5194/hess-21-4785-2017, 2017.

Hill, A. R., Devito, K. J., Campagnolo, S., and Sanmugadas, K.: Subsurface denitrification in a forest riparianzone: Interactions between hydrology and supplies ofnitrate and organic carbon, Biogeochemistry, 51, 193-223, https://doi.org/10.1023/A:1006476514038, 2000.

Humbert, G., Jaffrézic, A., Fovet, O., Gruau, G., and Durand, P.: Dry-season length and runoff control annual variability in stream DOC dynamics in a small, shallowgroundwater-dominated agricultural watershed, Water Resour. Res., 51, 7860-7877, https://doi.org/10.1002/2015WR017336, 2015.

Hytteborn, J. K., Temnerud, J., Alexander, R. B., Boyer, E. W., Futter, M. N., Fröberg, M., Dahné, J., and Bishop, K. H.: Patterns and predictability in the intra-annual organic carbon variability across the boreal and hemiboreal landscape, Sci. Total Environ., 520, 260-269, https://doi.org/10.1016/j.scitotenv.2015.03.041, 2015.

Lambert, T., Pierson-Wickmann, A.-C., Gruau, G., Jaffrezic, A., Petitjean, P., Thibault, J.-N., and Jeanneau, L.: Hydrologically driven seasonal changes in the sources and production mechanisms of dissolved organic carbon in a small lowland catchment, Water Resour. Res., 49, 5792-5803, https://doi.org/10.1002/wrcr.20466, 2013.

Le, S., Josse, J., and Husson, F.: FactoMineR: An R Package for Multivariate Analysis, J. Stat. Softw., 25, 1-18, DOI: 10.18637/jss.v025.i01, 2008.

Lemercier, B., Gaudin, L., Walter, C., Aurousseau, P., Arrouays, D., Schvartz, C., Saby, N. P. A., Follain, S., and Abrassart, J.: Soil phosphorus monitoring at the regional level by means of a soil test database, Soil Use Manage., 24, 131-138, https://doi.org/10.1111/j.1475-2743.2008.00146.x, 2008.

Le Moal, M., Gascuel-Odoux, C., Ménesguen, A., Souchon, Y., Étrillard, C., Levain, A., Moatar, F., Pannard, A., Souchu, P., Lefebvre, A., and Pinay, G.: Eutrophication: A new wine in an old bottle?, Sci. Total Environ., 651, 1-11, https://doi.org/10.1016/j.scitotenv.2018.09.139 , 2019.

Lintern, A., Webb, J. A., Ryu, D., Liu, S., Bende-Michl, U., Waters, D., Leahy, P., Wilson, P., and Western, A. W.: Key factors influencing differences in stream water quality across space, Wiley Interdisciplinary Reviews: Water, 5, e1260, https://doi.org/10.1002/wat2.1260, 2018.

Mardhel, V. and Gravier, A.: Carte de vulnérabilité intrinsèque simplifiée des eaux souterraines du Bassin Seine-Normandie, Report BRGM/RP54148-FR, 92 pp., 2004.

Martin, C., Aquilina, L., Gascuel-Odoux, C., Molénat, J., Faucheux, M., and Ruiz, L.: Seasonal and interannual variations of nitrate and chloride in stream waters related to spatial and temporal patterns of groundwater concentrations in agricultural catchments, Hydrol. Process., 18, 1237-1254, https://doi.org/10.1002/hyp.1395, 2004.

Martin, C., Molénat, J., Gascuel-Odoux, C., Vouillamoz, J. M., Robain, H., Ruiz, L., Faucheux, M., and Aquilina, L.: Modelling the effect of physical and chemical characteristics of shallow aquifers on water and nitrate transport in small agricultural catchments, J. Hydrol., 326, 25-42, https://doi.org/10.1016/j.jhydrol.2005.10.040, 2006.

Melland, A. R., Mellander, P. E., Murphy, P. N. C., Wall, D. P., Mechan, S., Shine, O., Shortle, G., and Jordan, P.: Stream water quality in intensive cereal cropping catchments with regulated nutrient management, Environ. Sci. Policy, 24, 58-70, https://doi.org/10.1016/j.envsci.2012.06.006, 2012.

Mengistu, S. G., Creed, I. F., Webster, K. L., Enanga, E., and Beall, F. D.: Searching for similarity in topographic controls on carbon, nitrogen and phopsphorus export from forest headwater catchments, Hydrol. Process., 28, 3201-3216, https://doi.org/10.1002/hyp.9862, 2014.

Minaudo, C., Dupas, R., Gascuel-Odoux, C., Roubeix, V., Danis, P.-A., and Moatar, F.: Seasonal and event-based concentration-discharge relationships to identify catchment controls on nutrient export regimes, Adv. Water Resour., 131, 103379, https://doi.org/10.1016/j.advwatres.2019.103379, 2019.

Minaudo, C., Meybeck, M., Moatar, F., Gassama, N., and Curie, F.: Eutrophication mitigation in rivers: 30 years of trends in spatial and seasonal patterns of biogeochemistry of the Loire River (1980–2012), Biogeosciences, 12, 2549-2563, https://doi.org/10.5194/bg-12-2549-2015, 2015.

Moatar, F., Floury, M., Gold, A. J., Meybeck, M., Renard, B., Ferréol, M., Chandesris, A., Minaudo, C., Addy, K., Piffady, J., and Pinay, G.: Stream Solutes and Particulates Export Regimes: A New Framework to Optimize Their Monitoring, Front Ecol Evol, 7, https://doi.org/10.3389/fevo.2019.00516, 2020.

Moatar, F. and Meybeck, M.: Riverine fluxes of pollutants: Towards predictions of uncertainties by flux duration indicators, C.R. Geosci., 339, 367-382, https://doi.org/10.1016/j.crte.2007.05.001, 2007.

Mulholland, P. J. and Hill, W. R.: Seasonal patterns in streamwater nutrient and dissolved organic carbon concentrations: Separating catchment flow path and in-stream effects, Water Resour. Res., 33, 1297-1306, https://doi.org/10.1029/97WR00490, 1997.

Musolff, A., Fleckenstein, J. H., Opitz, M., Büttner, O., Kumar, R., and Tittel, J.: Spatio-temporal controls of dissolved organic carbon stream water concentrations, J. of Hydrol., 566, 205-215, https://doi.org/10.1016/j.jhydrol.2018.09.011, 2018.

Musolff, A., Selle, B., Büttner, O., Opitz, M., and Tittel, J.: Unexpected release of phosphate and organic carbon to streams linked to declining nitrogen depositions, Global Change Biol., 23, 1891-1901, https://doi.org/10.1111/gcb.13498, 2017.

Mutema, M., Chaplot, V., Jewitt, G., Chivenge, P., and Blöschl, G.: Annual water, sediment, nutrient, and organic carbon fluxes in river basins: A global meta-analysis as a function of scale, Water Resour. Res., 51, 8949-8972, https://doi.org/10.1002/2014WR016668, 2015.

Onderka, M., Wrede, S., Rodný, M., Pfister, L., Hoffmann, L., and Krein, A.: Hydrogeologic and landscape controls of dissolved inorganic nitrogen (DIN) and dissolved silica (DSi) fluxes in heterogeneous catchments, J. Hydrol., 450-451, 36-47, https://doi.org/10.1016/j.jhydrol.2012.05.035, 2012.

Perrin, C., Michel, C., and Andréassian, V.: Improvement of a parsimonious model for streamflow simulation, J. Hydrol., 279, 275-289, https://doi.org/10.1016/S0022-1694(03)00225-7, 2003.

Plont, S., O'Donnell, B. M., Gallagher, M. T., and Hotchkiss, E. R.: Linking carbon and nitrogen spiraling in streams, Freshw. Sci., 39, 126-136, https://doi.org/10.1086/707810, 2020.

Poisvert, C., Curie, F., and Moatar, F.: Annual agricultural N surplus in France over a 70-year period, Nutr. Cycl. Agroecosyst., 107, 63-78, https://doi.org/10.1007/s10705-016-9814-x, 2017.

Pregitzer, K. S., Zak, D. R., Burton, A. J., Ashby, J. A., and MacDonald, N. W.: Chronic nitrate additions dramatically increase the export of carbon and nitrogen from northern hardwood ecosystems, Biogeochemistry, 68, 179-197, https://doi.org/10.1023/B:BIOG.0000025737.29546.fd, 2004.

Preston, S. D., Alexander, R. B., Schwarz, G. E., and Crawford, C. G.: Factors affecting stream nutrient loads: a synthesis of regional SPARROW model results for the continental United States, J. Am. Water Resour. As., 47, 891-915, https://doi.org/10.1111/j.1752-1688.2011.00577.x, 2011.

Raymond, S., Moatar, F., Meybeck, M., and Bustillo, V.: Choosing methods for estimating dissolved and particulate riverine fluxes from monthly sampling, Hydrolog. Sci. J., 58, 1326-1339, https://doi.org/10.1080/02626667.2013.814915, 2013.

Saby, N. P. A., Lemercier, B., Arrouays, D., Leménager, S., Louis, B. P., Millet, F., Schellenberger, E., Squividant, H., Swiderski, C., Toutain, B. F. P., Walter, C., and Bardy, M.: Le programme Base de Données des Analyses de Terre (BDAT) : Bilan de 20 ans de collecte de résultats d'analyses, Etude et Gestion des Sols, 21, 141-150, 2015.

Sobota, D. J., Harrison, J. A., and Dahlgren, R. A.: Linking dissolved and particulate phosphorus export in rivers draining California's Central Valley with anthropogenic sources at the regional scale, J. Environ. Qual., 40, 1290-1302, https://doi.org/10.2134/jeq2011.0010, 2011.

SoeS: NOPOLU-Agri. Outil de spatialisation des pressions de l'agriculture. Méthodologie et résultats pour les surplus d'azote et les émissions des gaz à effet de serre. Campagne 2010–2011. Ministere du Developpement durable et de l'Energie, 2013.

Taylor, P. G. and Townsend, A. R.: Stoichiometric control of organic carbon-nitrate relationships from soils to the sea, Nature, 464, 1178-1181, https://doi.org/10.1038/nature08985, 2010.

Temnerud, J. and Bishop, K.: Spatial Variation of Streamwater Chemistry in Two Swedish Boreal Catchments: Implications for Environmental Assessment, Environ. Sci. Technol., 39, 1463-1469, https://doi.org/10.1021/es040045q, 2005.

Thomas, O., Jung, A. V., Causse, J., Louyer, M. V., Piel, S., Baurès, E., and Thomas, M. F.: Revealing organic carbon–nitrate linear relationship from UV spectra of freshwaters in agricultural environment, Chemosphere, 107, 115-120, https://doi.org/10.1016/j.chemosphere.2014.03.034, 2014.

UNESCO, LIWQ.: International Initiative on Water Quality: promoting scientific research, knowledge sharing, effective technology and policy approaches to improve water quality for sustainable development - UNESCO Bibliothèque Numérique, 23 pp., https://unesdoc.unesco.org/ark:/48223/pf0000243651, 2015.

Van Meter, K. J., Chowdhury, S., Byrnes, D. K., and Basu, N. B.: Biogeochemical asynchrony: Ecosystem drivers of seasonal concentration regimes across the Great Lakes Basin, Limnol. Oceanogr., 9999, https://doi.org/10.1002/lno.11353, 2019.

Weigand, S., Bol, R., Reichert, B., Graf, A., Wiekenkamp, I., Stockinger, M., Luecke, A., Tappe, W., Bogena, H., Puetz, T., Amelung, W., and Vereecken, H.: Spatiotemporal Analysis of Dissolved Organic Carbon and Nitrate in Waters of a Forested Catchment Using Wavelet Analysis, Vadose Zone J., 16, doi:10.2136/vzj2016.09.0077, 2017.

Whitehead, P. G., Wilby, R. L., Battarbee, R. W., Kernan, M., and Wade, A. J.: A review of the potential impacts of climate change on surface water quality, Hydrolog. Sci. J., 54, 101-123, https://doi.org/10.1623/hysj.54.1.101, 2009.

Wickham, H.: ggplot2: Elegant Graphics for Data Analysis, Springer, 2016.

Wickham, H.: The Split-Apply-Combine Strategy for Data Analysis, J. Stat. Softw., 40, 1-29, DOI: 10.18637/jss.v040.i01, 2011.

Wood, S. N.: Generalized Additive Models : An Introduction with R, Second Edition, Chapman and Hall/CRC, 2017.

Zambrano-Bigiarini, M.: hydroGOF: Goodness-of-fit functions for comparison of simulated and observed hydrological time series. R package version 0.4-0. , DOI:10.5281/zenodo.839854., 2020.

Table 1. Headwater catchment descriptors identified as potential explanatory variables of spatial variability and temporal variation in dissolved organic carbon (DOC), nitrate (NO_3), and soluble reactive phosphorus (SRP) in stream and river water.

Type	Descriptor name	Unit	Definition	Source
Topography	Area	km^2	Drainage area of the monitoring station	Web Processing Service "Service de Traitement de Modèles Numériques de Terrain" and DEM 50 m by IGN
	Elevation	m	Elevation of headwater catchment	DEM 25 m by IGN
	Density_hn	$km.km^{-2}$	Density of the hydrographic network	BD Carthage by IGN
	Topo_i	$log(m^3)$	Topographic index of the headwater	
	IDPR	-	Hydrographic Network Development and Persistence Index	http://infoterre.brgm.fr/ BRGM data and geoservices portal (Mardhel and Gravier, 2004)
Geology	Granite_pm	%	Percentage of granite and gneiss area	Web Mapping Service "Carte des Sols de Bretagne" by UMR 1069 SAS INRAE - Agrocampus Ouest http://www.sols-de-bretagne.fr/
	Schist_pm	%	Percentage of schist and micaschist area	
	Other_pm	%	Percentage of various geological substrata	
Soil	Erosion	%	Percentage of area with high to very high erosion risk (derived from land use, topography and soil properties)	Erosion risk map estimated from MESALES by GIS Sol, INRAE from Colmar et al. (2010)
	OC_soil	$g.kg^{-1}$	Organic carbon content in the topsoil horizon (0-30 cm)	Web Mapping Service from BDAT database, Saby et al. (2015) by GIS Sol
	Thick_soil	cm	Class of dominant soil thickness	Web Mapping Service "Carte des Sols de Bretagne" by UMR 1069 SAS INRAE - Agrocampus Ouest
	TP_soil	$g.kg^{-1}$	Total phosphorus content in the topsoil horizon (0-30 cm)	Web Mapping Service from BDAT database by GIS Sol
Land use	SummerCrop	%	Percentage of summer crop land	OSO database, CESBIO, land-cover map 2016 (1 ha) from http://osr-cesbio.ups-tlse.fr/~oso/
	WinterCrop	%	Percentage of winter crop land	
	Forest	%	Percentage of forest land	
	Pasture	%	Percentage of pasture land	
	Urban	%	Percentage of urban land	
	Wetland	%	Percentage of potential wetlands	Web Mapping Service "Enveloppe des milieux potentiellement humides de France réalisée par les laboratoires Infosol et UMR SAS" by UMR 1069 SAS INRAE - Agrocampus Ouest / US 1106 InfoSol INRAE
Diffuse and point N and P sources	N_surplus	$kg.ha^{-1}.yr^{-1}$	Nitrogen surplus (= the maximum quantity on a given agricultural area that is likely to be transferred to the stream network)	CASSIS-N estimates by (Poisvert et al., 2017) from https://geosciences.univ-tours.fr/cassis/login
	P_surplus	$kg.ha^{-1}.yr^{-1}$	Phosphorous surplus	NOPOLU estimates by (SoeS, 2013)
	N_point	$kg.ha^{-1}.yr^{-1}$	Sum of nitrogen loads from domestic and industrial point sources	Data from Loire-Bretagne Water Agency data (2008-2012)
	P_point	$kg.ha^{-1}.yr^{-1}$	Sum of phosphorus loads from domestic and industrial point sources	Data from Loire-Bretagne Water Agency (2008-2012)

Hydrology	Qmean	$l.s^{-1}.km^{-2}$	Interannual mean flow	Calculated from flow data observations: HYDRO regional database by DREAL Bretagne & GR4J simulations (Perrin et al., 2003)
	QMNA	$l.s^{-1}.km^{-2}$	Median of annual minimum monthly specific discharge	
	BFI	%	Base flow index (Lyne et Hollick, 1979)	
	W2	%	Percentage of total discharge that occurs during the highest 2% of flows (Moatar *et al.*, 2013)	
	Rainfall	$mm.yr^{-1}$	Mean effective rainfall from 2008-2012	SAFRAN database (8 km²) by Météo France

Table 2. Coefficients of variation (spatial variability among catchments) of flow-weighted mean concentration (CVcmean) and mean stream flow (CVqmean), and the value of their ratio, for dissolved organic carbon (DOC), nitrate (NO_3), and soluble reactive phosphorus (SRP).

Parameter	CVcmean	CVqmean	CVcmean:CVqmean
DOC	0.2954	0.4614	0.6403
NO_3	0.3285	0.4709	0.6976
SRP	0.9207	0.4743	1.9412

Table 3. Spearman rank correlations between water quality indices and geographical descriptors for dissolved organic carbon (DOC), nitrate (NO_3), and soluble reactive phosphorus (SRP). Only significant correlations ($p \leq 0.05$) are shown, and bold text indicates $|r| \geq 0.40$.

		DOC				NO_3				SRP			
Spatial variable		C50	Ampli	SI	Load	C50	Ampli	SI	Load	C50	Ampli	SI	Load
Topography	Area	-	-0.24	-	-	-	-	-	-	-	-	-	-
	Elevation	**-0.46**	-0.18	-	-	-	-0.31	-0.20	0.19	-0.20	-	-	-
	Density_hn	-	-	-	-	-	-0.22	-	0.16	-0.30	-0.27	0.19	-
	Topo_i	**0.54**	-	-	-	-	**0.41**	0.25	-0.33	0.39	0.25	-	0.18
	IDPR	-	-	-	-	-	-	-	-	-0.21	-0.19	-	-
Geology	Granite_pm	-	-	0.21	**0.41**	-	**-0.43**	-0.31	0.27	-0.26	-0.24	-	-
	Schist_pm	-	-0.21	-0.37	-0.29	-0.16	0.25	0.22	-0.23	-	-	-	-0.20
	Other_pm	-	0.32	0.35	-	0.28	-	-	-	0.28	0.16	-	0.35
Soil	Erosion	-0.36	0.24	-	-	**0.48**	0.16	-0.26	0.39	0.24	0.17	-	0.33
	OC_soil	-0.27	-0.21	-	-	-	-0.29	-	0.18	-0.20	-0.19	-	-
	TP_soil	**-0.44**	-	-	0.38	-	**-0.51**	-0.34	**0.49**	**-0.40**	-0.32	-	-
Land use	SummerCrop	-0.30	0.28	**0.54**	-	**0.68**	-	**-0.47**	**0.54**	-	-	0.29	0.36
	WinterCrop	0.19	-	-0.20	-0.29	-	**0.48**	0.21	-0.23	0.17	-	-0.18	-
	Forest	-	-0.17	-0.30	0.23	-0.37	**-0.47**	-	-	-0.29	-0.19	-	-0.27
	Pasture	-	-	-	-	-0.30	-	0.26	-0.20	-	-	-	-
	Urban	-	-	-	-	-	-	-	-	0.23	-	-	-
N and P diffuse and point sources	N_surplus	-0.21	0.20	-	-	0.39	-	-	0.38	-	-	0.29	0.29
	P_surplus	-0.24	0.33	-	-0.22	**0.49**	-	-0.32	0.37	0.20	-0.19	-	0.35
	N_point	-	-0.17	-	-	-	-	-	-	-	-	-	-
	P_point	-	-0.16	-	-	-	-	-	0.21	-	-	-	0.21
Hydrology	Qmean	**-0.49**	0.19	-	**0.53**	0.16	**-0.58**	**-0.42**	**0.67**	-0.39	-0.31	0.21	0.18
	QMNA	**-0.52**	0.25	**0.41**	**0.48**	**0.42**	**-0.54**	**-0.56**	**0.76**	-0.34	-0.32	0.35	0.27
	BFI	**-0.41**	-0.27	**0.64**	0.38	**0.54**	**-0.52**	**-0.69**	**0.57**	-0.20	-0.23	0.32	0.23
	W2	**0.43**	-	**-0.61**	**-0.46**	**-0.49**	**0.54**	**0.68**	**-0.59**	0.20	0.20	-0.26	-0.24
	Precipitation	**-0.50**	-	-	**0.47**	-	**-0.60**	-0.39	**0.60**	**-0.43**	-0.33	0.18	-
	Wetland	0.16	-	0.31	0.38	-	-	-	-	-	-	-	0.35

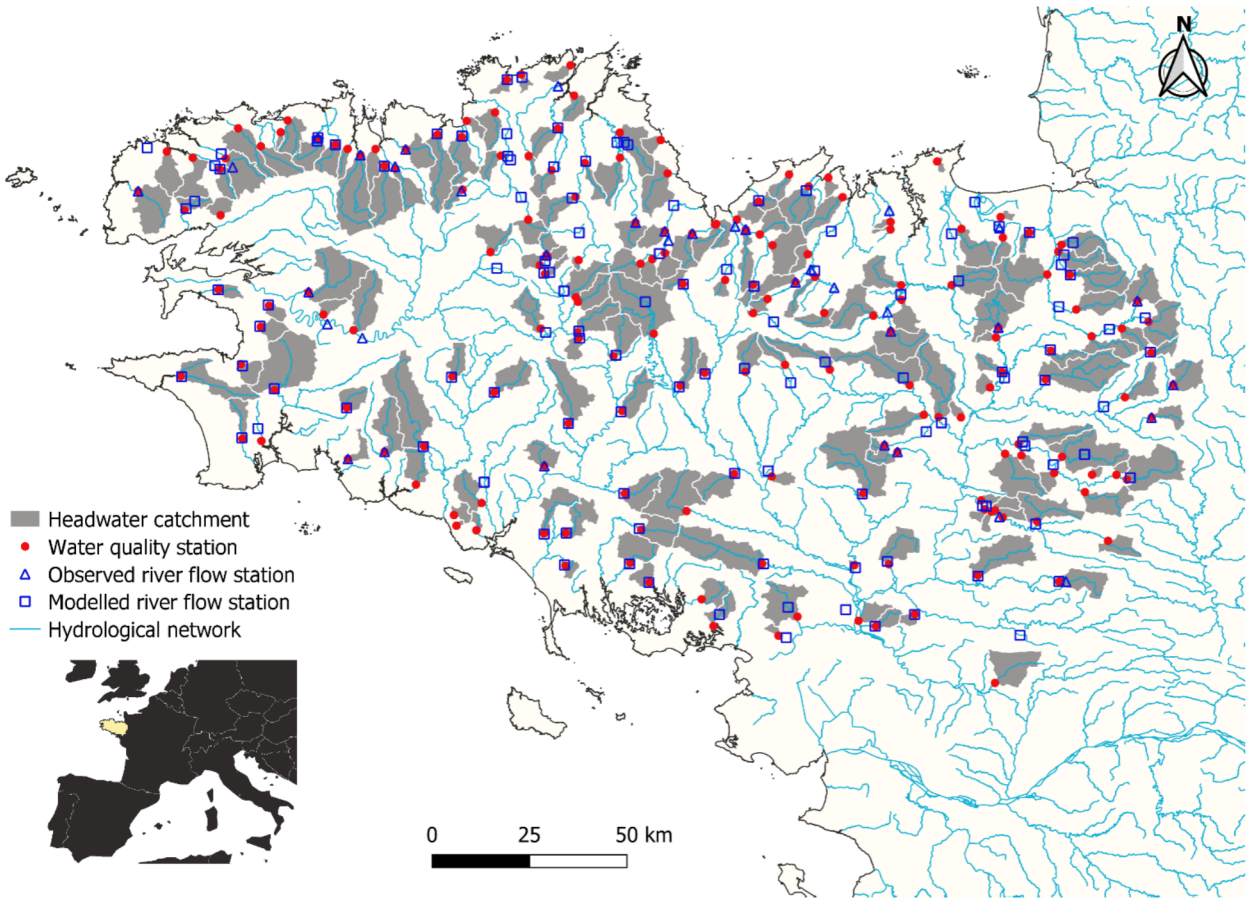

Figure 1. Locations of the 185 study headwater catchments where dissolved organic carbon, nitrate, and soluble reactive phosphorus concentrations were monitored monthly at the outlet from 2007-2016, and paired discharge stations where daily records of stream flow were available from observations or modeling.

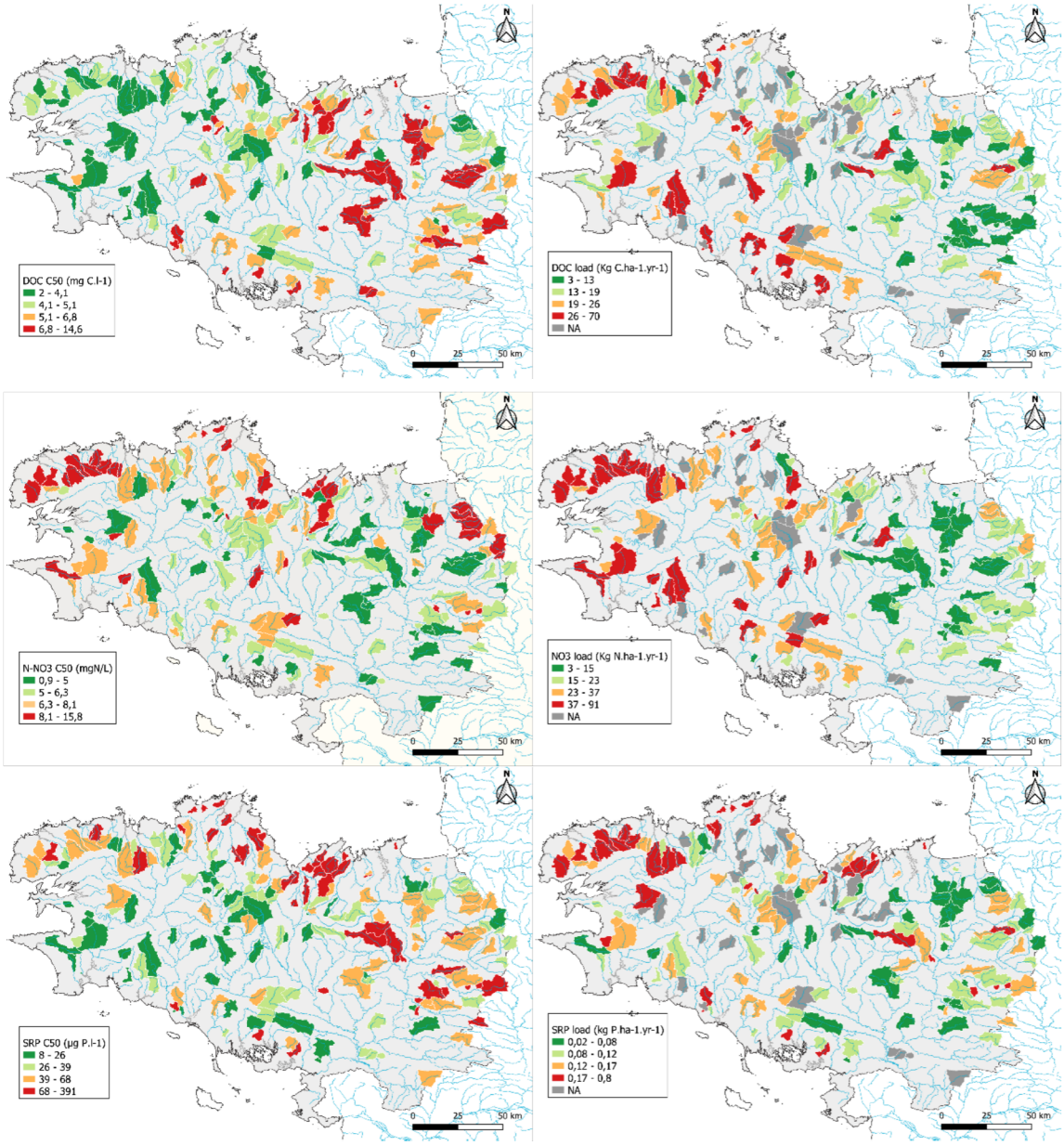

Figure 2. Map of median (left) concentrations C50 and (right) loads of dissolved organic carbon (DOC), nitrate N ($N\text{-}NO_3$), and soluble reactive phosphorus (SRP) for the 185 streams. The catchments in gray did not meet the criteria to estimate a mean average interannual load. Classes in the legends have equal numbers of catchments.

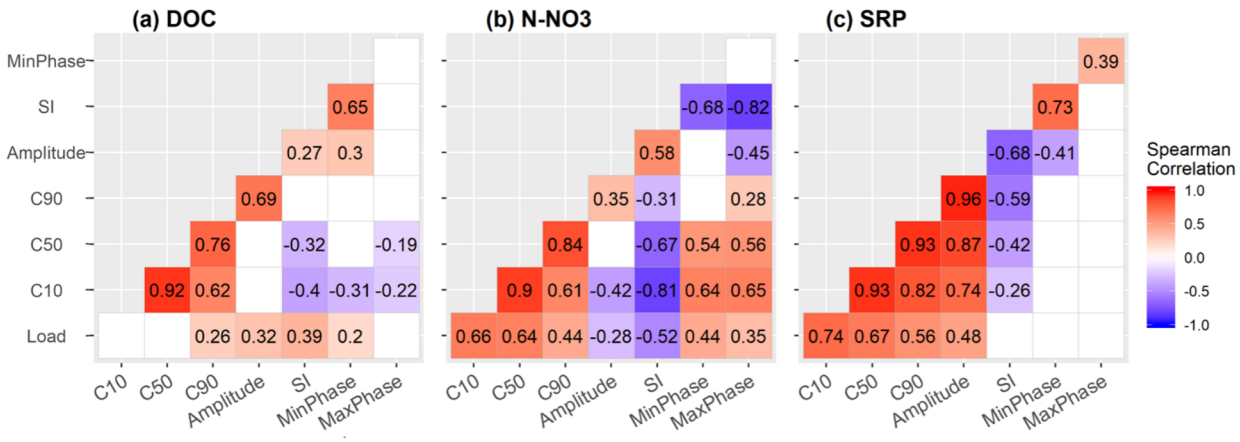

Figure 3. Matrices of Spearman's rank correlations of water quality (load, concentration percentiles (10th (C10), 50th (C50), and 90th (C90)), and seasonality metrics) for (a) dissolved organic carbon (DOC), (b) nitrate N (N-NO_3), and (c) soluble reactive phosphorus (SRP) (c). Only significant ($p \leq 0.05$) values are shown.

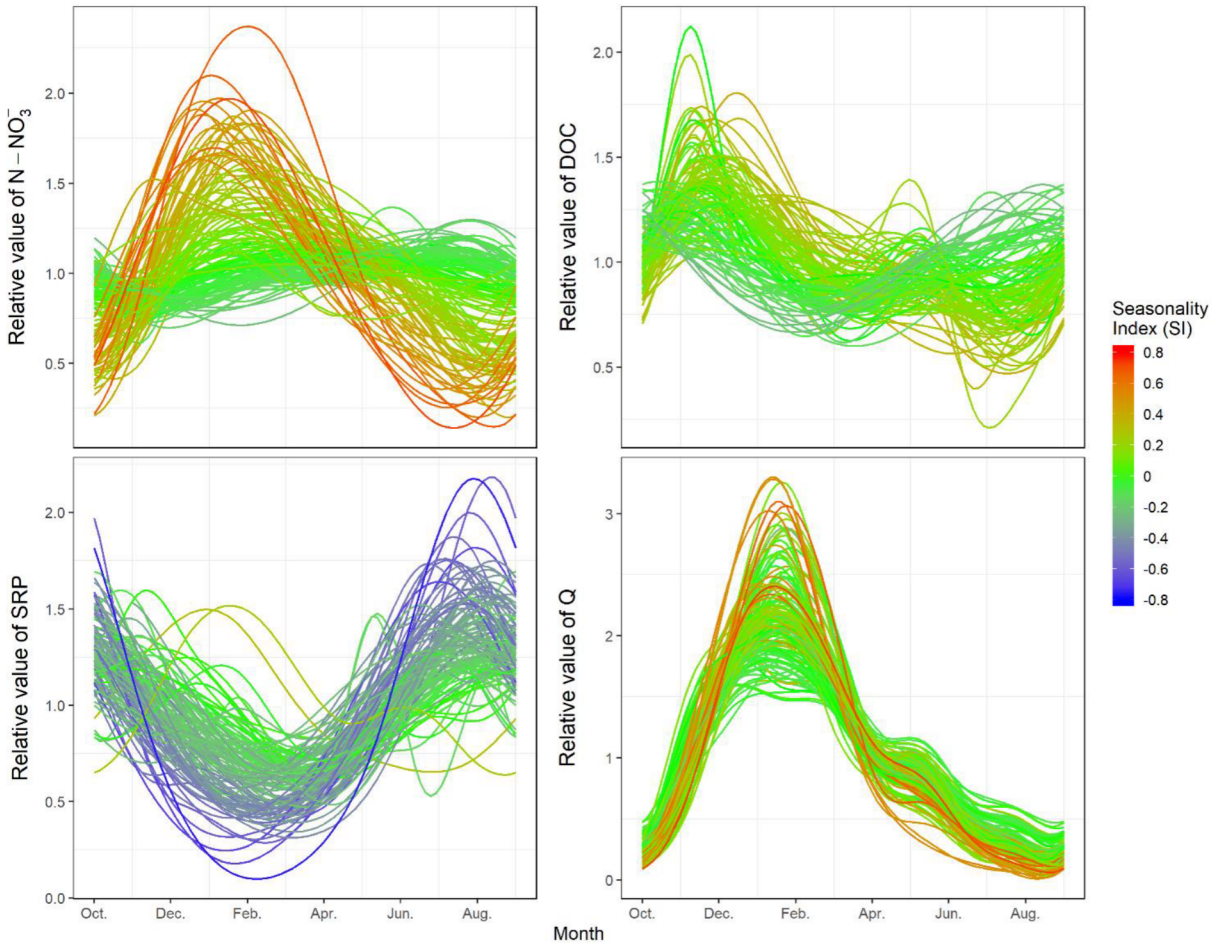

Figure 4. Seasonal dynamics of nitrate N (N-NO_3), dissolved organic carbon (DOC), soluble reactive phosphorus (SRP), and daily discharge modeled by Generalized Additive Models for 185 headwater catchments. To compare concentrations, they are standardized by their mean interannual concentration. The color gradient represents the seasonality index of each parameter; thus, a headwater catchment's color can vary among panels.

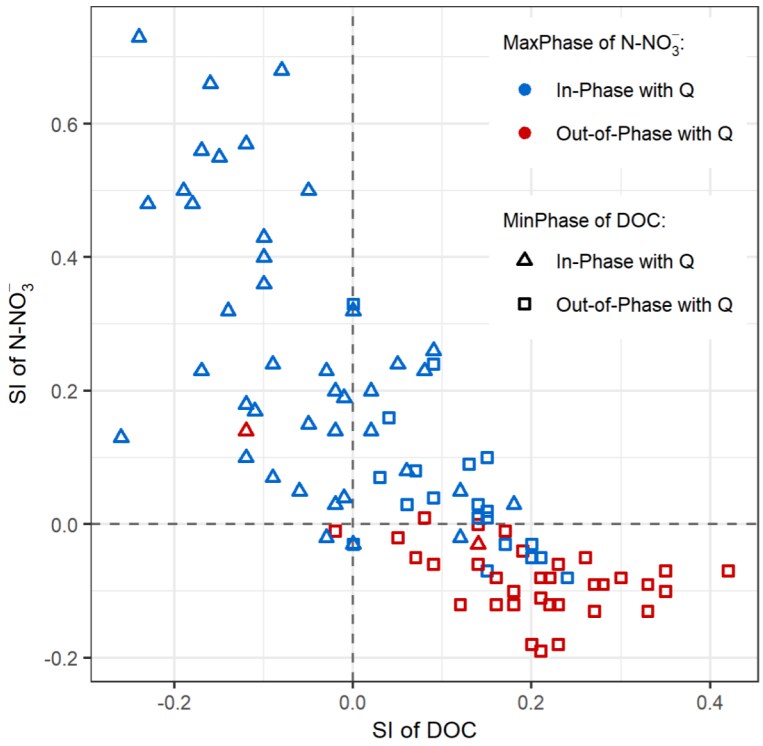

Figure 5. Relationship between the seasonality indices (SI) of nitrate N ($N\text{-}NO_3$) vs. dissolved organic carbon (DOC) in the headwater catchments for which seasonality was significant for both parameters (n=98). The color and shape of symbols identify the seasonality types based on the NO_3 MaxPhase and DOC MinPhase metrics. The threshold date was 1 May: MaxPhase that occurred before were classified as "in-phase" with discharge (Q), while those that occurred after were "out-of-phase" with Q. The DOC MinPhase metric is shown to highlight the synchrony between minimum DOC and maximum $N\text{-}NO_3$ concentrations.

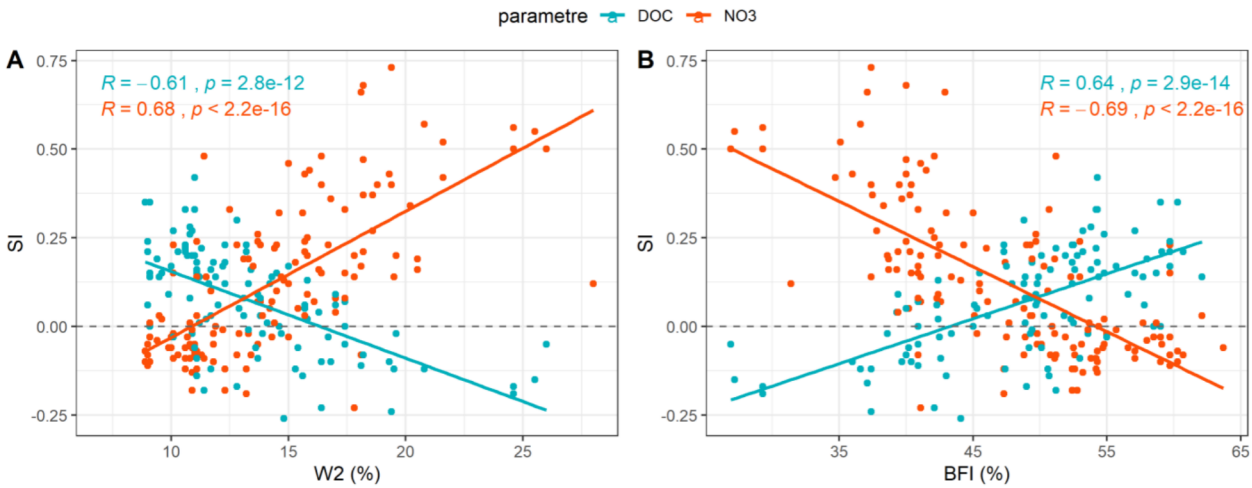

Figure 6. Relationship between the seasonality index (SI) of dissolved organic carbon (DOC) and nitrate (NO_3) and the hydrological reactivity descriptors (A) flow flashiness index (W2) and (B) base-flow index (BFI) for 124 headwater catchments.

Supplements for Spatio-temporal controls of C-N-P dynamics across headwater catchments of a temperate agricultural region from public data analysis

Stella Guillemot[1,2], Ophelie Fovet[1], Chantal Gascuel-Odoux[1], Gérard Gruau[3], Antoine Casquin[1], Florence Curie[2], Camille Minaudo[4], Laurent Strohmenger[1], and Florentina Moatar[5,2]

[1]INRAE, AGROCAMPUS OUEST/INSTITUT AGRO, UMR SAS, 35000 Rennes, France

[2]Université de Tours, EA 6293 GéHCO, 37200 Tours, France

[3]OSUR, Geosciences Rennes, CNRS, Université Rennes 1, 35000 Rennes, France

[4]EPFL, Physics of Aquatic Systems Laboratory, 1015 Lausanne, Switzerland

[5]INRAE, RIVERLY, 69625 Villeurbanne, France

Correspondence to: Ophelie Fovet (ophelie.fovet@inrae.fr)

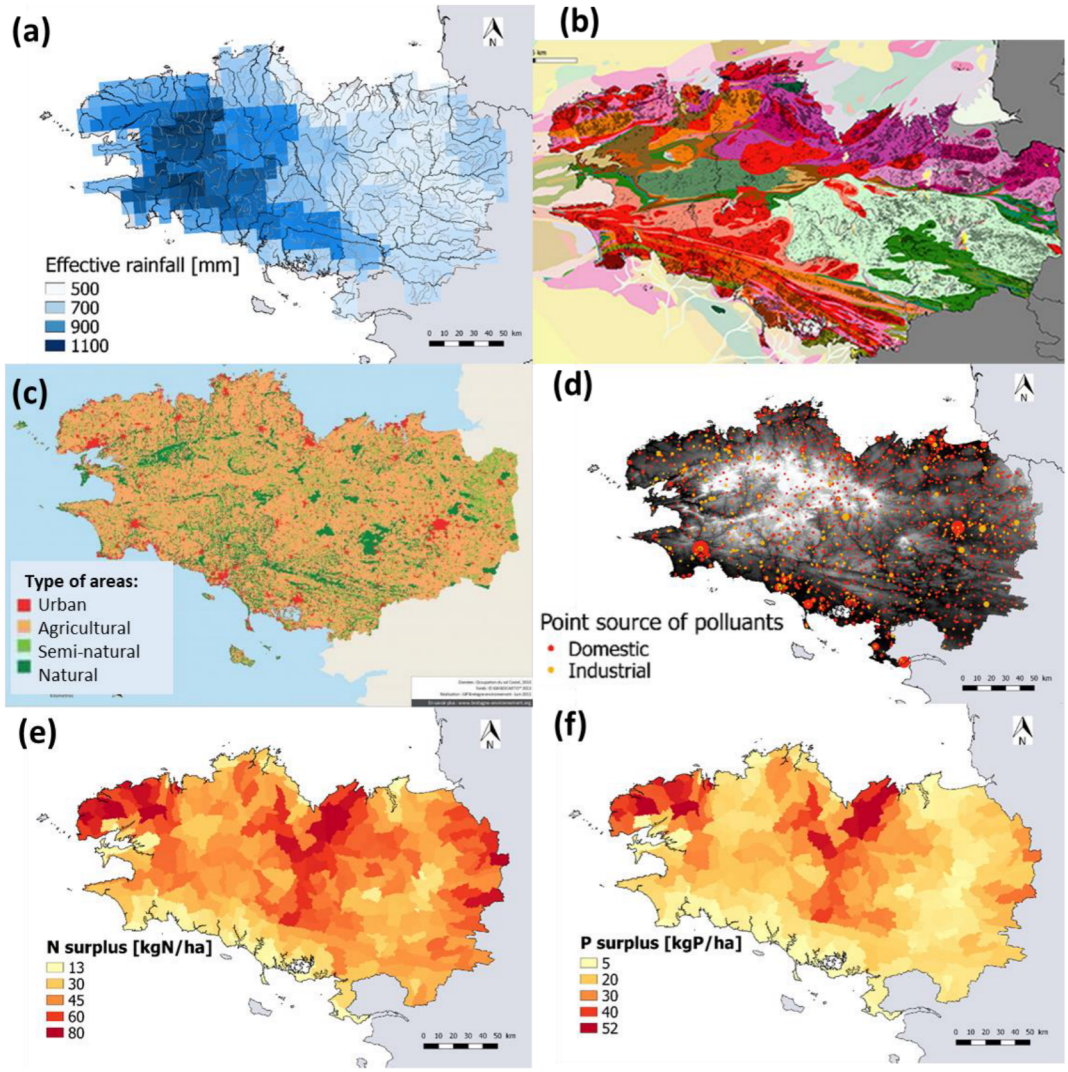

Figure S1. General characteristics of the Brittany region: (a) effective rainfall (SAFRAN database 2010), (b) geology (Sols de Bretagne database), (c) land use (OSO database), (d) nitrogen (N) and phosphorus (P) point sources (Agence de l'Eau Loire Bretagne database), (e) N surplus (NOPOLU model 2010), and (f) P surplus (NOPOLU model 2010).

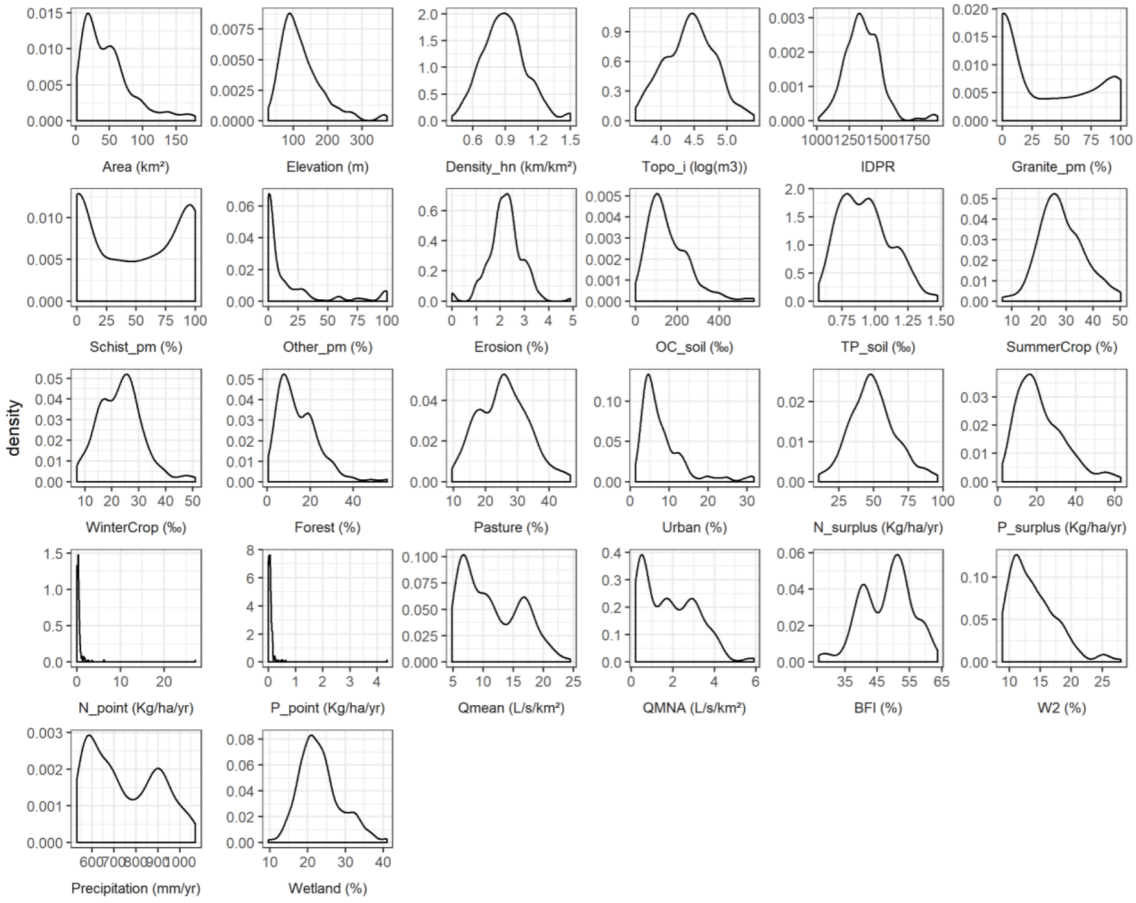

Figure S2. Density histograms of each catchment descriptor. See Table 1 for definitions, units, and sources.

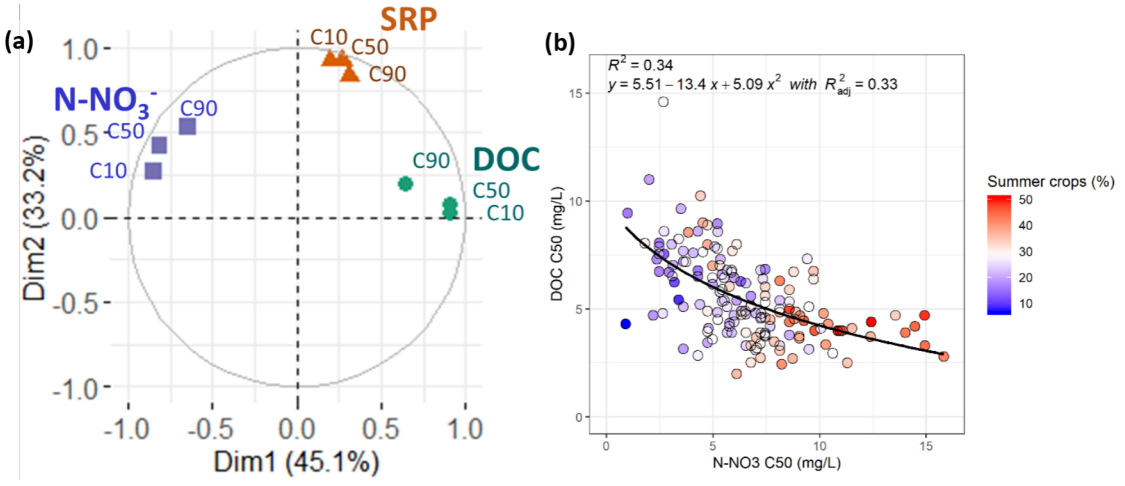

Figure S3. (a) Principal component analysis of 10th, 50th, and 90th percentiles (C10, C50 and C90) of nitrate ($N\text{-}NO_3$), dissolved organic carbon (DOC), and soluble reactive phosphorus (SRP) concentrations for the 185 headwater catchments analyzed; (b) Correlation between the medians (C50) of DOC and $N\text{-}NO_3$ concentrations for the 159 catchments

in which DOC and NO_3 were monitored from 2007-2017. The color gradient indicates the percentage of catchment area covered by summer crops.

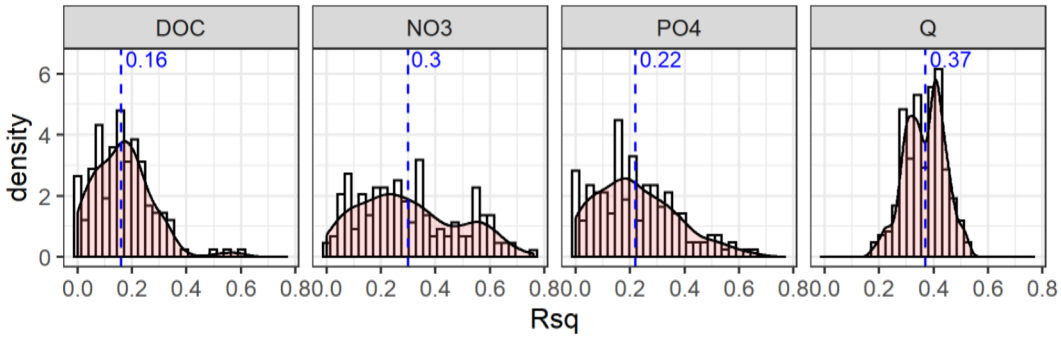

Figure S4. Density histogram of variance in the seasonal component explained by the Generalized Additive Models (GAMs) among headwater catchments for dissolved organic carbon (DOC), nitrate (NO3), soluble reactive phosphorus (noted PO4 here), and discharge (Q). Rsq is the coefficient of determination between observed concentrations and values calculated by the GAM. Dashed lines identify mean values.

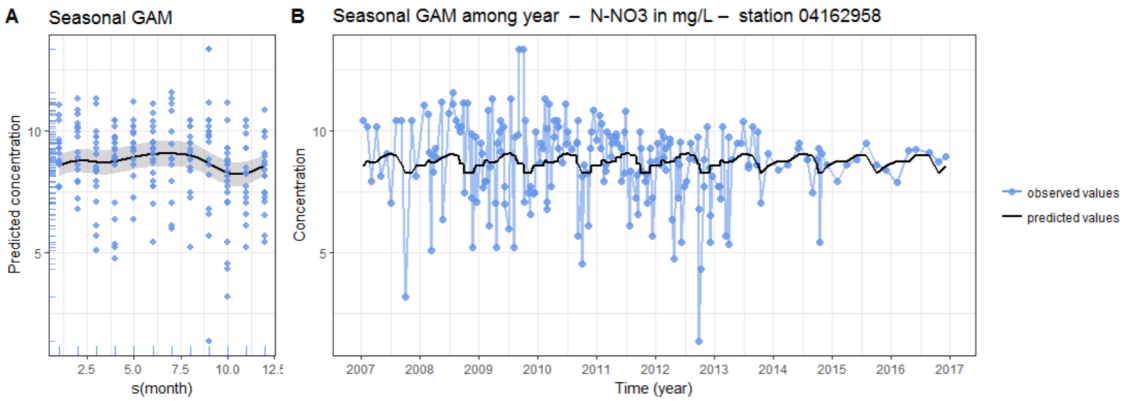

(1)

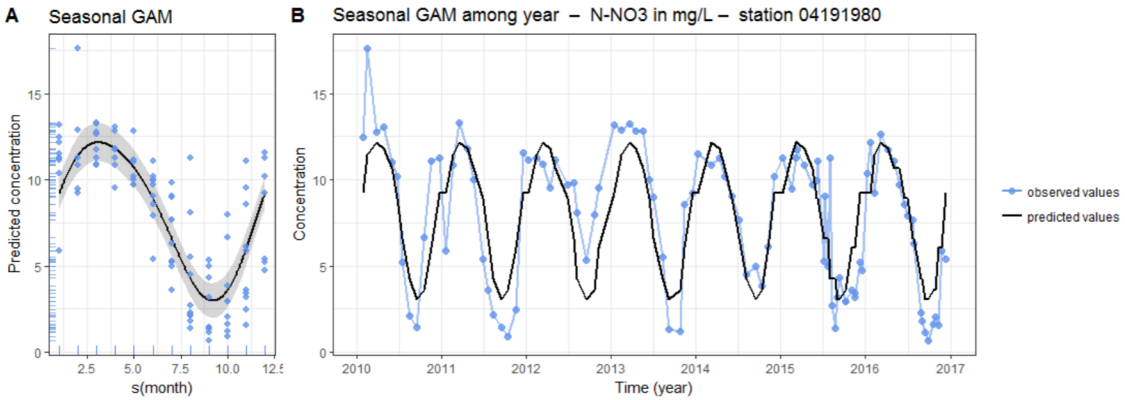

(2)

Figure S5. Two examples of Generalized Additive Model adjustments to nitrate (N-NO3) time series: (1) La Loisance River (station no. 04162958 in the OSUR database) illustrates poor adjustment quality (Rsq=0.02). (2) Saint Niel River/ tributary of the Blavet (station no. 04191980 in the OSUR database) illustrates good adjustment quality (Rsq=0.66).

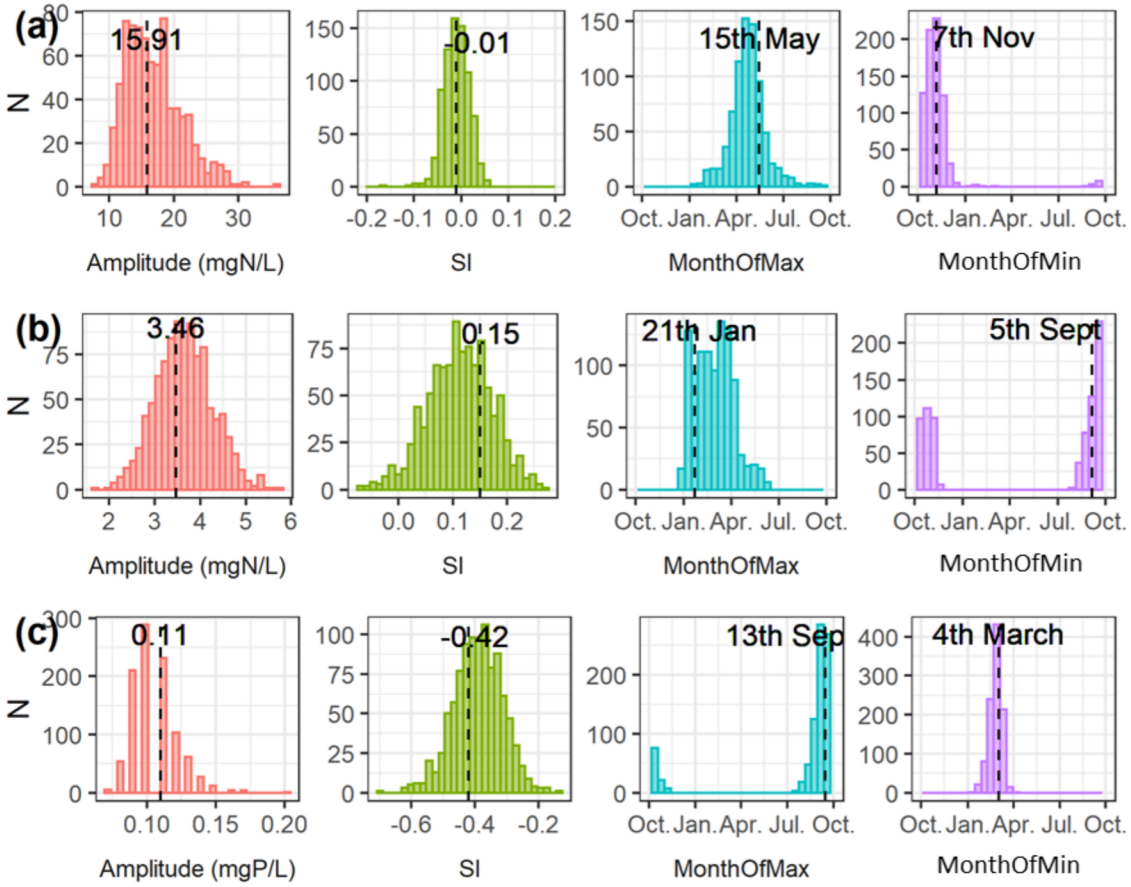

Figure S6. On average, the Generalized Additive Model (GAM) seasonal components were fitted to time series of monthly data, which is a low frequency for investigating intra-annual variations. We assumed that aggregating the 10 years would allow a relatively robust average seasonal pattern to be extracted. To verify this assumption, we analyzed how much the relatively low-frequency sampling influenced the seasonal metrics. We calculated differences between the seasonal indices calculated from GAMs adjusted to high-frequency data and those calculated from GAMs adjusted to monthly data, generated by random Monte Carlo draws (n=1000) from the high-frequency time series. This analysis was performed for three catchments Brittany for which NO_3 and SRP concentration data were available at higher frequency (not available for DOC data) from 2007-2016. The figure summarizes the variability in the seasonality indices (Ampli, seasonality index (SI), MaxPhase and MinPhase) calculated from the 1000 GAM models that were fitted to monthly concentration time series for (a) nitrate (NO_3) in the Kervidy-Naizin catchment, (b) NO_3 in the Néal catchment, and (c) soluble reactive phosphorus (SRP) in the Le Queffeuth catchment. Only significant GAM models (Rsq ≥ 0.10) are shown. Dashed lines indicate the value obtained by the GAM with the original daily (Kervidy-Naizin, AgrHyS observatory) or weekly (Néal and Le Queffeuth catchments) time series. The y-axis corresponds to the number of catchments (N). The comparisons show that the distribution of seasonality metrics obtained from lower-frequency time series were centered on the values obtained from the original time series. Despite some delay in phases, minimum and maximum concentrations were identified during the same season by both types of time series. For NO_3, the mean errors in seasonal metrics obtained from the monthly time series were -4.5% and 6.7% for amplitude, 21.0% and -7.2% for SI for the Kervidy-Naizin and Néal catchments respectively. PhaseMax was delayed by -1.0 to -1.5 months, and PhaseMin by 0 to 1 months. For SRP (Le Queffeuth catchment), the mean error was -4.0% for amplitude, -7.0% for SI, ±18 days for PhaseMax, and ±12 days for PhaseMin.

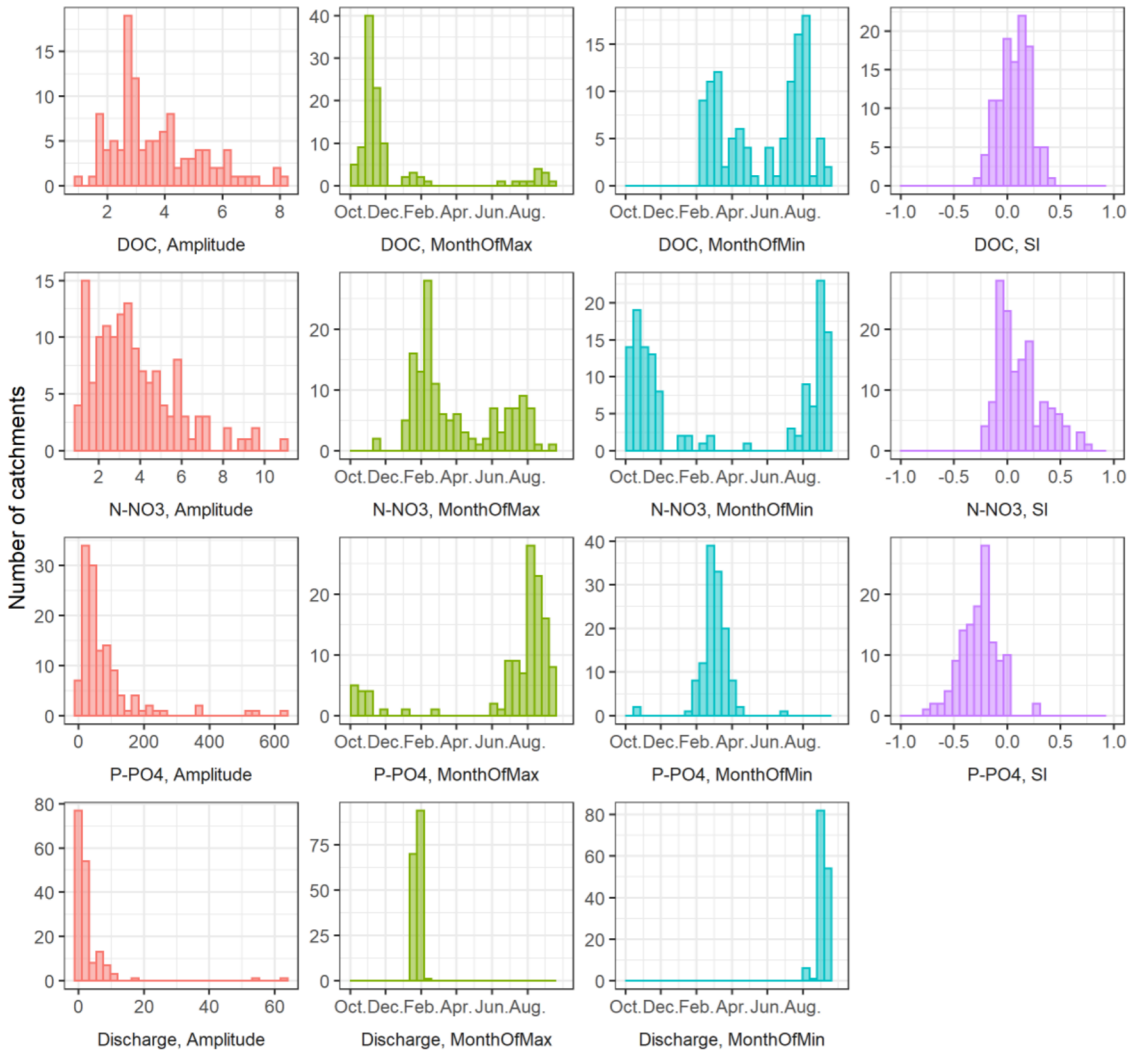

Figure S7. Histograms of water quality metrics and discharge, from left to right: absolute annual amplitude (mg.l^{-1}), annual minimum and maximum concentration phases (in months), and the seasonal index (only for concentrations). From top to bottom: for dissolved organic carbon (DOC) (n=113), nitrate (N-NO_3) (n=142), soluble reactive phosphorus (SRP) (n= 126), and discharge (Q) (n=124). Non-significant amplitudes (Rsq<0.1) are not shown.

DOCTORAT ECOLOGIE BRETAGNE GEOSCIENCES LOIRE AGRONOMIE ALIMENTATION

l'institut Agro agriculture • alimentation • environnement

AGRO CAMPUS OUEST

Titre : Influence du climat sur les transferts de carbone organique dissous, nitrate et phosphate dans une tête de bassin versant agricole

Mots clés : Hydrologie, agriculture, climat, carbone, azote, phosphore

Résumé : L'agriculture a provoqué des concentrations excessives en nitrate (NO_3) et phosphate (SRP) dans les écosystèmes aquatiques. Le climat influence aussi le transfert de ces éléments au sein d'un bassin versant. La compréhension de ces transferts est cruciale pour restaurer la qualité des eaux. L'objectif est d'identifier l'effet du climat sur les transferts de carbone organique dissous (DOC), NO_3 et SRP dans une tête de bassin versant agricole. Cette étude s'appuie sur un jeu de données hydro-climatiques et chimiques acquis sur le bassin versant de Kervidy Naizin (Morbihan, Bretagne, France). Le premier chapitre porte sur l'analyse de données pour identifier les conditions hydro-climatiques qui contrôlent les dynamiques long terme, saisonnières et évènementielles des concentrations dans le cours d'eau. Le second chapitre porte sur la modélisation couplée du débit, DOC et NO_3 dans le cours d'eau pour mieux contraindre leurs sources et chemins d'écoulement. Les résultats montrent que les pratiques agricoles et le climat contrôlent les concentrations sur le long terme, alors que les conditions hydrologiques en contrôlent les dynamiques saisonnières et évènementielles. La modélisation a montré que l'opposition du DOC et du NO_3 est contrôlée par la distribution spatiale de leurs sources dans deux compartiments dont les temps de résidence sont contrastés. Le climat influence indirectement les dynamiques des concentrations par son effet sur les chemins d'écoulement de l'eau dans le bassin versant.

Title : Climate influence on the transfer of dissolved organic carbon, nitrate and phosphate in an agricultural headwater catchment

Keywords : Hydrology, agriculture, climate, carbon, nitrogen, phosphorus

Abstract : Agriculture caused excessive nitrate (NO_3) and phosphate (SRP) concentrations in aquatic ecosystems. Climate also influences the transfer of these elements within catchment. Understanding these transfers is crucial in the aim of restoring water quality. The objective of this work is to identify the climate effect on dissolved organic carbon (DOC), NO_3 and SRP transfers in an agricultural catchment. This study used a dataset of hydro-climatic and chemical variables acquired on the Kervidy Naizin catchment (Morbihan, Brittany, France). The first chapter focuses on data analysis to identify the hydro-climatic conditions that control the long-term, seasonal and event-driven dynamics of the concentrations in the river. The second chapter deals with the coupled modeling of the discharge, DOC and NO_3 in the river to better constrain their sources and flow paths. The results show that agricultural practices and climate control concentrations over the long term, while hydrological conditions control seasonal and event-driven dynamics. Modelling showed that the opposition of DOC and NO_3 is controlled by the spatial distribution of their sources in two compartments with contrasting residence times. Climate indirectly influences the dynamics of the concentrations through its effect on water flow paths within the watershed.